Universidade de Lisboa
Faculdade de Medicina de Lisboa

EFFECT OF INFLAMMATION ON BONE BIOLOGICAL, STRUCTURAL AND MECHANICAL BEHAVIOR

JOANA RIBEIRO CAETANO LOPES

Doutoramento em Ciências Biomédicas
Especialidade de Ciências Biopatológicas

2011

Universidade de Lisboa

Faculdade de Medicina de Lisboa

EFFECT OF INFLAMMATION ON BONE BIOLOGICAL, STRUCTURAL AND MECHANICAL BEHAVIOR

JOANA RIBEIRO CAETANO LOPES

Tese orientada por

Professor Doutor João Eurico Fonseca

Professor Doutor Yrjö Tapio Konttinen

Doutoramento em Ciências Biomédicas

Especialidade de Ciências Biopatológicas

A impressão desta dissertação foi aprovada pelo Conselho Científico da Faculdade de Medicina de Lisboa em reunião de 19 de Julho de 2011.

Dissertação apresentada à Faculdade de Medicina da Universidade de Lisboa para obtenção do grau de doutor em Ciências Biomédicas.

A todos os que contribuíram
para esta tese

Não sou nada
Nunca serei nada
Não posso querer ser nada
À parte isso, tenho em mim todos os sonhos do mundo

"I am nothing
I shall always be nothing
I cannot wish to be anything
Aside from that, I have within me all the dreams of the world"

In Tabacaria
Álvaro de Campos, 1928

TABLE OF CONTENTS

FIGURES INDEX

ACKNOWLEDGEMENTS

Uma tese de doutoramento, como projecto de vida que é, é feita de momentos, uns bons outros menos bons, mas sempre acompanhada de pessoas que nos ajudam a ultrapassar obstáculos. A estas pessoas quero agradecer os momentos partilhados nesta viagem de descoberta científica.

During the work that lead to this dissertation thesis I wish to highlight the role of my two supervisors, professor João Eurico Fonseca and professor Yrjö Tapio Konttinen, which were fundamental to keep me on the route to accomplish the objectives proposed. Thank you for all the discussions, for the guidance, for the advice and for allowing me to think by myself and expose my point of view. But most of all, thank you for believing. João, é muito gratificante ver como a história da UIR se desenrolou durante estes curtos sete anos de vida e tal não seria possível sem a sua orientação e admirável capacidade de trabalho que conduziu à fusão de vários mundos numa só unidade.

À professora doutora Helena Canhão, minha tutora e super-mulher, não posso deixar de te expressar a minha admiração pela extraordinária pessoa que és e por seres uma imparável força da natureza. Obrigada pelos constantes desafios, pelas intermináveis discussões e por estares simplesmente presente e disponível ao longo de todo o trabalho. A tua velocidade de revisão e escrita de artigos, de projectos e trabalhos afins é incomparável! Foste tu quem me apresentou o RANKL, um senhor com muitos amiguinhos que eu vim a conhecer bem melhor mais tarde. Aos restantes membros do meu comité de tese, professora Fátima Vaz e doutora Sandra Casimiro o meu muito obrigada pelos vossos conselhos inestimáveis e pela constante disponibilidade.

In the first year I've been in Italy, in L'Aquila in a bone biology laboratory, supervised by Professor Anna Teti. It was short visit but during this time I've discovered the magic of the bone cell. Thank you for allowing me to enter your world and to get to know the scientist you are. To Dr. Nadia Rucci for being the center of the lab, for all the knowledge that she transmits to the students and for our several *panini* lunches talking about Lisbon. To Dr. Mattia Capulli for the constant jokes and for making everyone laugh even when the environment was somewhat tense and specially for asking me every single day "how is your writting?". To Anna Rufo for all the time she spent teaching me how to take bones from newborn mice to get cells. To Marta Cappanolo I have to thank the kindness, the never-ending questions, to showing me that although L'Aquila is a very small city the size doesn't matter. The history lesson that you gave me was truly impressive, almost as the 99 squares, 99 fountains and 99 churches of L'Aquila. If Marta showed me L'Aquila, Dr. Andrea Del Fattore gave me a tour of Rome. But not only the tourist Rome, he presented me some of his favorite places, the fontana di trevi, the colosseo, San Pietro and the small alleys of Trastevere. You also introduce me to a real *mamma italiana* which received me as a long-time friend. *Grazie mille*!

Na Unidade de Investigação em Reumatologia muito aconteceu desde que eu iniciei o meu trabalho, umas pessoas passaram outras ficaram mas todas me marcaram. João Cavaleiro, obrigada pela força, pela calma com que encaras a vida e por todos os *truques de bancada* que aprendi contigo. Zé Teles não posso deixar de te agradecer palavras que na altura não compreendi mas que agora fazem todo o sentido. Obrigada pela confiança e por me teres mostrado que uma imagem vale mais de mil palavras! Aos dois e à doutora Pamela Weinman, muito obrigada por me terem acolhido na UIR e por me mostrarem o que é trabalhar num laboratório de investigação translacional. Rita

Moura, nós vivemos muita da confusão inicial mas isso só nos tornou mais fortes e é com esta força que estamos neste momento a dar os últimos passos numa etapa das nossas vidas. Foi também desde o início que a Ana Margarida desenvolveu a biomecânica do osso e apesar de todos os percalços e idas e vindas entre o IST e o IMM, conseguimos estabelecer os ensaios que hoje em dia tanto usamos. Obrigada pela tua perseverança e pelas tardes que passámos a *desossar* ratinhos. A doutora Saba Abdulghani, a Inês Aleixo e a Catarina Vale foram também aqui peças importantes em estabelecer e afinar os detalhes da técnica. Como apoios, o Bruno, a Rita Cascão, a Ana Lopes e a Ana Farinho muito contribuíram para o bem-estar ao longo do trabalho. Diana, a minha companhia cultural, de que outra forma é que as nossas manhãs poderiam começar se não fosse esta? Um café e meia horinha de brainstorming sobre os problemas e experiências do momento! Mas melhor melhor, é quando os nossos dias acabam num espectáculo! Ângela, entraste numa fase mais tardia mas o tempo aqui não é o importante. Tens sido um apoio fundamental durante esta minha fase de eremita num projecto que eu acarinho muito e que está a renascer. À doutora Anita Gomes, uma enciclopédia de biologia molecular, muito obrigada pelos preciosos protocolos e conselhos.

A ti Inês, a minha companheira dos ossos duros de roer que foram as nossas experiências, obrigada pelos nossos momentos de bancada e pela infinita partilha de artigos. Talvez eu agora tenha tempo de os ler todos ... Conhecemo-nos sem sabermos quem éramos mas o que mais me impressionou foi a tua curiosidade, o querer saber tudo e não ter tempo. E a curiosidade transformou-se em força como o monócito se transforma em osteoclasto! Ao longo deste tempo crescemos e trabalhámos juntas com muito riso e muita lágrima, mas sempre nós.

Nada deste trabalho em amostras humanas seria possível sem a maltinha clínica! Filipa e Elsa, as nossas histórias vêm de um tempo diferente, de tardes e tardes a pôr dados em tabelas e de dias sem fim de colheitas de sangue. Obrigada pela vossa infinita paciência quando me explicavam o que é que cada uma das variáveis significa. Filipa, sempre despachada tu contagias todos à tua volta com essa energia positiva. Elsa, sempre tão preocupada e uma amiga incansável. Se há problema, resolve-se num jantar! Tu és tu, nunca sejas diferente! Nesta história entraste mais recentemente Ana Maria, mas entraste para ficar. Tornámo-nos tão cúmplices ao longo destes projectos que não conseguiria enumerar um momento especial. Trabalhar contigo é especial e nem pensar em escrever projectos ou artigos separadas, só nos dá mais trabalho. Muito muito obrigada por tudo! Um obrigada ainda para o Joaquim e Maria João pelas análises fora-de-horas e DXAs de urgência, à enfermeira Lurdes por estar sempre disponível e ao serviço de ortopedia (incluindo enfermeiras) pela constante colaboração.

Durante o doutoramento fui voluntária no Jardim Zoológico de Lisboa. O zoo é por si só um mundo à parte, com uma sociedade própria, um refúgio. A todos os voluntários, um muito obrigada por todos os momentos de companheirismo e cumplicidade. Muito especialmente ao Sr. Silvino, sempre no topo do torreão esquerdo, oficialmente coordenador de voluntários mas também psicólogo nas horas vagas. Nunca me esquecerei dos 10 minutos transformados em meia hora de conversa, nem de que "os animais também comem quando chove"! No Jardim Zoológico há sempre algo de novo para ver ... mesmo para quem lá ia todas as semanas. Apesar de o zoo ser enorme e de todas as áreas precisarem de ajuda, há um local muito especial – a baía dos golfinhos!! Que todos adoram golfinhos, inclusive eu, não é surpresa. Mas aquilo que ninguém vê, tudo o que se passa nos bastidores, as formiguinhas obreiras, aí, sim, está a

diferença. A equipa técnica da baía dos golfinhos faz um trabalho espectacular para produzir três espectáculos diários. E eu só tenho que lhes agradecer terem-me acolhido na sociedade, deixando-me fazer parte da sua família. Ana, tu és daquelas pessoas especiais e únicas. A tua coragem e força une a equipa e foi dessa força que nasceu a Beatriz. Tens sempre uma palavra amiga para dizer na hora certa, no momento certo. E tu Lourenço, sempre disposto a defender tudo e todos. Depois de te conhecer vi a tua generosidade, lealdade e dedicação e nasceu uma grande amizade. Não me vou esquecer nunca do *just breathe* e do sorriso que soprava para longe os problemas. Tu és uma pessoa muito especial. Não posso deixar ainda de referir o Hélio, o Duarte, o Dinis, o Lopes, a Joana, a Mariana, a Vanessa e a Marina pelos bons momentos passados, por todas as palavras amigas. À Cristina obrigada por seres a amiga das horas aflitas (porque quando aquece, a baía dos golfinhos torna-se um barril de pólvora), à companheira de aspiração, de limpeza, de espectáculos, à cúmplice de brincadeiras. Estivemos sempre juntas, no melhor e no pior, sempre angustiadas quando um animal estava doente, a vibrar de emoção quando no meio do show um golfinho salta e a baía explode em palmas, quando um golfinho nos encharca e vocaliza ou simplesmente quando a água está azul. Tenho imensas recordações do tempo aí passado, umas boas, outras mesmo muito más, mas o balanço final não poderia ser mais positivo. Tive o privilégio de vos conhecer e criar laços de amizade, estar presente na loucura do show das 15h, de ver a lagoa a nascer, a baía vazia, de ver nascimentos, doença, morte, mas sempre com o lema *the show must go on*. E sempre que durante um espectáculo, uma criança sorri, a nossa missão foi cumprida!

E, claro, ao meu fungagá da bicharada, Vicky, Soda, Kobie, Neo, Lair, Princesa, Storm, Joshua, Otarii, Seth, entre outros, obrigada pela vossa constante presença, dentadinhas amigáveis e sempre boa disposição! Ao Nazaré, uma estrelinha que nos visitou, quem te conconheceu nunca te esquecerá! E foram tantos os que tu tocaste ...

Obrigada por tudo, cresci muito como pessoa no zoo, convosco, e aí ficou também um bocadinho de mim.

A todos os amigos que acompanharam este meu projecto de vida, muito obrigada pelos momentos partilhados. Joana Lopes (a outra), estás longe mas sempre perto. Os nossos cafés todas as manhãs foram um *bem-vinda a este mundo clínico*. Nós somos tão iguais, mas tão diferentes ... obrigada por todos os momentos de cumplicidade e pela amizade que nos une. Marta às vezes uma conversa ao lanche faz milagres. E quando pensamos juntas tudo se encaixa, espero que nos cruzemos no futuro. Apesar de termos passado pouco tempo a trabalhar em conjunto Patrícia, nasceu uma grande amizade. Sempre com um jantar e um filme pelo meio, dás-me outra perspectiva da vida. A tua perseverança, calma e tranquilidade são extraordinárias; às vezes gostava que isso se transmitisse por osmose.

Não posso ainda deixar de agradecer à família, pais, avós e Romeu por não questionarem quando não percebem e pela paciência com que enfrentam a minha falta de tempo durante este percurso do doutoramento. E à Filipa, a minha pequena dançarina , obrigada por me encheres a vida de música, dança, princesas e magia Disney.

Obrigada a todos por terem embarcado comigo nesta viagem.

ABBREVIATIONS

2D	2 dimension
3D	3 dimension
ADAM	A disintegrin and metalloproteinase
ADAMTS2	A disintegrin-like and metalloproteinase (reprolysin type) with thrombospondin type 1, motif 2
ALP	Alkaline phosphatase
AP-1	Activator protein-1 (Fos/Jun)
APC	Adenomatous polyposis coli
AS	Ankylosing Spondylitis
ATP6V0D2	ATPase, H+ transporting, lysosomal 38kDa, V0 subunit d2
BAFF	B-cell activating factor
BIM	BCL2-like 11
BMC	Bone mineral content
BMD	Bone mineral density
BMP	Bone morphogenetic protein
BMU	Basic multicellular unit
BRC	Bone remodeling compartment
BSP	Bone sialoprotein
bp	Base pair
CALCR	Calcitonin receptor
CD	Cluster of differentiation
C/EBPα	CCAAT/enhancer-binding protein α
C-FMS	Colony stimulating factor 1 receptor
CIA	Collagen-induced arthritis
CLCN	Chloride channel
COL1A1	Type I collagen α1 chain
CT	Computed tomography
CTLA4	Cytotoxic T-Lymphocyte Antigen 4
CTSK	Cathepsin K
CTX	Carboxy-terminal cross-linked telopeptide of type I collagen

CXCL12	Chemokine (C-X-C motif) ligand 12
DAP12	DNAX-activation protein 12
DC	Dendritic cells
DC-STAMP	Dendritic cell-specific transmembrane protein
DKK1	Dickkopf homolog 1
DLX5	Distal-less homeobox 5
DMP1	Dentin matrix acidic phosphoprotein 1
DNA	Deoxyribonucleic acid
DPD	Deoxypyridinoline
DVL	Dishevelled
DXA	Dual X-ray absorptiometry
E11/gp38	Podoplanin
EFNB2	Ephrin-B2
EN-1	Homeobox protein engrailed-1
EPHB4	Ephrin receptor B4
ERK	Extracellular signal-regulated kinase
FGF	Fibroblast growth factor
FRA-1	FOS-like antigen 1
FLS	Fibroblast-like synoviocytes
FOS	FBJ murine osteosarcoma viral oncogene homolog
FZ	Frizzled
GM-CFU	Granulocyte-macrophage colony forming unit
GM-CSF	Colony stimulating factor 2 (granulocyte-macrophage)
HCl	Hydrogen chloride
HLA	Human leukocyte antigen
HSC	Hematopoietic stem cells
ICTP	Pyridinoline cross-linked carboxy-terminal telopeptide of type I collagen
IFN	Interferon
IGF	Insulin-like growth factor
IgG	Immunoglobulin G
IKK	Inhibitor of NF-κB kinase
IL	Interleukin
IL-6R	IL-6 receptor

ITAM	Immunoreceptor tyrosine-based activation motif
JIA	Juvenile idiopathic arthritis
JNK	C-Jun N-terminal kinase
kDa	kiloDalton
KRM	Kremen
LEF	Lymphoid enhancer factor
LPS	Lipopolysaccharide
LRP	Low density lipoprotein receptor-related protein
LT	Lymphotoxin
MAPK	Mitogen-activated protein kinase
MCP-1	Monocyte chemotactic protein-1
M-CSF	Colony stimulating factor 1 (macrophage)
MDL	DAP12-associating lectin
MEPE	Matrix extracellular phosphoglycoprotein
microCT	Microcomputed tomography
MIF	Macrophage migration inhibitory factor
MITF	Microphthalmia-associated transcription factor
mm	Milimeter
MMP	Matrix metalloproteinase
MPM	Multiphoton microscopy
MRI	Magnetic resonance imaging
mRNA	Messenger RNA
MSC	Mesenchymal stem cell
NFκB	Nuclear factor kappa B
NFATc1	Nuclear factor of activated T-cells, cytoplasmic, calcineurin-dependent 1
NK cells	Natural killer cells
NKT cells	Natural killer T cells
nm	Nanometer
NTX	Amino-terminal cross-linked telopeptide of type I collagen
OA	Osteoarthritis
OCL	Osteocalcin
OP	Osteoporosis
OPG	Osteoprotegerin

OPN	Osteopontin
OSCAR	Osteoclast associated, immunoglobulin- like receptor
OSE2	Osteoblast specific element
OSF-2	Periostin
OSX	Osterix
p38	Mitogen-activated protein kinase 14
P1CP	Procollagen 1 carboxy-terminal peptide
P1NP	Procollagen 1 amino-terminal peptide
PsA	Psoriatic Arthritis
PAMP	Pathogen-associated molecular pattern
PDGF	Platelet-derived growth factor
PHEX	Phosphate regulating endopeptidase homolog, X-linked
PI3K	phosphoinositide-3-kinase
PIR	Immunoglobulin-like receptor
PPAR	Peroxisome proliferator-activated receptor
PRDM1	PR domain zinc finger protein 1
PTH	Parathyroid hormone
PTPN22	Protein tyrosine phosphatase, non-receptor type 22
PYD	Pyridinoline
PU.1	Spleen focus forming virus proviral integration oncogene spi1
RA	Rheumatoid Arthritis
RANK	Receptor activator of nuclear factor kappa B
RANKL	RANK ligand
RANTES	Regulated upon activation, normal T cell expressed and secreted
RGD	Arg-Gly-Asp
RARG	Retinoic acid receptor γ
RNA	Ribonucleic acid
RSPO1	R-spondin homolog
RUNX	Runt-related transcription factor
S1P	Sphingosine-1-phosphate
SEM	Scanning electron microscopy
sFRP	Secreted frizzled-related protein
SHG	Second-harmonic generation

SIBLING	Small integrin-binding ligands with N-linked glycosylation
SIRP	Signal-regulatory protein
SP1	SP1 transcription factor
SRC	V-src sarcoma (Schmidt-Ruppin A-2) viral oncogene homolog
SOST	Sclerostin
SQSMT1	Sequestosome-1
SOX9	SRY (sex determining region Y)-box 9
TACE	TNF-α converting enzyme
TCF	T cell factor
TCR	T cell receptor
tg	Transgenic
TGF	Transforming growth factor
Th	T helper
TIE2	TEK tyrosine kinase, endothelial
TLR	Toll-like receptor
TNF	Tumor necrosis factor
TPE	Two-photon excitation
TRAcP5b	Tartrate-resistant acid phosphatase 5b
TRAF	TNF receptor-associated factor
TRAP	Acid phosphatase 5, tartrate resistant
Treg	Regulatory T cells
TREM	Triggering receptor expressed on myeloid cells
VEGF	Vascular endothelial growth factor
vQCT	Volumetric quantitative CT
ZAP-70	Zeta-chain-associated protein kinase 70

Gene names were based on the database of HUGO Gene Nomenclature Committee[1].

SUMÁRIO

O termo osteoimunologia foi usado pela primeira vez em 2000 para descrever a interacção entre células do sistema imunitário e do osso. Estes dois sistemas têm vários factores em comum, tais como citocinas, factores de transcrição e receptores. Consequentemente, a sua interacção ocorre, não só em condições fisiológicas, mas também patológicas. O objectivo desta dissertação de doutoramento é o de compreender o efeito da inflamação mediada pelo sistema imunitário no comportamento estrutural, mecânico e biológico do osso usando a artrite reumatóide e a regeneração de fracturas como modelos.

O primeiro estudo desta tese foca a análise do efeito da artrite no comportamento biomecânico do osso. Foi utilizado um modelo animal de artrite, o ratinho SKG, para avaliar o comportamento biomecânico do osso por testes de flexão de 3 pontos. A microscopia electrónica de varrimento e a microscopia multifotão foram utilizadas, respectivamente, para o estudo da estrutura óssea e da organização da rede de colagénio no osso trabecular. Os resultados deste estudo mostraram que o osso de ratinhos com artrite apresenta pior qualidade biomecânica comparando com os controlos. Observações por microscopia multifotão e microscopia electrónica de varrimento demonstraram alteração da organização do colagénio e da estrutura trabecular. Neste trabalho verificámos que a inflamação crónica *per se* conduz à degradação das propriedades biomecânicas, particularmente da rigidez, ductilidade e resistência.

No mesmo modelo animal, prosseguimos com o estudo do efeito da inflamação no metabolismo e organização do colagénio. A avaliação do osso incluiu ensaios mecânicos, microscopia electrónica de varrimento, microscopia multifotão e doseamento de marcadores

séricos de remodelação óssea, especificamente o péptido amino-terminal do procolagénio tipo I (P1NP) e o carboxi-terminal do telopéptido do colagénio tipo I (CTX). O osso dos ratinhos SKG revelou aumento da fragilidade óssea expresso pela deterioração das propriedades mecânicas. Em concordância, por microscopia electrónica de varrimento foi observado que a distância intertrabecular aumentou e a espessura trabecular reduziu e a microscopia multifotão demonstrou uma matriz desorganizada, com baixa densidade de colagénio. O metabolismo do colagénio foi ainda estudado no soro, encontrando-se aumentado nos ratinhos com artrite. Neste trabalho determinámos que o efeito de fragilidade óssea induzido pela artrite se deve à elevada remodelação óssea e desorganização da matriz de colagénio tipo I.

Seguindo os dados iniciais obtidos em modelo animal, os primeiros a descrever o efeito directo da artrite na estrutura do colagénio e na biomecânica do osso, confirmámos e detalhámos estas observações em osso humano com artrite reumatóide. Foram recrutados doentes com AR submetidos a artroplastia da anca. A microarquitectura do osso trabecular foi avaliada por microtomografia computadorizada e o comportamento biomecânico por teste de compressão de um cilindro de osso trabecular extraído da epífise femoral. A actividade das células ósseas foi analisada através do estudo da expressão génica no microambiente ósseo. Observou-se um aumento da expressão dos genes que codificam citocinas pró-inflamatórias, particularmente a IL-17, a qual desempenha um importante papel na estimulação da osteoclastogénese. O microambiente do osso com AR apresenta um perfil de expressão génico caracterizado pelo aumento das citocinas pró-osteoclastogénicas e de DKK1 e ainda do rácio de expressão RANKL/OPG. Paralelamente, verificou-se um aumento da expressão de factores indutores da actividade osteoblástica, tais como o IGF-I, FGF2 e PDGF, apesar da baixa expressão de colagénio tipo I. O DKK1 é um regulador negativo da via de sinalização WNT/β-catenina, sendo esta uma via chave na estimulação da diferenciação do osteoblasto. Assim, o aumento deste inibidor nos doentes com artrite reumatóide limita o efeito pró-osteoblastogénico do ambiente molecular do osso artrítico. A perda óssea associada às doenças crónicas inflamatórias, tal como a artrite reumatóide, parece, desta forma, resultar do aumento da reabsorção óssea e de uma diminuição na formação, conduzindo ao desequilíbrio da remodelação e precipitando a rápida perda de massa óssea. De facto, foram observadas diferenças na expressão génica entre o osso de doentes com artrite reumatóide e com osteoporose primária, apesar destes dois grupos de doentes terem microestrutura óssea e propriedades biomecânicas semelhantes. Estas observações parecem indicar que as diferenças encontradas a nível da expressão génica reflectem mecanismos biológicos específicos responsáveis pela fragilidade óssea na artrite reumatóide e a inibição do DKK1 poderá vir a ser uma possível estratégia terapêutica para diminuir os efeitos da artrite reumatóide sobre o osso.

No último trabalho desta tese, utilizámos a reacção inflamatória pós-fractura como modelo para caracterizar a cinética de expressão dos genes relacionados com a inflamação e remodelação óssea. Ao contrário da inflamação crónica, característica da artrite reumatóide, a regeneração de fracturas é um processo breve e cuidadosamente regulado. Foram incluídos neste estudo doentes submetidos a artroplastia da anca devido a fracturas de baixo impacto. Os doentes foram agrupados de acordo com o tempo decorrido entre a fractura e a cirurgia: osso colhido nos 3 dias após fractura, entre o 4º e o 7º dias, e uma semana após fractura. Um conjunto de genes relacionados com a inflamação e o metabolismo ósseo foram estudados no local de fractura. Os resultados obtidos indicam que a expressão dos genes relacionados com a inflamação, especialmente a

IL-6, estão aumentados nos primeiros dias após fractura; contudo, a partir do dia 4 verifica-se um desvio para os genes de remodelação óssea, sugerindo que a fase inflamatória activa a regeneração da fractura. A expressão da esclerostina, um inibidor da diferenciação do osteoblasto, está aumentada durante os primeiros dias após fractura e diminui após a redução da expressão dos genes pró-inflamatórios. Desta forma, propomos a existência de um processo em duas fases que conduz à regeneração de fracturas, dependente de um estímulo inicial inflamatório e uma diminuição subsequente dos efeitos relacionados com a esclerostina, com consequente estímulo osteoblástico. Assim, a indução local destes eventos poderá constituir uma intervenção promissora para acelerar a regeneração óssea após fractura.

O trabalho aqui discutido claramente demonstra o complexo papel da inflamação na regulação óssea. A identificação de factores reguladores chave deste sistema será crucial para o futuro tratamento da artrite reumatóide e das fracturas.

SUMMARY

The term osteoimmunology was used for the first time in 2000 to describe the interaction of cells from the immune system and bone These two systems have several regulatory factors in common, such as cytokines, transcription factors and receptors. Consequently, they interact with each other both in physiological and pathological conditions. The aim of this dissertation thesis was to understand the effect of immune mediated inflammation on bone structural, mechanical and biological behaviour, using rheumatoid arthritis (RA) and fracture healing as a model.

The first study of this thesis focused on the analysis of the effect of arthritis on bone biomechanical behavior. An animal model of arthritis, the SKG mice, was used and bone behavior was evaluated by mechanical three-point bending tests. Scanning electron microscopy (SEM) and multiphoton microscopy (MPM) were applied to study, respectively, bone structure and the collagen network organization in trabecular bone. Results from this study have shown that arthritic bones had poor biomechanical quality compared to control bones. MPM and SEM observations disclosed signs of impaired collagen organization and poor trabecular architecture. In this work we verified that chronic inflammation *per se* leads to impairment of bone biomechanics in terms of stiffness, ductility and ultimate strength.

In the same model, we then proceed to study the effect of inflammation on collagen metabolism and organization. The evaluation of bone included mechanical tests, SEM, MPM and serum bone turnover markers, specifically procollagen type - amino-terminal peptide (P1NP) and carboxy-terminal crosslinked telopeptide of type I

collagen (CTX). Femoral bones of SKG mice revealed increased fragility expressed by deterioration of mechanical properties. In accordance, as observed by SEM, intertrabecular distance was increased and trabecular thickness decreased. MPM depicted a disorganized matrix and loose collagen structure compared to controls. Moreover, the collagen metabolism assessed in the serum was also highly increased in arthritic mice. In this work we found that the bone weakening effect of arthritis was due to high bone turnover and disorganized collagen type I matrix.

Following these initial animal model data, the first to describe a direct effect of arthritis on collagen structure and bone biomechanics, we confirmed and further detailed these observations in human RA bone. Patients with RA submitted to hip replacement surgery were recruited. Trabecular bone microarchitecture was assessed by micro-computed tomography (microCT) and mechanical behavior by compression tests of a bone cylinder extracted from the femoral epiphysis. Bone cell activity was analyzed by studying gene expression in the bone microenvironment. Genes that code for pro-inflammatory cytokines were upregulated in RA patients, particularly IL-17, which plays an important role in stimulating osteoclastogenesis. RA bone microenvironment had a gene expression profile characterized by upregulated pro-osteoclastogenic cytokines and dickkopf homolog 1 (DKK1) and increased RANKL/OPG ratio. This was paralleled by raised expression of factors that promote osteoblastic activity, such as IGF-I, FGF2 and PDGF, but with low type I collagen expression. DKK1 is a negative regulator of the WNT/β-catenin signaling, which is a key pathway in the stimulation of osteoblast differentiation, meaning that its upregulation in RA patients is limiting the effects of pro-osteoblastic factors. Bone loss in a chronic inflammatory disease, such as RA, thus appears to result from enhanced bone resorption and impaired bone formation, which constitutes a detrimental imbalance of bone remodeling and precipitates the rapid loss of bone mass. Indeed, differences were observed in gene expression between RA and primary osteoporosis (OP) bone in spite of the fact that these two patient groups had similar bone microarchitecture and biomechanical properties. These observations might indicate that the differences in gene expression reflect biologically specific mechanisms responsible for bone fragility in RA and that the inhibition of DKK1 can be a possible treatment strategy for tackling the effects of RA on bone.

In the final work of this thesis, we have used the post-fracture inflammatory reaction as a model for characterizing the kinetics of inflammatory and bone remodeling related genes. Unlike the chronic inflammation seen in RA, fracture healing is a highly regulated and brief process. Patients submitted to hip replacement surgery after a low-energy hip fracture were enrolled in this study. Patients were grouped according to the time interval between fracture and surgery: bone collected within 3 days after fracture; between the 4th and 7th day; and one week after fracture. Inflammation and bone metabolism related genes were assessed at the fracture site. Our results indicate that the expression of inflammation related genes, especially IL-6, is highest at the very first days after fracture but from day 4 onwards there is a shift towards bone remodeling genes, suggesting that the inflammatory phase triggers bone healing. Sclerostin expression, an inhibitor of osteoblast differentiation, has an initial high expression level that is diminished after the reduction of inflammatory gene expression. We propose the existence of a two step process in bone healing, dependent on an initial inflammatory stimulus and a latter decrease in sclerostin-related effects, with a consequent pro-osteoblastic effect. Therefore, local promotion of these events might constitute a promising medical intervention to accelerate fracture healing.

The work herein discussed clearly shows that inflammation has a complex role in bone regulation. The identification of key regulators of this system will be crucial both for RA and fracture healing future management.

INTRODUCTION

BONE

Bone is one of the most dynamic human tissues, as it remains metabolically active throughout life and has pleiotropic functions in the organism. It not only protects the internal organs, supports the body and assists in its movement but also function as a mineral (calcium and phosphorus) and fat reservoir and harbours bone marrow, where haematopoiesis occur.

Bone is composed of three different cell types: osteoclasts, osteoblasts and osteocytes. These cells are responsible for the daily bone renewal in a tightly balanced process. On the other hand, the organization of bone as a tissue is dependent on complex interactions between three main players; collagen type I, hydroxyapatite crystals and cells.

From a structural perspective bone can be classified in hierarchical levels of complexity, all of which affect its mechanical properties. It must be stiff, slightly flexible and light in order to make loading possible and facilitate movement.

Additionally bone has a unique characteristic that distinguishes it from other tissues: it can respond according to the location and extent of the biomechanical loading and microdamage, remove the damaged tissue and replace it with new bone. Disequilibrium of this system is observed in bone metabolic diseases, such as primary osteoporosis (OP), or as consequence of systemic inflammatory diseases such as rheumatoid arthritis (RA). This will induce bone fragility and eventually low energy fractures.

How inflammation affects bone structure and mechanics and how different are the processes that occur in RA and OP are issues still not completely understood. In order to address these questions a comprehensive knowledge on bone structure, mechanics and biology, coupled with an understanding of the crosstalk between the immune system and bone is essential.

BONE STRUCTURE

At the macroscopic structural level, bones have diverse shapes accounting for the different supporting and/or protective functions they play. In the appendicular skeleton we can find long bones which provide stability against bending and buckling. Bone is covered by a shell, the cortical bone, which is filled in by a honeycomb-like structure, the trabecular bone[2]. Trabecular bone absorbs energy and is light and flexible. The cortical structure, on the other hand, has the ability to tolerate the peak loads that the long bones are subjected to[3].

Cortical bone is quite dense, with a porosity of only about 6%, mainly due to the presence of blood vessels. In fact, this type of bone is characterized by the presence of structures called osteons, comprising a blood vessel surrounded by concentric layers of bone, which form the Haversian system. Therefore, cortical bone consists of overlapping parallel osteons that block the propagation of microcracks. On top of that, damage propagation into the osteon is blocked by its surrounding cement line[3-4], which delimits each osteon, and by the concentric lamellae of mineralized collagen fibers[3]. Cortical bone contains Haversian and transversal Volkmann canal systems for vascular supply. These structures are surrounded by 5 to 15 concentric lamellae several microns thick with its fibers aligned parallel to each other, around the vascular canal. Haversian canals contain capillaries and small blood vessels, lymphatic vessels and connective tissue with osteoprogenitor cells. On the other hand, Volkmann canals are vascular channels which link the periosteum and bone[5].

Trabecular bone is composed of trabeculae arranged in a honeycomb-like network, which confers a porosity of about 80%. Each trabecula has a thickness of around 200µm and their orientation depends on load distribution. Trabeculae are surrounded by bone marrow and fat[2]. The trabecular structure is characterized by the number of trabeculae in a given volume of bone, their thickness as well as the distance and connectivity between them. Previously, observation of trabecular microarchitecture was only possible by two-dimensional histomorphometry but nowadays, new imaging techniques such as high-resolution microcomputed tomography (microCT), allow tri-dimensional observation of bone microstructure[6]. Trabecular bone is metabolically more active than cortical bone and this is why studies on bone quality have mainly focused on this component of bone.

Regarding collagen fiber arrangement, bone can be classified in woven bone and lamellar bone. In woven bone, which is predominantly present during fetus development, bone collagen fibers are randomly oriented and there are higher numbers of cells per unit area than in mature bone. In adults, woven bone can only be found in areas where bone is being remodeled. Lamellar bone, the mature form of bone, develops when the deposition rate is slow and it has a well-organized arrangement of collagen fibers. In general, it is formed only over pre-existing bone, either woven or lamella[5].

BONE MATRIX

Bone matrix is composed of two components, an organic phase (about 40% of the dry weight) made up of collagen, proteoglycans, glycoproteins, phospholipids and phosphoproteins, and an inorganic phase (about 60% of the dry weight) of calcium hydroxyapatite ($Ca_{10}(PO_4)_6(OH)_2$)[5].

COLLAGENS

Collagens are a group of natural occurring proteins that share common features. The widely accepted definition of collagen is "structural proteins of the extracellular matrix which contain one or more domains harboring the collagen triple helix"[7-8]. About 90% of bone matrix is composed of type I collagen that undergoes posttranslational modifications specific to this tissue. These modifications (hydroxylation and glycosylation) partly explain why mineralization only occurs in bone and not in other tissues[9].

The collagen fibril is the basic unit of bone matrix. This fibril results from the junction of 300nm long and 1.5nm thick collagen monomers which are produced by osteoblasts[10]. Each type I collagen molecule is composed of a repeating tripeptide sequence (Gly-X-Y) that form a left-handed helix containing two pro-α1 and one pro-α2 chains[11]. The three chains assemble in a right-handed triple helix, where the Gly residues are in the center and the lateral chains of X and Y are on the surface of the helix[8]. In the most common occurring triplets (10.5%)[12], X is a proline and Y is a hydroxyproline (Gly-Pro-Hyp), which is a unique characteristic of collagen and it is essential to stabilize the triple helix. These fibrils have high tensile strength and play a pivotal role in providing structural support for body structures, such as the skeleton, skin, blood vessels, intestine and fibrous capsules of organs[13]. In humans the α1 chain is coded by a gene located on chromosome 17 (17q21.3-q22), while the α2 chain is located on chromosome 7 (7q21.3-q22). Each messenger RNA (mRNA) is monocistronic[14] and several growth factors and hormones regulate with collagen synthesis at the transcriptional level. The Sp1 transcription factor (SP1)[15] and runt-related transcription factor (RUNX) 2[16], among others, bind to the promoter regions controlling collagen type I gene transcription. Several other factors contribute to the expression of this protein, either by modulating its mRNA levels or by stabilizing it. Transforming growth factor (TGF)β[17-18], insulin-like growth factor (IGF)-I[18-19] and interleukin (IL)-6[20] have been found to stimulate collagen mRNA synthesis while tumor necrosis factor (TNF)[21], interferon (IFN)γ[22], IL-1[23], parathyroid hormone (PTH)[24] and the active form of vitamin D_3[25] suppress it.

After transcription, the pre-mRNA undergoes maturation by exon splicing, capping, and addition of a poly(A) tail. These mRNAs are translated and the resulting proteins undergo extensive post-translational modifications before being assembled in a triple helix and released to the extracellular space. Both the pro-α1 and the pro-α2 chains undergo hydroxylation of proline to hydroxyproline, and glycosylation, which are the two critical modifications to obtain a stable triple helix. The triple helix formation is then started at the carboxy-terminal end of the molecule and extends towards the amino-terminal end[7]. Procollagen is thereafter secreted to the extracellular space where specific enzymes [a disintegrin-like and metalloproteinase (reprolysin type) with thrombospondin type 1, motif 2 (ADAMTS2) and bone morphogenetic protein (BMP)-1] cleave the propeptides, giving rise to mature collagen molecules which triggers spontaneous self-assembly of the collagen molecules into fibrils. The processed collagen monomers within fibrils are joined by covalent cross-links which mature with aging[26-27]. Cleavage of the propeptides reduces the solubility of the molecules and therefore a major extracellular function of carboxy propeptides is to prevent premature fibril formation, while the amino propeptides influence fibril shape and diameter[27].

The final assembly of fibrillar collagen involves the interaction with several proteins that have a role in the organization of the matrix pattern and control the diameter of the fibrils[28-29]. Of interest, biglycan and decorin, two proteoglycans highly expressed in extracellular bone matrix, interact with collagen molecules to facilitate fibril formation, which will later allow mineral deposition[30].

In clinical practice, products of the collagen processing or breakdown, either for the formation or degradation, act as markers of collagen turnover and are used to assess bone remodeling[31]. Collagen type I propeptides, amino-terminal (P1NP) and carboxy-terminal (P1CP) result from posttranslational cleavage of the pro-collagen molecule before its organization in fibrils[32]. The propeptides P1NP and P1CP are two small domains present in the procollagen molecule, which after secretion of the molecule into the extracellular space are enzimatically cleaved. Since both propeptides are stochiometrically produced from each new collagen molecule, P1NP and P1CP are considered quantitative measures of collagen formation. Moreover, P1NP serum levels correlate with bone formation indices assessed by histomorphometry[33]. The strength of the collagen fibers depends on the formation of covalent cross-links between the telopeptides and the adjacent helical domains of collagen molecules. The cross-linked telopeptides of type I collagen, amino (NTX) and carboxy-terminal (CTX), are products of the collagen cleavage. Both NTX and CTX are products of cathepsin K (CTSK) action and represent collagen breakdown. CTX contains epitopes prone to spontaneous isomerization: α-CTX is the native sequence, while β-CTX represents collagen maturation through translocation of an aspartic acid residue from position α to β. Therefore, the ratio α/β-CTX is an indicator of bone age, the lower the ratio, the older the bone[34]. As CTX, pyridinoline cross-linked carboxy-terminal telopeptide of type I collagen (ICTP) is also a product of collagen breakdown. ICTP epitope neighbors CTX but it is released as a result of MMP activity[35] and it measures a relatively large hydrophobic phenyl-alanine rich pyridinolines cross-link of the two α1 chains in the carboxy-terminal of matured collagen type I. However, since the helical part of the α-chain is strongly conserved among different types of collagen, the specificity of this marker in reflecting bone resorption is not the best[33].

NON-COLLAGENOUS PROTEINS

Although bone matrix is composed mostly of collagen, other non-collagenous bone proteins have been described since 1974[36]. Non-collagenous proteins, including osteopontin (OPN), bone sialoprotein

(BSP), osteonectin, osteocalcin (OCL), and proteoglycans may have a regulatory function controlling the size and orientation of deposited minerals. Through sequestration of calcium or enzymatic release of phosphate from these proteins, they may act as a reservoir for hydroxyapatite crystals formation[37]. Collagen acts as a scaffold for mineralization and these non-collagenous proteins are the nucleators of hydroxyapatite crystals[13].

Biglycan and decorin are two proteoglycans that are found in several tissues. In bone they contain chondroitin sulfate chains and bind to collagen fibers[38]. Biglycan is upregulated in osteoblasts and its expression is maintained in osteocytes. On the other hand, decorin is expressed during the preosteblast stage, maintained in fully mature osteoblasts and is downregulated when the cells differentiate towards the osteocyte phenotype[13]. As osteocytes probably act as bone mechanoreceptors[39], biglycan may act as transducer of shear forces within canaliculi. Biglycan-deficient mice are normal at birth but evidence reduced growth and bone mass, together with deterioration of bone biomechanical behavior by the third month of life[40]. Proving a relevant role of biglycan/decorin in bone biology, a double-knockout mouse for these proteins has severe osteopenia with alterations in the geometry of the bone collagen fibrils[41].

Osteonectin is a glycoprotein secreted by the osteoblast that binds collagen, calcium and hydroxyapatite. It is hypothesized that this molecule plays a role in the nucleation of hydroxyapatite crystals[42]. It regulates cell proliferation and stimulates angiogenesis and metalloproteinase production[43]. Osteonectin-deficient mice show decreased bone remodeling leading to severe osteopenia in older animals. Moreover, the bone of these mice is characterized by decreased trabecular connectivity and decreased mineral content but with increased hydroxyapatite crystal size[44-45].

Osteopontin is a member of the family of small integrin-binding ligands with N-linked glycosylation (SIBLING). This protein is expressed in several tissues, including bone, kidney and the immune and vascular systems. In bone it promotes osteoclast binding to the extracellular matrix and activates intracellular signaling pathways[43, 46]. Osteopontin is produced at the late stage of osteoblast maturation during matrix formation and mineralization[47]. Osteopontin-deficient mice develop normally but are resistant to ovariectomy-induced bone resorption. Moreover, these mice have increased mineral content although the crystals are smaller than in wild-type mice[48].

BSP, like osteopontin, contains both mineral and integrin-binding sites. It is expressed by hypertrophic chondrocytes, osteoclasts and mature osteoblasts[49]. In osteoblasts, induction of BSP expression coincides with the initiation of mineral deposition and this protein is upregulated by factors that induce osteoblast differentiation[50]. BSP is located at the mineralization front and, based on its affinity for collagen, it is believed to be a nucleator for crystals[51].

Osteocalcin is exclusively expressed in bone and dentin. It is a calcium-binding protein characterized by three gamma-carboxyglutamic acid residues. Due to its interaction with hydroxyapatite it is believed that OCL regulates the growth and maturation of bone crystals[43]. In fact, OCL measurements in serum have proven to be a valuable marker for bone turnover in metabolic bone diseases[31].

HYDROXYAPATITE CRYSTALS

In 1964, Hodge and Petruska[52] proposed the now widely accepted model for the mineralization of collagen in bone structure. In this model, collagen fibrils are coated with mineral crystals, arranged parallel to each other and to the axis of collagen fibrils. Crystal formation is triggered either by deposition of collagen or non-collagenous proteins that act as nucleation centers. After nucleation, crystals are elongated and, later on, grow in thickness. This very orderly process is crucial for bone nano-organization and resistance; disturbances in collagen conformation lead to bone fragility, such as osteogenesis imperfecta, where a mutation in the collagen gene occurs[53].

Bone crystals are composed of carbonate apatite mineral, called dahllite, which has hexagonal crystallographic structure, although crystals do not express this symmetry in their macroscopic shape. Instead, they assume the form of plates or tablets[54]. The plate-like crystals arise in the discrete spaces within the collagen fibrils, thereby limiting crystal growth and forcing it to be discrete and discontinuous. Crystals grow in such a way that their axis is roughly parallel to the long axis of the collagen fibrils[55-57].

The endpoint for matrix mineralization is the deposition of crystals between collagen fibers, a process that comprises two phases, an initial formation of apatite crystals within matrix vesicles and a subsequent propagation phase within the matrix. In the first phase of crystal formation, the ions that will later constitute the crystals form a cluster with the correct orientation, giving rise to a stable structure. This nucleation is facilitated by an increase in the local concentration of ions which increases the probability of association[58]. The initial phase of mineralization occurs inside matrix vesicles. These are released by budding from the surface of osteoblasts but have a special membrane composition[59] being enriched in alkaline phosphatase, nucleotide pyrophosphatase, phosphodiesterase, annexins and phosphatidyl serine[60-61]. It was proposed that the vesicle lipids could act as nucleation center for hydroxyapatite formation[62-63]. The minerals inside the vesicle precipitate initiating the formation of hydroxyapatite crystals that penetrate the membrane and give rise to calcification nodules in the extracellular fluid during the propagation phase of matrix mineralization[64-65]. The mineral crystals subsequently proliferate within and between the collagen fibrils[66].

Both collagen and non-collagenous proteins regulate the expansion of crystals, while cells can affect their maturation status[58].

BONE IMAGING

During the last 10 years high-resolution imaging techniques have been introduced for assessing bone quality parameters, primarily for research proposes. The new imaging studies provide information on bone morphometry, microarchitecture and on the relationship between bone microarchitecture and strength. Moreover these new imaging tests have proved to be useful for assessing the effect of new treatments.

Through radiography, the most common method to visualize bone, cortical and trabecular compartments are observed in a two-dimension (2D) format with a spatial resolution up to 40μm. Although this is a 2D image method, texture analysis parameters can be applied and have shown good correlation with three-dimension (3D) bone microarchitecture[67], biomechanical properties[68] and with several histological characteristics[69]. During the last 20 years, dual-emission X-ray absorptiometry (DXA) has been the most widely used method for measuring bone mineral density (BMD). Recent advances in DXA include software that calculates several other structural parameters that are important to determine bone fragility, such as hip-axis length, femoral neck cross-sectional area, moment of inertia and femoral neck shaft angle. The conventional method for evaluating bone microarchitecture is histomorphometry and stereology. In 1987, Parfitt developed and published[70] standardized nomenclature for histomorphometry parameters, reflecting trabecular size and spacing, as well as porosity. Through this technique bone is evaluated at a resolution of 1μm, although a biopsy is needed and three dimensional analysis is only achieved by serial sections of the tissue[71].

Computed tomography (CT)-based techniques have several advantages over the other bone imaging techniques. In contrast to DXA, volumetric quantitative CT (vQCT) offers 3D information of cortical and trabecular bone that can be separately analyzed. Currently, the imaging of specimens, bone biopsies and small animals for bone structure investigation is almost exclusively done with microCT. X-ray computed CT is an imaging technique that uses ionizing radiation and a method employing tomography created by computer processing. Digital geometry processing is used to generate a three-dimensional image of bone from a large series of two-dimensional X-ray images taken around a single axis of rotation[72].

Bone vQCT measurements are reported as true volumetric density. This technique can be used *in vivo* and trabecular and cortical bone can be evaluated separately. Moreover, vQCT is more sensitive than DXA in the detection of density differences[73-74] and can, thus, analyze both densitometry and geometrical components either of the entire bone or its cortical and trabecular compartments separately[74]. This technique also allows understanding how proximal femoral structural parameters explain bone strength, independently of BMD[75]. Recently, peripheral vQCT has been used for the evaluation of microarchitecture of the radial bone[76].

Until recently, bone histomorphometry was the standard for assessing trabecular and cortical architecture. Although this analysis provide unique information on cellularity and dynamic indices of bone remodeling, it has limitations with respect to assessment of bone microarchitecture, because structural parameters are derived from stereologic analysis of consecutive 2D sections, usually assuming that the underlying structure is plate-like[70, 77]. MicroCT, with a spatial resolution of 1 to 100μm, promises to replace histomorphometric analysis and allows the possibility of repeated *in vivo* investigation in small animals and human beings[72]. The accuracy of microCT morphology measurements has been compared with traditional measures from 2D histomorphometry both in animal[78] and in human[79-80] specimens. These studies showed that 2D and 3D measurements by microCT generally highly correlate with those from 2D histomorphometry. Therefore, microCT offers numerous advantages in the assessment of bone morphology *ex vivo*: it allows direct 3D measurement of trabecular morphology, such as trabecular thickness and separation; compared with 2D histology, a larger volume of interest can be evaluated; measurements can be performed with a much faster throughput and assessment of bone morphology by microCT scanning is non-destructive, thus, samples can be used subsequently for other assays[77].

Magnetic resonance imaging (MRI) reaches 150μm resolution and has several advantages other than assessing bone quality, namely the lack of ionizing radiation and the ability to investigate beyond bone structure, such as marrow fat content, diffusion and perfusion[81]. However, MRI acquisition is slower and technically more demanding than microCT. In addition, it is also much more expensive.

The scanning electron microscope (SEM) uses a focused beam of high-energy electrons to generate a variety of signals at the surface of solid specimens. The signals that derive from electron-sample interactions reveal morphology (texture) of the sample, chemical composition and crystalline structure. Areas ranging from approximately 1cm to 5μm in width can be imaged in a scanning mode using conventional SEM techniques (magnification ranging from 20X to approximately 30.000X, spatial resolution reaching 50 to 100 nm). Due to the very narrow electron beam, SEM micrographs have a large depth of field yielding a characteristic 3D appearance useful for understanding the surface structure of a sample. SEM analysis is considered to be "non-destructive"; that is, X-rays generated by electron interactions do not lead to volume loss of the sample, so it is possible to analyze the same samples repeatedly[82]. This technique enables the observation of the tissue topography in high-resolution images and has proven effective in the investigation of the activity of bone surfaces[83-84]. SEM is effective for the analysis of hierarchical composite structure and surface topography induced by microdamage accumulation and fracture due to its high resolution and large depth of field[85]. SEM has been used extensively to study the damage accumulation and fracture behavior of bone[86].

Multicolor non-linear microscopy of type I collagen arrangement can be obtained using second-harmonic generation (SHG) and two-photon excitation (TPE). SHG arises when the electric field of the exciting light is strong enough to deform a molecule. When this molecule is not symmetrical, such as the collagen superhelix, the resulting anisotropy creates an oscillating field with twice the energy, twice the frequency and half the wavelength, the so-called second harmonic. SHG microscopy is a powerful tool that has been developed to assess collagen with a high spatial resolution[87-88] and has already been applied to eye[89], teeth[90], tendons[91-92], cartilage[93], synovial membrane[94], wound repair[95], lung fibrosis[96] and metastatic growth[97-98]. In fact, spectral differences in the second-harmonic signal from normal and cancerous tissue have been described, opening up a possibility that might become a useful diagnostic tool in oncology[99-102]. A correlation between SHG intensity, fibrilar morphology, polarization anisotropy and signal orientation with impaired mechanical strength has been reported in osteogenesis imperfecta, a bone disease resulting from mutations in the collagen gene[103]. SHG microscopy offers also the possibility of providing submicrometer 3D spatial resolution images without the need for tissue processing or stain[104]. The signal is acquired by two opposing detectors, the backward-SHG channel detects the backscattered SHG signal and the forward-SHG channel receives the photons that are transmitted through the sample[105]. The development of quantitative SHG microscopy for clinical applications and studies will require the use of the backward SHG signal; therefore, is of major importance to understand this information. The forward/backward ratio has been used to access the thickness of fibril shells and the ionic strength of the surrounding medium[106]. In tendon, sclera and ear cartilage the preferred orientation of the collagen fibers was analyzed in both channels[92]. Moreover, multiphoton microscopy has become a powerful method for non-invasive high-resolution *in vitro*, *in situ* and *in vivo* imaging of extracellular matrix structures and cells in living intact native and tissue-engineered tissues[107]. Microendoscope prototypes have already been developed and applied to small animal research[108] and in dermatology as a method for noninvasive skin cancer detection[105, 109]. A study in collagen fibrils from tendon samples suggested that the forward-SHG channel reflects essentially the mature polymerized collagen and the backward-SHG channel represents the immature collagen fibril segments, indicating ongoing fibrilogenesis[106].

BIOMECHANICS OF BONE

In 1869 Julius Wolff, a German anatomist and surgeon, stated that bone adapts in response to the mechanical loads applied on it. More than one hundred years later we still believe that bone, as a natural material, has evolved and adapted to fill the needs posed by the function it exerts. Many of these needs are mechanical, such as the need to support static and dynamic loads created by the weight of the organism and the need to be resistant to fracture[110].

The bone mechanical properties describe the relationship between applied forces, or loads and bone deformation. The resistance of bone in response to these forces is known as stress and represents the intensity of the local force. The resultant deformation is referred to as strain and is defined as a relative change in size or shape. Normal strains represent elongation or shortening while shear strains represent distortion. Therefore, a load-deformation curve or a stress-strain curve are often used to define the biomechanical properties of bone[13].

The load-deformation curve (figure 1) reflects the structural behavior of bone and describes the amount of load needed to produce a unit of deformation. The analogous stress-strain curve reflects the material behavior of bone tissue and this curve is generated through a mechanically standardized (size and shape) test. Load and deformation have a linear relationship until the yield point is reached; at this time the slope of the curve is reduced. Before the yield point the material obey the Hooke’s law which states that there is a proportional relationship between stress and strain. This linear relationship is translated by the Young’s modulus, or bone stiffness, that measures the resistance of the bone to deformation[5, 111]. The yield point is the cross point of transition from an elastic behavior to a plastic one and corresponds to the occurrence of the first microfractures in bone tissue. If the bone is unloaded in the elastic region it returns to its original shape with no remaining deformation, while in the plastic region the load leads to permanent plastic deformations. If the bone continues to be loaded the ultimate or failure load is reached, after which the structure fails catastrophically (the bone fractures). Therefore, the slope of the elastic region defines bone stiffness while the strain energy, or toughness, is the energy required to initiate failure of the structure and is computed as the area under the curve[13, 111]. Through the analysis of the stress-strain curve several material characteristics can be established. A material is brittle when it only exhibits elastic deformation such as is the case with polymethylmethacrylate. On the other hand, a ductile material undergoes a large amount of plastic deformation before failure, like metals. In viscoelastic materials the stress-strain behavior is dependent on the time and rate of loading; these materials exhibit both fluid and solid-like properties with gradual deformation and recovery when subjected to loading and unloading. The response of viscoelastic materials is dependent on how quickly the load is applied or removed and the extent of deformation is dependent on the rate at which the deformation-causing loads are applied. On the other hand, a constantly maintained deformation will cause stress relaxation, that is, the force required to maintain the deformation diminishes with time. The stress-strain relationship for viscoelastic materials is a function of time rate at which the stress and strain are applied in the material. Biologic tissues such as articular cartilage, intervertebral disc, ligament, tendon and fresh bone all show a viscoelastic behavior[5, 112].

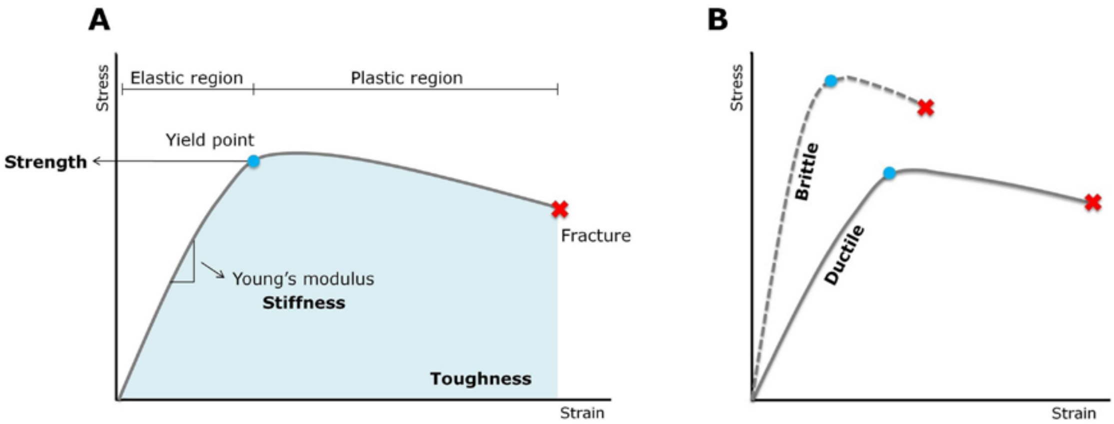

Figure 1 – *Graphical representation of the structural behavior of a material*. The relation between stress and strain, represented by the stress-strain curve (**A**), is reflected by the Young's modulus, or stiffness, that measures the bone resistance to deformation while the toughness is the energy required to induce failure of the structure and is computed as the area under the curve. The yield point is the cross point of transition from an elastic behavior to a plastic one and corresponds to the occurrence of the first microfractures. After this point, if the structure continues to be loaded the ultimate load or failure load is reached, after which a fracture will occur. This same curve also allows us to distinguish between ductile and brittle materials (**B**). The ductility of a material is a measure of the extent of which a material will deform before fracture. On the opposite, when a brittle material reaches the limit of its strength, fracture occurs. Therefore, while a ductile material undergoes large amounts of plastic deformation before fracture, a brittle material curve only exhibits elastic region.

Bone is a composite of hydroxyapatite crystals dispersed in a collagen matrix. Collagen is tough but not very stiff; on the other hand minerals are stiff but not very tough. Therefore, the mineral phase dominates the stiffness of bone and the toughness of the material arises from its hierarchical structure[110]. The toughness of the material increases with decreasing mineral content and increasing collagen content[113]. Bone stiffness is intermediate between that of hydroxyapatite and collagen, while its strength is higher than that of either components[111]. Therefore, bone combines the best properties of mineral and protein content, it is stiff to prevent bending and buckling, but it is also tough in order to avoid fracture when the load exceeds the normal range[2, 110].

The two types of bone, cortical and trabecular, also show different biomechanical performance. Cortical bone is stiffer than trabecular bone, resisting to higher stress but lower strain before failure. Due to its porous structure trabecular bone has a large capacity for energy storage[112]. Both cortical and trabecular bone mechanical properties are dependent on bone density[114]. In fact, studies have shown that density explains 60% to 90% of the variation in bone strength and stiffness[115] and that small changes in bone density lead to remarkable changes in mechanical behavior[116]. However, the correlation between bone mineral density assessed by DXA and bone strength is relatively low[117]. Cortical and trabecular bone are anisotropic materials since their mechanical properties depend on the loading direction. This characteristic reflects bone function and we can find higher strength and stiffness in the primary loading direction[2], although the degree of anisotropy varies with anatomical site and functional loading[118]. Bone, as a natural material, shows large variability in its mechanical behavior[113], in fact, mechanical properties of trabecular and cortical bone types vary from one bone to another and even within different regions of the same bone[119-120].

In vivo, bone is subjected to several different loading modes producing tension, compression, shear, bending, torsion and combined loading. During tensile loading the forces are directed away from the surface of the structure, leading to lengthening and narrowing. Fractures produced by tensile loading are typically seen in bones with a large proportion of trabecular bone. In compressive loading, equal and opposite loads are applied towards the surface of the structure, leading to shortening and widening. Clinically, fractures produced by compressive forces are found in the vertebrae, especially in the elderly with osteoporotic bone tissue. During shear, loading forces are applied parallel to the structure and shear stress and strain develop inside the structure. Therefore, the shear load deforms in an angular manner. Fractures that result from this loading are often seen in trabecular bone. In bending, a combination of tensile and compressive loads is applied in such a way that causes the structure to bend. Bending tests can be produced by three (three-point bending) or four (four-point bending) forces. Fractures produced by both types of bending are particularly common in long bones. Torsion loads are applied to a structure causing it to twist along an axis. Although each loading mode can be studied separately, bones *in vivo* are not only submitted to multiple different loads but also present irregular structure geometry[112, 121]. *In vivo* measurements of strain of a human adult tibia during walking demonstrated the complexity of the loading patterns during this common physiological activity. Stress values calculated from these strain measurements showed that during normal walking the stresses were compressive during heel strike, tensile during the stance phase and again compressive during push off. Moreover, the contraction of the muscles attached to the bone alters the stress distribution. During locomotion, bending moments are applied to the femoral neck and tensile stress is produced on the superior cortex. Contraction of the gluteus medius muscle produces compressive stress that neutralizes this tensile stress[112, 122-124].

A progressive loss of bone density occurs as part of the normal aging process. The reduction of bone mass, which occurs earlier and more extensively in trabecular than in cortical areas[74], is associated with impaired microarchitecture, increased fragility and risk of fracture. In osteoporotic bone, trabecular strength is reduced by loss of bone mass. Two different mechanisms were proposed to explain this phenomenon, a uniform thinning of all trabeculae and the complete removal of individual struts. Studies demonstrated that the random removal of struts is more harmful to bone strength than thinning of the trabeculae[2, 125]. Bone fragility is more prevalent among women than in men mainly because of estrogen deficiency after menopause. Although perforation and loss of connectivity between trabecula also occurs in men, trabecula thinning is primarily observed indicating that a reduction in bone formation predominates over an increase in bone resorption. Active remodeling also affects cortical bone. Cortical thinning and porosity reduce the resistance of bone to microcracks and, as a consequence, cortical bone can no longer absorb the energy imposed by a fall[3, 74].

Energy dissipation is achieved by the formation of plastic zones around the cracks, thereby protecting the integrity of the entire structure. At a nanoscale, deformation of individual collagen molecules involves hydrogen bonds which break allowing stretching and relaxation of the fibrils. At a higher scale we can find sliding and breaking of the bonds between tropocollagen molecules, which are critical in controlling deformation of bone. In fact, in older bones the collagen cross-links are increased, thereby reducing its ability to dissipate energy without failure. Continuous slide between the mineral particles and the tropocollagen molecules dissipates large amounts of energy and increases the resistance to fracture[126]. The mineralized fibrils are hold together by phosphorilated proteins, such as OPN and BSP. During deformation, the non-collagenous proteins resist separation of the fibrils. This suggests that collagen denaturation induced by mechanical loading is a possible mechanism for energy dissipation process. Since more energy dissipation capacity gives more toughness to bone, enhancing the properties of collagen may make the bone tough[127].

BONE BIOLOGY

Bone has three distinct cell types: the osteoclasts, or bone-resorbing cells; the osteoblasts, or bone-forming cells; and the osteocytes, which are osteoblasts entrapped within lacunae. Bone resorption and formation not only should be quantitatively balanced but must also be coupled in time and space. This tight coupling is essential for the repair of microscopic damages that result from constant impact[128].

In 1965, Frost described that groups of osteoclasts and osteoblasts constitute the bone multicellular unit (BMU)[129] which is a mediator mechanism linking individual cell activity to whole bone morphology[130]. Nowadays, this concept has evolved to include osteocytes[131]. Inside the BMU, cells move together with osteoclasts always in the front of the advancing BMU and osteoblasts in the back. At any given time, several millions of BMUs carry out turnover at multiple skeletal sites in a activation-reversal-formation cycle that in a healthy adult human lasts 6-9 months[132]. In order to balance bone formation and resorption in healthy individuals these two processes are coupled. That is to say that osteoblasts and its regulators determine osteoclastogenesis, while osteoclastogenesis and the products of the degraded matrix regulate osteoblastogenesis. In addition, both processes may be regulated by osteocytes and their products[133-135]. Resorption is much faster than formation: an area of bone can be resorbed in 2-3 weeks but it takes at least three months to rebuild it[13]. Bone resorption is probably the first event that occurs in response to a mechanical stress signal[134]. In fact, resorption and formation are tightly coupled, so that after resorption a formation phase occurs and, in normal bone, the amount of tissue resorbed will be rebuilt in the succeeding formation phase[135].

OSTEOCLAST

The osteoclast is the unique bone-resorptive cell and is highly specialized towards this process. For its specific work, the osteoclast matures as a giant polykaryon through cell-cell fusion from its precursors[136]. The mammalian osteoclast contains up to eight nuclei with an *in vitro* diameter of 300μm, thus covering large areas to operate efficiently[137]. Net bone resorption is a reflection of both the number of osteoclasts and the degrading capacity of each individual cell[138]. Osteoclastogenesis is a complex process that includes many stages, such as commitment, differentiation, multinucleation and activation of immature osteoclasts[139].

The earliest identifiable hematopoietic precursor able to form osteoclasts is the granulocyte-macrophage colony forming unit (GM-CFU)[140]. At this stage, the main transcription factors involved are spleen focus forming virus proviral integration oncogene spi1 (PU.1), microphthalmia-associated transcription factor (MITF) and FBJ murine osteosarcoma viral oncogene homolog (FOS). PU.1 is responsible for the earliest events in osteoclastogenesis; PU.1 null mice lack not only osteoclasts but also macrophages, although they preserve the ability to form monocytes[141]. Moreover, the transcription of colony stimulating factor 1 receptor (C-FMS) gene, which encodes the receptor of colony stimulating factor 1 (macrophage) (M-CSF), is dependent on PU.1 and M-CSF and also plays a role in the earliest events of osteoclastogenesis by stimulating the proliferation and preventing apoptosis of early osteoclast precursors[139]. MITF has also been implicated in differentiation and survival of several cell types, including osteoclasts. Moreover, this transcription factor is expressed in macrophages, osteoclasts and in the mononuclear precursor of these cell types[142]. By interaction with PU.1, MITF regulates target genes such as the ones that encode CTSK, acid phosphatase 5, tartrate resistant (TRAP) and osteoclast associated, immunoglobulin-like receptor (OSCAR), during osteoclast differentiation[143]. The protein FOS is a member of the transcription factor complex activator protein-1 (AP-1) and plays a role in early osteoclast differentiation as shown in animal model studies, where mice deficient in FOS develop osteopetrosis due to an osteoclast differentiation defect[144]. Moreover, FOS is a mediator of the lineage commitment between osteoclasts and dendritic cells (DC). The differentiation into an osteoclast or DC lineage is reciprocally inhibited by colony stimulating factor 2 (granulocyte-macrophage) (GM-CSF) and M-CSF, respectively[145].

In 1988 it was established that the osteoclast precursor belongs to the monocyte/macrophage lineage[146], as part of the cluster of differentiation (CD)14^{+}CD16^{-} monocyte subpopulation[147]. Moreover, it was demonstrated that osteoclasts could not be generated from bone marrow macrophages unless they were in contact with osteoblast-lineage cells[148]. But it was only ten years later that receptor activator of nuclear factor kappa B (RANK) ligand (RANKL), a member of the

TNF superfamily, was found to be expressed on the surface of osteoblast-lineage cells and to be responsible for osteoclast differentiation[149-150] through interaction with its receptor RANK at the surface of osteoclast precursors[151]. In a study using primary cultures of rat osteoclasts the authors settled that osteoprotegerin (OPG), a protein produced by osteoblasts, blocks RANKL and this effect was not only found on osteoclast precursors but also on mature osteoclasts[152]. Expression of RANKL and OPG regulates bone resorption by controlling the activation state of RANK on osteoclasts. The unique osteoclastogenic property of RANK is related to its ability to bind TNF receptor-associated factor (TRAF) 6, which stimulates mitogen-activated protein kinase (MAPK), phosphoinositide-3-kinase (PI3K) and nuclear factor kappa B (NFκB) pathways, as well as calcineurin[153]. Therefore, activation of RANK by its ligand leads to the expression of specific genes during differentiation, activation, participation in bone degradation and survival. At least five different intracellular cascades are induced during osteoclastogenesis and activation – inhibitor of NF-κB kinase (IKK), c-Jun N-teminal kinase (JNK), mitogen-activated protein kinase 14 (p38), extracellular signal-regulated kinase (ERK) and V-src sarcoma (Schmidt-Ruppin A-2) viral oncogene homolog (SRC) pathways[154]. As members of the TNF receptor family lack intrinsic enzymatic activity, the key preliminary step of this signalling cascade is the binding of TRAFs to specific cytoplasmic domains of RANK[155-156]. There are multiple TRAFs that can bind to RANK[157], however only TRAF6-deficient mice develop osteopetrosis due to impaired osteoclast function[158]. Therefore, TRAF6 acts as a key adaptor molecule of the signalling proteins that drive osteoclast-specific gene expression leading to cell differentiation and activation[159]. TRAF6 is not specific of RANK signalling but recent studies suggest that the quantitative difference in TRAF6-activation is probably the key mechanism that distinguishes RANK from other receptors regarding the osteoclastogenic potential[160]. NF-κB is one of the earliest signals following RANKL stimulation and it is required for precursor survival during commitment to the osteoclast lineage, as well as for full differentiation[161]. The importance of the NF-κB pathway for osteoclast formation was demonstrated in mice deficient in p50 and p52 (two NF-κB subunits), that are osteopetrotic, due to defective osteoclast differentiation[162].

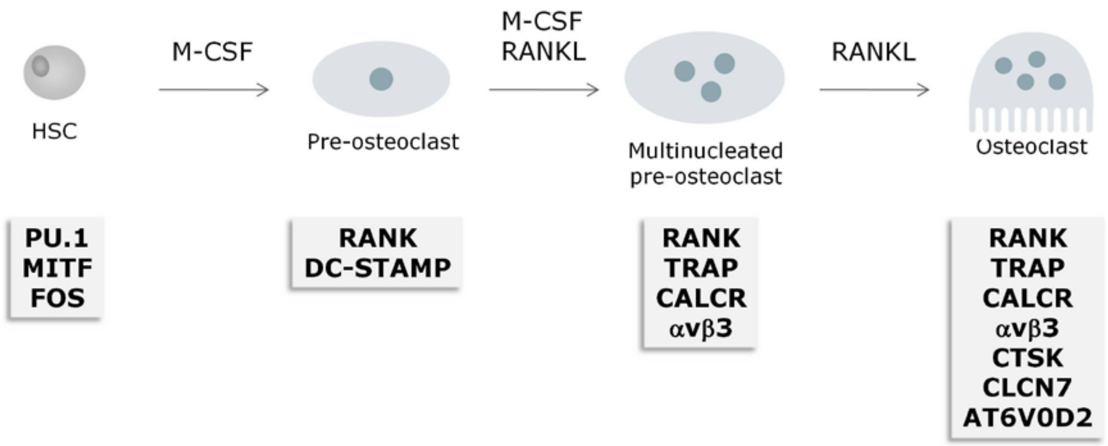

Figure 2 – *Osteoclast lineage*.

Osteoclasts derive from hematopoietic precursors and proliferation of mononuclear cells requires M-CSF. When these cells arrive at the resorption site they fuse together in the presence of RANKL and M-CSF. These multinucleated precursors express osteoclast-specific genes and after polarization acquire the capacity to resorb bone.

(αvβ3 - αvβ3 integrin; ATP6V0D2 - ATPase, H+ transporting, lysosomal 38kDa, V0 subunit d2; CALCR – calcitonin receptor; CLCN7 – chloride channel 7; CTSK – cathepsin K; DC-STAMP - dendritic cell-specific transmembrane protein; FOS - FBJ murine osteosarcoma viral oncogene homolog; HSC – hematopoietic stem cell; M-CSF – colony stimulating factor 1 (macrophage); MITF - microphthalmia-associated transcription factor; PU.1 – spleen focus forming virus proviral integration oncogene spi1; RANK - receptor activator of nuclear factor kappa B; RANKL – RANK ligand; TRAP - acid phosphatase 5, tartrate resistant)

In addition to RANKL, M-CSF is another essential cytokine to generate osteoclasts, as it promotes precursors proliferation and survival. This cytokine is produced by several cells, but cells from the osteoblast lineage are the major source during osteoclastogenesis[163]. Mice deficient in M-CSF (*op/op* mouse) are characterized by osteoclast-deficient osteopetrosis[164]. Together, M-CSF and RANKL are required to induce expression of osteoclast lineage-specific genes (figure 2), including those encoding TRAP, CTSK, calcitonin receptor (CALCR) and $\alpha v\beta_3$ integrin, leading to the development of mature osteoclasts[165].

Osteoclast precursors differentiate into TRAP$^+$ mononuclear cells after RANKL stimulation. These cells fuse with each other and differentiate into multinucleated osteoclasts[166]. Cell fusion is one of the most distinctive characteristic properties of osteoclasts. An osteoclast precursor cell in contact with a RANKL presenting cell will receive the RANKL signal to initiate a cascade of gene expression that includes the production of the chemokines monocyte chemotactic protein-1 (MCP-1) and regulated upon activation normal T cell expressed and secreted (RANTES) which are chemotactic signals for monocytes[167]. Osteoclast cell fusion occurs within RANK$^+$ mononuclear precursors in 2D directions and the major effect of multinucleation is the increase in cell size, creating multinucleated giant osteoclasts that resorb larger areas of bone tissue[136]. RANKL, via nuclear factor of activated T-cells, cytoplasmic, calcineurin-dependent 1 (NFATc1), induces the expression of two proteins dendritic cell-specific transmembrane protein (DC-STAMP) and ATPase, H$^+$ transporting, lysosomal 38kDa, V0 subunit d2 (ATP6V0D2) required for osteoclast multinucleation[168-169]. In DC-STAMP-deficient mice, osteoclast cell fusion is impaired despite normal expression of osteoclasts markers[170] and in another study this molecule was up-regulated following stimulation with RANKL[171-172]. The osteoclastic ability of DC-STAMP$^{-/-}$ mononuclear cells is impaired but not completely blocked; therefore, DC-STAMP is important for cell fusion but not essential for bone resorption activity. Moreover, inactivation of ATP6V0D2, an isoform of the osteoclast H$^+$ ATPase transporter, lead to resorptive dysfunction in mice by lack of efficient pre-osteoclast fusion[173]. The DC-STAMP-expressing osteoclast becomes the master-fusing cell and fuses with a DC-

STAMP-negative follower cell. Once fusion of the two cells is completed, a binucleated cell is formed and this cell becomes the master fuser and can fuse with other mono or multinucleated cells[174]. Overall, cell-cell fusion is a tightly regulated process involving several steps. Cells have to acquire the capacity to fuse and then, fusion-competent cells have to move towards each other, attach and bring their membranes in close contact. Finally, the cell membranes must be merged and the resultant multinucleated cell has to reorganize cellular components in order to become functional[175].

The mature osteoclast is rich in mitochondria to produce energy for the resorption process and is a polarized cell with the nuclei localized towards the resorptive surface. The osteoclast also contains a unique and complex ruffled membrane, which is the resorptive organelle. Although the origin of this specialized membrane was enigmatic for some time, it is now considered to be the most specific marker of the osteoclast since it appears only when the cell is resorbing bone[138]. Recent findings point to a lysossomal origin of this organelle. In fact, synaptotagmin VII, a calcium sensor protein that regulated exocytosis, is associated with lysosomes in osteoclasts and the absence of this protein inhibits CTSK secretion and formation of the ruffled border but without interfering with cell differentiation[176]. The ruffled border is formed upon contact of the cell with the bone surface by transport of acidified cytoplasmic vesicles to this area. This organelle is surrounded by an actin-rich structure known as actin ring or sealing zone which creates an isolated microenvironment where organic and inorganic components of bone are degraded[163]. The primary component of the osteoclast cytoskeleton is F-actin and this cell has a distinct actin complex known as podosome which mediates its attachment to bone[177]. The osteoclast attaches to bone surface via $\alpha v\beta 3$ integrin binding to the Arg-Gly-Asp (RGD) residues, a component of matrix proteins such as OPN and BSP. Upregulation of

$\alpha v\beta 3$ expression is characteristic of monocytes as they become osteoclasts and it is an important molecule in cell motility, adhesion to bone matrix and polarization. Osteoclasts of $\beta 3^{-/-}$ mice are not able to form actin rings and have attenuated ruffled membranes leading to diminished resorptive activity and increased bone mass[178]. In the osteoclast, $\alpha v\beta 3$ is maintained in a basal low-affinity state by interactions between the α and β subunits; during bone resorption the activated conformation is prevalent in the ruffled membrane whereas the basal form is present in the sealing zone. This conformation shift is modulated by M-CSF and integrin activation is necessary for the binding to RGD motifs present on bone matrix, leading to osteclast attachment to bone[179]. The cytoskeleton structure is controlled by interaction between $\alpha v\beta 3$ integrin and the M-CSF pathway. M-CSF binds to its receptor C-FMS and activates the integrin by targeting its cytoplasmic domain and changing the conformation of its extracellular ligand-binding region[180]. Consequently, osteoclasts stimulated with M-CSF undergo cytoskeletal reorganization, acquiring a motile phenotype mediated by the activation of Vav3/Rac pathway[181]. Bone resorption is a cyclic process in which the cell migrates to a resorptive site, degrades the underlying matrix, detaches and re-initiates the cycle. Optimal bone resorption depends upon these cycles and the $\alpha v\beta 3$ integrin is critical for all phases[182].

The osteoclast ability to resorb bone depends on the capacity of cytoskeletal organization to create an intimate microenvironment with bone surface. Observation of the pits formed by osteoclasts demonstrates that each cell typically produces a path that is longer than the cell width, indicating that migration is part of the resorption process. As the cell moves, it rearranges its cytoskeleton to form new sealing zones and dissolve old ones; in fact a single resorbing osteoclast can form several sealing zones[168]. Inside this specific microenvironment the key events that lead to bone degradation occur. The first study about the basic mechanism of bone degradation was performed in 1985 and established that the resorptive space is a highly acidified microenvironment[183]. The acidification process is initiated by a carbonic anhydrase[184] and the protons generated are transported to the resorptive lacunae via an ATP-dependent proton pump[185]. Concomitantly, intracellular pH is maintained by an energy-independent Cl^-/HCO_3^- exchanger on the cell anti-resorptive surface[186] and Cl^- ions are transported to the resorptive lacunae through chloride channel (CLCN) 7[187]. Therefore, acidification of the extracellular microenvironment represents production of hydrogen chloride (HCl) within this confined space. The low pH maintained in the resorptive lacunae is necessary and sufficient to dissolve the mineral phase of the matrix, which is followed by degradation of bone organic matrix[163]. The HCl dissolves the solid hydroxyapatite $[Ca_3(PO_4)_2]_3Ca(OH)_2$ to Ca^{2+}, HPO_4^- and H_2O[137]. Bone collagen degradation occurs through the action of a lysosomal enzyme, CTSK, which also polarizes to the ruffled membrane upon osteoclast attachment to bone[188].

Overall, the process of bone resorption can be divided into four steps. First, the mononuclear precursors fuse to form a polykaryon and target to the site of resorption. They will then attach to bone surface stimulating the reorganization of the actin cytoskeleton and forming the actin ring and the sealing zone. In the third step the ruffled border is created. Finally, the resorption lacunae will be acidified and proteases will be secreted into this space, resulting in mineral dissolution and organic matrix degradation. After resorption, the osteoclast will detach from the matrix, lose its polarization and either relocate to a new resorption site or undergo apoptosis[137].

Osteogenesis is a highly regulated process involving the differentiation of mesenchymal stem cells (MSC) into osteoblasts, which produce a characteristic extracellular collagenous matrix where hydroxyapatite crystals deposit. Osteoblasts can exhibit two opposite phenotypes. One is the osteogenic phenotype, which characterizes cells that secrete bone matrix at the bone resorption site, while the osteoclastogenic phenotype, supports osteoclast differentiation in old bone areas.

Osteoblasts are mononuclear, not terminally differentiated, specialized cells[189]. As they differentiate they acquire the ability to secrete bone matrix[190]. Osteoblasts resemble fibroblasts. In fact, the only morphological specific trait is located outside the cell in the form of a mineralized extracellular matrix. Moreover, all the genes expressed by fibroblasts are also expressed by osteoblasts. In fact, these cells have only two specific transcripts, one encoding RUNX2 and other encoding OCL[191].

Osteoblasts, chondrocytes, adipocytes, myoblasts, tendon cells and fibroblasts are all derived from MSC (figure 3). The lineages are determined by specific transcription factors[192]. RUNX2, osterix (OSX) and β-catenin are three factors necessary and sufficient to the differentiation of a MSC into an osteoblast[193]. RUNX2 directs mesenchymal progenitor cells to preosteoblasts, inhibiting their differentiation into adipocytes and chondrocytes, while OSX and β-catenin further direct the preosteoblasts to immature osteoblasts, completely eliminating the potential for differentiating into chondrocytes[192].

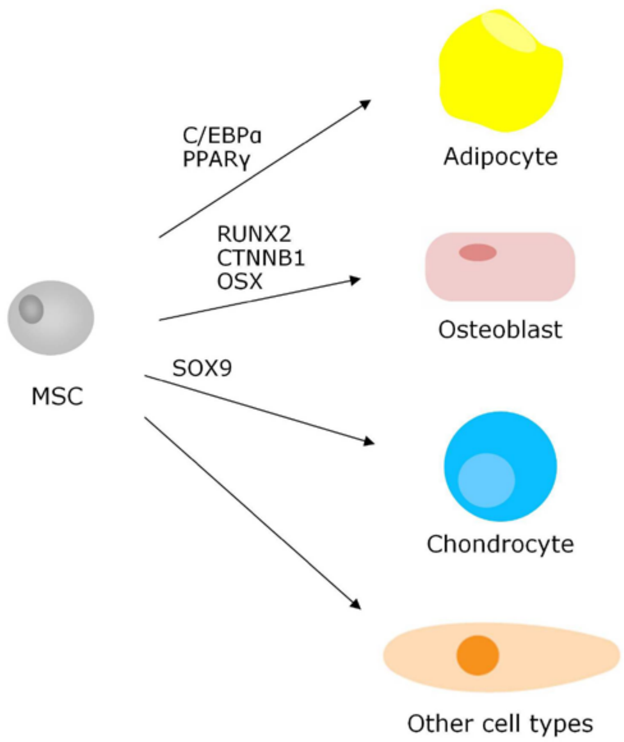

Figure 3 - *Mesenchymal precursors differentiate into several lineage cells*.
Mesenchymal stem cells give rise to several cell types depending on the transcription factors expressed. PPARγ and C/EBPα are required for adipocyte differentiation, while RUNX2, CTNNB1 and OSX are necessary for both osteoblast formation and chondrogenesis require SOX9.
(C/EBPα – CCAAT/enhancer-binding protein α; CTNNB1 - β-catenin; MSC – mesenchymal stem cell; OSX – osterix; PPARγ - peroxisome proliferator-activated receptor γ; RUNX2 – runt-related transcription factor 2; SOX9 - SRY (sex determining region Y)-box 9)

The progressive development of the osteoblast phenotype from a proliferating immature cell to a mature osteoblast that is able to synthesize bone proteins is characterized by a sequential expression of specific genes that identifies three periods of osteoblast phenotype development: proliferation, maturation and extracellular matrix synthesis, and matrix mineralization (figure 4)[194]. It is hypothesized that osteoblast proliferation is dependent on the matrix synthesis, whose maturation contributes to up-regulate the proliferation stage. During the active proliferation phase, osteoblast-committed progenitor cells express genes that support proliferation and several genes encoding for extracellular matrix proteins, such as type I collagen. These precursor cells are elliptical and unable to deposit bone matrix, but retain the proliferation capacity. At this point, BMP-2 and BMP-5 have a key role in increasing alkaline phosphatase (ALP) activity and OCL synthesis[194-195]. Immediately after growth arrest, a development sequence of specific genes that characterize osteoblasts (ALP, OCL) occurs. The accumulation of matrix proteins leads to the suppression of cell proliferation[196].

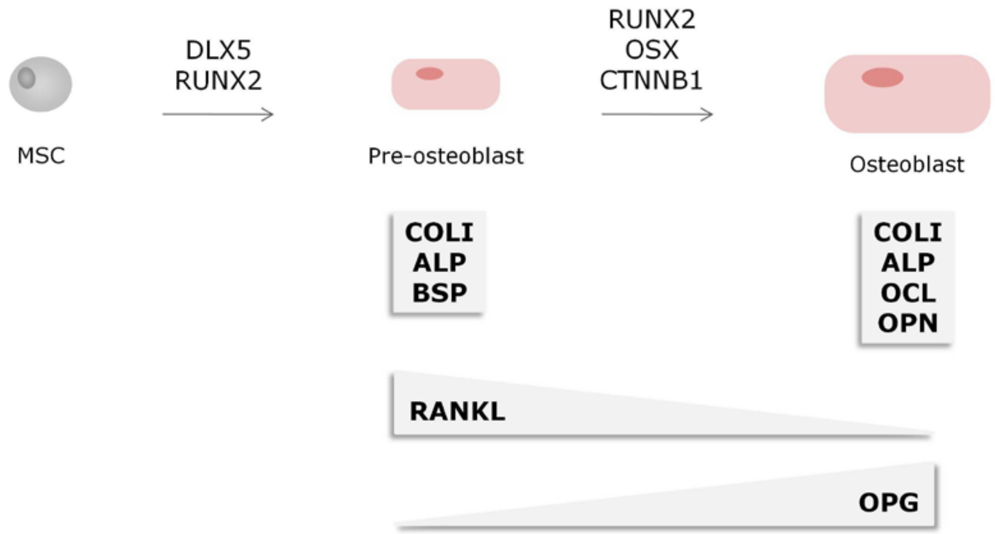

Figure 4 – *Osteoblast lineage*.

Osteoblasts derive from mesenchymal stem cells and differentiate only in the presence of DLX5, RUNX2, OSX and CTNNB1. The pre-osteoblast is unable to deposit bone matrix but maintains the proliferation capacity. Moreover, the amount of RANKL and OPG expressed by osteoblasts depend on their stage of differentiation: pre-osteoblast cells express high levels of RANKL and relatively low levels of OPG, thus stimulating osteoclast differentiation and function. Immediately after growth arrest, a development sequence of specific genes that characterize osteoblasts occurs.
(ALP – Alkaline phosphatase; BSP – bone sialoprotein; COLI – type I collagen; CTNNB1 - β-catenin; DLX5 - distal-less homeobox 5; MSC – mesenchymal stem cell; OPG – osteoprotegerin; OPN – osteopontin; OSX – osterix; RANKL - receptor activator of nuclear factor kappa B ligand; RUNX2 - runt-related transcription factor 2)

The active osteoblast is a cuboidal cell with an abundant rough endoplasmic reticulum and a large Golgi apparatus. In addition, osteoblasts form tight junctions with adjacent osteoblasts and have plasma membrane regions specialized in vesicular trafficking and secretion that facilitate the deposition of bone matrix[64, 197]. During the post-proliferative phase, which is characterized by high levels of ALP, the extracellular matrix progresses to the mineralization phase, in which osteoblasts synthesize several proteins associated with the mineralized matrix[198] including BSP[199], OPN and OCL[200]. OPN is expressed during active osteoblast proliferation, decreases immediately after the post-proliferative stage and increases again at the onset of mineralization, achieving a peak during mineralization[201]. On the other hand, OCL is expressed only in the post-proliferative phase, showing highest levels during mineralization[202]. At the end of the matrix synthesis and mineralization, expression of ALP diminishes[201] and osteoblasts either undergo apoptosis, become lining cells or maturate into osteocytes[194].

More than a decade ago, RUNX2 was established as essential for bone formation since mice deficient in this transcription factor showed no ossification[203]. RUNX2 is a member of the runt family of transcription factors that is expressed by MSCs at the onset of skeletal development and is present in osteoblasts throughout their differentiation[204]. Mice overexpressing RUNX2 exhibit osteopenia and multiple fractures, as a consequence of the reduced number of terminally differentiated osteoblasts and diminished number of osteocytes, whereas less mature osteoblasts expressing OPN accumulated in adult bone. Therefore, although essential for osteoblast lineage commitment and proliferation, RUNX2 inhibits differentiation at a later stage[205]. In bone lineage cells, RUNX2 binds to the osteoblast specific element (OSE2), that is found in the promoter region of all major osteoblast genes and controls their expression[206], including type I collagen α1 chain (COL1A1)[207], OPN[208], BSP[209] and OCL[207].

Osterix is another essential transcription factor for osteoblast differentiation. OSX-deficient mice show absence of osteoblasts and defective bone formation[210]; however, RUNX2 is expressed in these mice suggesting that OSX acts downstream of RUNX2. In fact, OSX transcription is positively controlled by RUNX2[211]. OSX acts by forming a complex with NFATc1 resulting both in the activation of the type I collagen promoter[212] and in the induction of WNT signaling pathway and bone formation[213].

The WNT signaling pathway regulates several aspects of osteoblast activities including commitment of mesenchymal stem cells, osteoblast progenitor amplification and cell death. The first evidence that WNT/β-catenin signalling plays an important role in bone formation came from studies in humans where mutations that inactivate the WNT co-receptor low density lipoprotein receptor-related protein (LRP)5 were shown to cause osteoporosis[214]. Moreover, gain-of-function mutations in this receptor increased WNT signalling and resulted in a high bone mass phenotype, both in humans and mice, due to an elevated number of active osteoblasts which seem to be protected from apoptosis[215].

WNTs are secreted glycoproteins that are found in all animal species. The human genome encodes 19 *WNT* genes that bind to cell-surface receptors and mediate a cascade of events that regulate a variety of cellular activities, including cell fate, determination, proliferation, migration, polarity and gene expression. The WNT/β-catenin pathway (figure 5) is frequently referred to as the canonical pathway and it promotes cell fate determination, proliferation and survival through the increase of β-catenin levels and alteration of gene expression by the transcription factor lymphoid enhancer factor/T cell factor (LEF/TCF)[216]. Activation of this signalling pathway occurs with binding of WNT to the receptor Frizzled (FZ) and the co-receptors LRP5/6[217-

[218]. In the absence of a WNT ligand, the cytosolic level of β-catenin is kept low by its phosphorylation and degradation, thereby suppressing the expression of WNT-responsive genes[216].

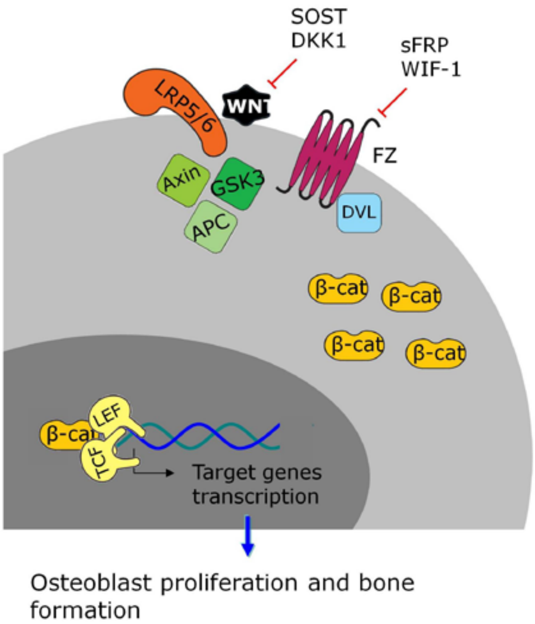

Figure 5 - *Wnt/β-catenin signaling pathway*.

Canonical Wnt signalling has multiple roles in osteoblastogenesis, is essential for osteoblast lineage differentiation and is involved in osteoblast proliferation, survival and lifespan. Binding of WNT to FZ and LRP5/6 receptors induce a signalling cascade that allows the accumulation of β-catenin in the cytoplasm. β-catenin then enters the nucleus where it promotes the transcription of target genes.
(APC – adenomatous polyposis coli; β-cat - β-catenin; DKK-1 – dickkopf-related protein 1; DVL – dishvelled; FZ – frizzled receptor; GSK3 – glycogen synthase kinase-3β; LRP5/6 - low-density lipoprotein receptor related protein 5/6; sFRP – secreted frizzled-related protein; SOST – sclerostin; WIF-1 – WNT inhibitory factor; LEF/TCF – lymphoid enhancer factor/T cell factor)

β-catenin activity is essential for the differentiation of mature osteoblasts and, consequently, for bone formation. In fact, conditional inactivation of β-catenin in either skeletal progenitor cells or at a later stage of osteoblast development in mouse embryos blocks osteoblast differentiation[219]. LRP5 is expressed at low levels in various tissues and constitutes a key factor in bone regulation. This factor forms a complex with FZ, leading to the activation of the canonical WNT signalling pathway[217-218, 220]. Moreover, recent studies have shown that OSX is able to inhibit WNT pathway activity during osteoblast differentiation either through disrupting the biding of TCF to DNA and inhibiting β-catenin transcription, or by activating the dickkopf homolog 1 (DKK1) promoter, an endogenous inhibitor of the WNT/β-catenin signaling[221-222]. Although this pathway has been extensively studied on osteoblastogenesis and bone formation, specific WNT proteins able to trigger its activation have still not been identified. In fact, several WNT genes, such as WNT1, WNT4, WNT5α, WNT9α/14 and WNT7b are expressed in either osteoblast precursors or adjacent tissues during development, and WNT3α and WNT10b are expressed in bone marrow[217], but only WNT10b mutants show a postnatal decrease in bone mass. WNT10b induces the expression of the transcription factors RUNX2[223-224], distal-less homeobox 5 (DLX5) and OSX[225] in mesenchymal progenitor cells *in vitro.* Additionally WNT10b blocks adipogenesis by inhibiting the transcription factors CCAAT/enhancer-binding protein α (C/EBPα) and peroxisome proliferator-activated receptor (PPAR)γ[223]. These observations substantiate the influence of WNT/β-catenin pathway on the differentiation of the mesenchymal stem cells towards an osteoblastic phenotype both by inhibiting adipogenesis and inducing osteoblast-specific transcription factors. LRP5/6 appears to regulate the number of osteoblasts and their proliferation[226] while β-catenin influences OPG production in osteoblasts and affects bone resorption but without having impact on their number[227]. Moreover, WNT/β-catenin signalling activation enhance osteoblast and osteocyte survival *in vitro*[219] and this pathway is also active during bone regeneration[228].

WNT signalling is tightly regulated by secreted antagonists. There are two classes of WNT inhibitors, the secreted frizzled-related protein (sFRP) class and the dickkopf class. Members of the sFRP class bind directly to WNTs and members of the dickkopf class, which comprise some dickkopf family of proteins and sclerostin (SOST), inhibit WNT signalling by binding to the LRP5/6 co-receptor[229-230]. The dickkopf family of proteins comprises four members. DKK1, the most studied one, is a secreted protein whose function is to prevent the activation of the WNT signalling pathway by binding to LRP5/6[231]. DKK1 inhibits the WNT pathway through interaction with another transmembrane receptor, Kremen (KRM)-1 and KRM-2, forming a ternary complex (DKK1-KRM-LRP5/6) and disrupting the signalling by promoting endocytosis and removal of the WNT receptor from the cell membrane[232]. Transgenic mice overexpressing DKK1 have reduced osteoblast numbers and severe osteopenia[233], whereas deletion of only one DKK1 allele increases all bone formation parameters without affecting bone resorption[234]. Single KRM mutants show normal bone formation while double mutants show increased bone mass parameters, both without interfering with bone resorption markers[235]. Canonical WNTs upregulate DKK2 expression which, in turn, controls some of the processes required for terminal osteoblast differentiation, mostly by removing the cells from the cell cycle. This protein is important in late stages of osteogenic differentiation, particularly for the formation of mineralized matrix. In fact, DKK2$^{-/-}$ mice are osteopenic, have increased numbers of osteoclasts and show elevated levels of RANKL; therefore, DKK2 seems to influence both osteoblast and osteoclast biology[236].

Sclerostin is a secreted protein expressed by mature osteocytes[237] and its expression is modulated by mechanical loading[238]. Like DKK1, SOST inhibits WNT/β-catenin pathway by binding to LRP5/6 co-receptor; however, it binds to a different region of LRP5/6 and it does not mediate receptor internalization[239]. SOST knockout mice have increased BMD, bone volume, bone formation and bone strength[240] while overexpression of SOST leads to osteopenia[241]. Mutations that reduce SOST function, in humans, cause sclerosteosis characterized by endosteal hyperostosis, most commonly of the skull and mandible [242].

BMPs, namely BMP-2, BMP-4 and BMP-7, are able to induce immature cells to differentiate into osteoblasts[243]. Specifically, BMP-7 induces the expression of RUNX2 indicating that this gene is a target of BMP signalling during osteoblast differentiation[244].

Osteoblasts have the ability to regulate bone resorption through the expression of RANKL, which binds to its receptor, RANK, on the surface of pre-osteoclast cells, inducing their differentiation. On the contrary, the soluble decoy receptor OPG, also produced by the osteoblast, is able to block RANK/RANKL interaction by binding to RANKL and thus prevent osteoclast differentiation and activation[245]. RANKL was initially identified as a cytokine produced by T cells and needed for their interaction with DCs[246]. RANKL is expressed by osteoblasts, bone marrow stromal cells, activated immune system cells[246-247], mammary epithelial cells[248], cells within the periodontal tissue[249], hypertrophic chondrocytes[149] and smooth muscle cells[250]. Evidence has shown that RANKL exists in two forms; a 40 to 45kDa membrane-bound form and a 31KDa soluble form[149, 251]. *In vitro* studies confirmed that the soluble form can be generated by proteolytic cleavage of the membrane-bound form by proteinases such as TNF-α converting enzyme (TACE)[252], a disintegrin and MMP (ADAM) 10 and MMP14[253]. In addition to proteolytic cleavage, in malignant cells a human soluble form of RANKL can be produced by alternative splicing[254-255]. However, some data suggest that the membrane-bound form is more potent than the soluble one[256] since shedding of RANKL from stromal cells inhibits osteoclastogenesis *in vitro* and mice with reduced RANKL shedding have increased osteoclast number[253]. Moreover, shedding of RANKL is suppressed either by binding of OPG or soluble RANK to RANKL[257] and transgenic mice overexpressing soluble RANKL are osteoporotic[258].

TNF family members mediate several biological processes and RANKL is especially important in bone, in the immune system[259] and in mammary epithelium[245]. Deletion of the RANKL gene in mice resulted in severe osteopetrosis and a complete lack of osteoclasts, as a result of an inability of osteoblasts to support osteoclastogenesis[260]. OPG was first identified in 1997 as being a protein that exhibits a protective effect on bone[261], although it is expressed ubiquitously and abundantly in many tissues and cell types[262]. OPG was identified only as a soluble protein[261, 263] which binds to its ligand, thereby preventing the activation of cellular targets. In fact, the main function of OPG is to antagonize RANKL effects, by interrupting the signalling between osteoblasts and osteoclast progenitors. Indeed, overexpression of OPG in mice also resulted in osteopetrosis due to inhibition of osteoclast maturation[261], whereas OPG-deficient mice exhibit osteoporosis[264]. In an *in vitro* study, RANKL mRNA levels were found to be increased in undifferentiated cells and decrease 5-fold during osteoblast differentiation, whereas OPG mRNA levels were much lower in undifferentiated cells and increased 7-fold during differentiation[265-266]. These findings are in agreement with the fact that only undifferentiated cells can support osteoclastogenesis, while partially or completely differentiated cells cannot. Accordingly, the amount of RANKL and OPG expressed by osteoblasts depend on their stage of differentiation: pre-osteoblast cells express high levels of RANKL and relatively low levels of OPG, thus stimulating osteoclast differentiation and function (figure 4). On the other hand, more mature osteoblasts express higher levels of OPG, in comparison to RANKL levels, inhibiting osteoclast differentiation and function[190]. Hence, a high RANKL/OPG ratio in bone microenvironment is the main molecular mechanism that determines osteoclastogenesis.

Following lineage commitment, osteoprogenitors undergo a proliferative stage. Subsequently, they exit cell cycling and begin to express genes encoding several proteins such as ALP, BSP and type I collagen as they start to produce and mature the extracellular matrix. Finally, osteoprogenitors express genes of proteins involved in the mineralization of the extracellular matrix such as OCL and OPN[267].

OSTEOCYTE

At the end of the bone formation phase osteoblasts have one of three possible fates: they can be embedded in the matrix and differentiate into osteocytes, they can be transformed to bone lining cells or they can undergo programmed cell death[268]. Thus, an osteocyte is an old osteoblast that was entrapped in its own matrix. It remains unclear if the decision for an osteoblast to become an osteocyte is determined by a specific pattern of gene expression, weather it is a cell autonomous response or one that is controlled by signals received by the surface cells from already embedded osteocytes. It is also not known whether every osteoblast can become an osteocyte or if there is a specific subpopulation with predefined fate[269]. Several investigators have reported heterogeneity in osteoblast gene and protein expression patterns, suggesting the existence of subpopulations of osteoblasts destined for different fates[270-271].

Osteocytes are non-proliferative, terminally differentiated cells and constitute the main cellular component of mammalian bone, representing more than 95% of bone cells. They reside both in mineralized matrix and in newly formed osteoid, locked inside small lacunae. Osteocytes have dendritic morphology. The cells are located in osteocytic lacunae and present cytoplasmic extensions, dendrites, which extend into channels in the matrix, called canaliculi. Although they are considered non-migratory, osteocytes are motile within the lacuno-canalicular system and they are able to retract and extend their cytoplasmic processes in the canals[272]. Osteocytes communicate with each other and with cells at bone surface via these dendrites and the lacuno-canalicular system constitutes a molecular exchange surface area[273]. Once embedded into the bone matrix, the osteocyte ceases its matrix synthetic activity and initiates the function as strain and stress sensor[274]. Another function of osteocytes within the bone cell network is the ability to deposit and resorb bone around the lacuna in which they are housed, thus changing the shape of the lacuna. This process is called osteocytic osteolysis and is limited to specific situations[275]. In an attempt to understand if the osteocyte can be released from its lacunae, it was found that when bone around embedded osteocytes is resorbed, osteocytes either appear to undergo cell death or they crawl out of the lacunae into the resorbed area[269]. However, the faith of the free cell is unknown.

During osteocytogenesis the embedding cell undergoes a dramatic transformation. In order for osteoblasts to differentiate into osteocytes they first need to arrest their motion on bone surface and adopt a dendritic morphology. At this phase, the organized expression of tubulin, vimentin and actin in cell bodies and dendrites of osteocytes are crucial to maintain their characteristic cytoskeletal shape[276]. Many researchers believe that the transformation process involves three cell types: preosteoblasts differentiate into osteoblasts which become trapped as osteocytes. During the transformation process there is a wide range of morphological changes such as decrease in size of the cell body (about 70% reduction in body volume), increase in the cellular processes and changes in intracellular organelles. In the nascent osteocyte, the structure of organelles is qualitatively similar to that of osteoblasts, although the size and number are diminished. In fact, with increasing distance from the mineralizing surface the rough endoplasmic reticulum, the Golgi apparatus and mitochondria decreases and glycogen accumulation increases[277-278]. During bone formation, processes of the osteocyte surface continue to grow to enable this cell to maintain contact with the active osteoblast layer and modulate their activity. When these processes stop growing they produce a signal that induces recruitment of those osteoblasts with which they are losing contact. The committed osteoblasts start differentiating into osteoblastic osteocytes[279]. Studies in the femoral metaphysis of 2-week old rabbits suggest that the transformation from osteoblast to osteocytes takes about three days[280]. During this time, the cell produces a volume of extracellular matrix three times its own cellular volume[278]. The osteoid osteocyte must perform two major functions simultaneously: regulate mineralization and form connective dendritic processes[281-282].

Osteocyte differentiation (figure 6) is accompanied by progressive reduction of several bone markers such as ALP, BSP, OCL, collagen type I and RUNX2. The expression of OPN and podoplanin (E11/gp38) is maintained. On the other hand, osteocytes start expressing new markers like CD44, dentin matrix acidic phosphoprotein 1 (DMP1) and matrix extracellular phosphoglycoprotein (MEPE)[274, 283]. After mineralization of the osteoid, the osteocyte undergoes morphological changes that lead to a decrease in protein synthesis. Although the molecular control of osteocytogenesis is largely unknown, this process is accompanied by increased expression of MEPE and DMP1, which have been associated with the osteocyte phenotype[284-285].

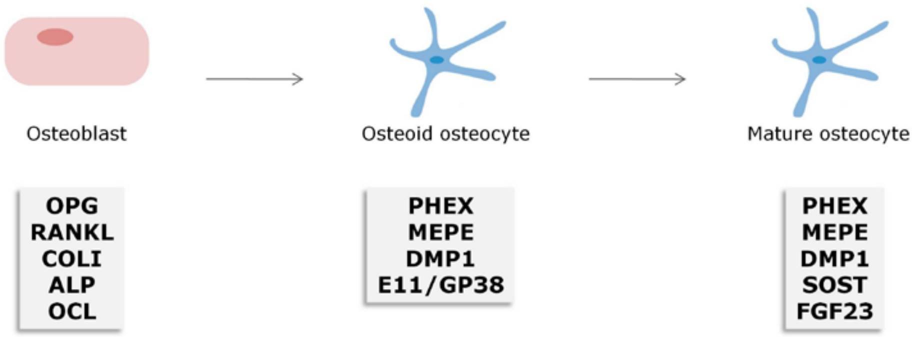

Figure 6 – *Osteocytogenesis*.

Osteocytes derive from matrix-secreting osteoblasts. By an unknown mechanism, osteocytes become entrapped in the bone matrix while maintaining contact with each other and with cells at the bone surface through cytoplasmic projections. During entrapment, the cell morphology changes until it acquires the typical morphology with a small cell body and numerous dendritic processes.
(ALP – Alkaline phosphatase; COLI – type I collagen; DMP1 - dentin matrix acidic phosphoprotein 1; E11/GP38 – podoplanin; FGF23 – fibroblast-growth factor 23; MEPE - matrix extracellular phosphoglycoprotein; OCL – osteocalcin; OPG – osteoprotegerin; PHEX - phosphate regulating endopeptidase homolog, X-linked; RANKL - receptor activator of nuclear factor kappa B ligand; SOST – sclerostin)

DMP1 is an extracellular matrix protein that has been implicated in osteocyte function and signaling[286]. DMP1 is a target for RUNX2 and is absent in RUNX2 knockout animals. In a DMP1 knockout model a hypomineralized phenotype is present and associated with elevated fibroblast growth factor (FGF)23 and defective lacuno-canalicular network formation[287]. Moreover E11/gp38 is highly expressed in osteocytes that are in the process of embedding or have recently been embedded, suggesting that this molecule may be important for the initial formation of dendrites but not for the subsequent maintenance of their morphology. *In vitro* studies suggest a link between this molecule and the dendritic nature of osteocytes since overexpression of E11/gp38 in osteoblasts initiates the development of cytoplasmic processes, while blockade inhibits them[288]. MMP-2 has also a role in osteocytogenesis. Recent work describes MMP-2 as a regulator of osteocyte production, generation and maintenance of an appropriate canalicular system, since in MMP-2 knockout mice the number of canaliculi is reduced[289]. Although osteocytes by themselves do not resorb or form bone, except in the lacunar area, they signal osteoblasts and osteoclasts to perform their functions. Osteocytes have been shown to produce RANKL and M-CSF and to support the generation of functional resorbing osteoclasts from their progenitors[290-291]. These cells also express OPG, influenced by β-catenin signaling[172, 282]. Mechanical pressures and loads are sensed by osteocytes and these cells are able to respond by modulating the expression and secretion of many molecules, including IGF-I, IGF-II, OCL[292] and type I collagen[293]. Osteocytes also produce two important inhibitors of osteoblast proliferation and differentiation SOST[241] and DKK1[233].

Osteocytes not only play a physiological role during their lifetime but also achieve functions through apoptosis. It has been observed that pro-apoptotic molecules are elevated in osteocytes found in the vicinity of microcracks, whereas anti-apoptotic molecules are expressed 1-2mm from the microcrack, suggesting that the apoptotic area may be restricted to the neighborhood of the damage[294]. The osteocyte apoptosis message travels through the lacuno-canalicular system to the bone surface and is sensed by the progenitor cells. This message leads to the initiation signals for remodeling, stimulating the bone resorption/formation cycle[295].

THE REMODELING PROCESS

Bone is continuously remodelled to ensure mineral homeostasis and to maintain the integrity and strength of the structure. Bone remodeling occurs at the BMU level and involves several sequential steps beginning with osteoclast formation, osteoclast-mediated bone resorption, a reversal period where the matrix will be prepared for the next phase and a long period of bone matrix formation mediated by osteoblasts, followed by mineralization of the matrix (figure 7)[296-297]. In this process cells are not in contact with bone marrow but are enclosed in a specialized vascular structure that Hauge called bone remodeling compartment (BRC). This compartment is covered by a canopy of cells that form the outer delineation that display the classic osteoblast lineage markers and, therefore, are most probably lining cells[298]. These cells communicate with each other and with osteocytes embedded in bone matrix via gap junctions. Capillaries infiltrate the canopy probably serving as a transportation system for the cells needed in the BMU. In fact, cells may enter the remodeling space either via diapedesis through lining cells or capillaries[131], since there are evidence that both osteoclast[146] and osteoblast[299] precursor cells are present in the circulation.

Essentially, BRC provides a closed microenvironment suitable for the tight regulation necessary for bone resorption-formation coupling and allows remodeling to proceed without interference from local factors liberated in the bone marrow. The BRC is the structure that translates microdamage sensed by the osteocyte network into osteoclast and osteoblast activity. Signals sensed by osteocytes are transmitted to the lining cells layer[300-301] and trigger osteoclast precursor recruitment. Coupling occurs inside the BMU; however, due to the separation in time and space of bone resorption and formation, the cell-cell contact between osteoclast precursors and active osteoblasts is highly unlikely[131]. Therefore it was proposed that lining cells, which express OPG and RANKL[302], might be responsible for cell-cell contact with osteoclast precursors. Bone surface is generally covered by lining cells[277] preventing direct contact between osteoblasts or osteoclasts and integrins or other adhesion molecules present on bone surface. Due to the fact that BRC formation involves detachment of lining cells from bone surface, BRC would be the only place where circulating osteoblasts and osteoclasts precursors are exposed to matrix constituents. Therefore, this structure eliminates the need of a “postal code” system to ensure that cells migrate and adhere to the areas where they are needed[131].

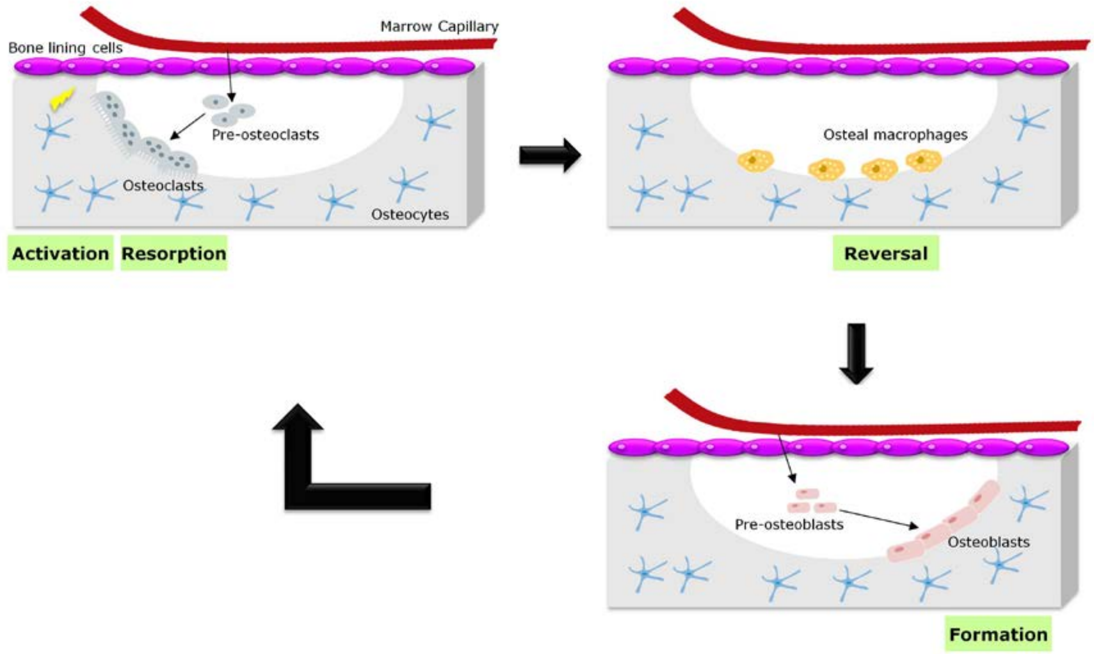

Figure 7 – *The remodeling process*.

The remodeling process takes place inside the bone remodeling compartment. Bone remodeling is hypothesized to be initiated by osteocyte apoptosis (activation phase), which sends a signal for the recruitment of osteclast precursors, which then differentiates and resorb bone in this closed microenvironment (resorption phase). Following osteoclast-mediated resorption, the lacunae remains covered with undigested demineralised collagen matrix and will be cleaned by osteal macrophages (reversal phase). At last, osteoblasts arrive at the bone remodeling compartment where they will deposit new bone (formation phase).

The trigger that initiates bone remodeling is thought to be osteocyte apoptosis[303]. Studies of mechanical loading in human bone *ex vivo* and of rat bone *in vivo* determined that osteocyte apoptosis is increased by loading and was accompanied by increased remodeling[304-305]. Under normal conditions, osteocytes secrete TGFβ, inhibiting osteoclastogenesis. When these cells undergo apoptosis, TGFβ levels diminishes, removing the osteoclastogenesis inhibitory signal and allowing osteoclast formation[306]. Moreover, osteocytes are able to secrete OPG and M-CSF and express RANKL, which enables them to control osteoclastogenesis[291, 307].

Osteoblasts respond to the stimuli generated by osteocytes and recruit osteoclast precursors to the remodeling site. During recruitment, osteoclast precursors migrate from the bloodstream into the extravascular space, through the endothelial cell layer. Studies have shown that two routes for this journey can be considered: either the precursors migrate via cell-cell junctions (paracellular migration)[308] or through the cell body of endothelial cells (transcellular migration)[166, 309]. At this time, osteoblast decrease the expression of OPG and enhance M-CSF and RANKL production in order to promote osteoclast differentiation and activity. Osteoblasts also produce MMPs in response to the remodeling signal[310]. These enzymes expose the RGD adhesion sites for osteoclast attachment to the matrix[178]. The structures at which attachment occur, known as podosomes, are rapidly assembled and disassembled allowing osteoclast movement and resorption across bone surface[296]. Osteoclasts anchor to bone creating a sealed acidic microenvironment where mineralized matrix is dissolved, producing the Howship's resorption lacunae. The remaining organic matrix is degraded by CTSK[311]. When its resorption cycles have been completed, osteoclasts die by apoptosis and leave the bone surface.

Following osteoclast-mediated resorption, the resorption pits remain covered with undigested demineralised collagen matrix[312]. Studies have shown that mononuclear cells remove the remaining collagen and prepare bone surface for subsequent osteoblast-mediated bone formation. This cell type has not yet been identified; it was proposed to be a monocytic phagocyte[313] but it can also belong to the osteoblast lineage[312]. From a functional perspective both osteal macrophages and bone lining cells facilitate events during the reversal phase of bone remodeling. Osteal macrophages are resident tissue macrophages located close to the bone surface and are required for full differentiation and maintenance of osteoblasts[314], while bone lining cells are terminally differentiated osteoblasts. After bone preparation by osteal macrophages and lining cells, the lining cells separate from underlying osteocytes and form a canopy over the bone to be remodelled, creating the BRC[298]. The ultimate role of the lining cells may be to receive and/or produce coupling signals to allow transition from bone resorption to bone formation inside the BMU; the nature of this signal remains elusive. It was initially proposed that molecules stored within bone matrix, such as IGF-I, IGF-II or TGFβ, could act as coupling signals[315]. However, in mice and humans with defective osteoclasts, bone formation is preserved and this finding has led to the hypothesis that osteoclasts themselves produce the coupling factor[135]. Several possible coupling mechanisms have been proposed, including the soluble molecule sphingosine-1-phosphate (S1P) and the bi-directional signalling mediated by ephrin receptor B4/ephrin-B2 (EPHB4/EFNB2). S1P is secreted by osteoclasts, induces osteoblast precursor recruitment and promotes mature cell survival[316]. EPHB4 receptors are expressed by osteoblasts while EFNB2 is located in osteoclasts. Forward signaling through EPHB4 into osteoblasts enhances osteogenesis and reverse signaling through EFNB2 into osteoclast precursor suppresses osteoclast differentiation by inhibiting the osteoclastogenic C-FOS-NFATc1 cascade[317]. However, as osteoblast recruitment and matrix deposition continues long after osteoclasts have abandoned the resorption lacunae, several mechanisms including both direct contact and soluble signal may be required to the coupling process. Mechanical stimulation can induce bone formation signals through osteocytes. Under resting conditions osteocytes express SOST[318] and, therefore, inhibit bone formation. Mechanical strain on bone inhibits osteocyte expression of SOST and removes the inhibition of WNT/β-catenin signaling allowing bone formation to occur[238].

Once osteoblast progenitors or mesechymal stem cells arrive to the resorption lacunae they differentiate and secrete molecules that replace the resorbed bone. For bone to assume its final composition, hydroxyapatite crystals are incorporated into this newly deposited osteoid. Once bone formation is completed and bone surface is covered with lining cells, the matrix continues to be mineralized in a process dependent on the signaling of osteocytes, particularly on the expression of DMP1, phosphate regulating endopeptidase homolog, X-linked (PHEX) and FGF23[287, 319]. The lost SOST expression returns towards the end of the remodeling cycle. Following mineralization, mature osteoblasts undergo apoptosis, revert to a lining cell phenotype or differentiate into osteocytes. When an equal amount of lost bone is replaced, the remodeling cycle is completed. The termination signal that informs all the machinery that the cycle has come to an end is unknown, however osteocytes may have a role in regulating this termination phase[320].

BONE REMODELING DISORDERS

Trabecular bone is the major site of bone remodeling. In normal bone, bone formation and resorption are two balanced and regulated processes in such a way that in adult healthy bone there are no major net changes in bone mass or mechanical strength after each remodeling cycle. In certain pathological conditions, an imbalance between bone formation and resorption may occur, leading to abnormal remodeling and bone disorders[321]. As an example, disorders such as OP, osteopetrosis, osteomalacia and Paget's disease are briefly addressed.

OP is the most common bone metabolic disease and is characterized by low bone mass and structural deterioration of bone, leading to increased fragility and susceptibility to fractures. About 40% of white postmenopausal women are affected by OP and in the context of an aging population, this number is expected to increase significantly in the near future. The patient with OP have an increased lifetime fracture risk, which most commonly occur in the spine, hip or wrist[322]. OP represents a group of distinct pathological conditions classified as primary or secondary depending on its aetiology. Primary OP can be further divided into two subtypes: post-menopausal (type I), which follows menopause in women, mainly due to the loss of the inhibitory effect of estrogens on osteoclastogenesis, and age-related (type II) that occurs in both genders but is twice more common in women[323]. In contrast, secondary OP is a consequence of an associated disease or medication that cause bone metabolism imbalance, such as the case of RA.

OP was operationally defined by the World Health Organization as a BMD measured by DXA with a T score lower than 2.5 (more than 2.5 standard deviations below the peak BMD for the same sex in a given population)[324]. Opposite to DXA scan, which gives us a static image of the bone, bone turnover markers reflect the total volume of bone in a time frame allowing us to indirectly assess osteoblast and osteoclast activity. The biochemical markers of bone turnover are measured both in blood and urine, have origin in the cellular metabolism or are products of the matrix remodeling and reflect bone turnover. These markers can be divided in two groups according to which function they reflect, either resorption or formation[31, 34]. However, in OP both groups are increased due to the coupling mechanisms between bone resorption and bone formation[325]. Currently the most widely used markers for bone formation are ALP, bone-specific ALP, OCL and the procollagen type I pro-peptides (P1CP and P1NP) (figure 8). On the other hand, pyridinium crosslinks (PYD and DPD) and the telopeptides of type I collagen (CTX and NTX) reflect bone resorption. For remodeling evaluation, the new biomarkers included recently are tartrate-resistant acid phosphatase 5b (TRAcP5b), CTSK, BSP and the ratio RANKL/OPG[326]. The major limitation for the clinical utility of all these biomarkers is the inter and intra-individual variation.

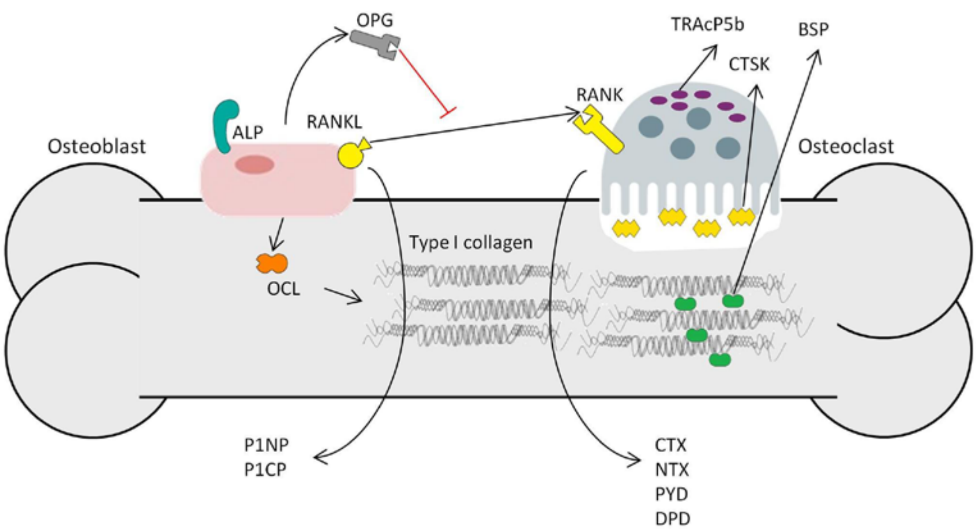

Figure 8 – *Bone turnover markers.*

Bone turnover markers can be divided in bone formation and bone resorption markers. Formation markers derive from osteoblast metabolism while the resorption markers originate from osteoclast action. The RANKL/OPG ratio is a marker of osteoclastogenesis.

(ALP – alkaline phosphatase; BSP – bone sialoprotein; CTSK – cathepsin K; CTX - carboxy-telopeptide of type I collagen; DPD – deoxypyridinoline; NTX - amino-telopeptide of type I collagen; OCL – osteocalcin; OPG – osteoprotegerin; P1CP - procollagen 1 carboxy-terminal peptide; P1NP - procollagen 1 amino-terminal peptide; PYD – pyridinoline; RANK - receptor activator of nuclear factor kappa B ; RANKL – RANK ligand; TRAcP5b - tartrate-resistant acid phosphatase 5b)

The contribution of genetic factors in bone remodeling, BMD variability and fracture risk has been extensively studied but without consensual results. However, for genes involved in the WNT/β-catenin pathway, RANK-RANKL-OPG interaction and estrogen receptors an association with both BMD and fracture risk have been established [327-328].

Age-related bone loss affects both women and men. Significant trabecular loss begins in the early thirties in both genders but after menopause women experience acceleration in bone loss due to the rapid decline in estrogen after menopause[329]. In men, age-related changes in the levels of sex steroids, including both androgen and estrogen, also contribute to the pathogenesis of osteoporosis[330]. A decline in bioavailable estrogen and androgen levels plays a role in the development of age-related osteoporosis in men by increasing osteoclast formation and function. Moreover, a decline in bioavailable androgen levels results in increased bone resorption as well as decreased bone formation[331-332]. In women, it is well established that both bone resorption and formation are increased in postmenopausal osteoporosis, although the balance of the two processes is shifted towards osteoclast-mediated bone resorption[333]. The variations in serum markers of bone turnover have been studied in a group of postmenopausal women showing that menopause induces a 79-97% increase in bone resorption marker levels and 37-52% increase in bone formation[334]. In early menopause, the acute phase of estrogen deficiency, the up-regulation of RANKL on bone-marrow stromal cells is associated with increased bone resorption[333, 335]. However, estrogen also stimulates the expression of OPG in mouse osteoblasts and stromal cells[336] and suppresses the expression of TNF, IL-1 and IL-6 in monocytes, osteoblasts and stromal cells[337]. Therefore, estrogen plays a protective role in bone loss by modulation of the

RANKL/OPG ratio and inhibition of pro-inflammatory cytokines secretion.

Osteopetrosis is a heterogeneous group of heritable conditions in which there is a defect in bone resorption by osteoclasts. The decrease in osteoclast activity also affects the shape and structure of the bone by altering its capacity to remodel during growth. In the most severe forms, the medullary cavity is filled with new bone, with little space remaining for hematopoietic cells. As a consequence of altered osteoclastic behavior osteopetrosis is associated with increased skeletal mass due to abnormally dense bone[338]. This contributes to the brittleness of bones and propensity for fractures characteristic of this disease. Osteopetrosis is genetically heterogeneous with autosomal dominant and recessive forms. There is a wide spectrum of phenotypes, the most severe caused by autosomal recessive inheritance[339]. Osteoclast development requires the presence of two growth factors, M-CSF and RANKL, and absence of either molecules leads to severe osteopetrosis in rodents, with lack of osteoclasts formation[340-341]. Also, loss-of-function mutations in either RANKL or RANK have recently been identified in osteoclast-poor cases of osteopetrosis[342-343]. Although a substantial percentage of osteopetrosis patients have no identifiable gene defect, three mutations that cause abnormal acidification of the resorption lacunae have been identified. The most common, found in 50-60% of the patients, results in a defect in the osteoclast vacuolar H^+-ATPase proton pump. The second most clinically significant form occurs in 10-15% of the patients with severe autossomal recessive osteopetrosis and affects CLCN7, a gene encoding the osteoclast specific chloride channel. Carbonic anhydrase II dysfunction is a feature of autossomal recessive osteopetrosis but accounts only for a small proportion of patients[339, 344].

Rickets and osteomalacia, also known as “soft bones” diseases, are characterized by a defect of mineralization due to calcium and/or phosphate deficiencies. Rickets is a disease of the growing skeleton and affects the bones in children, which are defective in strength and deformed. The prototype of this disease is vitamin D deficiency (nutritional) rickets. Osteomalacia is the adult counterpart[5]. In both diseases there is insufficient calcium and/or phosphorus to mineralize the skeleton. There may be less overall volume of bone, but more importantly, the bone fails to mineralize properly. Trabeculae are surrounded by unmineralized osteoid forming the so-called “osteoid seams”. Moreover, bone histomorphometry studies have shown that the mineralization lag time is higher than 100 days in rickets or in osteomalacia, contrasting with the normal 80-90 days[5]. Therefore, patients with osteomalacia present osteopenia or low BMD and frequently elevated levels of PTH, hypophosphatemia and elevated levels of ALP in circulation[345]. In a report of five cases with hypophosphatemic osteomalacia the authors reported an increase in the levels of ALP, both total and specific for bone, low levels of OCL and a slight increase in the collagen metabolism markers, particularly P1NP[346]. In vitamin D deficiency there is a reduction in the absorption of calcium from the gastrointestinal tract and an increase in the renal secretion of calcium that lead to lowering of blood calcium. This triggers a secondary hyperparathyroidism which brings the serum calcium to a normal level, but at the expense of bone loss[347]. The consequences of vitamin D deficiency in bone are inhibition of osteoblast progenitors, increase of RANKL and decrease of OPG. The immediate consequence is enhanced bone turnover and increased bone resorption[321, 348]. Mutational analysis in two families with autosomal recessive hypophosphatemic rickets showed the presence of mutations affecting the DMP1 start codon and a 7bp deletion disruption of the gene C-terminus. In addition, studies in mice demonstrated that absence of DMP1 resulted in defective osteocyte maturation leading to pathological changes in bone mineralization[287]. In another family with X-linked hypophosphatemic rickets analysis revealed a deletion of 52143bp including exons 1 to 3 in the PHEX gene[349].

Paget’s disease is characterized by a focal increase in bone turnover that affects one or more bones of the skeleton and becomes more prevalent with aging. Paget’s disease shows autosomal dominant inheritance and familial clustering has been recognized for over 50 years[350]. Between 15-40% of the patients have positive family history of the disease and studies have shown that the risk for relatives to develop Paget’s disease is increased between 7-10 times, compared with the risk of relatives of controls[351]. Paget’s disease is primarily a disorder of increased bone resorption with a secondary increase in osteoblast activity and new bone formation. The resulting trabecular bone is abnormal and disorganized[352]. A large histomorphometric study showed high bone turnover with a significant increase in bone resorption and bone formation indices leading to increased bone volume. A malignant transformation to osteosarcoma was observed in 0.8% of the patients[353]. Biochemical markers of bone turnover are increased in Paget's disease[354] and the same was observed for TRAcP5b[355]. Moreover, in Paget’s disease woven bone can be frequently found, with an irregular arrangement of collagen fibers. Therefore, the ratio of α-CTX/β-CTX is markedly increased, both in bone and urine[356]. The primary cellular abnormality resides in osteoclasts which have increased number of nuclei, are markedly increased in number and size, have an increased rate of formation and an increased bone resorption capacity per cell. In addition, osteoclast precursors from patients with Paget’s disease have increased responsiveness to RANKL[357]. Genetics play an important role in this bone remodeling disorder. In about one-third of the cases, Paget’s disease is inherited as an autosomal dominant disease with incomplete penetrance[339]. Several genetic loci have been linked to Paget's disease[358-359] but mutations in the genes RANK and particularly in sequestosome-1 (SQSMT1) have been reported to be associated with the disease[360-361] and are common causes of the classical Paget's disease[362]. SQSMT1 encodes p62, which is a scaffold protein in the NF-κB signaling pathway[363]. A total of twenty different SQSMT1 mutations have been identified, all of which cluster around the ubiquitin-associated domain of the protein product of this gene. SQSTM1 mutations are strongly associated with disease severity and complications of Paget's disease[364]. Between 30-50% of the patients with familial Paget's disease and 10-30% of patients without family history of the disease have mutations in this gene[365]. Studies in mice with targeted inactivation of SQSMT1 have impaired osteoclastogenesis in response to RANKL *in vivo*, suggesting that SQSMT1 plays a key role in regulating osteoclastogenesis[366]. Osteoclasts derived from peripheral blood monocytes from patients with Paget's disease were in higher numbers, contained more nuclei, were more resistant to apoptosis and exhibited greater bone-resorption capacity, compared to cells from healthy donors[367].

Overall, bone remodeling is a tightly regulated balanced process between bone resorption and formation. However, alterations to this equilibrium lead to bone remodeling disorders. Nowadays, the challenge is to replace the lost balance.

OSTEOIMMUNOLOGY

The term osteoimmunology was used for the first time in 2000[368] to describe the interaction of cells from the immune and skeletal systems for promoting osteoclastogenesis. This connection between bone and immune systems is not surprising, since precursors of immune cells reside in bone marrow, thus in the same environment as differentiated bone cells. Moreover, osteoclasts are of hematopoietic origin. Thus, a new concept is emerging in which bone exerts a quality control on immune responses by controlling the availability of hematopoietic stem cells (HSC)[369]. Osteoblasts play a crucial role in stem cell maintenance due to an intimate cell-cell contact via integrins[370-371]. Moreover, RUNX2-deficient mice are devoid of osteoblasts and are also characterized by the absence of bone marrow, although they show normal hematopoietic development in liver and spleen, suggesting an important role of osteoblasts in HSCs homing into the bone marrow cavity[372]. Osteoblasts can also control the pool of HSCs available by producing OPN, which inhibits their proliferation[373-374]. OPN is also required for the proper localization of the HSCs[373]. Adhesion of HSCs and osteoblasts appears to be mediated by interaction of N-cadherin and β-catenin[375]. In addition, TEK tyrosine kinase endothelial (TIE2) on HSCs and Angiopoietin-1 on osteoblasts also play a role in the inhibition of cell division of HSCs, while maintaining their capacity for self-renewal[376]. More recently, osteoclasts have been involved in the mobilization of HSCs. Indeed, stimulation of bone resorption increases the number of immature HSCs in circulation, suggesting that osteoclasts, by destroying the architecture of the niche, play a key function in mobilizing HSCs[377]. When mobilized, HSCs migrate through the bone marrow to meet the endothelial cells of the sinusoid vessels. These cells also form a niche for HSCs and support their proliferation, differentiation, as well as entry into the circulation[370].

Immune and skeletal systems have several regulatory factors in common, such as cytokines, transcription factors and receptors (figure 9). Consequently, these two systems interact with each other both in physiological and pathological conditions. All mammals are constantly being challenged by a variety of infectious agents, which produce some level of constant low grade immune system activation; therefore it is not difficult to imagine that crosstalk occurs throughout life between activated lymphocytes and bone cells. Furthermore, as we age there is accumulation in the bone marrow of memory T cells, which express RANKL on their surface. It is believed that these cells might influence bone turnover and be responsible for some of the changes that occur in the skeleton with aging[378].

Osteoblasts seem to have antigen-presenting properties, since cell lines were shown to express human leukocyte antigen (HLA) molecules besides the adhesion molecules CD54 and CD166, which are upregulated in the presence of IFN-γ and can activate T cells. Furthermore, osteoblasts express members of the toll-like receptor (TLR) family, in particular TLR-4, 5 and 9, indicating an active role in host immune response[379]. On the other hand, osteoclasts can send regulatory signals to T cells and potently suppress T cell response to mitogenic stimuli. They also have the capacity to attract and retain T cells at the bone surface, thus revealing a new role for osteoclasts[380]. These bone cells can also cross-present antigens to $CD8^+$ T cells, showing that osteoclasts are not just regulated by T cells but they can also modulate these cells forming a feedback control loop[381].

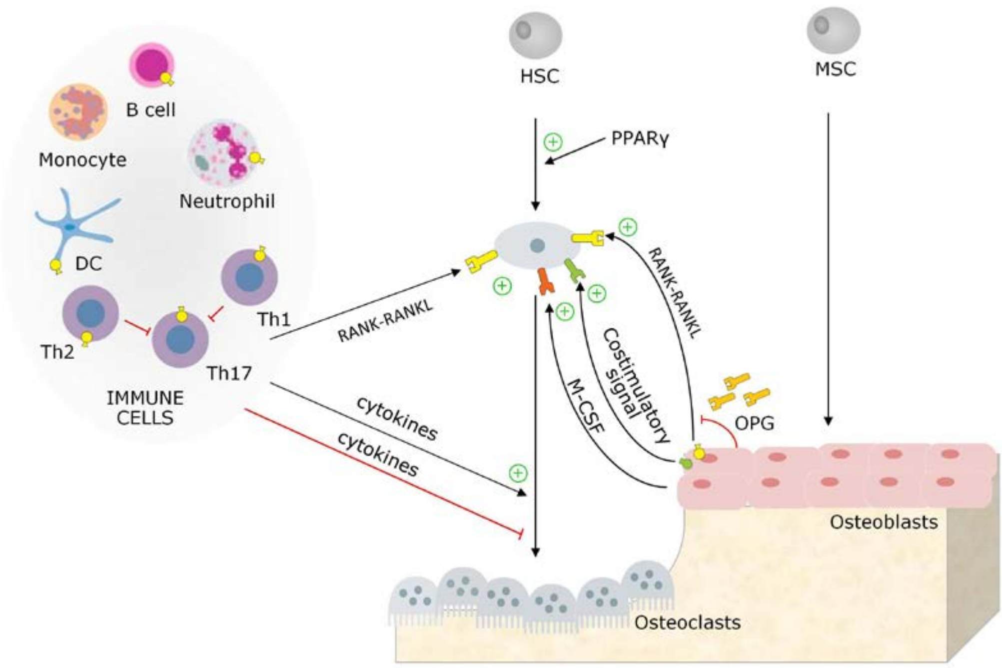

Figure 9 – *Interaction between bone and the immune system*.

Osteoclastogenesis makes use of three signals, RANK-RANKL, M-CSF and a costimulatory signal. However, there are also several factors produced by immune cells that also influence bone remodeling. Immune cells express RANKL and, therefore, can support osteoclastogenesis; on the other hand, these cells secrete several cytokines that can have either a pro-osteoclastogenic or an anti-osteoclastogenic effect.

(DC – dendritic cell; HSC – hematopoietic stem cell; M-CSF - colony stimulating factor 1 (macrophage); MSC – mesenchymal stem cell; OPG – osteoprotegerin; PPARγ – peroxisome proliferator activated receptor γ; RANK - receptor activator NF-κB; RANKL – RANK ligand; Th – T helper)

RHEUMATOID ARTHRITIS AND BONE

RA is a chronic inflammatory disease that targets the synovial membrane, cartilage and bone. It affects around 0.5-1% of the world population and is associated with significant morbidity and increased mortality[382-383].

In this disease, autoimmune phenomena, which manifest as the production of antibodies specific for immunoglogulin G (IgG, also known as rheumatoid factor) or specific for cyclic citrullinated peptides, precedes the clinically detectable onset of arthritis. In some patients these markers emerge years before the onset of the disease and probably contribute to its development and perpetuation[384]. Several genes have been proposed to be associated with susceptibility and severity of RA[385]; in fact, studies in twins suggest that genetic factors account for 60% of the RA onset[386]. There are two genes strongly associated with RA, the HLA system[387-390] and the protein tyrosine phosphatase non-receptor type 22 (PTPN22)[391]. A recent study has shown that citrullination generates "altered-self" peptides that are recognized preferentially by a subset of HLA-DR1 alleles that encode a conserved sequence of alleles known as the "shared epitope"[392]. Several other genes were found to be related with RA in a genome-wide association study, however only CD28, PR domain zinc finger protein 1 (PRDM1) and the attachment complex CD2/CD58 were considered risk factors for the disease[393]. In genetically susceptible individuals, specific environmental factors such as smoking habits, trauma or infection can activate potentially pathogenic immune pathways, contribute to disease development and its perpetuation, leading to chronic inflammation, joint destruction and systemic manifestations[382].

After the onset of RA, the normally hypocellular synovial membrane becomes hyperplasic, comprising a superficial lining layer of synovial fibroblasts and macrophages that expands from just one layer to several layers, covering an interstitial zone that contains a marked cellular infiltrate which includes synovial fibroblasts, macrophages, mast cells, $CD4^+$ and $CD8^+$ T cells, natural killer (NK) cells, natural killer T (NKT) cells, B cells and plasma cells. The inflamed synovium invades adjacent cartilage and bone, promoting joint destruction, which is mediated by the activities of osteoclasts, chondrocytes and synovial fibroblasts. In turn, joint damage is a source of neo-antigens, thereby promoting further autoimmune reactivity.

The inflammatory environment that occurs in RA induces bone remodeling disturbances, contributing not only to bone erosions but also to the development of secondary OP. In fact, RA patients have an increased risk of vertebral fractures, which is independent of BMD and corticosteroid use[394]. In addition, a high hip fracture risk was also noted in RA patients not exposed to corticosteroids[395]. Thus, RA itself seems to predispose to fractures although the underlying mechanisms are not yet completely understood.

During chronic inflammation, the balance between bone resorption and formation is skewed towards osteoclast-mediated bone resorption. Moreover, in inflamed joints, osteoclasts are located in the interface between the inflamed synovium and bone[396]. We can consider two essential key mechanisms for the formation of osteoclasts in the joints, the accumulation of precursors and their stimulation to differentiate into the osteoclast lineage. It is not clear whether the osteoclasts that enter the inflamed joint are already committed to the osteoclast lineage or are triggered locally within the synovium. Nevertheless, experimental evidences support the view that the peripheral monocytic population changes during inflammation towards an increase in the number of osteoclast precursors[397]. In collagen-induced arthritis (CIA) mice, the number of cells expressing RANK increases as arthritis progresses and, in areas of abundant $RANK^+$ cells, $TRAP^+$ multinucleated osteoclasts are also present. Sites of RANK expression were also co-localized with RANKL[398], which appeared to be overexpressed in pannus tissue from active RA patients[399]. Interestingly, RANK and RANKL are also essential for the development of secondary lymphoid tissues[400]. Denosumab, a fully humanized monoclonal anti-RANKL antibody, administered in association with methotrexate reduced erosion scores at 6 months after administration. The protection from focal bone erosion was accompanied by a decrease in bone turnover markers and an increase in BMD at 12 months[401]. Moreover, in another study, the authors reported that these effects were independent of concomitant bisphosphonate or glucocorticoid use[402]. Denosumab therapy in RA patients was also reported to decrease progression of erosions in the hands while increasing BMD and reducing cortical bone loss at 12 months after therapy[403-404].Therefore, as in physiological conditions, RANKL-RANK-OPG system is a major player in bone resorption in RA[405].

It is presently accepted that in RA both innate and adaptative immune responses are disturbed. Cytokines are implicated in both early and late phases of the pathogenesis of RA, promoting perpetuation of immune activity, maintaining chronic inflammatory synovitis and driving the destruction of adjacent joint tissues[406]. TNF[407-408], IL-1[409-410] and IL-6[411-412] are among the most important mediators of rheumatoid arthritis pathogenesis. Activated T and B cells are present in rheumatoid synovia[413-414] and synovial inflammation is the result of complex interactions between immune cells. Antigen-presenting cells communicate with T cells but their full activation requires a second co-stimulatory signal mediated by CD28-B7 receptor family. B cells participate in this complex environment by functioning both as antigen-presenting cells and as antibody-producing cells. Macrophages are activated by T cells and are key producers of pro-inflammatory cytokines such as TNF, IL-1 and IL-6[382]. On the other hand, cytokines regulate the phenotype of effector and regulatory T cells in the synovium. T cell activation is critical to the initiation and maintenance of RA and maximum T cell responses usually require co-stimulatory signals. Abatacept, a chimeric fusion protein composed of IgG1 Fc and extracellular domain of Cytotoxic T-

Lymphocyte Antigen 4 (CTLA4) that blocks T cell activation by disrupting the co-stimulatory signal, is effective for RA treatment by interfering with co-stimulation[415]. RANKL is not only expressed by osteoblasts, but also by several immune system cells, particularly by activated T cells, suggesting that these cells have a role in osteoclastic bone resorption[416]. However, some T cells are classical anti-osteoclastogenic cells as they produce cytokines that inhibit bone resorption, especially IFN-γ, the most potent inhibitor of RANKL signalling by downregulation of TRAF6[417].

DCs express RANK and they can be found in RA joints. It is thought that they mediate osteoimmune interactions indirectly by activating T cells to produce RANKL, which can then lead to osteoclastogenesis[418]. Moreover, DCs can even transdifferentiate *in vitro* into osteoclasts in the presence of M-CSF and RANKL and the resulting cells express the typical markers of osteoclasts[419-421].

Several studies have classified rheumatoid arthritis as a Th1 mediated disease and, therefore it was thought to be driven by a population of T cells producing interferon IFN-γ, lymphotoxin (LT)-β and TNF[422-423]. However, a new model is emerging that implicates Th17 cells as crucial effectors, since inhibition of IL-17 or its overexpression in mouse joints suppress or worsen joint inflammation and damage, respectively[424]. IL-17 drives neutrophil differentiation, maturation and activation, as well as monocyte and synovial fibroblast activation and cytokine, chemokine, prostaglandin and MMP production[425]. A synergistic effect has been observed with low concentrations of IL-17, IL-1β and TNF, which together lead to synovial fibroblast activation and cytokine production, indicating a pathogenic role for these inflammatory cascades[426-427]. In the synovial fluid of RA patients, OPN levels correlate with IL-17 production and the frequency of Th17 cells and OPN play a direct role in Th17 cell differentiation *in vitro*[428]. Recently, Th17 cells were identified as a typical pro-osteoclastogenic Th subset[429] due to the fact that they express RANKL at higher levels than Th1 or Th2, do not produce high amounts of IFN-γ and secrete pro-inflammatory cytokines. In addition, IL-17 induces RANKL expression on osteoblasts, and also enhances inflammatory cytokines production by other cells, thereby increasing RANKL expression and activity[424, 430]. Moreover, IL-17 induces the synthesis of MMPs, inducing bone and cartilage degradation[431]. IL-17 overexpression in CIA mice not only enhances RANKL expression, but also upregulates RANKL/OPG ratio in the synovium[432]. Treatment with a neutralizing anti-IL-17 antibody significantly reduces arthritis severity and suppresses joint damage. In addition, IL-6 levels are markedly reduced after treatment, as well as the number of IL-1β and RANKL positive cells in the synovium[433]. By comparing functional levels of IL-17 in synovial explants cultures from RA, osteoarthritis (OA) and healthy joints, it was found that IL-17 is spontaneously produced by cells from RA synovium[434]. In another study, authors described an enrichment of IL-17 producing $CD4^+$ T cells in the synovial fluid from RA patients as compared to blood. Moreover, Th17 cells from RA synovial fluid produce more TNF than the same cells from blood[435] and both the frequency of Th17 cells and IL-17 levels are increased compared to healthy joints[436].

Regulatory T cells (Treg) represent another T cell subpopulation with the main function of suppressing immune system activation[437]. Naturally occurring Tregs have been detected in the synovium of patients with active disease and particularly in synovial fluid[438-439] and, in some cases, in peripheral blood[440]. These observations raised the question of whether Tregs that are present in RA joints are dysfunctional or are functional but unable to prevent the disease[441]. Indeed, there is evidence for both effective and dysfunctional Treg cell activity in this disease setting. The support for the efficacy of

Tregs arose from studies of patients with juvenile idiopathic arthritis (JIA), where higher numbers of circulating Tregs were associated with mild forms of the disease[442]. On the other hand, Treg cells isolated from RA patients exhibit reduced suppressor function[443-444] but after anti-TNF treatment, these cells acquire the ability to suppress cytokine production by effector cells[443]. Treg cells, which express high levels of CTLA4, block osteoclast formation independently of RANKL by binding to CD80 and CD86 in the pre-osteoclasts[445]. Tregs also secrete anti-inflammatory cytokines like IL-4, IL-10 and TGFβ that also suppress osteoclastogenesis[446-448]. Recently, CTLA4 from Treg cells was reported to suppress *in vitro* osteoclastogenesis and recombinant CTLA4 was shown to reduce *in vivo* resorption in an arthritis model[449-450]. Tregs prevent the development of CIA which is accompanied by a decrease in serum levels of the pro-inflammatory cytokines TNF and IL-6. Moreover, anti-osteoclastogenic cytokines, such as GM-CSF, IFN-γ, IL-5 and IL-10 were drastically increased, suggesting that Treg cells not only inhibit osteoclastogenesis but also regulate cytokine production and improve clinical symptoms in the CIA mice model[451]. In another study, it was shown that blood markers of bone resorption inversely correlate with the amount of circulating Treg cells in healthy controls and RA patients, further demonstrating that Tregs may control bone destruction *in vivo*[452]. A reciprocal relationship was also found between Th17 cells and Tregs, suggesting that the factors that lead to the recruitment or survival of these two cell populations will lead to a predominance of either one of the subtypes. These data support the hypothesis that Th17 cells are key players in the pathogenesis of inflammatory arthritis and bone erosions[453]. Therefore, in pathological conditions, the effects of T cells on osteoclastogenesis depend on the balance between positive and negative regulating factors produced by them.

Naïve and memory B cells infiltrate and accumulate in the synovial tissue, where there is continuous activation of selected B cell clones with a high migratory capacity[454]. In addition to autoantibody production and immune-complex formation, B cell lineage also contributes to RA pathogenesis by the production of cytokines and chemokines such as IL-6, IL-10 and LT-β and through their role as antigen-presenting cells. Of interest, B cell depletion therapy with Rituximab[415] prevents the formation of ectopic germinal centres and the optimal activation of T cells[455] and markedly diminished clinical signs and symptoms of RA. Bone also interacts with B cells as RANKL is known to influence their development, increasing pro-B cell proliferation[456]. Progression of B cells along the lymphopoiesis requires physical contact with osteoblasts and stromal cells[457-459]. Interaction between B cell progenitors and stromal cells involves growth factors, chemokines and their receptors, among which chemokine (C-X-C motif) ligand 12 (CXCL12) and IL-17 are crucial[460-461]. In mice lacking CXCL12, the number of B cell progenitors is severely reduced in the bone marrow[461]. B cells from osteoporotic bone marrow show a higher density of RANKL than healthy individuals[335]. Moreover, it was reported that B cell progenitors have the ability of differentiating into osteoclasts *in vitro*, and peripheral blood B cells can support osteoclastogenesis[462]. B cells also cooperate with T cells in basal bone turnover. B cells regulate bone homeostasis through OPG production, which is promoted by T cells via CD40-CD40L costimulation. B cell knockout mice exhibit severe reduction in OPG levels and elevated bone resorption[420, 463]. Studies in animal models have shown that the loss of OPG increases pro and mature B cells, while the loss of RANKL or RANK has the opposite effect[464]. Moreover, in osteopenic mice B cell number decreased specifically by a reduction in the expression of CXCL12 and IL-7 by stromal cells, associated with lower osteoblastic engagement determined by the numbers of ALP positive cells[465].

Recent data increasingly implicate other innate immune response effector pathways in rheumatoid synovitis. Innate immune pathways remain of critical importance throughout the course of the disease[466]. Natural killer (NK) cells act as a bridge between the innate and the adaptative immune systems and respond to a variety of insults through cytokine secretion and cytolytic activity[467]. Recently, NK cells were shown to express both RANKL and M-CSF and appear frequently associated with $CD14^+$ monocytes in RA synovium. Moreover, when NK cells are co-cultured with monocytes, they trigger their differentiation into osteoclasts, in a RANKL and M-CSF dependent process. It was also shown that depletion of NK cells in CIA mice reduces the severity of arthritis and prevents bone erosion[468]. Mast cells are similarly implicated at the crossroad of innate and adaptative synovial immunity. They are widely distributed in rheumatoid arthritis synovial tissue and express several proteases and pro-inflammatory cytokines, including IL-17[469-470]. Neutrophils are present in high numbers in synovial fluid and traffic through the synovial membrane. Although their primary role in the pathology of RA is disputed, they synthesize a wide variety of cytokines including TNF, IL-1, IL-18, IL-15, IL-6 and B-cell activating factor (BAFF), and therefore could support a range of pathological events[471]. Neutrophils rapidly invade inflammatory sites where they act as first-responders by phagocytosis and release of toxic and pro-inflammatory molecules[472]. One of the most important chemotactic factors for neutrophils is IL-8, which is produced in response to inflammatory stimuli by osteogenic cells, linking osteoblasts with neutrophil infiltration[473]. Neutrophil-mediated inflammatory response appears to suppress osteoblastic differentiation from MSCs while enhancing chondrogenesis[474]. In addition, RA synovial fluid neutrophils strongly express RANKL and activate osteoclastogenesis in coculture systems and direct cell-cell contact between neutrophils and osteoclasts was observed[420, 475]. In another study, neutrophils from RA synovial fluid not only expressed

RANKL but also RANK and OPG, although peripheral neutrophils only express RANKL[476]. TNF is clearly of primary importance in the pathogenesis of rheumatoid arthritis[406]. This cytokine is present in most synovial biopsies and its inhibition suppresses several arthritis models, whereas overexpression of TNF induces spontaneous erosive inflammatory arthritis[477].

Immune cells have the ability to induce osteoclast differentiation and, consequently, bone resorption. These cells are also known for producing a variety of pro-inflammatory cytokines that contribute to bone damage by potentiating the effects of the RANK-RANKL signalling[405]. TNF, IL-1β, IL-3, IL-6, IL-7, IL-11, IL-15 and IL-17 potentiate bone loss either by increasing osteoclast generation and activation or by inducing RANKL expression on osteoblasts. On the other hand, IL-4, IL-5, IL-10, IL-12, IL-13, IL-18, IL-33, IFN-α, IFN-β and IFN-γ are inhibitors of osteoclastogenesis by blocking RANKL signalling[462]. IL-6 is an important monocyte-derived effector cytokine. Its levels were found elevated in synovial fluid of RA patients and were related to disease activity[411]. Moreover, IL-6 knockout mice are protected from developing joint symptoms in an arthritis model[478], and in humans blockade of the IL-6 signalling has been accomplished with an anti-IL-6 receptor (IL-6R) antibody (tocilizumab) with very good results[479-480]. IL-6 is a pro-inflammatory cytokine with pro-osteoclastogenic effects which not only contributes to the inflammatory response in RA but also induces osteoclast differentiation by promoting RANKL expression[481]. Blockade of IL-6R reduced osteoclast differentiation and bone resorption in monocyte cultures stimulated with RANKL. Moreover, IL-6R blockade in TNF-transgenic (tg) mice did not inhibit joint inflammation but strongly reduced osteoclast formation in swollen joints as well as bone erosions, suggesting an independent effect on bone metabolism[482]. Targeting IL-6R in a CIA mouse model results in a decrease in Th17 cells recruitment to the affected joint that is paralleled by a decrease in inflammatory activity[483]. In a CIA monkey model treated with tocilizumab, there was suppression of RANKL production and a decrease in the number of osteoclasts[484]. Moreover, patients with moderate to severe RA under tocilizumab therapy showed marked reduction in bone and cartilage degradation markers and an increase in bone formation four weeks after infusion[485]. IL-1α and IL-1β are expressed in the synovium of patients with RA[486] and, similar to the response in adjuvant arthritic rats, RA patients treated with IL-1Ra showed a modest anti-inflammatory activity[486-487]. Interestingly, IL-1β is a stimulator of TRAF6 expression in the osteoclast, thereby potentiating RANKL-RANK signalling cascade[488], whereas IFN-γ is known to downregulate TRAF6 by proteosomal degradation abrogating osteoclast formation[417]. IL-1β can also indirectly facilitate osteoclastogenesis by acting on the osteoblast inducing RANKL expression[430]. Arthritis in IL-1β-deficient mice is not associated with the occurrence of erosions[489-490], and even arthritic joint destruction of TNF-tg mice can be inhibited by anti-IL-1β-receptor antibody[491].

TNF favours leukocyte and endothelial cell activation, synovial fibroblast activation and survival, pain-receptor sensitization and angiogenesis, which together represent key pathological features of rheumatoid arthritis[406]. Therapeutic blockade of TNF yields clinical responses in approximately 60% of patients with established rheumatoid arthritis[492] and it results in a rapid decrease of IL-6 levels and acute-phase proteins, suppression of leukocyte migration and recovery of regulatory T cell function[443, 493]. Osteogenic differentiation of MSCs is blocked by IL-1β and TNF that not only suppress mineralization but also inhibit the expression of ALP, type I collagen, RUNX2 and OSX, blunting osteoblast formation[494]. Moreover, TNF increases proliferation and differentiation of pre-osteoclast in the presence of RANKL. TNF alone cannot induce osteoclast formation but combined with IL-1β[495] or TGFβ[496] it results in osteoclastic activity independent of RANKL. TNF is a potent inhibitor of osteoblast differentiation from its precursor cells, acting during the early stage of phenotype selection[497]. *In vitro*, TNF induces reduction in ALP activity, OCL expression and type I collagen synthesis[194]. Osteoblasts treated with TNF were also unable to regulate matrix mineralization[498].

Other factors contribute to the complex regulation of osteoclast differentiation. GM-CSF inhibits osteoclast differentiation by suppressing the transcription factors FOS and FOS-like antigen 1 (FRA-1), which would otherwise drive monocytes to differentiate into DCs[499]. Moreover, the combination of IL-4 and GM-CSF abolished monocytic differentiation into osteoclasts and induced DC differentiation, even in the presence of M-CSF and RANKL. GM-CSF and RANKL up-regulate TACE activity in monocytes, causing ectodomain shedding of M-CSF receptor, resulting in the inhibition of osteoclast formation[500]. The role of TGFβ on osteoclastogenesis is somehow controversial. TGFβ signalling, which primarily involves the Smad pathway, induces osteoclast apoptosis through up-regulation of BCL2-like 11 (BIM)[501]. On the other hand, the canonical TGFβ receptor complex is involved in the survival response and TGFβ-induced NF-κB activation is essential for TGFβ-mediated osteoclast survival[502]. Moreover, TGFβ induces osteoblast proliferation as an immediate response but decreases matrix production as a late response. Expression levels of osteoblast markers are down-regulated upon TGFβ stimulation and they acquire an osteoclast-recruiting phenotype[503]. In T cells, TGFβ by itself does not induce the expression of RANKL, but it can be synergistically induced by the combined stimulation with TGFβ and T cell receptor (TCR), significantly contributing to bone destruction during autoimmune arthritis[504].

Another important feature of rheumatoid synovitis is the deficiency of regulatory cytokines, which contributes to an imbalance between pro and anti-inflammatory stimuli in the joints. Therefore, although anti-inflammatory cytokines are expressed by synovial mononuclear cells, they are not present in sufficient concentrations to inhibit the dominant pro-inflammatory milieu[505].

Although M-CSF and RANKL are essential factors for osteoclast differentiation, it was hypothesized that costimulatory molecules like immunoglobulin-like receptors (PIR) are the third essential factor required for osteoclastogenesis (figure10). Among these molecules are OSCAR and PIR-A, that signals through FcRγ. Interestingly, OSCAR and PIR-A trigger receptors expressed on myeloid cells (TREM)-2 and signal-regulatory protein (SIRP)-β1[506], that signal through DNAX-activation protein 12 (DAP12)[507], and both activate an intracellular calcium cascade. This signalling leads to dephosphorylation of calcineurin, thereby activating the auto-amplification of NFATc1, which consequently promotes osteoclast differentiation[430]. Concordantly, DAP12-deficient mice develop osteopetrosis and *in vitro* osteoclast differentiation yield immature cells with attenuated bone resorption activity[507]. Moreover, DAP12$^{-/-}$ FcRγ$^{-/-}$ bone marrow cells fail to differentiate into multinucleated osteoclasts *in vitro* and show impaired phosphorylation of the Syk tyrosine kinase, suggesting that the recruitment of Syk to phosphorylated immunoreceptor tyrosine-based activation motif (ITAM) is critical for osteoclastogenesis[508]. Because DAP12 has no extracellular binding domain it must combine with a cell surface receptor for signal transduction. From the 15 different DAP12-associating receptors, DAP12-associating lectin (MDL)-1 receptor was identified as a key regulator of synovial injury and bone erosion during autoimmune joint inflammation[509]. Therefore, FcRγ and DAP12 are adaptor molecules that associate with immunoglobulin-like receptors helping their expression and transducing signals through ITAM[506, 510]. RANKL also interacts with ITAM by inducing its phosphorylation, thus increasing expression of PIR and enhancing ITAM signal[462].

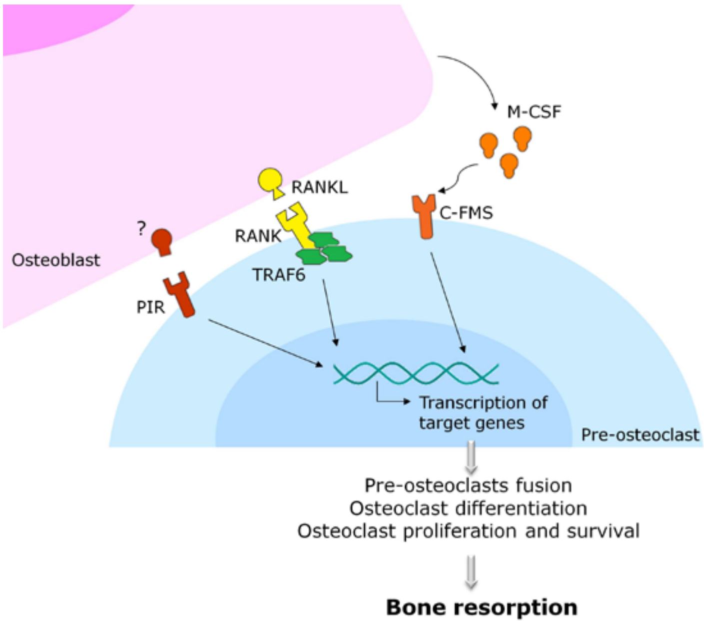

Figure 10 – *The three signals of osteoclastogenesis*.

Although RANK-RANKL and M-CSF are essential factors for osteoclastogenesis, currently it is believed that this process needs a third signal. This co-stimulation is mediated through immunoglobulin-like receptors present in the pre-osteoclast that are stimulated by a yet unknown ligand on the osteoblast.
(C-FMS - colony stimulating factor 1 receptor; M-CSF - colony stimulating factor 1 (macrophage); PIR - immunoglobulin-like receptor; RANK - receptor activator NF-κB; RANKL – RANK ligand; TRAF6 – tumor necrosis factor receptor-associated factor 6)

Further modulation of osteoclastogenesis is provided by TLRs. TLR expression was detected on bone cells and direct signalling through TLR activates a TRAF6 mediated cascade leading to the activation of transcription factors such as NF-κB and AP-1 family factors and to the synthesis and release of pro-inflammatory cytokines[456, 511-512]. However, the outcome of TLR activation depends on the stage of differentiation of the osteoclast. In early precursor cells, TLR inhibit osteoclastogenesis, but in cells that have already started to develop into osteoclasts TLR is a potent pro-osteoclastogenic factor. In mature osteoclasts, TLR signalling promotes cell survival. On the other hand, osteoblasts were also found to express TLR, namely TLR-4, TLR-5 and TLR-9, and exposure of these cells to pathogen-associated molecular patterns (PAMPs) induces the secretion of pro-inflammatory cytokines[511]. Moreover, TLR-9 is activated by CTSK, a protease expressed by osteoclasts and, although in low levels, in DCs. Inhibition of CTSK suppresses autoimmune inflammation in the joints as well as osteoclast-mediated bone resorption. Moreover, targeted disruption of CTSK resulted in defective TLR-9 signalling in DCs and attenuated induction of Th17 cells, suggesting that CTSK plays an important role in the immune system[513]. In fibroblast-like synoviocytes (FLS) from RA patients, TLR-2, TLR-3 and TLR-4 activation induces not only RANKL expression, but also production of IL-1β. However, it had no effect on IL-17 or TNF. Co-culture of monocytes with TLR-3 activated RA FLS, increased the expression of TRAP, RANK, CTSK, CALCR and MMP-9, reflecting the differentiation of monocytes into osteoclasts[514-515]. In fact, MMP-9 is strongly expressed in osteoclasts from RA patients and cleaves both soluble and insoluble type I collagen[516]. At the molecular level, TLR ligands suppressed osteoclastogenesis by inhibiting RANK expression and down-regulating the M-CSF receptor[517]. Therefore, TLRs contribute to the modulation of osteoclastogenesis by modulating the function of both osteoblasts and osteoclasts[511].

In RA joints, the presence of osteoclasts and pro-inflammatory cytokines leads to pathological bone destruction, joint damage and loss of function. Although an *in vitro* study showed that the capacity to generate osteoclasts varies greatly among individuals, RA patients presented significantly higher numbers and larger osteoclasts after 21 days of culture than controls[518] or patients with OP[519]. Higher osteoclast numbers associate with increased resorptive activity, further accounting for the excessive bone loss observed in RA[520]. Moreover, RA patients present both higher percentage of $CD14^+$ osteoclast precursors and lower apoptosis than the control group, suggesting that these two factors contribute to the large number of cells found in RA[518]. Osteoclasts formed from precursors obtained in RA patients show increased bone-resorbing activity compared to controls[521] and bone resorption by cells isolated from synovial fluid precursors was even higher[522]. In RA, there is little evidence of bone erosion repair, which is surprising considering that bone formation is coupled to bone resorption and increased rate of resorption should be accompanied with increased formation. Furthermore, in arthritic bone, mineralization of newly formed bone in areas adjacent to inflammation sites is reduced compared with bone surfaces adjacent to normal bone marrow, which suggest that the inflammatory tissue impairs osteoblast activity. In arthritic bone, there are abundant RUNX2-expressing cells but a limited number of cells expressing ALP and OCL indicating that osteoblasts have reduced capacity to form bone. Therefore, osteoblast activity at sites of focal bone erosion does not compensate the excessive osteoclastic resorption leading to an uncoupling of these two activities[523]. The sequence and quantity of bone formation is controlled both by the temporal regulation and the level of expression of DKK1[233]. Trabecular bone volume is increased in DKK1 mutant mice and is inversely proportional to the expression level of this protein. Trabecular number and thickness, as well as cortical thickness, are also increased in the low DKK1 expressing genotypes[524]. Inhibition of DKK1 was able to reverse the bone destruction observed in a mouse model of arthritis and to induce new bone formation. TNF was identified as the key inducer of DKK1 both in animal models and in human RA[525]. Indeed, both *in vitro* and *in vivo*, TNF increases DKK1 expression, blocking osteoblast differentiation, and inhibition of DKK1 not only rescued osteoblast formation but also neutralises TNF-mediated SOST expression in fully differentiated osteoblasts[526]. TNF increased the expression of inhibitors of the WNT signalling pathway such as DKK1 and SOST and could precipitate a destructive combination of low bone formation and high bone resorption[527]. Inhibitors of WNT, such as DKK1, are expressed in synovial fluid of RA patients, suggesting that bone formation is suppressed. Moreover, fully differentiated osteoblasts are rarely seen in arthritic bone erosions indicating that there is no major bone formation taking place in these lesions[523]. Low bone formation during inflammation may arise from impaired WNT signalling, which could also explain enhanced bone resorption, since active WNT signalling is associated with OPG expression[227, 527]. Increased DKK1 in rheumatoid arthritis patients treated with anti-TNF therapy was also associated with higher risk of progression of bone erosions independently of age, gender or disease activity[528]. It was recently found that DKK1 levels were correlated with markers of inflammation (C-reactive protein and erythrocyte sedimentation rate) and X-ray erosive score. Moreover, RA patients treated with anti-TNF (infliximab) or with IL-1Ra (anakinra) showed significantly lower levels of DKK1[529]. Ankylosing spondylitis (AS) patients have higher levels of DKK1 comparing with healthy individuals or patients with RA and psoriatic arthritis (PsA). However, DKK1 levels did not correlate with markers of inflammation or disease activity[530-531]. In a TNF transgenic mouse model, blockade of DKK1 had no effect on inflammatory sacroiliitis but reduced bone erosions and osteoclast number. Moreover, DKK1 blockade induced formation of hyperthrophic chondrocytes and fusion of the sacroiliac joints[532]. In another study, PsA patients presented higher levels of circulating DKK1 than healthy donors or patients with psoriasis and DKK1 levels were more increased in erosive PsA than in non-erosive disease[533]. On the other hand, it was reported that in caucasian women with more than 65 years of age enrolled in the Study of Osteoporotic

Fractures, high serum DKK1 levels were associated with a diminished risk of radiographic hip OA[534].

Like DKK1, SOST is an inhibitor of the WNT pathway. A study comparing bone SOST expression in AS, RA, OA and healthy individuals found that whereas the majority of osteocytes in healthy individuals and RA patients were SOST positive, the expression was reduced in OA patients and almost absent in AS. Moreover, the frequency of empty osteocyte lacunae was increased in RA patients compared to the other groups[535].

Recently, the WNT pathway modulator R-spondin homolog (RSPO1) was reported to be effective in the preservation of the joint structure in a TNF-tg model of arthritis. RSPO1 protected bone and cartilage by antagonizing DKK1 in mouse MSCs, while it induced differentiation and expression of OPG. Therefore, RSPO1 promotes osteoblast differentiation and osteoblast-mediated bone formation while blocking osteoclastogenesis during inflammatory arthritis.[536]

In summary, the immune system has several crosstalk points with the skeletal system, T and B lymphocyte interact with bone cells, cytokine and chemokine influence bone resorption, TLR signalling is activated, costimulatory molecules help osteoclast differentiation and WNT pathway is tightly controlled by immune system related molecules.

Bone is one of the few organs that retain the ability of regeneration in adult life. In fact, unlike other tissues that heal by formation of a poor quality scar, when a fracture occurs, bone restores all its pre-fracture properties.

Fracture healing recapitulates certain aspects of skeletal development and growth, involving the interplay of cells, growth factors and extracellular matrix. Each of the four stages of bone repair, inflammation, soft callus formation, hard callus formation and remodeling, is characterized by a specific set of events, although there is some overlap between them (figure 11).

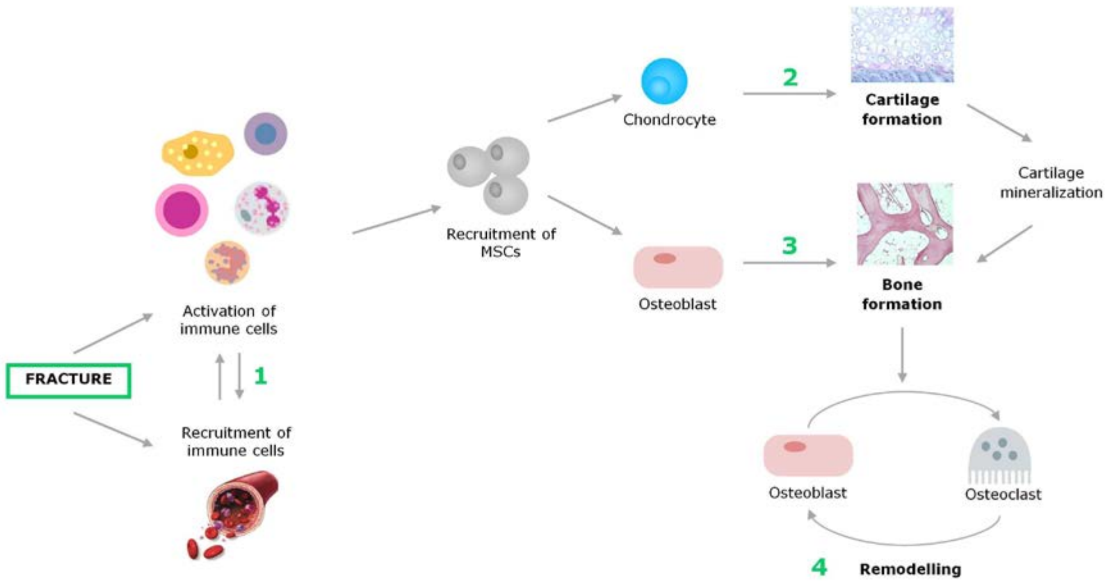

Figure 11 – *Cellular events of fracture healing*.

The fracture event leads to the activation of an inflammatory cascade (1), inducing the migration and activation of immune system cells that produce pro-inflammatory cytokines that recruit more immune cells and MSCs. These will then differentiate either in condrocytes or osteoblasts. Chondrocytes are responsible for cartilage synthesis and the soft callus formation (2) and osteoblasts produce bone and, consequently, the hard callus (3). In the final step, the newly formed bone is remodelled by the action of osteoclasts and osteoblasts in a coupled process (4). (MSC – mesenchymal stem cell)

At the cellular level, inflammatory cells, osteochondral progenitors and osteoclasts are the key players of the repair process[537]. Recently, osteal macrophages were found to be present at the injury site and to be required for collagen deposition and bone mineralization[538]. At the molecular level, fracture repair is mainly driven by pro-inflammatory cytokines and growth factors, pro-osteogenic and angiogenic factors[539].

Following injury, a local inflammatory reaction is triggered. Simultaneously, vasculature disruption occurs leading to the formation of a hematoma around the fracture site that becomes infiltrated by inflammatory cells[540-541]. Although the concentration of leukocytes in the fracture hematoma remains similar to the periphery for several hours after injury[542], within 24 hours there is a major influx of cells. The predominant leukocytes that infiltrate the tissue are neutrophils[474], which are later replaced by macrophages and T cells, whereas no B cells are found at any stage of fracture healing[543]. The hematoma is the source of several signalling molecules that induce an inflammatory cascade of cellular events that initiate healing[544]. These factors are secreted, not only by endothelial cells, platelets, macrophages, monocytes, but also by MSCs, chondrocytes, osteocytes and osteoblasts[541, 545]. Therefore, the hematoma contains cytokines and chemokines produced by the infiltrated inflammatory cells. Disturbance of this inflammatory phase impairs fracture healing. Indeed, in a rat femur fracture model the fracture hematoma was removed 30 minutes, 2 or 4 days after the injury, leading to a significant decrease in the mechanical characteristics of the new bone[546]. After inflammation, the fracture hematoma becomes osteogenic and angiogenic and this was demonstrated in a study where the transplantation of a 4-day-old hematoma into muscle tissue induced extraskeletal bone formation[547] and angiogenesis[548]. A recent study has shown, using a mouse model of slow-healing fracture, that covering the fracture with muscle cells accelerated healing and these cells differentiate into osteoblasts and formed bone nodules *in vitro*. Moreover, low concentrations of TNF recruited muscle-derived stromal cells for the fracture site, contributing for the initial phase of fracture healing[549]. Within several days of the initial inflammatory response, there is a sequence of events that results in the formation of new bone through a structure named callus. This is a newly developed tissue of fibrocartilage and bone that surrounds the fracture site[545]. Most fractures heal by a combination of intramembranous and endochondral ossification[550]. During the intramembranous ossification stage, bone is formed without the development of an intermediate cartilage tissue. The resulting structure is histologically described as hard callus[551]. This stage represents the most active period of osteogenesis and is characterized by high levels of osteoblast activity and bone matrix mineralization[537]. Endochondral ossification begins with chondrogenesis and involves recruitment and proliferation of MSCs that will later originate the avascular cartilage[541]. The soft callus, not only provides mechanical support for the fracture, but also acts as a scaffold for the bone that will be later formed[537]. The second process of endochondral bone formation, partially overlapping with the first, is a sequence of events that comprises cartilage calcification and removal, and bone formation. Chondrocytes release enzymes, proteases and phosphatases, which degrade proteoglycans and provide phosphate ions that precipitate in the extracellular matrix and, together with calcium released by mitochondria of hypertrofic chondrocytes, mineralize the cartilage[541]. Condrocytes undergo apoptosis and chondroclasts are formed and activated to resorb the mineralized cartilage matrix, which sends signals to enable vascularization of the newly formed tissue[552]. During the final stage, MMPs degrade cartilage and bone, allowing infiltration of blood vessels[551]. The differentiation and activity of osteoblasts allows the replacement of the calcified matrix with woven bone[541, 552]. The last stage of fracture repair is the replacement of the newly formed woven bone by the definitive tissue, the lamellar bone, and restoration of the normal vascular supply. BMUs require 1 to 4 years to replace woven by lamellar bone. The callus is then reshaped mainly by the action of osteoclasts that act to remodel the external surface of bone[541].

Although local controlled inflammation is essential for bone repair, evidence has shown that increased or prolonged inflammation within the fracture hematoma impairs fracture healing[540]. In a study, inflammation was induced by lypopolysaccharide (LPS) injection in rats with femur fractures. LPS is known to be a potent trigger of the inflammatory response and was administrated either locally at the site of fracture, or systemically by intraperitoneal injection. Both forms of administration led to larger but more immature callus production, with reduced bone mineral content (BMC) and BMD, suggesting that increased callus production appears to compensate for immaturity. Moreover, systemic administrated LPS reduced mechanical strength[553]. In another study, rats treated with anti-neutrophil serum showed decreased cartilaginous tissue markers such as SRY (sex determining region Y)-box 9 (SOX9) and type II collagen, along with increased expression of OCL and RUNX2[474]. Therefore, one can speculate that high neutrophil counts and neutrophil priming, leading to an increased influx of cells into the fracture hematoma, play an important role in the pathogenesis of impaired fracture healing after systemic inflammation. These findings suggest that neutrophils may stimulate chondrogenesis and inhibit osteogenesis and prolonged influx of neutrophils into the fracture hematoma during systemic inflammation may indeed impair fracture healing through stimulation of chondrogenesis. On the other hand, monocytes can differentiate towards several types of macrophages depending on the environmental circumstances. IFN-γ and LPS exposure induces a classically activated proinflammatory phenotype, while the regenerative phenotype is triggered by IL-4 or IL-13[554-555]. In addition, it has been shown that severe injury induces T cell unresponsiveness, characterized by both reduced proliferation and IL-2 production[556]. These findings indicate that unresponsiveness of T cells during systemic inflammation may also contribute to reduced osteogenesis after systemic inflammation. On the other hand, absence of γ/δ T cells improved fracture healing *in vivo,* through increased expression of bone and cartilage matrix proteins, as well as BMP-2 at a critical reparative phase. The result was improved stability at the repair site and an overall better biomechanical strength[557]. In summary, systemic inflammation induces several changes in leukocyte characteristics such as neutrophil priming, altered monocyte differentiation, T cell anergy and increased γ/δ T cell activation that influence bone healing.

Mononuclear cells and cell-free fluids from experimental wounds have shown to have immunosuppressive properties. Several cytokines were upregulated in a time-dependent manner in the fracture hematoma; IL-10 peaked in the first 24 hours after fracture, IL-6 in the first 48 hours, IL-8 after the first 48 hours and IL-12 on days 4-7. IL-6, IL-8, IL-10 and IL-12 levels could even be detected in the plasma of injured patients[558]. Indeed, cellular components, particularly the immune cell population of the fracture hematoma, changes very quickly within hours after fracture[542]. In order to better understand the cellular and molecular events in the initial phase of fracture healing, several studies have used animal models to evaluate the expression pattern during this process. IL-1, IL-6 and TNF are secreted by inflammatory cells and act as chemotactic factors for the recruitment of other inflammatory cells and MSCs. Tsangari *et al* studied a cohort of patients that suffered a fragility fracture of the femoral neck, and showed that the expression of IL-6 and RANKL/OPG ratio was increased in fracture patients as compared with age-matched controls. IL-6 mRNA expression correlated with RANKL, which reinforced the concept that IL-6 induces RANKL mRNA expression in osteoblasts[559]. In addition, studies in IL-6 knockout mice have shown that there was a delay in callus formation and lower osteoclast density[560]. IL-1β has a paradoxical effect, as it is upregulated in response to the fracture event, but in IL-1β knockout mice there is no change in callus formation and bone and cartilage matrix production[561]. On the other hand, in the absence of TNF signaling, there was a 2-4 days delay in chondrogenic differentiation and a 2-3 weeks delay in endochondral tissue resorption[562]. The expression of RANKL, OPG and M-CSF is increased after initial injury and later during the period of mineralized cartilage resorption. On the contrary, during the bone formation phase, RANKL, OPG and M-CSF are downregulated[563]. SOX9 is a key transcription factor for chondrogenesis that is expressed in the callus, together with RUNX1 and RUNX2. These transcription factors appear at an early fracture repair response and SOX9 is modulated by the mechanical microenvironment, influencing the fate decision between osteogenic and chondrogenic lineage commitment[564].

Platelets release platelet-derived growth factor (PDGF) and TGFβ play a role in initiating fracture repair by contributing for MSCs migration, activation and proliferation, angiogenesis, chemotaxis of inflammatory cells and further aggregation of platelets[565]. TGFβ is produced by osteoblasts and chondrocytes and induces the production of matrix proteins such as collagen, proteoglycans, OPN, osteonectin and ALP. FGFs are synthesized by immune cells, MSCs, osteoblasts and chondrocytes. These factors induce growth and differentiation of several cells, such as fibroblasts, myocytes, osteoblasts and chondrocytes. FGFs are present during the early stages of fracture repair where they play a crucial role in angiogenesis and MSCs proliferation[566]. Simultaneously, BMPs released by osteoprogenitor cells, osteoblasts and bone matrix induce the differentiation of MSCs into chondrocytes and osteoblasts, and osteoprogenitor cells into osteoblasts[551, 565]. Although BMPs are structurally and functionally related with each other, they present different temporal patterns of expression at different stages of fracture healing[551]. BMP-2 shows maximal expression within 24 hours of injury and its expression levels are maintained, suggesting that this factor is involved in initial callus formation[567]. In fact, in the absence of BMP-2, MSCs at the repair site do not differentiate and fracture healing is impaired[568]. On the other hand, expression of BMP-3, -4, -7 and -8 is restricted to the stage of calcified cartilage resorption and active osteoblastic recruitment. BMP-5 and -6 have a regulatory effect on both intramembranous and endochondral ossification and therefore, their expression is maintained from day 3 until day 21 post-fracture[550, 567]. BMPs may also stimulate the synthesis and secretion of other bone and angiogenic growth factors, such as vascular endothelial growth factor (VEGF) and IGF-I. IGF-I promotes bone matrix formation by inducing synthesis of type I collagen and noncollagenous matrix proteins by osteoblasts. IGF-II acts at a later stage of endochondral bone formation where it stimulates type I collagen production and cartilage matrix synthesis[551]. OPN, an extracellular matrix protein, plays an important role in angiogenesis and osteoclastic bone remodeling, two vital processes for bone healing. OPN deficiency *in vivo* altered but did not prevent bone healing and remodeling of fractures. The presence of OPN is essential for normal early callus formation, neovascularization and biomechanical strength and ductility. Moreover, OPN deficiency delayed the time-course of the remodeling phase in late stage healing[569]. Macrophage migration inhibitory factor (MIF) is a potent proinflammatory cytokine involved in the inflammatory response and its expression was reported to be upregulated during fracture healing in rats. MIF deficiency in a tibia fracture model showed worse mechanical behaviour, mainly due to increased osteoid volume, and delay in its mineralization within the fracture callus. These mice also presented lower number of osteoclasts, as well as suppression of MMPs, CTSK and ALP[570].

Some experimental studies made an effort to relate temporal gene expression with the sequence of events of bone healing. In a work with Sprague-Dawley rats, the gene expression on days 3 and 11 post-fracture was evaluated. The authors showed that different molecular pathways of gene expression regulate different phases of bone healing. At day 3 there was a predominance of cell proliferation and protein metabolism genes, as required for the proliferation of the periosteal mesenchymal cells of the soft callus. On the other hand, genes that predominated at day 11 were consistent with maturation of the callus during endochondral bone formation[571]. In C57bL/6 mice it was observed that the inflammatory cluster of genes was expressed from day 1 post-fracture until day 5. Chondrogenic phase started at day 4 and was prolonged for 7 days; finally, the remodeling phase started on day 10 post-fracture and was prolonged at least until day 21[572].

The contribution of the WNT/β-catenin pathway to fracture healing depends on the function of β-catenin in the different stages of fracture repair, namely in the commitment and regulation of osteoblasts[573]. Moreover, an *in vivo* study showed that the WNT pathway members (WNT5A, FZ2 and β-catenin) and the target genes [fibronectin, connexin 43, periostin (OSF-2) and retinoic acid receptor γ (RARG)] were upregulated in the fracture site. They also assessed other pathway members [WNT4A, WNT5B, dishevelled (DVL)1-3, TCF, LEF and LRP5] as well as target genes [homeobox protein engrailed-1 (EN-1), PPARδ and CD44] and found increased levels in the fractured bones, particularly at 5 days after fracture, when active bone and cartilage formation was occurring. The only exception was the transcription factor LEF, which was found downregulated between days 3 and 14, coinciding with the peak of osteoblast differentiation[574]. Since LEF inhibits RUNX2-dependent activation of OCL it is not surprising that this transcription factor is downregulated during fracture repair[575]. As healing progresses, at 21 days post fracture, the process of intramembranous ossification slows down and LEF expression is restored to the levels found in intact bone[574]. Therefore, the authors suggest a role for WNTs in the early stages of healing that involve intramembranous bone formation. The importance of WNT/β-catenin signaling was also reported by other groups[573, 576]. Tissue-specific inactivation of β-catenin in committed osteoblasts led to a significant reduction in calcified callus formation, along with incomplete bone bridging across the fracture gap. On the other hand, overexpression of β-catenin in committed osteoblasts enhanced fracture healing[573, 577]. Loss of the negative regulator axin2, a protein from the adenomatous polyposis coli (APC) complex that stabilizes β-catenin in the cytoplasm, results in prolonged amplification of the WNT signal and, consequently, on increased proliferation rate at the injury site. When WNT was supplied to the injury site after the initial inflammatory period, cells proliferated and accelerated their differentiation into osteoblasts and, consequently, stimulated bone healing[578-579].

Three recent studies analyzed the effect of DKK1 on bone healing in skeletally mature mice. Administration of DKK1 to the fracture site reduced β-catenin levels and inhibited chondrogenesis during the first week after fracture by blunting the expression of SOX9 and RUNX2. The fracture failed to heal and the injury site contained undifferentiated mesenchymal-like tissue[573]. In another report, DKK1 prevented activation of the WNT/β-catenin pathway during the first week of healing and reduced bone regeneration by 84%. DKK1 did not restrain angiogenesis or induce cell death at the repair site but suppressed the expression of osteogenic genes, specifically RUNX2[580]. A third report showed that DKK1 serum levels were increased during the second week of fracture healing, suggesting that DKK1 might be involved in slowing the anabolic response at later stages of bone repair[576]. Only one study in young mice has addressed the expression levels of SOST during fracture repair and they found that this protein was downregulated during the process[581]. In two recent studies, administration of a SOST monoclonal antibody in both rat and monkey models of fracture healing significantly increased bone mass and strength at the site of fracture. In monkeys, ten weeks after fracture, in the SOST antibody group callus presented less cartilage and smaller fracture gaps, containing more bone and fibrovascular tissue[582-583]. Overall, these data demonstrate the central role of β-catenin in orchestrating the cellular events that mediate fracture repair. DKK1 and SOST prevent the early stages of bone repair by blocking WNT/β-catenin signaling and the differentiation of MSCs into chondrocytes or osteoblasts[577].

The management of fragility fractures associated with osteoporosis is difficult due to several factors including inadequate fixation strength of implants used to stabilize the fracture until bone union occurs. In particular, the fragility fractures affecting the metaphyseal region of long bones are associated with an increased rate of complications. Several studies report nonunion in 2-10%, malalignment after surgery in 4-40%, metal work failure in 1-10%, and reoperation in 3-23% of the cases[584]. Experimental studies have shown that the decline in the capacity for fracture repair is age related. Disturbance of the full redevelopment of mechanical strength within fracture calluses in the elderly has been shown in experimental rat models[585-

[586]. In humans, it is possible that fracture healing is affected by aging, particularly in the elderly osteoporotic patients[587]. In a study it was described that in 6, 26 and 52 weeks old rats, there is a delay in radiographic progression of fracture healing upon aging but the expression of the key genes involved in this process is not age-dependent [584, 588-589]. Moreover, in another work the authors found age-related changes translated in delay in cell differentiation, decrease in bone formation, delay in angiogenesis and impairment of bone remodeling. However, they observed that the amount of cartilage formed in the fracture site was not affected by age[590]. While resorption augments with age, formation decreases, possibly due to lower number of osteoblasts[591]. Osteoblasts originate from MSCs that reside in the periosteum and bone marrow, together with hematopoietic stem cells. These two stem cell types cooperate with each other through direct cell-cell interactions; however, bone marrow environment changes with age resulting in unfavorable stimuli towards differentiation into osteoblasts. As an end result, total marrow fat increases with age and there is an inverse relationship between marrow adipocytes and osteoblasts with aging[592].

Bone turnover markers are widely used to monitor the course of callus consolidation during bone healing. Their levels vary throughout the course of fracture repair with changing rates dependent on the size of the fracture and the time it takes to heal. In a longitudinal study where the serum levels of biochemical markers associated with bone metabolism were assessed before, during and after fracture repair, the authors showed that a few hours after fracture there were no changes in bone turnover markers when compared to the levels measured before fracture. In opposition, markers of bone formation and resorption were significantly increased four months after fracture and bone turnover remained elevated up to 12 months after fracture[593]. In another study, authors observed that ALP levels increased only one week after surgery while bone resorption markers were increased immediately after fracture. Overall, bone turnover markers reached their peak values at 3-5 weeks after fracture, reflecting remodeling during the healing process[594]. Inhibition of osteoblast synthesis occurs after fracture, as shown by decreased levels of bone specific ALP and P1CP in the immediate post-fracture period. On the other hand, OCL was reported to be increased at this time and it is hypothesized that this represents the release of OCL from its bone-bound form[595]. The role of osteoclast in bone healing is somewhat controversial. In an *in vivo* study in sheep, authors found that resorption takes place in an early phase of fracture healing as observed by an increase in osteoclast density in the first six weeks after fracture. The authors hypothesized that osteoclasts not only resorb bone but they participate in the overall healing mechanism by maintaining and improving the structural strength of bone tissue[596]. This early phase healing was also measured in patients with tibial shaft fracture by bone turnover markers in order to identify patients with normal or delayed healing[597]. The authors found that in the first week after fracture, CTX levels decreased dramatically in the cases of delayed healing. By the fourth and eight weeks, the changes observed were a reduction in the value of TRAcP5b, whereas no changes were identified in the levels of ALP or P1NP[598].

The interplay between fracture healing and inflammation, highlight once more bone and immune system close relationship[599-601].

AIMS

The present work aims to address the interaction between skeletal and immune systems through the study of the effect of inflammation on bone biological, structural and mechanical behavior.

The specific aims of this work are:

I. Address to what extent biomechanical properties of bone are influenced by arthritis in an animal model;

II. Study the influence of arthritis on the trabecular bone collagen network in an animal model;

III. Compare bone gene expression between RA and primary OP patients, matched for BMD and major clinical fracture risk factors;

IV. Study the profile of genes involved in inflammation and bone remodeling during the three major steps of the early phase of callus formation in human bone after a hip fragility fracture.

RESULTS

In agreement with the Decreto-Lei 388/70, art. 8º, the results presented and discussed in this thesis were published or submitted for publication in the following scientific peer-reviewed journals:

I. **Caetano-Lopes J***, Nery AM*, Henriques R, Canhão H, Duarte J, Amaral PM, Vale M, Moura R, Pereira PA, Weinmann P, Abdulghani S, Souto-Carneiro M, Rego P, Monteiro J, Sakagushi S, Viana Queiroz M, Konttinen YT, Graça L, Vaz MF, Fonseca JE. Chronic arthritis induces quantitative and qualitative bone disturbances leading to compromised biomechanical properties. *Clinical and Experimental Rheumatology* 2009, 27(3):475-482

   (*Caetano-Lopes J and Nery AM contributed equally for this work)

II. **Caetano-Lopes J**, Nery AM, Canhão H, Duarte J, Cascão R, Rodrigues A, Perpétuo IP, Abdulghani S, Amaral PM, Sakaguchi S, Konttinen YT, Graça L, Vaz MF, Fonseca JE. Chronic arthritis leads to disturbances in the bone collagen network. *Arthritis Research and Therapy* 2010 15; 12(1):R9

III. **Caetano-Lopes J**, Rodrigues A, Lopes A, Vale AC, Pitts-Kiefer MA, Vidal B, Perpétuo IP, Monteiro J, Konttinen YT, Vaz MF, Nazarian A, Canhão H, Fonseca JE. Rheumatoid arthritis bone fragility is associated with increased DKK1 expression and disturbances in the bone turnover regulating genes. Submitted for publication in May 2011.

IV. **Caetano-Lopes J**, Lopes A, Rodrigues A, Fernandes D, Perpétuo IP, Monjardino T, Lucas R, Monteiro J, Konttinen Y, Canhão H#, Fonseca JE#. Upregulation of Inflammatory Genes and Downregulation of Sclerostin Gene Expression Are Key Elements in the Early Phase of Fragility Fracture Healing. *PLoS ONE* 2011 6(2): e16947. doi:10.1371/journal.pone.0016947

PART I

Chronic arthritis induces quantitative and qualitative bone disturbances leading to compromised biomechanical properties

Chronic arthritis directly induces quantitative and qualitative bone disturbances leading to compromised biomechanical properties

J. Caetano-Lopes[1], A.M.Nery[1,2,3], R. Henriques[4,5], H. Canhão[1,6], J. Duarte[7,8], P.M. Amaral[2,3], M. Vale[1,9], R.A. Moura[1], P.A. Pereira[1], P. Weinmann[1], S. Abdulghani[1], M. Souto-Carneiro[8], P. Rego[9], J. Monteiro[9], S. Sakagushi[10], M.V. Queiroz[6], Y.T. Konttinen[11], L. Graça[7,8], M.F. Vaz[2,3], J.E. Fonseca[1,6]

[1]Rheumatology Research Unit, Instituto de Medicina Molecular, Faculdade de Medicina da Universidade de Lisboa, Lisbon, Portugal; [2]Instituto de Ciência e Engenharia de Materiais e Superfícies, Instituto Superior Técnico, Lisbon, Portugal; [3]Departamento de Engenharia de Materiais, Instituto Superior Técnico, Lisbon, Portugal; [4]Unidade de Biologia Celular, Instituto de Medicina Molecular, Faculdade de Medicina da Universidade de Lisboa, Lisbon, Portugal; [5]Instituto de Sistemas e Robótica, Instituto Superior Técnico, Lisbon, Portugal; [6]Serviço de Reumatologia e Doenças Ósseas Metabólicas, Hospital de Santa Maria, Lisbon, Portugal; [7]Cellular Immunology Unit, Instituto de Medicina Molecular, Faculdade de Medicina, Universidade de Lisboa, Lisbon, Portugal; [8]Instituto Gulbenkian de Ciência, Oeiras, Portugal; [9]Serviço de Ortopedia, Hospital de Santa Maria, Lisbon, Portugal; [10]Department of Experimental Pathology, Institute for Frontier Medical Sciences, Kyoto University, Kyoto 606-8507, Japan; [11]University of Helsinki, ORTON Orthopaedic Hospital of the Invalid Foundation, Helsinki, COXA Hospital for Joint Replacement, Tampere, Finland.

Abstract

Objectives

Rheumatoid arthritis (RA) is associated with an increased risk of fragility fractures. In RA patients, the direct effect of inflammation on bone is difficult to study because their skeleton is also affected by medication with corticosteroids and other drugs as well as aging and menopause, which contribute to bone fragility. This study used an animal model of chronic arthritis to evaluate the direct impact of chronic inflammation on biomechanical properties and structure of bone.

Methods

In the SKG mouse chronic arthritis model three point bending tests were performed on femoral bones and compression tests on vertebral bodies. Collagen structure was analysed using second-harmonic generation (SHG) imaging with a two-photon microscope, ultramorphology by scanning electron microscopy (SEM) coupled with energy dispersive x-ray spectroscopy (EDS) and bone density using water pycnometer.

Results

Arthritic bones had poor biomechanical quality compared to control bones. SHG, SEM and pycnometry disclosed variable signs of impaired collagen organization, poor trabecular architecture and low bone density.

Conclusion

Present data demonstrate for the first time that chronic inflammation per se, without confounding influence of drugs and aging, leads to impairment of bone biomechanics in terms of stiffness, ductility and ultimate strength (fracture).

Key words

Rheumatoid arthritis, SKG mice, osteoporosis, bone, mechanical tests, multiphoton microscopy.

Clinical and Experimental Rheumatology 2009; **27**: 475-482.

*Joana Caetano-Lopes, PhD student**
*Ana Margarida Nery, MSc**
Ricardo Henriques, PhD student
Helena Canhão, MD, PhD
Joana Duarte, PhD student
Pedro M. Amaral, PhD
Mário Vale, MD
Rita A. Moura, PhD student
Patrícia A. Pereira, MSc
Pamela Weinmann, PhD
Saba Abdulghani, PhD
Margarida Souto-Carneiro, PhD
Paulo Rego, PhD
Jacinto Monteiro, MD, PhD
Shimon Sakaguchi, PhD
Mário Viana Queiroz, MD, PhD
Yrjö T. Konttinen, MD, PhD
Luís Graça, MD, PhD
Maria Fátima Vaz, PhD
João Eurico Fonseca, MD, PhD

**Both authors contributed equally to this study.*

This work was supported by the PTDC/SAU-BEB/65992/2006 grant from Fundação para a Ciência e Tecnologia.

Please address correspondence and reprint requests to:
João Eurico Fonseca,
Rheumatology Research Unit,
Instituto de Medicina Molecular,
Edifício Egas Moniz,
Faculdade de Medicina da Universidade de Lisboa, Av. Professor Egas Moniz, 1649-028 Lisboa, Portugal.
E-mail: jefonseca@netcabo.pt

Received on November 19, 2008; accepted in revised form on March 3, 2009.

Conflict of interest: Dr Y.T. Konttinen has received support from the Sigrid Jusélius Foundation, evo grants, Finska Läkaresällskapet and the ORTON Foundation; the other co-authors have declared no competing interests.

Introduction

Rheumatoid arthritis (RA) is a chronic inflammatory disease, of unknown aetiology, which affects around 1% of the world-population (1). Bone erosions can develop in the first few months of the disease. These bone erosions are caused by the inflammatory synovial membrane, which attaches to the joint surface (*pannus*) and invade cartilage and bone (2). Recent evidences suggest that bone remodelling disturbances also contribute to bone erosions and in particular to the development of secondary osteoporosis (OP). In fact, RA patients have an increased risk of vertebral fractures, which is independent from bone mineral density and corticosteroid use (3). In addition, an elevated hip fracture risk was also noted in RA patients not exposed to corticosteroids (4). Thus, RA seems in itself to predispose to fractures although the underlying mechanisms and their effects on bone are not completely understood yet.

The connection between OP and RA can be partially explained by the activation of the Receptor Activator of Nuclear Factor κB (RANK) by RANK Ligand (RANKL) (5) produced by activated T lymphocytes (6) and osteoblasts (7). This activates signalling leading to pre-osteoclast priming and osteoclast activation, which contribute to the formation of bone erosions and reduction of the bone mineral density. RANK/RANKL interaction is antagonised by osteoprotegerin (OPG) (5), a soluble decoy receptor. In RA the RANKL/OPG ratio is increased (8).

Osteoclasts dissolve mineralized bone matrix (mainly hydroxyapatite crystals) and destroy the exposed non-mineralized organic bone matrix (mainly type I collagen) (9). However, it is not clear if, how, and to what extent the bone structure itself is affected by inflammation although it is known that the arrangement of bone trabeculae and the orientation of collagen fibres and hydroxyapatite crystals in relation to load play an important role for bone strength (10). The main objective of the present work was to study to what extent the biomechanical properties of bone are influenced by the destructive arthritic changes.

Due to multiple confounding factors involved, like the use of glucocorticosteroids and other drugs as well as aging and hormonal changes, it is difficult to specifically study the effect of arthritis *per se* on the structure and biomechanics of bone in RA. The use of a mouse model of chronic arthritis would reduce such variability and allow access to bones for *ex vivo* testing. Animal models are already widely used in the development of new drugs for OP (11). The recently described SKG mouse arthritis model resembles in many aspects human RA. These mice develop a rheumatoid factor positive, erosive chronic polyarthritis that affects both large and small joints and present some of the systemic features of RA. The SKG mouse has a BALB/c background (12) with a single recessive point mutation in the ZAP-70 gene, a G→T substitution that alters codon 163 from tryptophan to cystein. This gene encodes a protein, which has an important role for T cell signal transduction and its mutation leads to changes in the thymic selection threshold. As a result SKG mice maintain otherwise negatively selected autoreactive T cell clones. Unlike their normal BALB/c counterparts, SKG mice are genetically prone to spontaneously develop chronic polyarthritis, the onset of which can be precipitated by zymosan or by other dectin-1 agonist (12, 13). This experimental arthritis model was used to study the direct effect of chronic arthritis on bone structure and biomechanics.

Material and methods

SKG arthritis model and BALB/c controls

Twenty-five female SKG and sixteen female BALB/c mice were bred and maintained under pathogen free conditions. All experiments were conducted according to the guidelines from the Animal User and Institutional Ethics Committee. A single intraperitoneal injection of 2mg of zymosan (Sigma-Aldrich Co, USA) was administered at 2 months of age. Joint swelling was monitored by inspection as follows: 0, no joint swelling; 0.1, swelling of one finger joint; 0.5, mild swelling of wrist or ankle; and 1.0, severe swelling of wrist or ankle, with a range of the total sum score varying from 0 to 5 (12). At five months the SKG and BALB/c mice were sacrificed and femoral bones and vertebrae were dissected free of soft tissues and stored at -20°C. Immediately before testing, the samples were defrosted at room temperature.

Mechanical testing

All mechanical tests were performed using a universal testing machine (Instron 5566™, Instron Corporation, Canton, USA) with a load cell of 500 N. The biomechanical strength variables were displayed in stress-strain curves by the Bluehill 2 Software (Instron, Copyright 1997-2007) and analysed using MatLab 7.1 software (R14 SP3, The Mathworks, Inc, Copyright 1984-2006). The software has the ability to build stress-strain representations from load-displacement points, once initial dimensions are provided for each specimen.

Femoral bones were submitted to three-point bending tests (Fig. 1A) and vertebrae to compression tests (Fig. 1B).

For three-point bending tests the span between the outer loading points was 5 mm with the load being applied to the centre of the femoral shaft at a cross-head speed of 0.01 mm/s. The parameters analysed from the stress-strain curves were Young's modulus (E), yield stress (σ_y), ultimate stress (σ_u), ultimate strain (ε_u) and work/energy until ultimate stress (W_u) (Fig. 1C).

The second (L2) and fourth (L4) lumbar vertebrae were used for compression tests. In these tests a cross head speed of 0.01 mm/s was used, and then obtained Young's modulus (E), yield stress (σ_y), maximum stress (σ_M), work until yield stress (W_y) and work until maximum stress (W_M) (Fig. 1D).

Assuming that femurs behave like cylinders (14), stress-strain curves can be built according to the following equations (1 and 2):

$$\sigma = \frac{L \cdot s}{\pi\left(\frac{d_f}{2}\right)^3} \quad (Pa) \qquad (1)$$

$$\varepsilon = \frac{12\left(\frac{d_f}{2}\right)\Delta l}{s^2} \cdot 100 \quad (\%) \qquad (2)$$

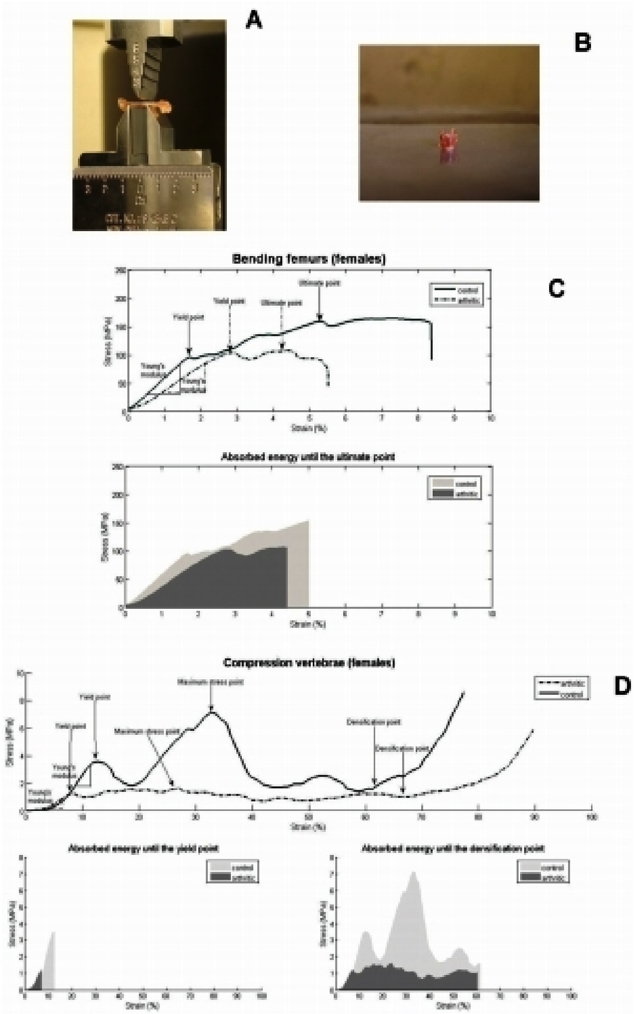

Fig. 1. Experimental setup and stress-strain representations obtained after mice femurs bending and vertebrae compression. Images of a three point bending test setup (A), and a vertebra standing on the inferior plate of a compression test setup (B). Femurs (arthritic and control) bending curves (C) were obtained in order to determine the analysed parameters directly from the graphic: Yield point=(yield strain, yield stress) and Ultimate point=(ultimate strain, ultimate stress), or after calculations:
Young's modulus – slope of the curve between the origin and the yield point;
Energy until ultimate point – area under the graphic from the origin until the ultimate point, calculated using trapezoidal numerical integration.
Vertebrae (arthritic and control) compression curves (D) were obtained from the mechanical test in order to determine the analysed parameters directly from the graphic: First yield point=(first yield strain, first yield stress), Second yield point = (second yield strain, second yield stress) and Densification point = (densification strain, densification stress), or after calculations:
Young's modulus – slope of the curve between the origin and the first yield point;
Energy until first yield, or densification points – area under the graphic from the origin until the first yield point or until densification point, calculated using trapezoidal numerical integration.

Where σ - stress (Pa); L = load (N); s = support span (mm); d_f = femoral outer diameter (mm); ε = strain (%); Δl = displacement (mm).

All the calculations were done for the middle cross-section area, applied to the centre of the femoral shaft, by the upper load support. From these curves the mechanical parameters were read, except for the Young's modulus, which was obtained from the slope of the elastic regime of the stress-strain curves, and the energies absorbed until determined points that were calculated using trapezoidal numerical integration, with using MatLab 7.1 software.

For vertebrae, compression tests were made (14). Equations (3 and 4) show how stress-strain curves can be obtained, assuming that a cylinder, of homogenous material, is being compressed:

$$\sigma = \frac{L}{\pi\left(\frac{d_v}{2}\right)^2} \quad (Pa) \tag{3}$$

$$\varepsilon = \frac{\Delta h}{h_0} \cdot 100 \quad (\%) \tag{4}$$

Where d_v = vertebral diameter (mm); h_0 = initial vertebral height (mm); Δh = compression suffered by the vertebra (displacement) (mm).

As for femurs, the biomechanical parameters were read from the stress strain curves and the Young's modulus as well as the energies calculated using MatLab 7.1 software.

Even though, in this paper, all the vertebrae tested refer to the same lumbar position (L2 and L4) and the long bones were all femurs, there was always variability in dimensions associated with the fact that each bone comes from a different animal. In order to normalize this parameter, and allow all samples to be compared against each other, instead of load (L) – displacement (d) values, we used stress (σ) – strain (ε) representations. Stress is the load applied on a sample, per area unit (a) (equations 1 and 3), and the strain is the deformation suffered, when compared with the initial dimension of the bone (equations 2 and 4).

In this study it was assumed that both femurs and vertebrae were similar to cylinders, but with different orientations and dimensions, according to the mechanical test (three point bending for femurs and compression for vertebrae) performed in each case.

In this way, the results from the control and arthritic groups could be compared between each other, even if the dimensions were different, because this effect was already contemplated in the stress-strain analysis.

Second-harmonic generation and two-photon excitation microscopy

Mice vertebrae and femurs were decalcified, embedded in paraffin, cut to 7µm sections using a microtome and deparaffinised to be inspected in a Zeiss LSM510 META laser scanning microscope featuring a Coherent Mira 900 femtosecond multiphoton excitation laser. Multicolour nonlinear microscopy of collagen was done through second-harmonic generation (SHG) using two-photon excitation (TPE). The signal was acquired by two opposing detectors: 1) the META spectral detector configured for bandpass detection between 390-430 nm collecting light from a Zeiss Fluar 20x/0.75 objective; this signal was associated with a green look up table (LUT) and is referred to as backward-SHG and 2) the non-descanned detector (NDD) collecting light from a Zeiss 0.8 numerical aperture (NA) condenser and filtered by a 390-430 nm bandpass filter; this signal was associated with the blue LUT and is referred to as forward-SHG. The backward-SHG channel detects the backscattered SHG signal and the forward-SHG channel the SHG receives the photons that are transmitted through the sample (15). The wavelength of the laser was set to 820 nm. The Jefferies' method (16) was applied to all acquired images to quantify the amount of trabecular area occupied by collagen detected by the forward-SHG channel (essentially mature polymerized collagen) and by collagen detected by the backward-SHG channel (mainly immature collagen fibril segments, indicating ongoing fibrillogenesis) (17).

Image analysis was done using NIH ImageJ software (W. Rasband, National Institute of Health, Bethesda, USA) by applying a 40-255cps intensity threshold for each channel to cover only the extracellular collagen matrix. All the trabecular area was covered using a lower 20-255cps threshold.

Scanning electron microscopy

Bone samples were inserted into an epoxidic and transparent resin and mounted in a mixture of Résine Mecaprex MA2 (04008) and Durisseur pour résine Mecaprex MA2 (Presi SA. Tavernolles, 38320 Brie & Angonnes, France) in 100:12 ratio. After 24 hours the surfaces of the vertebrae samples were polished using grid papers with 1000, 800, 600, 320 and 200 µm granulometries. After deposition of a uniform and thin gold layer the samples were observed with an electron beam energy of 25 keV in a scanning electron microscope (Hitachi model S2400 SEM. Hitachi, Ltd. Tokyo, Japan).

The images obtained were analysed with the software ImageJ, already mentioned for the MPM images. In this case the region of interest was the vertebral body, where pictures were taken and parameters such as the area occupied by trabeculae (%), inter-trabecular distance (µm), trabecular thickness (t^-, µm) and cortical thickness (c^-, µm) were determined. These measurements were made according to Heyn's and Jefferies' methods (16).

Energy dispersive x-ray spectroscopy

The energy dispersive x-ray spectroscopy (EDS) analysis was performed to measure the proportion of calcium and phosphorus in the bone samples using an analytical SEM with Rontec standard EDS detector (Hitachi S2400, Tokyo, Japan).

Density measurements

The densities of both femoral bones and vertebrae were measured prior to mechanical testing with a water pycnometer. The pycnometer was filled with water, with corrections being made to the ambient temperature following the Archimedes' principle. Bone density was calculated using equation (5):

$$\rho = (m_1 - m_0)\rho_L \frac{1}{(m_3 - m_0) - (m_2 - m_1)} \tag{5}$$

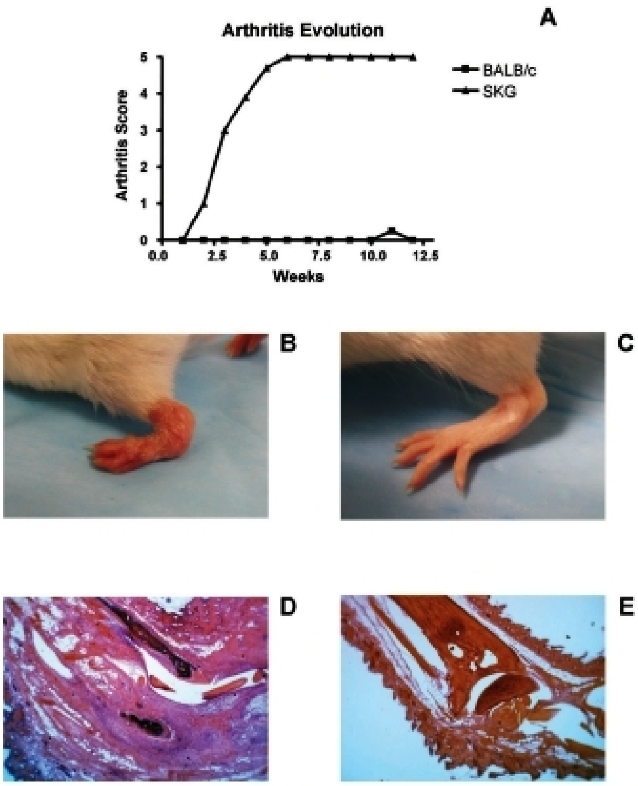

Fig. 2. SKG mice developed a severe destructive polyarthritis after zymosan injection. Joint swelling was monitored by inspection and scored as follows: 0: no joint swelling; 0.1: swelling of one finger joint; 0.5: mild swelling of wrist or ankle; and 1.0: severe swelling of wrist or ankle. Scores for all fingers and toes, wrists and ankles were totalled for each mouse. Graph (A) shows that the scores evaluation started at week zero and peak in the arthritis group at week 6 (squares and triangles represent median scores). BALB/c mice did not develop arthritis (C, E) and were used as controls to SKG mice (B, D), which showed evident swelling of the ankle joints and an erosive synovitis at 5 months of age (haematoxylin and eosin staining, magnification ×400).

Where ρ - bone density; ρ_L - water density at ambient temperature; m_0 - mass of the empty pycnometer; m_1 - mass of the pycnometer and the bone sample; m_2 - mass of the pycnometer, the bone sample and water; m_3 - mass of the pycnometer filled with water.

Statistical analysis
Results were represented by mean and standard deviation values. According to their distribution either t test for independent-samples or non–parametric Mann-Whitney test were used to compare continuous variables. Significance level was set at 0.05. Statistical analyses were performed using the Statistical Package for Social Sciences (SPSS) Manager software (SPSS, Inc, Chicago, IL, USA).

Results
Female SKG mice develop chronic arthritis
Twenty-five female SKG mice, injected with a single intraperitoneal injection of 2mg of zymosan at two months of age, developed chronic arthritis (in small and large joints) after one week and reached peak activity by the sixth week. By the time of sacrifice (5 months of age), the SKG mice had approximately 3 months of disease activity and all had a clinical score of 5. Inflammatory joint infiltration was severe and destructive (Fig. 2). The sixteen control BALB/c mice, after the 2mg zymosan injection, did not develop arthritis. These two strains of mice are identical, differing only in a point mutation in the ZAP-70 protein that only affects the selection of T lymphocytes in the thymus. BALB/c mice are widely used as a control for SKG mice.
A significant reduction in body weight of the SKG mice was observed in comparison to the BALB/c mice (18.60±1.04g and 24.08±0.81g respectively, $p<0.001$).

Chronic arthritis reduces mechanical properties of femurs and vertebrae
Mechanical 3-point bending test results (Table I and Fig. 1C) showed that arthritic femurs have a significantly lower: elastic (Young's) modulus (reflecting reduced stiffness), yield stress (less force was needed to cause the first microfractures and to start a plastic and definitive deformation of bone), ultimate stress (reflecting the maximum strength of the bone at fracture) and energy until ultimate stress (reflecting the energy required to cause fracture, thus the toughness of the bone) as compared to control femurs.
In the case of vertebrae compression tests (Table II and Fig. 1D), significant differences were found between arthritic and control L2 and L4 vertebras with regards to elastic (Young's) modulus, yield stress, ultimate stress and energy until yield stress, as compared to control vertebrae.

Bone collagen content is preserved during chronic arthritis
The SHG technique with MPM was not appropriate for the study of cortical bone as the images produced were homogenous and did not allow us to characterize the presence and organization of collagen molecules. However, images obtained in vertebral trabecular bone were very informative. Five control and 5 arthritic vertebrae were used to study bone collagen

Table I. Mean and standard deviation values calculated from mechanical tree-point bending test of mice female femurs.

	SKG mice (n=9)	BALB/c mice (n=8)	*p*-value
Diameter (mm)	1.10 ±0.03	1.04 ± 0.02	0.001**
Stiffness (N/mm)	147.65 ± 18.87	197.84 ± 27.55	<0.001**
Yield stress (MPa)	108.68 ± 18.12	221.35 ± 62.72	0.001**
Ultimate stress (MPa)	171.57 ± 33.06	289.12 ± 48.28	<0.001**
Young's modulus (GPa)	6.79 ± 1.16	11.36 ± 1.96	0.001*
Ultimate strain (%)	5.69 ± 1.40	5.80 ± 1.50	0.564*
Energy until ultimate stress (N.mm/mm³)	5.16 ± 2.32	8.30 ± 2.58	0.019**

Values are mean ± standard deviation.
*Mann-Whitney test.
**Independent-samples *t*-test.

content and structure. Quantitative image analysis of the collagen content showed no statistical differences between BALB/c control mice and SKG arthritic mice (Fig. 3A and 3B). The calculated percentage of collagen occupied areas depicted by forward-SHG channel in SKG and control vertebrae were 40.87±6.89% and 47.00±14.26%, respectively. This percentage was very similar to the one obtained by using the backward-SHG channel (52.81±6.05% and 53.90±11.03% for arthritic and control samples, respectively) (Fig. 3C). These percentages have to be calculated separately, as the channels in this imaging technique are individually analysed, so there is no direct correlation between values found for each group from the two channels. Furthermore, the ratio of mature collagen to immature collagen (the percentage obtained in the forward-SHG channel dividing by the one obtained in the backward -SHG channel) was of 0.775±0.179 for arthritic animals and 0.907±0.363 for control bones (*p*-value of 0.372).

As mature polymerised collagen has a signal present predominantly in the forward-SHG channel and amorphous collagen fibril segments in the backward-SHG channel one can assume that the relative distribution of these two types of collagen and the total amount of collagen per bone surface are equivalent in the arthritic and control groups. However, qualitative analysis of mice vertebrae using SHG microscopy revealed structural differences in the mature collagen organization in the arthritic group images in comparison to controls. In fact, in the SKG mice (arthritic group) areas of a nodular pattern in the collagen organization were observed among the longitudinal fibrils of the mature collagen (Fig. 3A and 3B).

Vertebrae from arthritic mice have a higher inter-trabecular distance and a decreased trabeculae thickness

In arthritic SKG mice vertebrae the trabeculae thickness was reduced giving rise to an increased inter-trabecular distance in comparison to BALB/c mice vertebrae, as highlighted by SEM images (Table III and Fig. 4). Moreover, vertebral cortical thickness was significantly lower in the SKG bone as compared to the controls. However, the trabeculae area, as assessed by SEM, was similar between the 2 groups.

Chronic arthritis reduces bone density

The density measurements were lower in the arthritic group as compared to the control group (Table IV). These results were statistically different for femurs and L2 vertebrae.

Mineral bone composition is not affected by arthritis

The results from the EDS analysis did not reveal any significant difference in the bone mineral composition in terms of calcium and phosphorous proportion between the arthritic and control bone samples, both in femurs (arthritic femur: calcium = 73% (72-75%) and phosphorus = 27% (25-28%); control femur: calcium = 73% (73-74%); and phosphorus = 27% (26-27%); no statistically significant differences between groups) and in vertebrae (arthritic vertebrae: calcium = 72% (42-79%) and phosphorus = 28% (21-58%); control vertebrae: calcium = 71% (52-79%);

Table II. Mean and standard deviation values calculated from mechanical compression stress-strain curves of female mice vertebrae L2 and L4.

	L2			L4		
	SKG mice (n=7)	BALB/c mice (n=6)	*p*-value	SKG mice (n=7)	BALB/c mice (n=5)	*p*-value
Height (mm)	2.82 ± 0.39	3.28 ± 0.46	0.077*	3.23 ± 0.25	3.67 ± 0.30	0.015*
Diameter (mm)	2.99 ± 0.15	2.97 ± 0.14	0.824*	2.82 ± 0.14	2.96 ± 0.07	0.063*
Young's Modulus (MPa)	20.17 ± 4.74	42.60 ± 18.70	0.007**	16.81 ± 2.33	30.29 ± 16.28	0.138*
Yield stress (MPa)	2.14 ± 0.61	3.85 ± 1.39	0.029*	2.06 ± 1.08	4.45 ± 1.83	0.028**
Energy until yield stress (Nmm/mm³)	0.13 ± 0.08	0.22 ± 0.10	0.109*	0.12 ± 0.09	0.30 ± 1.15	0.028**
Maximum stress (MPa)	4.73 ± 0.92	6.89 ± 1.58	0.015**	3.35 ± 1.09	6.13 ± 0.87	0.005**
Energy until maximum stress (Nmm/mm³)	1.13 ± 0.68	1.10 ± 0.54	0.668**	0.66 ± 0.15	0.57 ± 0.17	0.268**

Values are mean ± standard deviation.
*Mann-Whitney test; **Independent-samples *t*-test.

and phosphorus = 29% (24-48%); no statistically significant differences between groups).

Discussion

It is well established that RA is associated with secondary osteoporosis and an increased risk of fractures. This is apparently the end result of multiple factors, such as the use of corticosteroids, aging, menopause and inflammation. Thus, the direct contribution of the effect of chronic inflammation on bone in RA patients is difficult to assess. The primary aim of this study was to assess the influence of chronic inflammation in the SKG mouse chronic arthritis model on the biomechanical strength of the bone. The secondary aim was to study femoral bones and vertebral bodies, using new methods to assess the effect of chronic inflammation on the collagen and mineral structure of bone tissue. This is the first report in the literature demonstrating a deleterious and direct effect of chronic inflammation *per se* on the biomechanical quality of bone. This may in part clarify the increased fracture risk in RA patients.

Due to the anatomical qualities of the femoral bones and vertebral bodies it was necessary to use two different types of tests to measure their biomechanical strength. First, the femoral bones were tested using a three point bending test. In this test increasing force is applied to the femoral shaft using a cross-head. This leads first to fully elastic deformation of the bone so that if the force is released, the bone assumes its former shape. This property of the bone is usually expressed as its elastic Young's modulus and the maximum stress still enabling such reversible changes is referred to as the yield point. When more stress is applied, bone tissue starts to undergo microfractures and truly irreversible plastic changes occur, as it is characteristic of a ductile material. Upon release of the stress force, it can be observed that the morphological bone changes are now permanent. The maximum stress the bone can tolerate without breakage reveals its ultimate strength, after which a macroscopic fracture soon follows. In this study, it was for the first time shown that arthritic

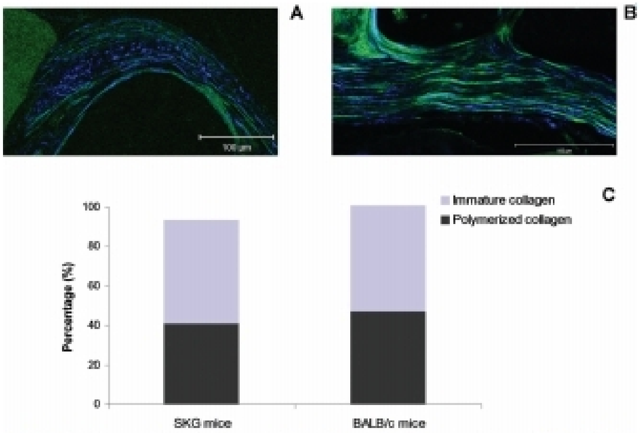

Fig. 3. Multiphoton microscopy images obtained from (A) SKG mouse vertebrae and (B) BALB/c mouse vertebrae. The green colour (backward-SHG channel) corresponds to immature collagen fibril segments, indicating ongoing fibrillogenesis and the blue colour (forward-SHG channel) corresponds to the mature polymerized collagen. (C) The content of collagen in the vertebrae was not affected by arthritis. Scale bars correspond to 100μm.

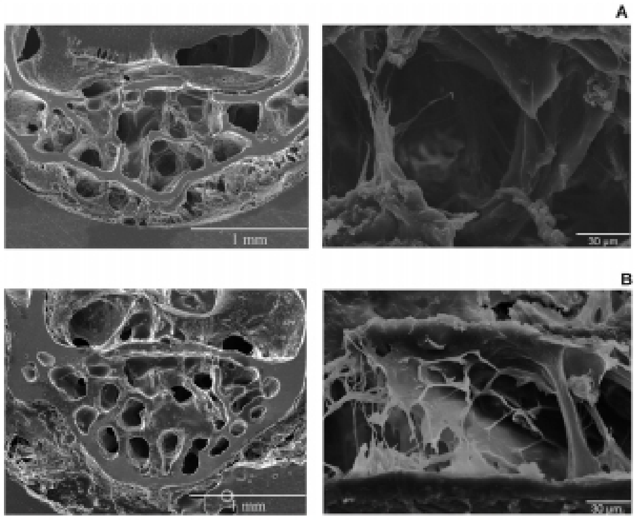

Fig. 4. Vertebrae from arthritic mice have a decreased trabeculae thickness and a higher inter-trabecular distance. Scanning electron microscopy images from female mice vertebrae with (A) and (B) without arthritis, showing a higher inter-trabecular distance and a decreased trabeculae thickness. Scale bars correspond to 1mm (left) and 30μm (right).

femoral bones have impaired elasticity, ductility and ultimate (fracture) strength compared to healthy control femoral bones. In accordance with these results, the compression test used to characterize the biomechanics of the vertebral bodies also showed impairment in the arthritic mice. This could be expected by the low trabeculae area of the cancellous vertebral bone (SEM analysis) as well as by the abnormal nodular structural organisation of its collagen

Table III. Trabeculae and cortical measurements of lumbar vertebrae, as determined by scanning electron microscopy.

	SKG mice (n=6)	BALB/c mice (n=4)	*p*-value
Cortical thickness (μm)	82.40 ± 23.71	99.81 ± 27.44	<0.001*
Trabeculae occupied area (%)	18.91 ± 5.39	21.63 ± 8.22	0.540**
Trabeculae thickness (μm)	57.18 ± 16.78	70.91 ± 23.66	<0.001*
Inter-trabecular distance (μm)	218.92 ± 88.18	188.04 ± 72.54	0.017*

Values are mean ± standard deviation.
*Mann-Whitney test; **Independent-samples t-test.

Table IV. Density measurements for femurs and vertebra.

	SKG mice (n=6)	BALB/c mice (n=7)	*p*-value
Femur density (g/cm^3)	1.17 ± 0.02	1.35 ±0.07	0.002**
Vertebra L2 density (g/cm^3)	0.82 ± 0.10	0.94 ±0.07	0.034*
Vertebra L4 density (g/cm^3)	0.89 ± 0.08	1.03 ±0.25	0.268*

Values are mean ± standard deviation.
*Mann-Whitney test; **Independent-samples t-test.

architecture in the vertebral bone (SHG analysis). However, differences might be even greater than the ones depicted by our results as the squared vertebral body is supported by a slowly remodelling cortical bone shell, which, as a strong and stiff structure, protects the more vulnerable trabeculae bone interior and could mask the impact of the mechanical test.

Interestingly, SHG, independently both in the forward and backward mode, as well as the SEM-coupled EDS methods disclosed that the bulk collagen content and relative proportions of bone embedded minerals do not differ between arthritis and healthy controls. Although the reasons for the impaired quality of arthritic bone remain at present unclear, based on the current work it seems that they may relate to the mineral content and quality (architecture) of bone rather than to its total collagen content or the composition of the hydroxyapatite laid down in the organic bone matrix.

The results of this study clearly show that chronic inflammation directly induces a reduction in bone density and a change in the pattern of bone organization. This is the first report to indicate that arthritis is associated with an impairment of the bone mechanical properties, namely impaired elasticity, ductility and ultimate (fracture) strength. These observations encourage pharmacological intervention studies to analyze if it would be possible to counteract these arthritis-associated and fracture-predisposing changes by targeting also the bone metabolism, apart from controlling the arthritis itself.

References

1. ALAMANOS Y, DROSOS AA: Epidemiology of adult rheumatoid arthritis. *Autoimmun Rev* 2005; 4: b130-6.
2. NEUMANN E, GAY S, MULLER-LADNER U: The RANK/RANKL/osteoprotegerin system in rheumatoid arthritis: new insights from animal models. *Arthritis Rheum* 2005; 52: 2960-7.
3. ORSTAVIK RE, HAUGEBERG G, MOWINCKEL P *et al.*: Vertebral deformities in rheumatoid arthritis: a comparison with population-based controls. *Arch Intern Med* 2004; 164: 420-5.
4. VAN STAA TP, GEUSENS P, BIJLSMA JW *et al.*: Clinical assessment of the long-term risk of fracture in patients with rheumatoid arthritis. *Arthritis Rheum* 2006; 54: 3104-12.
5. RAISZ LG: Pathogenesis of osteoporosis: concepts, conflicts, and prospects. *J Clin Invest* 2005; 115: 3318-25.
6. LAMGHARI M, TAVARES L, CAMBOA N *et al.*: Leptin effect on RANKL and OPG expression in MC3T3-E1 osteoblasts. *J Cell Biochem* 2006; 98: 1123-9.
7. HORWOOD NJ, KARTSOGIANNIS V, QUINN JM *et al.*: Activated T lymphocytes support osteoclast formation in vitro. *Biochem Biophys Res Commun* 1999; 265: 144-50.
8. FONSECA JE, CORTEZ-DIAS N, FRANCISCO A *et al.*: Inflammatory cell infiltrate and RANKL/OPG expression in rheumatoid synovium: comparison with other inflammatory arthropathies and correlation with outcome. *Clin Exp Rheumatol* 2005; 23: 185-92.
9. THEILL LE, BOYLE WJ, PENNINGER JM: RANK-L and RANK: T cells, bone loss, and mammalian evolution. *Annu Rev Immunol* 2002; 20: 795-823.
10. VIGUET-CARRIN S, GARNERO P, DELMAS PD: The role of collagen in bone strength. *Osteoporos Int* 2006; 17: 319-36.
11. PEREL P, ROBERTS I, SENA E *et al.*: Comparison of treatment effects between animal experiments and clinical trials: systematic review. *BMJ* 2007; 334: 197.
12. HIROTA K, HASHIMOTO M, YOSHITOMI H *et al.*: T cell self-reactivity forms a cytokine milieu for spontaneous development of IL-17+ Th cells that cause autoimmune arthritis. *J Exp Med* 2007; 204: 41-7.
13. SAKAGUCHI N, TAKAHASHI T, HATA H *et al.*: Altered thymic T-cell selection due to a mutation of the ZAP-70 gene causes autoimmune arthritis in mice. *Nature* 2003; 426: 454-60.
14. AKHTER MP, CULLEN DM, GONG G *et al.*: Bone biomechanical properties in prostaglandin EP1 and EP2 knockout mice. *Bone* 2001; 29: 121-5.
15. HELMCHEN F, DENK W: Deep tissue two-photon microscopy. *Nat Methods* 2005; 2: 932-40.
16. JEFFERIES Z, KLINE AH, ZIMMER EB: The determination of grain size in metals. *Trans AIME* 1916; 57: 594-607.
17. WILLIAMS RM, ZIPFEL WR, WEBB WW: Interpreting second-harmonic generation images of collagen I fibrils. *Biophys J* 2005; 88: 1377-86.

PART II

Chronic arthritis leads to disturbances in the bone collagen network

arthritis research&therapy

RESEARCH ARTICLE Open Access

Chronic arthritis leads to disturbances in the bone collagen network

Joana Caetano-Lopes1, Ana M Nery[1,2,3], Helena Canhão[1,4], Joana Duarte[5,6], Rita Cascão[1], Ana Rodrigues[1,4], Inês P Perpétuo[1], Saba Abdulghani[1], Pedro M Amaral[2,3], Shimon Sakaguchi[7], Yrjö T Konttinen[8,9], Luís Graça[5,6], Maria F Vaz[2,3] and João E Fonseca*[1,4]

Abstract

Introduction: In this study we used a mice model of chronic arthritis to evaluate if bone fragility induced by chronic inflammation is associated with an imbalance in bone turnover and also a disorganization of the bone type I collagen network.

Methods: Serum, vertebrae and femur bones were collected from eight-month-old polyarthritis SKG mice and controls. Strength of the femoral bones was evaluated using three-point bending tests and density was assessed with a pycnometer. Bone turnover markers carboxy-terminal collagen cross-linking telopeptides (CTX-I) and amino-terminal propeptide of type I procollagen (PINP) were measured in serum. The organization and density of bone collagen were analyzed in vertebrae using second-harmonic generation (SHG) imaging with a two-photon microscope and trabecular bone microstructure was assessed by scanning electron microscope (SEM).

Results: Femoral bones of SKG mice revealed increased fragility expressed by deterioration of mechanical properties, namely altered stiffness ($P = 0.007$) and reduced strength ($P = 0.006$), when compared to controls. Accordingly, inter-trabecular distance and trabecular thickness as observed by SEM were reduced in SKG mice. PINP was significantly higher in arthritic mice (9.18 ± 3.21 ng/ml) when compared to controls (1.71 ± 0.53 ng/ml, $P < 0.001$). Bone resorption marker CTX-I was 9.67 ± 3.18 ng/ml in arthritic SKG mice compared to 6.23 ± 4.11 ng/ml in controls ($P = 0.176$). The forward-to-backward signal ratio measured by SHG was higher in SKG animals, reflecting disorganized matrix and loose collagen structure, compared to controls.

Conclusions: We have shown for the first time that chronic arthritis by itself impairs bone matrix architecture, probably due to disturbed bone remodeling and increased collagen turnover. This effect might predispose patients to bone fragility fractures.

Introduction

Bone is a dynamic tissue composed mainly of a type I collagen matrix that constitutes the scaffold for calcium hydroxyapatite crystal deposition. Remodeling is a continuous process in which osteoclast-mediated bone resorption is coupled with osteoblast-mediated bone matrix production. Biochemical markers of bone turnover are produced during this process and released into circulation [1], providing a read-out of its pace and the balance between bone loss and formation [2]. More specifically, bone-resorbing osteoclasts secrete hydrochloric acid, followed by resorption of the demineralized organic type I collagen matrix by cathepsin K, leading to release of carboxy-terminal collagen cross-linking telopeptides (CTX-I) [1] as a marker for bone degradation. During the formation, phase type I collagen is synthesized *de novo*, and this leads to the release of the amino-terminal propeptide of type I procollagen (PINP) [3] as a marker of bone formation.

The mechanical and physical properties of bone depend on a hierarchical spatial arrangement of its collagen fibrils [4], which leads the deposition pattern of the extracellular hydroxyapatite crystals and consequently influences the overall bone strength. One of the consequences of the remodeling process is the alignment of

* Correspondence: jefonseca@netcabo.pt
[1] Rheumatology Research Unit, Instituto de Medicina Molecular, Faculdade de Medicina da Universidade de Lisboa, 1649-028 Lisbon, Portugal

collagen fibrils along the direction of the load in the mature lamellar bone, thus providing maximal strength to the structure [5]. Precisely due to this nanolevel architecture and the nonsymmetric protein arrangement in a crystalline array, collagen has the ability to generate a second-harmonic signal [6]. Second-harmonic generation (SHG) arises when the electric field of the exciting light is strong enough to deform a molecule. When a molecule, like collagen superhelix, is not symmetrical, the resulting anisotropy creates an oscillating field at twice the frequency, the so-called second harmonic. This method has an additional advantage of not dissipating energy into the sample, so that the sample retains its properties. As a matter of fact, due to its helical structure, SHG signal generated by type I collagen fibers is very strong and practically unaffected by most of the sample processing methods so that either unstained or stained routine histological sections can be subjected to this method. SHG microscopy is a powerful tool that has been developed to assess the bone collagen with a high spatial resolution [7] and has already been applied to mice tail tendons, wound repair, and metastatic growth. A correlation between the SHG intensity, fibrillar morphology, polarization anisotropy, and signal orientation with impaired mechanical strength has been reported in osteogenesis imperfecta [8].

In a recent paper, we used the SKG mouse model to demonstrate the weakening effect of chronic arthritis on the biomechanical properties of the affected vertebral and femoral skeleton in terms of stiffness, ductility, and ultimate (fracture) strength, besides the minimum effects observed on bone density [9]. We now hypothesize that this effect would be due, at least in part, to the inflammatory derangement of normal bone remodeling, leading to a higher bone turnover and consequently to a disorganized collagen type I matrix. To test this hypothesis, we have used a mice model of arthritis and assessed markers of bone collagen metabolism associated with modern SHG-assisted collagen architecture analysis, bone structure, and mechanical evaluation.

Materials and methods

SKG arthritis model and BALB/c controls

The SKG mice model of arthritis develops an erosive chronic polyarthritis that affects both large and small joints, is rheumatoid factor-positive, and presents some of the systemic features of rheumatoid arthritis (RA). The SKG mouse has a BALB/c background [10] with a recessive point mutation in the *zap*-70 gene, which encodes a protein that has an important role in T-cell signal transduction. As a result, this mutation leads to a positive selection of otherwise eliminated autoimmune T cells. SKG mice are genetically prone to develop chronic polyarthritis triggered by zymosan or other dectin-1 agonists [11].

Ten female SKG and ten female BALB/c mice were bred and maintained under specific pathogen-free conditions. All experiments were conducted according to the guidelines of the Animal User and Institutional Ethics Committee, and the study was approved by the local ethics committee. A single intraperitoneal injection of 2 mg of zymosan (Sigma-Aldrich, St. Louis, MO, USA) was administered at 2 months of age. Joint swelling was monitored by inspection as follows: 0, no joint swelling; 0.1, swelling of one finger joint; 0.5, mild swelling of wrist or ankle; and 1.0, severe swelling of wrist or ankle, with a range of the total score varying from 0 to 5 [10]. At 8 months, SKG and BALB/c mice were sacrificed and femoral bones as well as lumbar vertebrae were dissected free of soft tissues and stored at -20°C. Immediately before testing, the samples were defrosted at room temperature.

Biochemical analysis of collagen turnover markers

Determination of bone turnover markers was performed on morning fasting samples that were obtained just before the sacrifice. Two biochemical markers were assayed by enzyme-linked immunosorbent assay (ELISA): CTX-I as a measurement of bone resorption and PINP for bone formation. Both protein serum concentrations were determined according to the guidelines of the manufacturer (Immunodiagnostic Systems, Boldon, Tyne and Wear, UK) by ELISA with sensitivities of 2.0 and 0.7 ng/mL, respectively.

Density measurements

The densities of femoral bones were measured prior to mechanical testing with a water pycnometer. The pycnometer was filled with water, with corrections being made to the ambient temperature following the Archimedes' principle, as previously described [9].

Mechanical testing

All mechanical tests were performed using a universal testing machine (Instron 5566™; Instron Corporation, Norwood, MA, USA) with a load cell of 500 N. The biomechanical parameters were displayed from stress-strain curves by Bluehill 2 Software (copyright 1997-2007; Instron Corporation) and analyzed using MatLab 7.1 software (R14 SP3, copyright 1984-2006; The MathWorks, Inc., Natick, MA, USA). The software has the ability to build stress-strain representations from load-displacement points once initial dimensions are provided for each specimen. Femoral bones were collected at the time of sacrifice and were submitted to three-point bending tests [12].

For these tests, the span between the outer loading points was 5 mm, with the load being applied to the center of the femoral shaft at a cross-head speed of 0.01 mm/s. The parameters analyzed from the stress-strain curves were Young's modulus, ultimate stress, ultimate strain, stiffness, and work/energy until maximum stress. When an increasing force is applied to the femoral shaft using a cross-head, it leads first to fully elastic deformation of the bone so that if the force is released the bone assumes its former shape. This property of the bone is assessed by its stiffness and elastic Young's modulus. The maximum stress still enabling such reversible changes is referred to as the yield point. When more stress is applied, bone tissue starts to undergo microfractures and truly irreversible plastic changes, which are characteristic of a ductile material, occur. The maximum stress the bone can tolerate without breakage reveals its ultimate strength, beyond which a macroscopic fracture soon follows. Stress-strain curves were obtained as previously described [9].

Second-harmonic generation and two-photon excitation microscopy

The third lumbar (L3) vertebrae was decalcified, embedded in paraffin, cut to 7- μm sections using a microtome, and deparaffinized to be inspected in a Zeiss LSM510 META laser scanning microscope (Carl Zeiss, Jena, Germany) featuring a Coherent Mira 900 femtosecond multiphoton excitation laser (Coherent, Inc., Santa Clara, CA, USA). Multicolor nonlinear microscopy of collagen was done through SHG using two-photon excitation. The signal was acquired by two opposing detectors: (a) the META spectral detector that was configured for bandpass detection between 390 and 430 nm and that collected light from a Zeiss Fluar × 20/0.75 objective; this signal was associated with a green look up table (LUT) and is referred to as backward SHG; and (b) the non-descanned detector that collected light from a Zeiss 0.8 numerical aperture condenser and that was filtered by a 390- to 430-nm bandpass filter; this signal was associated with the blue LUT and is referred to as forward SHG. The backward SHG channel detects the backscattered SHG signal, and the forward SHG channel receives the photons that are transmitted through the sample. The wavelength of the laser was set to 820 nm. The method of Jefferies [13] was applied to all acquired images to quantify the amount of trabecular area occupied by collagen detected by the forward SHG channel and by collagen detected by the backward SHG channel [14].

Image analysis was done using National Institutes of Health (NIH) ImageJ software (Wayne Rasband, NIH, Bethesda, MD, USA) by applying a 40- to 255-cycle per second (cps) intensity threshold for each channel to cover only the extracellular collagen matrix. All of the trabecular area was covered using a lower 20- to 255-cps threshold.

The forward-to-backward signal ratio (the fraction of the percentage obtained in the forward SHG channel divided by the one obtained in the backward SHG channel) was determined. This ratio reflects the collagen matrix organization and density, and a higher ratio is associated with a less dense matrix [8].

Scanning electron microscopy

The first lumbar vertebrae (L1) was inserted into an epoxidic and transparent resin and mounted in a mixture of *Résine Mecaprex MA2* (04008) and *Durisseur pour résine Mecaprex MA2* (Presi SA, Tavernolles, Brié-et-Angonnes, France) in 100:12 ratio. After 24 hours, the surfaces of the vertebrae samples were polished using grid papers with granulometries of 1,000, 800, 600, 320, and 200 μm. After deposition of a uniform and thin gold layer, the samples were observed with an electron beam energy of 25 keV in a scanning electron microscope (Hitachi model S2400 scanning electron microscope; Hitachi, Ltd., Tokyo, Japan).

The images obtained were analyzed with the software ImageJ (W. Rasband, NIH). In this case, the region of interest was the vertebral body, where pictures were taken at a magnification of × 100 and parameters such as the inter-trabecular distance (micrometers) and trabecular thickness (micrometers) were determined. These measurements were made according to the methods of Heyn and Jefferies [13].

Statistical analysis

Results were presented as mean and standard deviation values. According to the distribution of the variables, either the *t* test for independent samples or the nonparametric Mann-Whitney test was used to compare continuous variables. Significance level was set at 0.05. Statistical analyses were performed using the Statistical Package for Social Sciences Manager software (SPSS, Inc., Chicago, IL, USA).

Results

Female SKG mice develop chronic arthritis

Ten female SKG mice injected with a single intraperitoneal injection of 2 mg of zymosan at 2 months of age developed chronic arthritis after 1 week (in both small and large joints), and the arthritis reached peak activity by the sixth week. During the first weeks after zymosan administration, scores were calculated every week and then every 2 weeks until sacrifice. By the time of sacrifice (8 months of age), the SKG mice had a disease duration of approximately 6 months and all presented a clinical activity score of 5, indicating persistent active disease. BALB/c mice were used as controls since they have the same genetic background as SKG and, consequently, the bone phenotype is common between these two strains before the development of arthritis. Control BALB/c mice (n = 10) did not develop arthritis (arthritis score = 0) after zymosan administration. At 8 months, SKG mice had a lower body weight than their BALB/c controls (18.9 ± 2.1 g versus 25.6 ± 1.8 g, $P < 0.001$).

Bone collagen turnover is increased in chronic arthritis

PINP, the marker for bone formation, was higher in arthritic mice (9.18 ± 3.21 ng/mL) compared with controls (1.71 ± 0.53 ng/mL, $P < 0.001$). CTX-I, the serum marker for bone resorption, was also higher in arthritic mice (9.67 ± 3.18 ng/mL) compared with controls (6.23 ± 4.11 ng/mL) but without reaching statistical significance ($P = 0.178$).

Chronic arthritis has reduced impact on bone density

The density measurements were lower in the arthritic group (1.26 ± 0.10 g/cm^3) as compared with the control group (1.43 ± 0.23 g/cm^3), although the results were not statistically different ($P = 0.180$).

Chronic arthritis reduces mechanical properties of femurs

Mechanical three-point bending test results (Table 1) showed that arthritic femoral bones had a low elastic (Young's) modulus (reflecting reduced stiffness, $P = 0.007$) and ultimate stress strength (reflecting the maximum strength of the bone, measured at the point of fracture, $P = 0.006$) compared with control bones. The ultimate strain (ductility) and energy absorbed until ultimate point (toughness) did not differ.

Bone collagen structure is modified by chronic arthritis

The percentage of collagen areas was calculated by analyzing the forward and the backward SHG channels separately. The values for the forward channel were 29.49% ± 7.36% in SKG mice and 23.19% ± 6.59% in controls. The corresponding values for the backward channels were 50.22% ± 9.70% and 53.85% ± 8.87%, respectively. The forward-to-backward signal ratio (the fraction of the percentage obtained in the forward SHG channel divided by the one obtained in the backward SHG channel) was higher in arthritic animals (0.566 ± 0.125) than in controls (0.453 ± 0.100, $P = 0.005$), reflecting a lower collagen matrix organization and density (Figure 1) [8].

Vertebrae from arthritic mice have a higher inter-trabecular distance and a decreased trabecular thickness

In arthritic SKG mice vertebrae, the trabecular thickness was reduced, giving rise to an increased inter-trabecular distance in comparison with BALB/c mice vertebrae, as determined by scanning electron microscopy (Table 2).

Discussion

We have previously shown that arthritic mice bone has altered mechanical properties as compared with those from healthy mice [9]. We now show that this bone fragility is induced, at least in part, by chronic inflammation, leading to increased bone turnover that is coupled with impaired microarchitecture of the bone type I collagen network. In fact, we have documented that bone in arthritic animals has a higher remodeling rate, the increase in the bone-forming marker PINP being particularly evident, suggesting that an active bone-repairing process is ongoing. This may be due to inflammation-induced catabolism and bone destruction, which via coupling of bone resorption to bone formation lead to a compensatory osteoblast response in the form of increased bone matrix synthesis in an attempt to reinstall bone homeostasis. The question is whether this high rate of collagen production is able to fully compensate, both quantitatively and qualitatively, for the loss of bone organic matrix. It was therefore of interest to use the newly discovered potential of multiphoton microscopy to analyze this issue in more detail. Multiphoton microscopy in the forward and backward SHG mode was used to calculate the forward-to-backward signal ratio. This

Table 1: Values calculated from mechanical bending stress-strain curves of mice femur

	SKG	BALB/c	P value
Young's modulus, gigapascals	3.6 ± 0.8	6.1 ± 1.6	0.007
Ultimate stress, megapascals	123.7 ± 18.5	164.7 ± 22.5	0.006
Ultimate strain, percentage	6.9 ± 2.5	5.6 ± 1.5	0.280
Energy until ultimate point, Newton-millimeters per cubic millimeters	4.0 ± 1.9	4.7 ± 0.7	0.390

Values are presented as average ± standard deviation.

Table 2: Trabecular measurements of L1 lumbar vertebrae, as determined by scanning electron microscopy

	SKG	BALB/c	*P* value
Trabecular thickness, micrometers	85.41 ± 43.54	99.12 ± 53.85	0.002
Inter-trabecular distance, micrometers	170.1 ± 74.9	142.2 ± 47.2	0.007

Values are presented as average ± standard deviation.

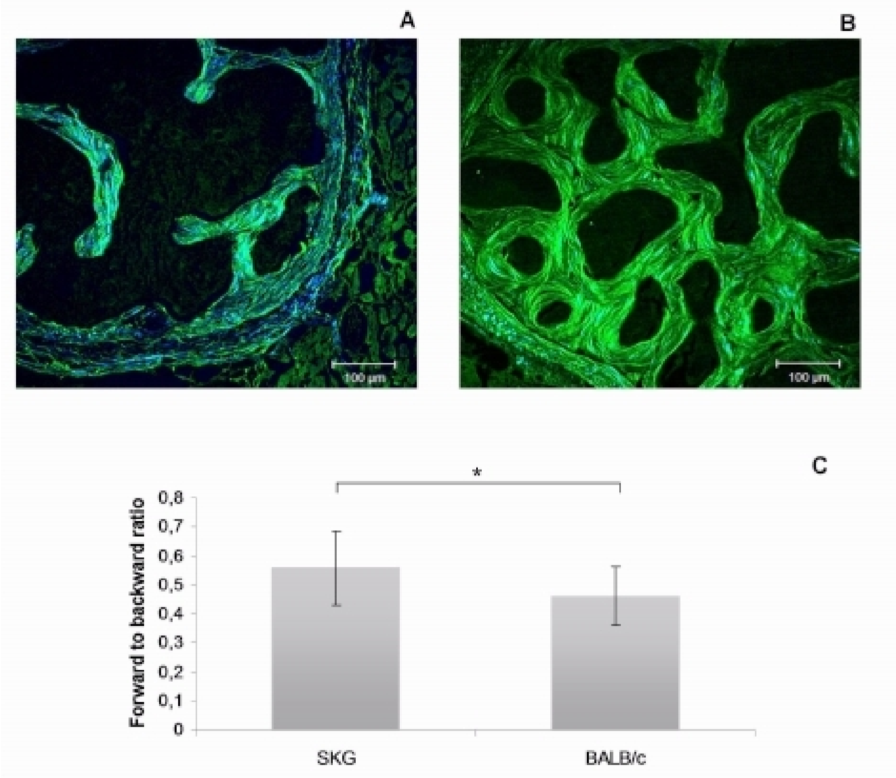

Figure 1 Multiphoton microscopy images obtained from (a) SKG mouse vertebrae and (b) BALB/c mouse vertebrae. The green color corresponds to backward SHG channel and the blue color to forward SHG channel. **(c)** The collagen organization, represented by the forward to backward ratio, was changed by arthritis. Scale bars = 100 µm. $*P < 0.05$. SHG, second-harmonic generation.

ratio, reflecting the bone collagen density and matrix organization [8], clearly showed that bone in the vertebrae of arthritic SKG mice had lower density and organization of collagen fibrils than the healthy control bone. An association between the SHG collagen pattern and mechanical strength was previously established in osteogenesis imperfecta [8], suggesting, together with our data, that this is a reliable method to assess bone collagen spatial organization.

Our results suggest that PINP is actually a more sensitive marker for increased bone turnover rate than CTX-I and this is quite in line with earlier studies of human RA. In fact, intervention studies with etidronate in RA suggest that the impact of the osteoclast-targeting treatment is actually more prominent on bone collagen type I synthesis than on collagen degradation markers [15]. The outcome of the collagen resorption versus synthesis observed by multiphoton microscopy analysis showed that there was a net loss of bone type I collagen in arthritis and that this is not due to diminished synthesis, as verified by the serum markers. Furthermore, SHG images clearly disclosed the disturbed and somewhat haphazard organization of the bone collagen fiber bundles in arthritic bone compared with the better organized lamellar architecture of the healthy control bone (Figure 1). Thus, it is concluded that in spite of the enhanced metabolic bone turnover rate in arthritic mice, this reparative attempt is able to maintain neither collagen mass nor its architectural quality (SHG signals assessed by multiphoton microscopy).

Collagen fiber orientation determines the topography and extent of the deposition of hydroxyapatite bone mineral in the extracellular bone matrix. Collagen further influences the elasticity of bone and is mainly responsible for its ability to absorb energy until the point of fracture, which can be assessed using the three-point bending test of arthritic and healthy control femoral bones. Indeed, it was shown that arthritic femoral bones had an impaired elasticity and relatively low ultimate (fracture) strength compared with healthy control femoral bones. This further supports our interpretation that the collagen component of arthritic bone is strongly affected by the inflammatory process and ultimately this interferes with bone mechanical performance. In addition, scanning electron microscopy findings showed that SKG mice exhibit thinner and more spaced trabeculae as compared with controls, suggesting the lack of a normal matrix-repairing process, which in this case is affecting the mineral deposition pattern and contributing directly to the low strength observed in the mechanical tests.

Conclusions

In summary, we have concluded that the high remodeling rate of arthritic bone affects bone collagen fiber density and organization and leads to the deterioration of bone microstructure and mechanical properties.

Abbreviations

cps: cycle per second; CTX-I: carboxy-terminal collagen cross-linking telopeptides; ELISA: enzyme-linked immunosorbent assay; LUT: look up table; NIH: National Institutes of Health; P1NP: amino-terminal propeptide of type I procollagen; RA: rheumatoid arthritis; SHG: second-harmonic generation.

Competing interests

The authors declare that they have no competing interests.

Authors' contributions

HC, YTK, and JEF helped to conceive the study and draft the manuscript. SS and LG helped to conceive the study. JD, RC, and IPP evaluated the mice and collected their biological material. AMN, MFV, FMA, and SA carried out the mechanical tests and scanning electron microscopy studies. JC-L did the immunoassays and the multiphoton microscopy, statistically analyzed the data, and helped to draft the manuscript. AR helped to draft the manuscript. All authors read and approved the final manuscript.

Acknowledgements

This work was supported by the PTDC/SAU-OSM/65992/2006 grant from Fundação para a Ciência e Tecnologia.

Author Details

[1]Rheumatology Research Unit, Instituto de Medicina Molecular, Faculdade de Medicina da Universidade de Lisboa, 1649-028 Lisbon, Portugal,
[2]Instituto de Ciência e Engenharia de Materiais e Superfícies, Instituto Superior Técnico, Av. Rovisco Pais, 1049-001 Lisbon, Portugal,
[3]Departamento de Engenharia de Materiais, Instituto Superior Técnico, Av. Rovisco Pais, 1049-001 Lisbon, Portugal,
[4]Serviço de Reumatologia e Doenças Ósseas Metabólicas, Hospital de Santa Maria, 1649-035 Lisbon, Portugal,
[5]Cellular Immunology Unit, Instituto de Medicina Molecular, Faculdade de Medicina, Universidade de Lisboa, 1649-028 Lisbon, Portugal,
[6]Instituto Gulbenkian de Ciência, 2780-156 Oeiras, Portugal,
[7]Department of Experimental Pathology, Institute for Frontier Medical Sciences, Kyoto University, Kyoto 606-8507, Japan,
[8]University of Helsinki, Department of Medicine; ORTON Orthopaedic Hospital of the Invalid Foundation, 00281 Helsinki, Finland and
[9]COXA Hospital for Joint Replacement, 33101 Tampere, Finland

Received: 9 September 2009 Revisions Requested: 16 November 2009
Revised: 20 November 2009 Accepted: 15 January 2010 Published: 15 January 2010

References

1. Cremers S, Garnero P: Biochemical markers of bone turnover in the clinical development of drugs for osteoporosis and metastatic bone disease: potential uses and pitfalls. *Drugs* 2006, 66:2031-2058.
2. Caetano-Lopes J, Canhão H, Fonseca JE: Osteoimmunology - The hidden immune regulation of bone. *Autoimmun Rev* 2009, 8:250-255.
3. Seibel MJ: Molecular markers of bone turnover: biochemical, technical and analytical aspects. *Osteoporos Int* 2000, 11(Suppl 6):S18-29.
4. Seeman E, Delmas PD: Bone quality--the material and structural basis of bone strength and fragility. *N Engl J Med* 2006, 354:2250-2261.
5. Viguet-Carrin S, Garnero P, Delmas PD: The role of collagen in bone strength. *Osteoporos Int* 2006, 17:319-336.
6. Cox G, Kable E, Jones A, Fraser I, Manconi F, Gorrell MD: 3-dimensional imaging of collagen using second harmonic generation. *J Struct Biol* 2003, 141:53-62.
7. Cox G, Kable E: Second-harmonic imaging of collagen. *Methods Mol Biol* 2006, 319:15-35.
8. Nadiarnykh O, Plotnikov S, Mohler WA, Kalajzic I, Redford-Badwal D, Campagnola PJ: Second harmonic generation imaging microscopy studies of osteogenesis imperfecta. *J Biomed Opt* 2007, 12:051805.
9. Caetano-Lopes J, Nery AM, Henriques R, Canhão H, Duarte J, M AP, Vale M, Moura R, Pereira PA, Weinmann P, Abdulghani S, Souto-Carneiro M, Rego

P, Monteiro J, Sakagushi S, Konttinen Y, Graça L, Viana Queiroz M, Vaz MF, Fonseca JE: **Chronic arthritis induces quantitative and qualitative bone disturbances leading to compromised biomechanical properties.** *Clin Exp Rheumatol* 2009, 27:475-482.
10. Hirota K, Hashimoto M, Yoshitomi H, Tanaka S, Nomura T, Yamaguchi T, Iwakura Y, Sakaguchi N, Sakaguchi S: **T cell self-reactivity forms a cytokine milieu for spontaneous development of IL-17+ Th cells that cause autoimmune arthritis.** *J Exp Med* 2007, 204:41-47.
11. Kobayashi K, Suda T, Nan-Ya K, Sakaguchi N, Sakaguchi S, Miki I: **Cytokine production profile of splenocytes derived from zymosan A-treated SKG mice developing arthritis.** *Inflamm Res* 2006, 55:335-341.
12. Akhter MP, Cullen DM, Gong G, Recker RR: **Bone biomechanical properties in prostaglandin EP1 and EP2 knockout mice.** *Bone* 2001, 29:121-125.
13. Jefferies Z, Kline AH, Zimmer EB: **The determination of grain size in metals.** *Trans AIME* 1916, 57:594-607.
14. Williams RM, Zipfel WR, Webb WW: **Interpreting second-harmonic generation images of collagen I fibrils.** *Biophys J* 2005, 88:1377-1386.
15. Valleala H, Laasonen L, Koivula MK, Mandelin J, Friman C, Risteli J, Konttinen YT: **Two year randomized controlled trial of etidronate in rheumatoid arthritis: changes in serum aminoterminal telopeptides correlate with radiographic progression of disease.** *J Rheumatol* 2003, 30:468-473.

doi: 10.1186/ar2908
Cite this article as: Caetano-Lopes *et al.*, Chronic arthritis leads to disturbances in the bone collagen network *Arthritis Research & Therapy* 2010, **12**:R9

PART III

Rheumatoid arthritis bone fragility is associated with increased DKK1 expression and disturbances in the bone turnover regulating genes

Rheumatoid arthritis bone fragility is associated with increased DKK1 expression and disturbances in the bone turnover regulating genes

Joana Caetano-Lopes[1], Ana Rodrigues[1,2], Ana Lopes[1], Ana Catarina Vale[3], Michael A. Pitts-Kiefer[4], Bruno Vidal[1], Inês Perpétuo[1], Jacinto Monteiro[5], Yrjö T Konttinen[6], Maria F Vaz[3], Ara Nazarian[5], Helena Canhão[1,2#], João E Fonseca[1,2#]

1- Rheumatology Research Unit, Instituto de Medicina Molecular, Faculdade de Medicina da Universidade de Lisboa, Lisbon, Portugal

2- Serviço de Reumatologia e Doenças Ósseas Metabólicas, Hospital de Santa Maria, Lisbon, Portugal

3- Department of Mechanical Engineering, Instituto Superior Técnico, ICEMS, Lisbon, Portugal

4- Center for Advanced Orthopaedic Studies, Department of Orthopaedic Surgery, Beth Israel Deaconess Medical Center, Harvard Medical School, Boston, USA

5- Orthopaedics Department, Hospital de Santa Maria, Lisbon, Portugal

6- University of Helsinki, Department of Medicine; ORTON Orthopaedic Hospital of the Invalid Foundation, Helsinki; COXA Hospital for Joint Replacement, Tampere, Finland

# Both authors contributed equally

Corresponding Author:

João Eurico Fonseca

Rheumatology Research Unit, Instituto de Medicina Molecular, Edifício Egas Moniz, Faculdade de Medicina da Universidade de Lisboa

Av. Professor Egas Moniz

1649-028 Lisboa

Tel: +351-217999545, Fax: +351-217999459,

E-mail: jefonseca@netcabo.pt

Manuscript word count - 2999

Abstract

Introduction: Rheumatoid arthritis (RA) and primary osteoporosis (OP) induce bone fragility. In this study we aimed at identifying differences in the mechanisms involved in bone fragility by comparing gene expression between RA and OP bone samples with similar fracture risk factors. .

Methods: Patients with RA submitted to hip replacement surgery were recruited. Trabecular bone microarchitecture was assessed by micro-computed tomography and bone mechanical behavior by compression tests. Bone cell activity was analyzed by studying gene expression. RA patients compared with OP patients were matched for bone mineral density (BMD) and major clinical fracture risk factors (age, gender, BMI, FRAX).

Results: Twenty four patients were included, ten with RA, seven with primary established OP and seven with normal BMD. Bone microarchitecture did not differ between the groups, but mechanical bone properties were similarly decreased in RA and primary OP patients compared to the normal BMD group. RA bone microenvironment, compared to primary OP, had a gene expression profile characterized by upregulated pro-osteoclastogenic cytokines and Dkk-1, increased RANKL/OPG ratio, paralleled by raised expression of factors that promote osteoblastic activity, but with low COL1A1 expression.

Conclusion: Bone fragility in RA patients is induced by an unbalanced bone turnover that is qualitatively different from the pathobiologic phenomena that occur in primary OP. The type of bone gene disturbances is suggestive of a pivotal role for Dkk-1 in this process, suggesting that it could be used as a therapeutic target to prevent RA bone damage.

Keywords

Rheumatoid arthritis, bone turnover, bone microCT, bone gene expression

Introduction

Rheumatoid arthritis (RA) is a chronic immune-mediated inflammatory disease of unknown aetiology, characterized by synovial inflammatory infiltration leading to cartilage destruction and juxta-articular bone erosions [1]. Evidence suggests that bone remodeling disturbances contribute not only to bone erosions but also to the development of secondary osteoporosis (OP) in RA. In fact, RA patients have an increased risk of vertebral fractures, which is independent of bone mineral density (BMD) and glucocorticosteroid use [2]. In addition, a high hip fracture risk was also noted in RA patients not exposed to glucocorticosteroids [3]. Thus, RA itself seems to predispose to fractures, although the underlying mechanisms are not yet completely understood.

The connection between bone and inflammation can be partially explained by the activation of the Receptor Activator of Nuclear Factor κB (RANK) by RANK Ligand (RANKL). The downstream signaling of RANK-RANKL interaction leads to pre-osteoclast priming and osteoclast activation, which contribute to the occurrence of erosions and disturbances in bone remodeling [4]. In RA, the ratio between RANKL and its decoy receptor, osteoprotegerin (OPG), is increased [5], shifting the balance towards bone resorption. Immune and skeletal systems communicate with each other in such a way that all immune cells can interact with osteoblasts, osteoclasts, and their respective progenitors [6-7]. Pro-inflammatory cytokines such as tumor necrosis factor (TNF), interleukin (IL)-1β, IL-6 and IL-17 are potent inducers of RANKL expression and, consequently, of osteoclast formation [8]. These cytokines are elevated in the serum and synovial fluid of RA patients since the first weeks of disease [9].

Osteoblasts play a role in this network as they produce RANKL and OPG upon differentiation and maturation. Their differentiation is characterized by the expression of the key pro-osteogenic transcription factors runt-related transcription factor 2 (RUNX2) [10] and osterix (OSX) [11]. Maturation is marked by the expression of alkaline phosphatase (ALP) and type I collagen (COL1A1) and, later on, by production of non-collagenous proteins such as osteocalcin (OCL) [12-13].

In a recent study we used the SKG arthritis model to demonstrate the weakening effect of chronic arthritis on bone biomechanical properties [14-15]. Moreover, we observed that this effect was due to inflammation-driven derangement of bone matrix, caused by disturbed bone remodeling and increased collagen turnover [16]. We hypothesize that bone fragility in RA patients is induced by an unbalanced bone turnover that is qualitatively different from the biologic phenomena that occur in OP. Thus, our aim was to compare bone gene expression between RA and primary established OP patients, matched for BMD and major clinical fracture risk factors.

Methods

Study population

Patients older than 50 years diagnosed with RA according to the 2010 ACR/EULAR revised classification criteria [17] and submitted to hip replacement surgery between 2007 and 2010 were included in this study. The hip replacement surgery was either due to fragility fracture or secondary osteoarthritis (OA). Patients were excluded if had other causes of secondary osteoporosis such as malignancies, untreated thyroid disease, terminal renal disease and hypogonadism. Pre-menopausal women were also excluded. Two groups of patients matched for gender, age and body mass index (BMI) were used for comparison. One group was submitted to hip arthroplasty due to hip fragility fracture, had a matched femoral neck BMD and no secondary causes for OP. The second group had normal BMD, was submitted to hip arthroplasty due to OA and did not have any other clinical risk factor for OP. None of the patients reported a history of other metabolic bone diseases, bone metastasis or primary bone tumors or osteomyelitis.

A clinical protocol was applied at the time of surgery in order to assess clinical risk factors for OP – age, gender, BMI, prior fragility fracture, family history of hip fracture, long term use of oral glucocorticoids (≥3 months), current smoking and alcohol intake (≥ 3 units/day). The probability of fracture at ten years was calculated using the FRAX tool available online (http://www.shef.ac.uk/FRAX/), calibrated to the epidemiology of fracture and life expectancy of Spain. Femoral neck BMD of the contralateral hip was measured by dual-emission X-ray absorptiometry (DXA) scan using a Lunar Prodigy densitometer (GE Healthcare, United Kingdom) within one week after surgery.

For RA patients, disease duration, age at disease onset, rheumatoid factor, C reactive protein (CRP), disease activity score (DAS28 ESR3V), presence of erosions and RA therapy was also assessed.

Written informed consent was obtained from all patients, and this study was conducted in accordance with the regulations governing clinical trials such as the Declaration of Helsinki, as amended in Seoul (2008), and was approved by the local Ethics Committee.

This was a nested case-control study from a cohort of 387 consecutive patients submitted to hip replacement surgery in Hospital de Santa Maria, accordingly to the above mentioned inclusion and exclusion criteria.

Biochemical markers of bone turnover

Blood samples were collected at the time of surgery to assess serum calcium and phosphorus, ALP, bone-specific ALP (BSALP) and OCL. Serum carboxyl-terminal cross-linked telopeptides of type I collagen (CTX-I) and serum amino-terminal propeptides of type I procollagen (P1NP) were measured by fully automated Elecsys® electro-chemiluminescent immunoassay analyzers (Roche Diagnostics, Switzerland).

Micro-Computed Tomography

The femoral epiphyses were immediately stored at -80°C after surgery.

A small cylinder of trabecular bone (5mm diameter) was drilled from femoral epiphysis. The sample was processed through fixation, dehydration, impregnation and inclusion in methylmetacrylate solution.

Sequential transaxial images through the entire specimen were obtained using micro-computed tomography (microCT 40, Scanco Medical AG, Brüttisellen, Switzerland) at an isotropic voxel size of 20µm, integration time of 250ms and beam energy and current of 55keV and 0.145mA, respectively. A three-dimensional Gaussian filter (σ=0.8) with a limited, finite filter support was used to suppress the noise. The images were binarized to separate bone from other tissues or background using an adaptive thresholding procedure. After thresholding, bone volume fraction (BV/TV), bone surface density (BS/TV), specific bone surface (BS/BV), trabecular number (Tb.N), trabecular thickness (Tb.Th), trabecular spacing (Tb.Sp), degree of anisotropy (DA= length of the longest mean intercept length (MIL) tensor divided by the shortest MIL tensor), and connectivity density (Conn.D) were assessed for all samples.

Mechanical Compression Tests

Bone cylinders were obtained by drilling through the highest load direction using a perforating drill with a diameter of 15mm (method adapted from [18]). The cylinders (with only trabecular bone) were de-fatted for three hours using a chloroform and methanol solution and were hydrated overnight in a phosphate-buffered saline solution.

Compression tests were performed in a universal testing machine (Instron 5566™, Instron Corporation, Canton, USA) with a 10kN load cell and a cross-head rate of 0.1mm/s. Stress-strain curves were obtained for each specimen by the *Bluehill 2 software* (Instron, Copyright 1997-2007). This software has the ability to build stress-strain representations from load-displacement points, normalized for the dimensions of the specimen. Analyses of the curves were performed in order to obtain the mechanical bone parameters: stiffness (Young modulus), strength (yield stress) and toughness (energy absorbed until fracture).

RNA extraction

Small trabecular bone pieces were collected and pulverized using a mortar and pestle. RNA was extracted using TRIzol reagent (Invitrogen, UK) with proteinase K (Bioline, UK) digestion [19] to better dissolve extracellular matrix. 80mg of bone powder was placed in TRIzol reagent and homogenized. Lipids were solubilized with 0.2 volumes of chloroform and the fraction containing RNA was preserved. Proteinase K digestion (3.25µg proteinase K/mg bone) was performed at 55°C. RNA was precipitated with 1 volume of ice-cold isopropyl alcohol. RNA pellet was dissolved in RNase/DNase-free water. RNA was cleaned using a commercial kit (RNeasy mini kit, Qiagen, Germany) and genomic DNA contaminants were removed by DNaseI treatment (Qiagen, Germany) (Adapted from [20-21]). RNA concentration was determined spectrophotometrically (Nanodrop ND-1000 Spectrophotometer, Thermo Fisher Scientific, USA) and its integrity was assessed by lab-on-a-chip technology (Agilent RNA 6000 Nano Kit, Agilent technologies, USA) according to the manufacturer's instructions. RNA was stored at -80°C until further use.

Quantitative reverse transcription-polymerase chain reaction (PCR)

Reverse transcription cDNA synthesis was performed on 60ng of RNA from each sample using the DyNAmo cDNA synthesis kit (Finnzymes, Finland) and 300ng of random hexamer primers, according to the manufacturer's instructions.

Each cDNA template (3ng/µl) was amplified in duplicate with DyNAmo Flash SYBR green qPCR kit (Finnzymes, Finland) on a Rotor-Gene thermocycler (Qiagen, Germany) according to the manufacturer's instructions. Reactions were incubated at 50°C for 2 minutes and at 95°C for 7 minutes, followed by denaturation at 95°C for 10 seconds and annealing/extension at 60°C for 10 seconds. The reactions were validated by the presence of a single peak in the melt curve analysis.

Primers for the housekeeping and target genes (supplementary table) were designed using the software Probefinder (http://qpcr.probefinder.com, Roche, Switzerland) in order to anneal in separate exons preventing amplification of contaminating genomic DNA.

Real time PCR results were analyzed using the standard curve analysis. The cycle threshold (C_T) is defined as the number of cycles required for the fluorescent signal to cross the threshold and exceed the background level. The efficiency of the PCR should be 100%, meaning that for each cycle the amount of product doubles. A good reaction should have an efficiency of 90-

100%, which corresponds to a slope between -3.58 and -3.10. The conversion of the C_T value in relative expression levels was performed with the slope and the Y intersect extracted from the standard curve and applying the equation $10^{(Y\ intersect-CT/slope)}$ [22-23]. The values obtained were normalized with the housekeeping genes β-2-microglobulin (B2M) and phosphomannomutase 1 (PMM1).

Statistical analysis

Values are presented as mean and standard deviation or frequencies for continuous or categorical variables, respectively. The RA patients group was compared with the normal BMD and primary OP groups. For continuous variables, normality was confirmed using Shapiro-Wilk test and groups were compared with independent samples t test. For categorical data, chi-squared or Fisher exact test were used. Statistical significance was set for p value at 0.05.

Analysis was conducted using the Statistical Package for Social Sciences manager software, version 19.0 (SPSS, Inc, Chicago, IL, USA).

RESULTS

Study population

Twenty-four patients were recruited for this study, 10 with RA, 7 with primary OP and 7 with normal BMD (table 1).

RA patients had a mean age of 68±11 years, 90% women, with a disease duration of 4±3 years, CRP was of 2.1±2.1 mg/dl, the mean DAS28 3V was of 4.05±2.21 and 44% of the patients had DAS28 3V above 3.2. 50% were positive for rheumatoid factor and 50% had erosive disease. All RA patients were on a low glucocorticosteroid dose (<10mg/day) and synthetic disease-modifying anti-rheumatic drug monotherapy, nine on methotrexate and one on leflunomide. None of the patients had used biological therapy.

Clinical risk factors for fracture were comparable between groups. FRAX score (both for major and hip fractures) was similar in RA and primary OP patients. FRAX score was lower in the normal BMD group ($p<0.05$) than in the two other groups. We did not find any differences between groups regarding markers of bone turnover.

Table 1 – Characteristics of the study populations.

	RA patients	Primary OP‡	p-value	Normal BMD†	p-value
Age (years)	68±11	71±4	0.324	66±10	0.803
Women (%)	90	86	1	71	0.732
BMI (Kg/m^2)	26.9±4.6	23.7±4.9	0.210	33.6±9.7	0.104
BMD (g/cm^2)	0.68±0.06	0.71±0.09	0.576	1.03±0.22	0.005
Tscore	-2.6±0.7	-2.6±1.0	0.993	0.0±0.9	0.001
Previous fracture (%)	11	43	0.262	0	1
Smoking (%)	33	29	1	0	0.213
Alcohol intake (%)	11	0	1	0	1
Family history of fracture (%)	11	0	1	0	1
Corticotherapy (%)	100	14	0.001	0	<0.001
FRAX major fracture (%)	16.3±10.0	9.8±3.7	0.389	4.0±3.6	0.015
FRAX hip fracture (%)	9.1±7.5	7.9±2.0	0.554	1.4±1.8	0.030
Calcium (mg/ml)	9.8±4.0	7.9±0.4	0.283	8.5±4.5	0.461
Phosphorus (mg/dl)	3.4±0.4	3.1±0.8	0.445	2.8±0.8	0.123
Osteocalcin (ng/ml)	10.2±11.3	13.2±8.8	0.671	8.9±5.4	0.809
ALP (u/l)	99.2±53.0	81.6±38.1	0.545	57.6±35.6	0.138
BSALP (µg/l)	12.3±5.1	9.6±3.2	0.365	11.7±5.7	0.877
P1NP (ng/ml)	43.0±32.4	31.8±16.8	0.544	43.0±21.5	0.997
CTX-I (ng/ml)	0.40±0.26	0.35±0.21	0.697	0.25±0.15	0.230
PTH (pg/ml)	31.0±27.3	42.5±10.3	0.400	37.1±13.2	0.637

Values represent mean±standard deviation or frequencies.
† p-value from comparison between patients with RA and normal BMD individuals; ‡ p-value from comparison between RA patients and primary OP individuals
RA – rheumatoid arthritis; BMD – bone mineral density; BMI – body mass index; ALP – alkaline phosphatase; BSALP – bone-specific ALP; P1NP – procollagen type I amino-terminal propeptide; CTX-I - carboxy-terminal collagen type I crosslinks; PTH – parathormone.

Bone microstructure

Sequential transaxial images through each specimen (213±44 slices per sample) were obtained using microCT. We did not find significant differences regarding trabecular structure between groups (table 2).

Table 2 – MicroComputed Tomography of the trabecular bone specimens.

	RA patients	Primary OP‡	p-value	Normal BMD†	p-value
BV/TV (%)	0.245±0.096	0.231±0.102	0.782	0.252±0.081	0.882
BS/BV (mm^{-1})	13.8±2.6	14.6±3.4	0.605	13.6±3.0	0.865
Conn.D (mm^{-3})	6.103±2.750	5.442±2.632	0.634	6.025±2.010	0.951
Tb.N (mm^{-1})	1.730±0.420	1.661±0.400	0.744	1.694±0.186	0.824
Tb.Th (mm)	0.197±0.037	0.191±0.043	0.771	0.201±0.043	0.838
Tb.Sp (mm)	0.596±0.141	0.616±0.192	0.579	0.553±0.076	0.781
DA	1.55±0.14	1.55±0.25	0.949	1.46±0.14	0.213

Values represent mean±standard deviation.
† p-value from comparison between patients with RA and normal BMD individuals; ‡ p-value from comparison between RA patients and primary OP individuals
RA – rheumatoid arthritis; BMD – bone mineral density; BV/TV – percent bone volume; BS/BV – bone specific surface; Conn.D – connectivity density; Tb.N – trabecular number; Tb.Th – trabecular thickness; Tb.Sp – trabecular separation; DA – degree of anisotropy.

Mechanical bone behavior

RA bone had significantly lower stiffness than normal BMD bone (p=0.051) but was similar to primary OP bone. Regarding bone strength, RA patients had slightly lower values than controls with normal BMD (not significant). No differences among groups were found in toughness (figure 1).

Gene expression

The expression of genes reflecting bone microenvironment is detailed in figure 3 and table 3.

Cytokines and adipokines

Genes related with inflammation were increased in RA patients. IL-1β and IL-17 expression levels were significantly higher in RA patients compared to the primary OP group (p=0.029 and p=0.030, respectively). The same behavior was observed for IL-6 and TNF, although these differences did not reach statistical significance. The expression of fibroblast growth factor (FGF)-2 (p=0.047), platelet-derived growth factor (PDGF)-β (p=0.086) and insulin-like growth factor (IGF)-I (p=0.036) were increased in RA patients in comparison to the primary OP group.

Regarding adipokines, leptin (LEP), leptin receptor (OB-R), adiponectin (ADIPOQ) and peroxidase proliferator-activated receptor (PPAR)γ, there were no significant differences between groups.

RANKL-OPG ratio

RANKL/OPG ratio showed a tendency to be increased in RA patients compared to the normal BMD group (p=0.066). No differences were observed in the expression levels of RANK between groups.

Osteoclast-related genes

Measurement of the osteoclast-related genes tartrate-resistant acid phosphatase (TRAP), ATPase H^+ transporter, V0 subunit d2 (ATP6V0D2), subunit β3 of αvβ3 integrin (ITGB3) and cathepsin K (CTSK) disclosed that the primary OP group expressed higher levels of ITGB3 (p=0.015) compared to RA patients.

Osteoblast and osteocyte related genes

To characterize osteoblast metabolism the expression levels of RUNX2, OSX, ALP, COL1A1 and OCL were analyzed. The transcription factor OSX was increased in RA patients compared to the primary OP group (p=0.048). COL1A1 was slightly lower in RA patients than in the primary OP group (p=0.099) but OCL was increased (p=0.054). RUNX2 and ALP were similar in all groups.

Regarding osteocyte-related genes, phosphate-regulating endopeptidase homolog, X-linked (PHEX) was decreased in RA in comparison with the normal BMD group (p=0.062) but no differences were found in dentin matrix acidic phosphoprotein 1 (DMP1) expression.

WNT pathway

Several components of the Wnt signaling pathway, low-density lipoprotein receptor related protein (LRP)5, LRP6, dickkopf-related protein (Dkk)-1 and secreted frizzled-related protein (sFRP)1 were analyzed. Both LRP5 and LRP6 were increased in RA patients compared to the primary OP group, although only LRP6 reached statistical significance (p=0.045). Regarding Wnt inhibitors, we did not find any difference in sFRP1. We also did not find significant differences regarding SOST between the groups, although SOST gene expression levels were relatively low in RA and in primary OP patients. However, Dkk-1 was upregulated in RA patients (p=0.036), when compared with primary OP patients.

Table 3 – Comparison between relative gene expression levels between RA patients and normal BMD group or primary OP patients.

	RA patients	Primary OP[‡]	p-value	Normal BMD[†]	p-value
IL1β	0.0016±0.0015	0.0003±0.0004	0.029	0.0007±0.0006	0.110
IL17	1.221±1.104	0.045±0.062	0.030	0.336±0.322	0.083
IL6	0.0038±0.0053	0.0024±0.0020	0.535	0.0028±0.0054	0.330
TNF	0.015±0.016	0.0061±0.0099	0.198	0.030±0.024	0.144
FGF2	0.083±0.109	0.0036±0.0078	0.047	0.073±0.071	0.836
PDGFβ	0.027±0.037	0.0027±0.0045	0.086	0.022±0.017	0.731
IGF-I	0.140±0.164	0.0105±0.0251	0.036	0.340±0.354	0.200
LEP	5.52±2.60	8.60±12.20	0.535	8.75±8.78	0.405
OB-R	0.081±0.109	0.014±0.019	0.088	0.063±0.063	0.708
ADIPOQ	1.35±1.94	0.109±0.123	0.075	0.86±0.90	0.508
PPARγ	0.051±0.067	0.018±0.013	0.157	0.035±0.032	0.590
RANKL	0.077±0.077	0.293±0.297	0.105	0.112±0.148	0.606
OPG	0.028±0.022	0.050±0.041	0.215	0.053±0.051	0.303
RANKL/OPG	3.8±3.0	7.5±7.4	0.296	1.3±1.6	0.066
RANK	0.002±0.002	0.002±0.001	0.591	0.002±0.002	0.586
RUNX2	0.043±0.041	0.040±0.020	0.845	0.052±0.032	0.646
OSX	0.031±0.032	0.007±0.004	0.048	0.019±0.018	0.419
COL1A1	0.037±0.033	0.198±0.219	0.099	0.132±0.131	0.104
ALP	0.024±0.025	0.037±0.022	0.288	0.046±0.051	0.367
OCL	0.034±0.043	0.003±0.004	0.054	0.055±0.056	0.405
PHEX	0.259±0.203	0.647±1.188	0.463	1.057±1.089	0.062
DMP1	2.65±1.90	2.50±2.43	0.894	1.74±1.03	0.307
LRP5	0.029±0.029	0.011±0.017	0.163	0.032±0.033	0.856
LRP6	0.043±0.047	0.008±0.014	0.045	0.035±0.041	0.712
DKK-1	0.238±0.296	0.007±0.011	0.036	0.110±0.115	0.378
sFRP1	0.018±0.023	0.004±0.007	0.101	0.035±0.041	0.334
SOST	0.012±0.012	0.014±0.012	0.824	0.034±0.031	0.113
TRAP	0.030±0.022	0.060±0.043	0.219	0.061±0.050	0.247
ATP6V0D2	0.089±0.085	0.081±0.034	0.820	0.046±0.049	0.262

ITGB3	0.013±0.010	0.030±0.011	0.015	0.013±0.010	0.974
CTSK	0.414±0.495	1.09±0.89	0.102	0.397±0.311	0.946

Values represent mean±standard deviation.

† p-value from comparison between patients with RA and normal BMD individuals; ‡ p-value from comparison between RA patients and primary OP individuals

(ADIPOQ – adiponectin; ALP – alkaline phosphatase; ATP6VOD2 - ATPase H^+ transporter; COL1A1 – Collagen type 1α1; CTSK – cathepsin K; DKK1 – dickkopf-related protein 1; DMP1 – dentin matrix acidic phosphoprotein 1; FGF2 – fibroblast growth factor 2; IGF1 – insulin growth factor-1; IL1 - Interleukin-1; IL6 – interleukin-6; IL17 – inteleukin-17; ITGB3 – subunit β3 of the integrin αvβ3; LEP – leptin; LRP5/6 – low-density lipoprotein receptor related protein 5/6; OB-R – leptin receptor; OCL – osteocalcin, OPG – osteoprotegerin; OSX – osterix; PDGF - platelet derived growth factor β; PHEX – phosphate-regulating endopeptidase homolog, X-linked; PPARγ - peroxidase proliferator-activated receptor γ; RANK - receptor activator of nuclear factor κB; RANKL – RANK ligand; RUNX2 – runt-related transcription factor 2; sFRP1 – secreted frizzled-related protein 1; SOST – sclerostin; TNF – tumor necrosis factor; TRAP - tartrate-resistant acid phosphatase)

Discussion

In this study we found that RA bone microenvironment has a gene expression profile characterized by upregulation of several pro-osteoclastogenic cytokines and Dkk-1, increased RANKL/OPG ratio, paralleled with a raised expression of factors that promote osteoblastic activity. These observations were obtained in comparison with an established primary OP group with similar BMD, FRAX score, trabecular bone mechanics and microstructural organization.

As expected genes that code for pro-inflammatory cytokines were upregulated in RA patients, particularly IL-17, which plays an important role in stimulating osteoclastogenesis. In accordance, RANKL/OPG expression ratio was higher in RA than in controls with normal BMD. Overall osteoclast related gene expression was similar between RA and established OP patients, with the exception of ITGB3, which was lower in RA patients, suggesting an intriguing disturbance in osteoclast adherence to bone matrix [24].

RA patients had increased FGF2 and IGF-I expression levels, which together with the upregulation of bone OSX, might represent a compensatory osteoblastic activity response that we have also previously observed in a mice model of arthritis [16, 25]. Interestingly, OSX is involved in the induction of Dkk-1 [26], which is coherent with our observation of an increase in the expression of this gene in RA bone. In addition, Dkk-1 induces LRP6 accumulation both at the cell surface and in endosomes [27] and in fact our observations showed that the increased expression of Dkk-1 in RA was paralleled by an upregulation of LRP6. Dkk-1 is a negative regulator of the Wnt/β-catenin signaling, which is a key pathway in the stimulation of osteoblast differentiation [28], meaning that its upregulation in RA patients is limiting the effects of pro-osteoblastic factors, as can be inferred by low COL1A1 expression in RA bone. Dkk-1 was previously shown to be present in joint sections from RA patients [29] and neutralization of Dkk-1 completely protects hTNFtg mice from inflammatory bone loss by preventing impaired osteoblast function and enhanced osteoclast activity [30]. Curiously, the other Wnt pathway inhibitor sclerostin (SOST), exclusively expressed by osteocytes, was not increased in RA bone. This uncoupling with Dkk-1 expression might be explained by increased osteocyte apoptosis in RA [31] and/or by an inhibitory effect of Dkk-1 on SOST expression [32].

Differences were observed in gene expression between RA bone and established primary OP bone in spite of the fact that these two patient groups were matched for BMD and major fracture risk factors. Moreover, neither bone microarchitecture nor biomechanics of the trabecular bone showed any significant difference between the two groups. However, RA and established OP bone samples had impaired bone biomechanical properties compared to the normal BMD control group. These details are relevant as they might indicate that the differences in gene expression that were observed reflect biologically specific mechanisms responsible for bone fragility in RA. Finally, another interesting point is that patients belonging to the RA group had a relatively short disease duration, low erosive rate and low microstructural damage (as evaluated by microCT) reinforcing the idea that these differences in gene expression occurred in the absence of major clinically meaningful bone damage in RA.

We have tried to reach the highest possible intra-group homogeneity, minimizing a major issue in the analysis of human bone, but by doing that we have considerably reduced the sample size. However, the results are perfectly in line with our previous animal observations [16]. An aspect that cannot be completely clarified solely based on this study is the eventual impact of low dose glucocorticosteroids, used by all our RA patients (a standard practice in the management of RA in Portugal), on the expression of the genes analysed. From a clinical perspective, low dose glucocorticosteroids have a minor effect on RA bone [2-3] but their effects on bone gene expression are not precisely known [33]. In fact, to our knowledge this is the first study where bone quality and gene expression were assessed in human samples in the context of a chronic inflammatory condition.

In conclusion, RA bone microenvironment has a gene expression profile characterized by upregulated pro-osteoclastogenic cytokines, increased RANKL/OPG expression ratio, paralleled simultaneously by a raised expression of factors that promote osteoblastic activity. However, the marked Dkk-1 expression observed in RA patients might limit this tentative osteoblast-mediated bone repair activity as it is suggested by the low COL1A1 expression. Our observations reinforce the position of Dkk-1 as an attractive target for treating RA induced systemic bone disease.

Acknowledgements

We wish to thank Drª. Viviana Tavares from Hospital Garcia de Orta for the help in clinical evaluation.

This work was supported from an unrestricted grant from Institut de Recherché Internationals, Servier.

Conflict of Interest

The authors confirm that there are no conflicts of interest.

REFERENCES

1. Alamanos Y, Drosos AA. Epidemiology of adult rheumatoid arthritis. *Autoimmun Rev* 2005, **4**:130-136.
2. Orstavik RE, Haugeberg G, Mowinckel P, et al. Vertebral deformities in rheumatoid arthritis: a comparison with population-based controls. *Arch Intern Med* 2004, **164**:420-425.
3. van Staa TP, Geusens P, Bijlsma JW, et al. Clinical assessment of the long-term risk of fracture in patients with rheumatoid arthritis. *Arthritis Rheum* 2006, **54**:3104-3112.
4. Raggatt LJ, Partridge NC. Cellular and molecular mechanisms of bone remodeling. *J Biol Chem* 2010, **285**:25103-25108.
5. Fonseca JE, Cortez-Dias N, Francisco A, et al. Inflammatory cell infiltrate and RANKL/OPG expression in rheumatoid synovium: comparison with other inflammatory arthropathies and correlation with outcome. *Clin Exp Rheumatol* 2005, **23**:185-192.
6. Gruber R. Cell biology of osteoimmunology. *Wien Med Wochenschr* 2010, **160**:438-445.
7. Takayanagi H. Osteoimmunology: shared mechanisms and crosstalk between the immune and bone systems. *Nat Rev Immunol* 2007, **7**:292-304.
8. Schett G. Osteoimmunology in rheumatic diseases. *Arthritis Res Ther* 2009, **11**:210.
9. Cascao R, Moura RA, Perpetuo I, et al. Identification of a cytokine network sustaining neutrophil and Th17 activation in untreated early rheumatoid arthritis. *Arthritis Res Ther* 2010, **12**:R196.
10. Komori T, Yagi H, Nomura S, et al. Targeted disruption of Cbfa1 results in a complete lack of bone formation owing to maturational arrest of osteoblasts. *Cell* 1997, **89**:755-764.
11. Nakashima K, Zhou X, Kunkel G, et al. The novel zinc finger-containing transcription factor osterix is required for osteoblast differentiation and bone formation. *Cell* 2002, **108**:17-29.
12. Marie PJ. Transcription factors controlling osteoblastogenesis. *Arch Biochem Biophys* 2008, **473**:98-105.
13. Caetano-Lopes J, Canhao H, Fonseca JE. Osteoblasts and bone formation. *Acta Reumatol Port* 2007, **32**:103-110.
14. Abdulghani S, Caetano-Lopes J, Canhao H, et al. Biomechanical effects of inflammatory diseases on bone-rheumatoid arthritis as a paradigm. *Autoimmun Rev* 2009, **8**:668-671.
15. Caetano-Lopes J, Nery AM, Henriques R, et al. Chronic arthritis induces quantitative and qualitative bone disturbances leading to compromised biomechanical properties. *Clinical and Experimental Rheumatology* 2009, **27**:475-482.
16. Caetano-Lopes J, Nery AM, Canhao H, et al. Chronic arthritis leads to disturbances in the bone collagen network. *Arthritis Res Ther* 2010, **12**:R9.
17. Aletaha D, Neogi T, Silman AJ, et al. 2010 Rheumatoid arthritis classification criteria: an American College of Rheumatology/European League Against Rheumatism collaborative initiative. *Arthritis Rheum* 2010, **62**:2569-2581.
18. Smith CB, Smith DA. Relations between age, mineral density and mechanical properties of human femoral compacta. *Acta Orthop Scand* 1976, **47**:496-502.
19. Egyhazi S, Bjohle J, Skoog L, et al. Proteinase K added to the extraction procedure markedly increases RNA yield from primary breast tumors for use in microarray studies. *Clin Chem* 2004, **50**:975-976.
20. Ireland D. Analysis of Gene Expression in Bone by Quantitative RT-PCR. In *Bone Research Protocols.* Edited by Helfrich MH, Ralston SH. New York: Humana Press; 2003: 433-440
21. Caetano-Lopes J, Lopes A, Rodrigues A, et al. Upregulation of inflammatory genes and downregulation of sclerostin gene expression are key elements in the early phase of fragility fracture healing. *PLoS One* 2011, **6**:e16947.
22. Wong ML, Medrano JF. Real-time PCR for mRNA quantitation. *Biotechniques* 2005, **39**:75-85.
23. Heid CA, Stevens J, Livak KJ, et al. Real time quantitative PCR. *Genome Res* 1996, **6**:986-994.
24. Zou W, Teitelbaum SL. Integrins, growth factors, and the osteoclast cytoskeleton. *Ann N Y Acad Sci* 2010, **1192**:27-31.
25. Baek WY, de Crombrugghe B, Kim JE. Postnatally induced inactivation of Osterix in osteoblasts results in the reduction of bone formation and maintenance. *Bone* 2010, **46**:920-928.
26. Zhang C. Transcriptional regulation of bone formation by the osteoblast-specific transcription factor Osx. *J Orthop Surg Res* 2010, **5**:37.

27. Li Y, Lu W, King TD, et al. Dkk1 stabilizes Wnt co-receptor LRP6: implication for Wnt ligand-induced LRP6 down-regulation. *PLoS One* 2010, **5**:e11014.
28. Glass DA, 2nd, Bialek P, Ahn JD, et al. Canonical Wnt signaling in differentiated osteoblasts controls osteoclast differentiation. *Dev Cell* 2005, **8**:751-764.
29. Walsh NC, Reinwald S, Manning CA, et al. Osteoblast function is compromised at sites of focal bone erosion in inflammatory arthritis. *J Bone Miner Res* 2009, **24**:1572-1585.
30. Diarra D, Stolina M, Polzer K, et al. Dickkopf-1 is a master regulator of joint remodeling. *Nat Med* 2007, **13**:156-163.
31. Appel H, Ruiz-Heiland G, Listing J, et al. Altered skeletal expression of sclerostin and its link to radiographic progression in ankylosing spondylitis. *Arthritis Rheum* 2009, **60**:3257-3262.
32. Heiland GR, Zwerina K, Baum W, et al. Neutralisation of Dkk-1 protects from systemic bone loss during inflammation and reduces sclerostin expression. *Ann Rheum Dis* 2010, **69**:2152-2159.
33. Dovio A, Micossi I, Bianco E, et al. Determinants of glucocorticoid action in the bone microenvironment. *J Endocrinol Invest* 2008, **31**:7-15.

FIGURE LEGENDS

Figure 1 – Mechanical behavior of bone was analyzed by compression tests of trabecular bone cylinders. Strength, stiffness and toughness were considered to characterize bone mechanics.

Figure 2 – Several genes were analyzed translating three important components of the interaction between immune system and bone – inflammation, osteoblastogenesis and osteoclastogenesis.

(ADIPOQ – adiponectin; ALP – alkaline phosphatase; ATP6VOD2 - ATPase H^+ transporter; COL1A1 – Collagen type 1α1; CTSK – cathepsin K; DKK1 – dickkopf-related protein 1; DMP1 – dentin matrix acidic phosphoprotein 1; FGF – fibroblast growth factor; IGF1 – insulin growth factor-1; IL1 - interleukin-1β; IL6 – interleukin-6;IL17 – inteleukin-17; ITGB3 – subunit β3 of the integrin αvβ3; LEP – leptin; LRP5/6 – low-density lipoprotein receptor related protein 5/6; MSC – mesenchymal stem cell; OB-R – leptin receptor; OCL – osteocalcin, OPG – osteoprotegerin; OSX – osterix; PDGF - platelet derived growth factor β; PHEX – phosphate-regulating endopeptidase homolog, X-linked; PPARγ - peroxidase proliferator-activator receptor γ; RANK - receptor activator of nuclear factor κB; RANKL – RANK ligand; RUNX2 – runt-related transcription factor 2; sFRP1 – secreted frizzled-related protein 1; SOST – sclerostin; TNF – tumor necrosis factor; TRAP - tartrate-resistant acid phosphatase)

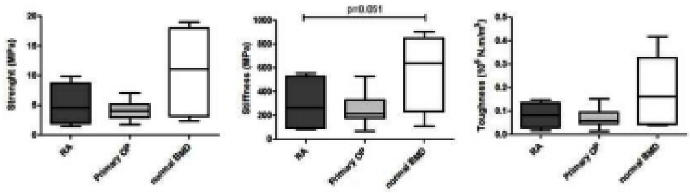

70x20mm (300 x 300 DPI)

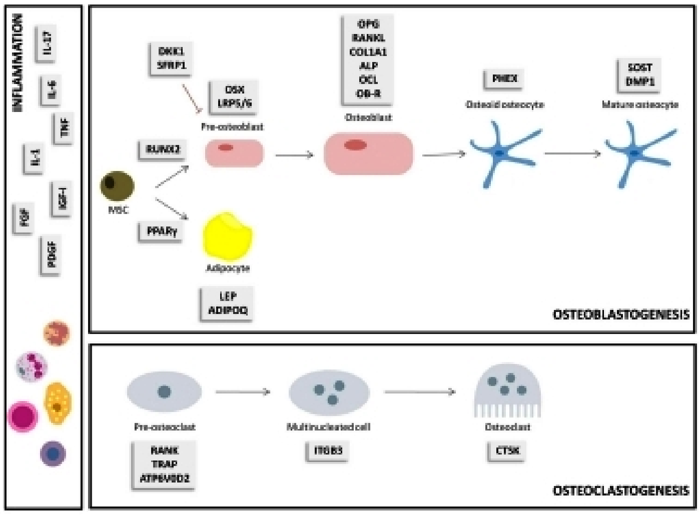

190x142mm (300 x 300 DPI)

Table. Real time PCR primer sequences of the genes studied.

Gene	GenBank number	Primer sequences	
ADIPOQ	NM_004797	F: GGTGAGAAGGGTGAGAAAGGA	R: TTTCACCGATGTCTCCCTTAG
ALP	NM_000478	F: AGAACCCCAAAGGCTTCTTC	R: CTTGGCTTTTCCTTCATGGT
ATP6V0D2	NM_152565	F: CATTCTTGAGTTTGAGGCCG	R: CCGTAATGATCCGCTACGTT
B2M	NM_004048	F: CTATCCAGCGTACGCCAAAGATTC	R: CTTGCTGAAAGACAAGTCTGAATG
COL1A1	NM_000088	F: ACGAAGACATCCCACCAATC	R: AGATCACGTCATCGCACAAC
CTSK	NM_000396	F: GCCAGACAACAGATTTCCATC	R: CAGAGCAAAGCTCACCACAG
DKK1	NM_012242	F: CAGGCGTGCAAATCTGTCT	R: AATGATTTTGATCAGAAGACACACATA
DMP1	NM_004407	F: TGGGCATAGATTTCCTCTTTG	R: CCTGGTTACTGGGAGAGCAC
FGF2	NM_002006	F: TTCTTCCTGCGCATCCAC	R: TTCTGCTTGAAGTTGTAGCTTGAT
IGFI	NM_001111283	F: TGTGGAGACAGGGGCTTTTA	R: ATCCACGATGCCTGTCTGA
IL1B	NM_000576	F: TACCTGTCCTGCGTGTTGAA	R: TCTTTGGGTAATTTTTGGGATCT
IL6	NM_000600	F: GATGAGTACAAAAGTCCTGATCCA	R: GATGAGTACAAAAGTCCTGATCCA
IL17A	NM_002190	F: TTCCCCCGGACTGTGATGGTCA	R: CAGGGTCCTCATTGCGGTGGAGA
ITGB3	NM_000212	F: GGGCAGTGTCATGTTGGTAG	R: CAGCCCCAAAGAGGGATAAT
LEP	NM_000230	F: TTGTCACCAGGATCAATGACA	R: GTCCAAACCGGTGACTTTCT
LRP5	NM_015835	F: GAACATCAAGCGAGCCAAG	R: TGGCTCAGAGAGGTCAAAACA
LRP6	NM_002336	F: ATCCGAAAGGCACAAGAAGA	R: GACTCGGAACTGAGCTCACAA
OB-R	NM_002303	F: ATTTTCAGAAGCCAGAAACG	R: CAGTTGTTGGCATCATCTCA
OCL	NM_199173	F: CCAGGCAGGTGCGAAG	R: TCAGCCAACTCGTCACAGTC
OPG	NM_002546	F: CGCTCGTGTTTCTGGACAT	R: GTAGTGGTCAGGGCAAGGG
OSX	NM_152860	F: CATCTGCCTGGCTCCTTG	R: CAGGGGACTGGAGCCATA
PDGFB	NM_002608	F: CTGGCATGCAAGTGTGAGAC	R: CGAATGGTCACCCGAGTTT
PHEX	NM_000444	F: CGATCCTCTTTCTAGTGAGTCAAG	R: TAGCTTGGCATATCTTCGGG
PMM1	NM_002676	F: GAATGGCATGCTGAACATCT	R: TCCCGGATCTTCTCTTTCTTG
PPARγ	NM_138712	F: AGCCTTTAACGAAATGACCA	R: TCTGCAACCACTGGATCTGT
RANK	NM_003839	F: GAACATCATGGGACAGAGAAATC	R: GGCAAGTAAACATGGGGTTC
RANKL	NM_003701	F: AGAGAAAGCGATGGTGGATG	R: TATGGGAACCAGATGGGATG
RUNX2	NM_004348	F: CGGAATGCCTCTGCTGTTA	R: TCTGTCTGTGCCTTCTGGGT
sFRP1	NM_003012	F: GCTGGAGCACGAGACCAT	R: TGGCAGTTCTTGTTGAGC
SOST	NM_025237	F: AGACCAAAGACGTGTCCGAG	R: GGGATGCAGCGGAAGTC
TNF	NM_000594	F: CAGCCTCTTCTCCTTCCTGAT	R: GCCAGAGGGCTGATTAGAGA
TRAP	NM_001111034	F: CGGCCACGATCACAATCT	R: GCTTTGAGGGGTCCATGA

ADIPOQ – adiponectin; ALP – alkaline phosphatase; ATP6V0D2 - ATPase H^+ transporter; B2M – β2-microglobulin; COL1A1 – Collagen type 1,α1; CTSK – cathepsin K; DKK1 - dickkopf-related protein 1; DMP1 – dentin matrix acidic phosphoprotein 1; FGF2 – fibroblast growth factor 2; IGF1 – insulin growth factor-1; IL1B - interleukin-1β; IL6 – interleukin-6; IL17A – interleukin-17; ITGB3 – subunit β3 of the integrin αvβ3; LEP – leptin; LRP5/6 – low-density lipoprotein receptor related protein 5/6; OB-R – Leptin receptor; OCL – osteocalcin, OPG – osteoprotegerin; OSX – osterix; PDGFB - platelet derived growth factor β; PHEX – phosphate-regulating endopeptidase homolog, X-linked; PMM1 - phosphomannomutase 1; PPARγ - peroxidase proliferator-activator receptor γ; RANK – receptor activator of nuclear factor κB; RANKL – RANK ligand; ; RUNX2 – runt-related transcription factor 2; sFRP1 - secreted frizzled-related protein 1; SOST – sclerostin; TNF – tumor necrosis factor; TRAP - tartrate-resistant acid phosphatase.

PART IV

Upregulation of Inflammatory Genes and Downregulation of Sclerostin Gene Expression Are Key Elements in the Early Phase of Fragility Fracture Healing

OPEN ACCESS Freely available online

PLoS one

Upregulation of Inflammatory Genes and Downregulation of Sclerostin Gene Expression Are Key Elements in the Early Phase of Fragility Fracture Healing

Joana Caetano-Lopes[1], Ana Lopes[1], Ana Rodrigues[1,2], Diana Fernandes[1], Inês P. Perpétuo[1], Teresa Monjardino[3,4], Raquel Lucas[3,4], Jacinto Monteiro[5], Yrjö T. Konttinen[6,7,8], Helena Canhão[1,2¶], João E. Fonseca[1,2*¶]

1 Rheumatology Research Unit, Faculdade de Medicina da Universidade de Lisboa, Instituto de Medicina Molecular, Lisbon, Portugal, 2 Serviço de Reumatologia e Doenças Ósseas Metabólicas, Hospital de Santa Maria, Lisbon, Portugal, 3 Department of Hygiene and Epidemiology, University of Porto Medical School, Porto, Portugal, 4 Institute of Public Health, University of Porto, Porto, Portugal, 5 Orthopaedics Department, Hospital de Santa Maria, Lisbon, Portugal, 6 Department of Medicine, University of Helsinki, Helsinki, Finland, 7 ORTON Orthopaedic Hospital of the Invalid Foundation, Helsinki, Finland, 8 COXA Hospital for Joint Replacement, Tampere, Finland

Abstract

Background: Fracture healing is orchestrated by a specific set of events that culminates in the repair of bone and reachievement of its biomechanical properties. The aim of our work was to study the sequence of gene expression events involved in inflammation and bone remodeling occurring in the early phases of callus formation in osteoporotic patients.

Methodology/Principal Findings: Fifty-six patients submitted to hip replacement surgery after a low-energy hip fracture were enrolled in this study. The patients were grouped according to the time interval between fracture and surgery: bone collected within 3 days after fracture (n = 13); between the 4th and 7th day (n = 33); and after one week from the fracture (n = 10). Inflammation- and bone metabolism-related genes were assessed at the fracture site. The expression of pro-inflammatory cytokines was increased in the first days after fracture. The genes responsible for bone formation and resorption were upregulated one week after fracture. The increase in RANKL expression occurred just before that, between the 4th–7th days after fracture. Sclerostin expression diminished during the first days after fracture.

Conclusions: The expression of inflammation-related genes, especially IL-6, is highest at the very first days after fracture but from day 4 onwards there is a shift towards bone remodeling genes, suggesting that the inflammatory phase triggers bone healing. We propose that an initial inflammatory stimulus and a decrease in sclerostin-related effects are the key components in fracture healing. In osteoporotic patients, cellular machinery seems to adequately react to the inflammatory stimulus, therefore local promotion of these events might constitute a promising medical intervention to accelerate fracture healing.

Citation: Caetano-Lopes J, Lopes A, Rodrigues A, Fernandes D, Perpétuo IP, et al. (2011) Upregulation of Inflammatory Genes and Downregulation of Sclerostin Gene Expression Are Key Elements in the Early Phase of Fragility Fracture Healing. PLoS ONE 6(2): e16947. doi:10.1371/journal.pone.0016947

Editor: Eliana Abdelhay, Instituto Nacional de Câncer, Brazil

Received November 22, 2010; **Accepted** January 18, 2011; **Published** February 11, 2011

Funding: This work was supported by two grants from the Portuguese Foundation of Science and Technology (Fundação para a Ciência e Tecnologia)(PTDC/SAU-BEB/65992/2006, SFRH/BD/36825/2007). (*www.fct.mctes.pt*). The funders had no role in study design, data collection and analysis, decision to publish, or preparation of the manuscript.

Competing Interests: The authors have declared that no competing interests exist.

* E-mail: jefonseca@netcabo.pt

¶ These authors contributed equally to this work.

Introduction

The management of fragility fractures associated with osteoporosis is difficult due to several factors including inadequate fixation strength of implants used to stabilize the fracture until union of bone occurs. In particular, the fragility fractures affecting the metaphyseal region of long bones are associated with an increased rate of complications. Several studies report nonunion in 2–10%, malalignment after surgery in 4–40%, metal work failure in 1–10%, and reoperation in 3–23% [1]. Experimental studies have shown that the decline in the capacity for fracture repair is age related. Disturbance of the full redevelopment of mechanical strength within fracture calluses in elderly animals has been shown in experimental rat models. In the human being it is possible that fracture healing is affected by aging [2], particularly in the elderly osteoporotic patients [3]. In another study it was described that in 6, 26 and 52 weeks old rats, there is upon aging a delay in radiographic progression of fracture healing but the expression of the key genes involved in this process is not age-dependent [1,4,5]. The fracture healing response and its temporal gene expression in elderly patients with osteoporosis has not been adequately investigated at the cellular and molecular level. Identification of the mechanisms that lead to fracture healing disturbances in patients with osteoporosis is of outstanding importance because they could allow prevention and better management of these healing complications. In addition, the biological processes behind fracture healing in osteoporosis might hold the key for future medical interventions.

Fracture healing recapitulates certain aspects of skeletal development and growth, involving interplay of cells, growth factors and extracellular matrix. Following injury, a blood clot is formed in the fracture site [6,7]. This hematoma is the source of several signaling molecules that induce an inflammatory cascade of events that initiate healing [8,9]. Based on histological observations of healing fractures, bone repair was defined in animal models by an initial inflammatory phase (lasting for about three days), a catabolic phase where damaged tissues are removed, and an anabolic phase where new bone is rebuilt. Within several days of the initial inflammatory response there is a sequence of events that results in the formation of new bone through the development of a structure named callus. Experimental studies have related temporal gene expression with bone healing. In a study with Sprague-Dawley rats, gene expression was evaluated on days 3 and 11 post-fracture. The authors showed that different molecular pathways of gene expression regulate different phases of bone healing [10].

This work aims to study the profile of genes involved in inflammation and bone remodeling during the 3 major steps of the early phase of callus formation in human bone after a hip fragility fracture.

Results

Study population

Fifty-six patients 80±7 years of age, 75% of female gender, which suffered a hip fragility fracture, were enrolled in this study. There were no statistical significant differences in age and gender between the 3 study groups (Table 1): those who had surgery less than three days after fracture (group 1), between four and seven days (group 2) and eight or more days post-fracture (group 3).

Inflammation and growth factors genes

The local expression of nine genes related to the inflammatory phase of bone healing (IL-1β, IL-6, TNF, BMP2, BMP4, TGF-β1, IGF-I, FGF-2 and PDGF-β) was analyzed (Figure 1, Table 2). IL-1β, IL-6 and TNF are cytokines that have an important role in potentiating the inflammatory cascade. Concordantly, the expression of these genes was highest during the first 3 post-fracture days and decreases thereafter. Specifically, *IL6* had a higher expression in group 1 than in group 2 (p-value = 0.021) and *IL1B*, although expressed at low levels, remained stable, decreasing slightly after the 4^{th}–7^{th} day post-fracture (p-value = 0.087). On the contrary, *TNF* expression was stable, showing only a slight tendency to decrease over time (p-value = 0.208).

BMPs are a set of growth factors and cytokines belonging to the TGF-β superfamily and are involved in the creation of bone tissue architecture. In fracture healing, BMP-2 and BMP-4 play important roles in osteoblast differentiation. Accordingly, it was observed that the expression levels of *BMP2* were highest until 3 days post-fracture and decreased thereafter (p-value = 0.023), while *BMP4* expression remained fairly constant in all groups (p-value = 0.852). *TGFB* exhibited a constant negative slope between the three groups (p-value = 0.051).

IGF-I is a hormone involved in bone matrix synthesis and there were no differences in its expression levels in the three groups analyzed (p-value = 0.817). The growth factors FGF-2 and PDGF-β are involved in the formation of new blood vessels. Their expression tended to decrease slightly from group 1 to group 2 and was clearly decreased after 8 days post-fracture (*FGF2*: p-value = 0.091 and *PDGFβ*: p-value = 0.043).

Overall, these findings suggest that the expression levels of inflammatory genes and growth factors are particularly high during the three first days post-fracture and decrease from the day 4 onwards.

Osteoprotegerin, RANK and RANKL

OPG is a negative regulator of bone resorption and, as expected, its expression was slightly lower in group 3 than in group 1 (p-value = 0.168) (Figure 2A, Table 2). On the other hand, *RANK* produced by osteoclast precursors showed a tendency to increase over time (p-value = 0.072). Finally, *RANKL* expressed by osteoblasts, stromal cells and immune system cells had its highest level at days 4 to 7 post-fracture (group 2) and decreased thereafter (p-value = 0.267).

The ratio RANKL/OPG regulates the balance between remodeling and formation. In this study, the ratio *RANKL/OPG* mRNA peaked in group 2 and tended to decrease later on (p-value = 0.078).

Steoblast-related genes

The expression of three genes that play important functions in the osteoblast and its activity was studied (Figure 2B, Table 2). Core-binding factor, alfa subunit 1/runt-related transcription factor 2 (CBFA1/RUNX2) and osterix (OSX) are transcription factors that play a crucial role in osteoblast differentiation, and ALP is an enzyme expressed at a later stage being involved in bone matrix maintenance. In our results, *CBFA1/RUNX2* expression was slightly higher in group 2 than in group 1 and then remained constant and was similar in groups 2 to 3 (p-value = 0.521). On the other hand, *OSX* expression levels were similar in groups 1 and 2 and marginally higher in group 3 (p-value = 0.149). Regarding *ALP*, levels were slightly lower in group 2 as compared to group 1 but were similar between groups 2 and 3 (p-value = 0.726).

Osteocyte-related genes

Sclerostin (SOST) is produced by the osteocyte and regulates negatively osteoblast differentiation by inhibiting Wnt/β-catenin

Table 1. Description of the study population divided between the event of fracture and surgery.

	Group 1	Group 2	Group 3	p-value
	Until 3 days post-fracture	4 to 7 days post-fracture	8 or more days post-fracture	
Number of patients	13	33	10	
Age (years)	80±5	79±7	83±7	0.326
Female gender (%)	85	79	50	0.121

Values represent mean±standard deviation.
Comparisons between groups performed with ANOVA or chi-square tests.
doi:10.1371/journal.pone.0016947.t001

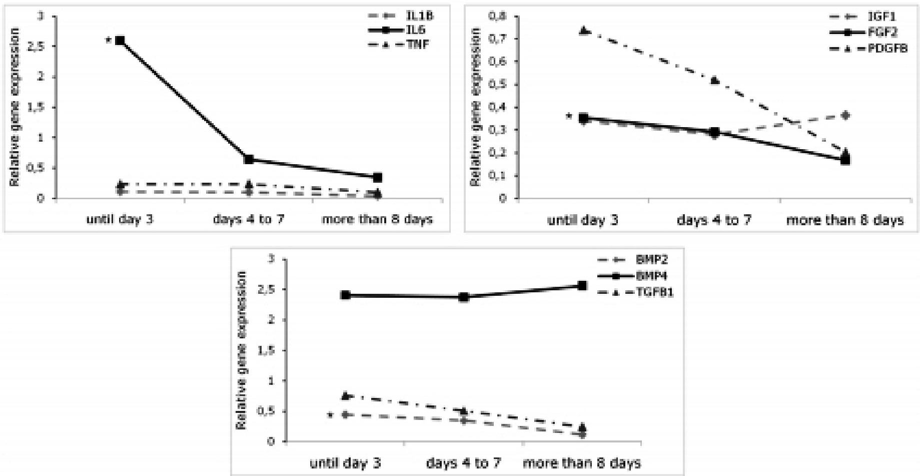

Figure 1. Relative expression of inflammation and growth factors genes grouped according to the time between the event of fracture and the surgery. Each gene was normalized to the expression of the housekeeping genes *B2M* and *PMM1*. *p-value<0.05 for comparisons between the three groups. (Points represent median values). IL1B = Interleukin-1β; IL6 = Interleukin-6; TNF = tumor necrosis factor; IGF1 = Insulin growth factor-1 ; FGF2 = fibroblast growth factor 2 ; PDGFB = platelet derived growth factor β; BMP = Bone morphogenetic protein; TGFB1 = transforming growth factor β1.
doi:10.1371/journal.pone.0016947.g001

signaling. In this work we found a highly significant reduction in *SOST* levels overtime (p-value = 0.001) (Figure 2C, Table 2).

Osteoclast-related genes

Four genes that regulate osteoclast differentiation and function were studied (Figure 2D, Table 2). Tartrate-resistant acid phosphatase (TRAP) is an enzyme expressed by pre-osteoclasts and active osteoclasts; on the other hand, cathepsin K (CTSK), β3 subunit of the αvβ3 integrin (ITGB3) and ATPase H^+ transporter (ATP6V0D2) are proteins involved in the process of bone resorption.

We observed a marked increase in *TRAP* and a more modest change in *CTSK* and *ATP6V0D2* expression over the post fracture period (*TRAP*: p-value = 0.009; *CTSK*: p-value = 0.027 and *ATP6V0D2*: p-value = 0.076). On the other hand, the expression of *ITGB3* remained constant (p-value = 0.658).

Discussion

Although some studies have addressed the sequence of events in fracture healing, the research was mainly based on histological examination of healthy individual's tissue and on molecular studies in animal models. Based on these previous histological and molecular studies of healing fractures the initial stages of these process have been proposed to include an early inflammatory and unspecific anabolic phase (first 24 hours up to third day), immediately followed by a non specific catabolic phase (up to the end of the first week) that sets the conditions for a more bone specific anabolic phase (first week and thereafter) [10,11,12,13,14]. Thus, in our study, patients were grouped into these three phases according to the time between fracture and surgery and the main objective was to address the gene expression variations during early callus formation in patients that have suffered a hip fragility fracture. We showed that many inflammation-related genes have higher levels of expression until 3 days post-trauma while genes related to osteoblast and osteoclast activity increase at day 4 and thereafter.

Cytokine gene expression (*IL1B*, *IL6* and *TNF*) was more pronounced during the first days after fracture, as described in younger individuals. Specifically, the decrease in *IL6* expression levels was far more pronounced than what was observed with the other pro-inflammatory cytokines evaluated. Of interest, reports state that *IL1B* is upregulated in response to the fracture event but in *IL1B* knockout mice there was no change in callus formation and bone and cartilage matrix production [15]. On the other hand, in the absence of TNF signaling there was a 2–4 days delay in chondrogenic differentiation and a 2–3 weeks delay in endochondral tissue resorption [16]. Regarding IL-6, studies in knockout mice have shown that there was a delay in callus formation and lower osteoclast density [17]. Therefore, in accordance with our results, IL-6 appears to have a pivotal role in the early phase of fracture healing, probably through the increase in the pro-osteoclastogenic stimuli. Moreover, expression levels of *TGFB*, *BMP2*, *BMP4*, *PDGFB* and *FGF2* was highest during the first 3 days post-fracture. The variation encountered in these elderly fragility fracture patients is similar to the findings obtained in animal models studies [8] and in healthy younger subjects [18] where the inflammatory phase occurs before day 3 post-fracture, being IL-6 a crucial player in this early phase of fracture healing.

Regarding the RANK-RANKL-OPG system, *OPG* expression diminished gradually after fracture, releasing the inhibitory signal for osteoclast differentiation. Concordantly, *RANKL* peaks at 4^{th}–7^{th} day after trauma, creating a stimulus for osteoclast differen-

Table 2. Comparison between the relative gene expression levels of patients submitted to hip replacement surgery due to low-energy fracture in relation to the days between fracture and surgery.

	Fragility fracture patients			p-value*
	Until 3 days post-fracture	**4–7 days post-fracture**	**8 or more days post-fracture**	
IL1B	0.111 (0.07–0.30)	0.101 (0.03–0.16)	0.039 (0.02–0.11)	0.087
IL6	2.596 (0.94–5.23)	0.643 (0.24–2.46)	0.348 (0.08–0.90)	0.021
TNF	0.236 (0.20–0.63)	0.238 (0.09–0.43)	0.102 (0.08–0.56)	0.208
TGFB1	0.759 (0.28–0.94)	0.507 (0.25–0.83)	0.244 (0.17–0.49)	0.051
BMP2	0.443 (0.20–1.32)	0.344 (0.09–0.55)	0.114 (0.03–0.41)	0.023
BMP4	2.406 (1.16–6.66)	2.372 (0.72–5.54)	2.516 (0.86–3.26)	0.852
IGFI	0.341 (0.13–2.24)	0.280 (0.16–0.80)	0.365 (0.27–0.66)	0.817
FGF2	0.354 (0.25–1.08)	0.292 (0.12–0.85)	0.168 (0.10–0.36)	0.091
PDGFB	0.738 (0.30–1.71)	0.520 (0.19–0.82)	0.203 (0.08–0.58)	0.043
OPG	3.340 (1.63–4.56)	1.938 (0.99–4.18)	0.979 (0.85–2.09)	0.168
RANKL	13.803 (5.46–22.36)	25.838 (8.11–39.20)	15.305 (3.86–32.70)	0.267
RANK	0.095 (0.06–0.37)	0.290 (0.14–0.52)	0.438 (0.24–0.86)	0.072
RANKL/OPG	4.887 (2.71–7.78)	11.362 (5.32–22.28)	5.581 (3.08–23.08)	0.078
CBFA1/RUNX2	1.954 (1.08–2.63)	2.574 (1.31–4.02)	2.178 (1.12–2.58)	0.521
OSX	0.629 (0.28–1.86)	0.655 (0.24–0.87)	0.888 (0.68–2.71)	0.149
ALP	5.393 (2.53–7.86)	4.407 (2.47–5.95)	4.054 (2.64–10.05)	0.726
SOST	1.402 (1.07–3.66)	0.668 (0.39–1.18)	0.274 (0.19–0.77)	0.001
TRAP	4.204 (1.31–11.46)	9.660 (3.78–34.41)	22.758 (9.18–83.48)	0.009
CTSK	30.276 (8.72–132.81)	63.593 (15.67–250.62)	151.91 (87.71–558.88)	0.027
ITGB3	2.045 (1.43–2.97)	1.619 (1.16–2.79)	1.292 (0.82–2.48)	0.658
ATP6V0D2	4.898 (2.78–10.71)	9.839 (4.51–25.20)	32.378 (7.65–68.59)	0.076

Values represent median (Q1–Q3).
Comparisons between the 3 groups performed with Kruskall-Wallis H test.
*p-value for comparison between the 3 groups.
IL1B – interleukin-1β; IL6 – interleukin-6; TNF – tumor necrosis factor; TGFB1 – transforming growth factor β1; BMP – Bone morphogenetic protein; IGF1 – insulin growth factor-1; FGF2 – fibroblast growth factor 2; PDGFB – platelet derived growth factor β; OPG – osteoprotegerin; RANK – receptor activator of nuclear factor κB; RANKL – RANK ligand; CBFA1/RUNX2 – core binding factor α1/runt-related transcription factor 2; OSX – osterix; ALP – alkaline phosphatase; SOST – sclerostin; TRAP – tartrate-resistant acid phosphatase; CTSK – cathepsin K; ITGB3 – subunit β3 of the integrin αvβ3; ATP - ATPase H^+ transporter.
doi:10.1371/journal.pone.0016947.t002

tiation from its precursors. Therefore, the ratio *RANKL/OPG* was high during days 4–7 post-fracture, not only due to an increase in *RANKL* but also to a decrease in *OPG* expression switching the balance to a pro-resorptive status, as described in a young mouse model [9].

Concerning osteoblast differentiation and activity, it was observed that *CBFA1/RUNX2* and *OSX*, two regulatory factors essential for its differentiation [19], had a weak increase indicating the beginning of an initial osteogenic phase. *CBFA1/RUNX2* increases from the initial phase of bone healing whereas *OSX* increases after 4 days post-fracture sustaining the evidence that *OSX* acts later than *CBFA1/RUNX2* in osteoblast lineage commitment [20]. On the other hand, *ALP*, a marker for osteoblast activity, decreases from early stages of bone healing.

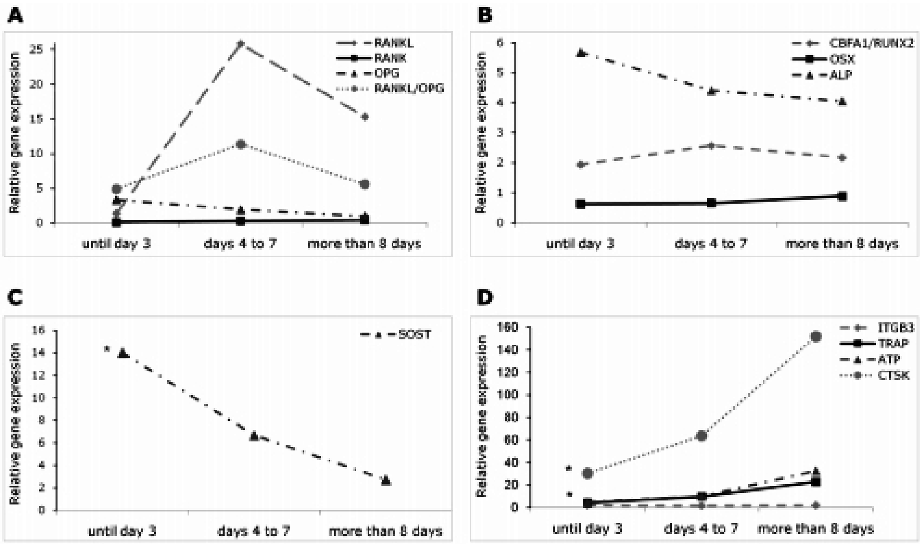

Figure 2. Relative expression of bone metabolism-related genes divided according to the time between the event of fracture and the surgery. *RANK*, *RANKL* and *OPG* (**A**), osteoblast (**B**), osteocyte (**C**) and osteoclast-specific genes (**D**) were studied in the three study groups. Each gene was normalized to the expression of the housekeeping genes *B2M* and *PMM1*. *p-value<0.05 for comparisons between the three groups. (Points represent median values). RANK = receptor activator of nuclear factor κB; RANKL = RANK ligand; OPG = osteoprotegerin; CBFA1/RUNX2 = core binding factor α1/runt-related transcription factor 2; OSX = osterix; ALP = alkaline phosphatase; SOST = sclerostin; ITGB3 = subunit β3 of the integrin αvβ3; TRAP = tartrate-resistant acid phosphatase; ATP - ATPase H^+ transporter; CTSK = cathepsin K.
doi:10.1371/journal.pone.0016947.g002

This gene expression profile had been already observed in other studies [18,21,22] and it is not entirely surprising, since this enzyme is involved in bone matrix production and our study is focused on the early changes related to fracture, in a stage where the formation of new bone matrix is still not occurring.

Sclerostin is a protein produced by the osteocyte that inhibits canonical Wnt/β-catenin signaling, thus blocking osteoblast proliferation and differentiation. The contribution of this pathway to fracture healing depends on the function of β-catenin in different stages of fracture repair, namely in the commitment and regulation of osteoblasts [23]. Only one study in young mice has addressed the levels of expression of sclerostin during fracture repair and they found that this protein was downregulated during the process [24]. In fact, our results, the first obtained in fragility fracture patients, showed that *SOST* expression decreases significantly from the beginning of the healing cascade, suggesting that there is an initial blockage of osteoblast proliferation and differentiation that is subsequently released over the period of fracture healing.

The role of the osteoclast in bone healing is somewhat controversial. Bone formation overcomes the loss of continuity and osteoclasts seem to play a role at a later phase, in the remodeling stage. Moreover, in a longitudinal study where the serum levels of biochemical markers associated with bone metabolism were assessed, the authors showed that the markers for bone resorption remained elevated up to four months after fracture [21]. At gene expression level, we found that the osteoclast-specific genes *TRAP*, *CTSK* and *ATP6V0D2* were significantly increased from day 8 onward after fracture, pointing to an activation of osteoclast function. In fact, the RANKL/OPG ratio is highest in group 2, whereas the CTSK values are increased in group 3, indicating that during 4–7 days after fracture, osteoclastogenesis stimulus was ongoing intensively whereas at day 8 and later osteoclasts containing cathepsin K had already been formed in relatively high numbers. The active role of osteoclast during the early phase of fracture healing was already described in sheep where it was proposed that these cells not only resorb bone but adjust the system, together with osteoblasts, in order to improve bone strength [25].

Due to the fact that we are dealing with human subjects, the study had to have a cross-sectional design. Thus, it is not possible to rule out the intrinsic variability of different individuals. However, the statistical significance for many of the changes described seems to refute this. Besides, the RNA used was extracted from the site of fracture (trabecular bone) that not only has the bone cells that we are interested in, but also other cell types, such as adipocytes, bone marrow cells and cells infiltrating the tissues during the initial healing phase. However, the bone remodeling genes studied are relatively specific for bone cells and it is unlikely that this technical aspect represent a relevant confounding factor in our study.

Taken together, our results indicate that in patients with hip fragility fractures, the expression of inflammation-related genes is highest during the first days after fracture but from day 4 onwards there is a shift towards bone cell remodeling genes, suggesting that the machinery of bone healing is conserved in osteoporotic bone.

Table 3. Real time PCR primer sequences of the genes studied.

Gene	GenBank number	Primer sequences
B2M	NM_004048	F: CTATCCAGCGTACGCCAAAGATTC
		R: CTTGCTGAAAGACAAGTCTGAATG
PMM1	NM_002676	F: GAATGGCATGCTGAACATCT
		R: TCCCGGATCTTCTCTTTCTTG
IL1B	NM_000576	F: TACCTGTCCTGCGTGTTGAA
		R: TCTTTGGGTAATTTTTGGGATCT
IL6	NM_000600	F: GATGAGTACAAAAGTCCTGATCCA
		R: GATGAGTACAAAAGTCCTGATCCA
TNF	NM_000594	F: CAGCCTCTTCTCCTTCCTGAT
		R: GCCAGAGGGCTGATTAGAGA
TGFB1	NM_000660	F: GCAGCACGTGGAGCTGTA
		R: CAGCCGGTTGCTGAGGTA
BMP2	NM_001200	F: CGGACTGCGGTCTCCTAA
		R: GGAAGCAGCAACGCTAGAAG
BMP4	NM_001202	F: CTGCAACCGTTCAGAGGTC
		R: TGCTCGGGATGGCACTAC
FGF2	NM_002006	F: TTCTTCCTGCGCATCCAC
		R: TTCTGCTTGAAGTTGTAGCTTGAT
PDGFB	NM_002608	F: CTGGCATGCAAGTGTGAGAC
		R: CGAATGGTCACCCGAGTTT
IGFI	NM_001111283	F: TGTGGAGACAGGGGCTTTTA
		R: ATCCACGATGCCTGTCTGA
CBFA1/RUNX2	NM_004348	F: CGGAATGCCTCTGCTGTTA
		R: TCTGTCTGTGCCTTCTGGGT
OSX	NM_152860	F: CATCTGCCTGGCTCCTTG
		R: CAGGGGACTGGAGCCATA
ALP	NM_000478	F: AGAACCCCAAAGGCTTCTTC
		R: CTTGGCTTTTCCTTCATGGT
TRAP	NM_001111034	F: CGGCCACGATCACAATCT
		R: GCTTTGAGGGGTCCATGA
ITGB3	NM_000212	F: GGGCAGTGTCATGTTGGTAG
		R: CAGCCCCAAAGAGGGATAAT
CTSK	NM_000396	F: GCCAGACAACAGATTTCCATC
		R: CAGAGCAAAGCTCACCACAG
ATP6V0D2	NM_152565	F: CATTCTTGAGTTTGAGGCCG
		R: CCGTAATGATCCGCTACGTT
SOST	NM_025237	F: AGACCAAAGACGTGTCCGAG
		R: GGGATGCAGCGGAAGTC
RANK	NM_003839	F: GAACATCATGGGACAGAGAAATC
		R: GGCAAGTAAACATGGGGTTC
RANKL	NM_003701	F: AGAGAAAGCGATGGTGGATG
		R: TATGGGAACCAGATGGGATG
OPG	NM_002546	F: CGCTCGTGTTTCTGGACAT
		R: GTAGTGGTCAGGGCAAGGG

B2M – β2-microglobulin; PMM1 - phosphomannomutase 1; IL1B – interleukin-1β; IL6 – interleukin-6; TNF – tumor necrosis factor; TGFB1 – transforming growth factor β1; BMP – Bone morphogenetic protein; IGF1 – insulin growth factor-1; FGF2 – fibroblast growth factor 2; PDGFB – platelet derived growth factor β; OPG – osteoprotegerin; RANK – receptor activator of nuclear factor κB; RANKL – RANK ligand; CBFA1/RUNX2 – core binding factor α1/runt-related transcription factor 2; OSX – osterix; ALP – alkaline phosphatase; SOST – sclerostin; TRAP – tartrate-resistant acid phosphatase; CTSK – cathepsin K; ITGB3 – subunit β3 of the integrin αvβ3; ATP - ATPase H^+ transporter.

doi:10.1371/journal.pone.0016947.t003

In addition, the changes observed in IL-6 expression profile suggest that this pro-inflammatory cytokine plays a pivotal role in triggering the healing cascade. Moreover, sclerostin expression is quickly reduced after fracture and we hypothesize that this allows osteoblasts to escape from its inhibitory effect, thus promoting the expression of bone formation genes. Interestingly, RANKL expression is subsequently increased, generating the stimulus for osteoclast activity, as confirmed also by the later rise in the expression of the bone resorption-related genes. Our findings bring new insights for clarifying bone fracture healing process in osteoporotic patients. We propose that an initial inflammatory stimulus and a decrease in sclerostin-related effects are key events for an adequate fracture healing. Thus, in osteoporotic patients, locally promoting these events might provide promising medical interventions for accelerating fracture healing and reduce the rate of complications.

Methods

Sample collection

Patients that suffered a low-energy hip fracture and underwent total hip replacement surgery at the Orthopedic Department of Hospital de Santa Maria were consecutively recruited for this study from 2007 until 2009. Epidemiological and clinical data such as age, gender and days between the fracture and surgery were collected. Patients with other metabolic bone diseases and with bone metastases were excluded.

Written informed consent was obtained from all patients and the study was conducted in accordance with the ethical principles for medical research involving human subjects expressed in the Declaration of Helsinki, as amended in Edinburgh (2000), and was approved by Santa Maia Hospital Ethics Committee.

According to the time between fracture and surgery, patients were divided in three groups: those who had hip replacement surgery between zero and three days after fracture (group 1), four and seven days after fracture (group 2) or eight or more days after fracture (group 3).

After the medical procedure, the femoral epiphyses were snap-frozen at −80°C.

RNA extraction

Without defrosting the bone specimen, small trabecular bone pieces were collected from the site of fracture and pulverized using a mortar and pestle. RNA was then extracted using TRIzol reagent (Invitrogen, UK) with proteinase K (Bioline, UK) digestion [26] to better dissolve the dense extracellular matrix.

The procedure used was a modified version of the protocol described by Ireland [27]. Briefly, 80mg of bone powder was placed in TRIzol reagent and homogenized. Lipids were solubilized with 0.2 volumes of chloroform and the fraction containing RNA was preserved. Proteinase K digestion (3.3µg proteinase K/mg bone) was performed at 55°C. RNA was precipitated with 1 volume of ice-cold isopropyl alcohol. RNA pellet was dissolved in RNase/DNase-free water. As this method leaves residual chemical contaminants, RNA was cleaned using a commercial kit (RNeasy mini kit, Qiagen, Germany) and genomic DNA contaminants were removed by

DNaseI treatment (Qiagen, Germany). RNA concentration was determined spectrophotometrically (Nanodrop ND-1000 Spectrophotometer, Thermo Fisher Scientific, USA) and its integrity was assessed by lab-on-a-chip technology (Agilent RNA 6000 Nano Kit, Agilent technologies, USA) according to the manufacturer's instructions. RNA was stored at −80°C until further use.

Quantitative reverse transcription-polymerase chain reaction (PCR)

Reverse transcription cDNA synthesis was performed on 60ng of RNA from each sample using the DyNAmo cDNA synthesis kit (Finnzymes, Finland) and 300ng of random hexamer primers according to the manufacturer's instructions.

Each cDNA template (3ng/µl) was amplified in duplicate with DyNAmo Flash SYBR green qPCR kit (Finnzymes, Finland) on a Rotor-Gene thermocycler (Qiagen, Germany) according to the manufacturer's instructions. Reactions were incubated at 50°C for 2 minutes and at 95°C for 7 minutes, followed by denaturation at 95°C for 10 seconds and annealing/extension at 60°C for 10 seconds. The reactions were validated by the presence of a single peak in the melt curve analysis.

Primers for the housekeeping and target genes (Table 3) were designed using the software *Probefinder* (http://qpcr.probefinder.com, Roche, Switzerland) in order to anneal in separate exons preventing amplification of contaminating genomic DNA.

Real time PCR results were analyzed using the standard curve analysis. The cycle threshold (C_T) is defined as the number of cycles required for the fluorescent signal to cross the threshold and exceed the background level. The efficiency of the PCR should be 100%, meaning that for each cycle the amount of product doubles. A good reaction should have an efficiency of 90–100%, which corresponds to a slope between −3.58 and −3.10. The conversion of the C_T value in relative expression levels was performed with the slope and the Y intersect extracted from the standard curve and applying the equation $10^{(Y\ \mathrm{intersect}-CT/\mathrm{slope})}$ [28,29]. The values obtained were normalized with the housekeeping genes β-2-microglobulin (*B2M*) and phosphomannomutase 1 (*PMM1*).

Statistical analysis

To define the exposure variable, patients were divided, according to the number of days between the event of fracture and the surgery, in three groups. The distributions of continuous variables were compared between groups using either analysis of variance (ANOVA), for normally-distributed characteristics, or Kruskal-Wallis H test, for distributions with significant deviation from normality (according to Shapiro-Wilk test). For nominal variables, chi-squared test was used. Significance level was set at 0.05.

Statistical analysis was performed using the Statistical Package for Social Sciences manager software, version 17.0 (SPSS, Inc, Chicago, IL, USA).

Acknowledgments

We wish to thank Dr. A. Gomes from Molecular Immunology Unit, Instituto de Medicina Molecular da Faculdade de Medicina de Lisboa for advice in real time PCR experiment setup.

Author Contributions

Conceived and designed the experiments: YTK HC JEF. Performed the experiments: JCL AL DF IP. Analyzed the data: TM RL. Contributed reagents/materials/analysis tools: AR JM. Wrote the paper: JCL AR HC JEF.

References

1. Giannoudis P, Tzioupis C, Almalki T, Buckley R (2007) Fracture healing in osteoporotic fractures: is it really different? A basic science perspective. Injury 38 Suppl 1: S90–99.
2. Lu C, Miclau T, Hu D, Hansen E, Tsui K, et al. (2005) Cellular basis for age-related changes in fracture repair. J Orthop Res 23: 1300–1307.
3. Nikolaou VS, Efstathopoulos N, Kontakis G, Kanakaris NK, Giannoudis PV (2009) The influence of osteoporosis in femoral fracture healing time. Injury 40: 663–668.
4. Desai BJ, Meyer MH, Porter S, Kellam JF, Meyer RA, Jr. (2003) The effect of age on gene expression in adult and juvenile rats following femoral fracture. J Orthop Trauma 17: 689–698.
5. Meyer RA, Jr., Desai BR, Heiner DE, Fiechtl J, Porter S, et al. (2006) Young, adult, and old rats have similar changes in mRNA expression of many skeletal genes after fracture despite delayed healing with age. J Orthop Res 24: 1933–1944.
6. Giannoudis PV, Einhorn TA, Marsh D (2007) Fracture healing: the diamond concept. Injury 38 Suppl 4: S3–6.
7. Marzona L, Pavolini B (2009) Play and players in bone fracture healing match. Clinical cases in Mineral and Bone Metabolism 6: 159–162.
8. Einhorn TA, Majeska RJ, Rush EB, Levine PM, Horowitz MC (1995) The expression of cytokine activity by fracture callus. J Bone Miner Res 10: 1272–1281.
9. Kon T, Cho TJ, Aizawa T, Yamazaki M, Nooh N, et al. (2001) Expression of osteoprotegerin, receptor activator of NF-kappaB ligand (osteoprotegerin ligand) and related proinflammatory cytokines during fracture healing. J Bone Miner Res 16: 1004–1014.
10. Rundle CH, Wang H, Yu H, Chadwick RB, Davis EI, et al. (2006) Microarray analysis of gene expression during the inflammation and endochondral bone formation stages of rat femur fracture repair. Bone 38: 521–529.
11. Schindeler A, McDonald MM, Bokko P, Little DG (2008) Bone remodeling during fracture repair: The cellular picture. Semin Cell Dev Biol 19: 459–466.
12. Bais M, McLean J, Sebastiani P, Young M, Wigner N, et al. (2009) Transcriptional analysis of fracture healing and the induction of embryonic stem cell-related genes. PLoS One 4: e5393.
13. Street J, Bao M, deGuzman L, Bunting S, Peale FV, Jr., et al. (2002) Vascular endothelial growth factor stimulates bone repair by promoting angiogenesis and bone turnover. Proc Natl Acad Sci U S A 99: 9656–9661.
14. Khan SN, Solaris J, Ramsey KE, Yang X, Bostrom MP, et al. (2008) Identification of novel gene expression in healing fracture callus tissue by DNA microarray. HSS J 4: 149–160.
15. Lange J, Sapozhnikova A, Lu C, Hu D, Li X, et al. (2010) Action of IL-1beta during fracture healing. J Orthop Res 28: 778–784.
16. Gerstenfeld LC, Cho TJ, Kon T, Aizawa T, Tsay A, et al. (2003) Impaired fracture healing in the absence of TNF-alpha signaling: the role of TNF-alpha in endochondral cartilage resorption. J Bone Miner Res 18: 1584–1592.
17. Yang X, Ricciardi BF, Hernandez-Soria A, Shi Y, Pleshko Camacho N, et al. (2007) Callus mineralization and maturation are delayed during fracture healing in interleukin-6 knockout mice. Bone 41: 928–936.
18. Lyritis G, Nikiforidis P, Papadopoulou Z, Castrisios E, Hartofilakidis-Garofalidis G (1976) The values of some plasma components during the early phases of fracture healing in man. Acta Orthop Scand 47: 264–266.
19. Caetano-Lopes J, Canhao H, Fonseca JE (2007) Osteoblasts and bone formation. Acta Reumatol Port 32: 103–110.
20. Zhang C (2010) Transcriptional regulation of bone formation by the osteoblast-specific transcription factor Osx. J Orthop Surg Res 5: 37.
21. Ivaska KK, Gerdhem P, Akesson K, Garnero P, Obrant KJ (2007) Effect of fracture on bone turnover markers: a longitudinal study comparing marker levels before and after injury in 113 elderly women. J Bone Miner Res 22: 1155–1164.
22. Ikegami S, Kamimura M, Nakagawa H, Takahara K, Hashidate H, et al. (2009) Comparison in bone turnover markers during early healing of femoral neck fracture and trochanteric fracture in elderly patients. Orthopedic Reviews 1: e21.
23. Chen Y, Whetstone HC, Lin AC, Nadesan P, Wei Q, et al. (2007) Beta-catenin signaling plays a disparate role in different phases of fracture repair: implications for therapy to improve bone healing. PLoS Med 4: e249.
24. Dean DB, Watson JT, Jin W, Peters C, Enders JT, et al. (2010) Distinct functionalities of bone morphogenetic protein antagonists during fracture healing in mice. J Anat: In press.
25. Schell H, Lienau J, Epari DR, Seebeck P, Exner C, et al. (2006) Osteoclastic activity begins early and increases over the course of bone healing. Bone 38: 547–554.
26. Egyhazi S, Bjohle J, Skoog L, Huang F, Borg AL, et al. (2004) Proteinase K added to the extraction procedure markedly increases RNA yield from primary breast tumors for use in microarray studies. Clin Chem 50: 975–976.
27. Ireland D (2003) Analysis of Gene Expression in Bone by Quantitative RT-PCR. In: Helfrich MH, Ralston SH, eds. Bone Research Protocols. New York: Humana Press. pp 433–440.
28. Wong ML, Medrano JF (2005) Real-time PCR for mRNA quantitation. Biotechniques 39: 75–85.
29. Heid CA, Stevens J, Livak KJ, Williams PM (1996) Real time quantitative PCR. Genome Res 6: 986–994.

DISCUSSION

It is well established that in certain inflammatory conditions bone remodeling is disturbed, shifting the balance towards bone resorption, which ultimately leads to the development of secondary osteoporosis. However the interaction between immune and skeletal systems can also have a beneficial effect when after a fracture inflammation triggers the healing cascade. The aim of this dissertation thesis was to understand the effect of inflammation on bone structural, mechanical and biological behavior.

The first study of this thesis (part I) focused on the analysis of the direct effect of chronic inflammation on bone biomechanical behavior. In part II we studied the effect of inflammation on collagen metabolism and organization and found that the bone weakening effect of arthritis was due to high bone turnover and disorganized collagen type I matrix. Following these initial animal model observations, the first to describe a direct effect of arthritis on collagen structure and bone biomechanics, we confirmed and further detailed these observations in human RA bone, assessed by bone microenvironment gene expression, microCT structure analysis and bone mechanics. We have identified DKK1 as a major potential regulatory factor of bone disturbances in RA, suggesting that this could be an interesting target for future treatment interventions. Finally, we have used the post-fracture inflammatory reaction as a model for characterizing the kinetics of inflammatory and bone remodeling related genes (part IV). Our results indicate that the expression of inflammation-related genes, especially IL-6, is highest at the very first days after fracture but from day 4 onwards there is a shift towards bone remodeling genes, suggesting that the inflammatory phase triggers bone healing. We propose that an initial inflammatory stimulus and a decrease in sclerostin-related effects are the key components in fracture healing. Therefore local promotion of these events might constitute a promising medical intervention to accelerate fracture healing.

It is relevant to emphasize that the animal model that we have used is the most similar to human RA. In fact, SKG mice develop a rheumatoid factor positive, erosive chronic polyarthritis that affects both large and small joints and present some of the systemic features of RA such as interstitial pneumonitis with various degrees of perivascular and peribronchiolar cellular infiltration, infiltration of inflammatory cells in the skin and subcutaneous rheumatoid-like nodules. The SKG mice have a BALB/c background with a single recessive point mutation in the zeta-chain-associated protein kinase 70 (ZAP-70) gene, a G→C substitution that alters codon 163 from tryptophan to cystein[602]. In our study group, penetrance of arthritis was of 100%, as evaluated by a semiquantitative arthritis score. In femoral and vertebral bone we have used standard mechanical tests to assess osteoporotic bone and for the test of new anti-osteoporotic drugs[603]. When an increasing force is applied to bone it leads first to a fully elastic deformation so that if the force is released the structure will assume its former shape. This property of the bone is translated by its stiffness. When more stress is applied, bone tissue starts to undergo microfractures and truly irreversible plastic changes occur. For vertebrae, compression tests were used, while 3-point bending was the appropriate for femurs and all tests were corrected for the size of the specimen. Analysis from the stress-strain curves have shown that bones from mice with arthritis have impaired elasticity, ductility and ultimate fracture strength when compared with bones from BALB/c mice that do not develop arthritis.

The results obtained by the biomechanical tests were sustained by the findings of bone structure obtained by SEM, which enables the observation of tissue topography through high-resolution images and has proven effective in investigating the activity states of bone surfaces[83-84]. In SKG mice there was less trabecula-occupied area, increased distance between trabeculae and decreased trabecular and cortical thickness than in control mice, consistent with increased bone fragility induced by arthritis. In addition, we assessed the collagen network in these mice through multiphoton microscopy and by biochemical turnover markers. Multicolour non-linear microscopy of type I collagen was analyzed using SHG and TPE in the backward and forward SHG mode. The backward-SHG channel detects the backscattered SHG signal and the forward-SHG channels receives the photons that are transmitted through the sample[105]. Forward-to-backward signal ratio reflects collagen matrix organization and density and a higher ratio is associated with a less dense matrix[103]. Moreover, a study in collagen fibril from tendon samples suggested that the forward-SHG channel translates essentially the mature polymerized collagen and the backward-SHG channel represents the immature collagen fibril segments, indicating ongoing fibrilogenesis[106]. In this work we found that vertebral body trabecular bone from SKG animals have a higher forward-to-backward ratio reflecting lower density and organization of collagen fibrils than the healthy control bone. Moreover, multiphoton microscopy images disclosed a disturbed organization of fiber bundles in arthritic bone compared with the organized lamellar architecture of healthy bone. Although two studies have assessed collagen density and organization on bone[102-103], this was the first report to address the disorganized collagen matrix in the context of arthritis. On the other hand, formation and degradation of bone matrix can be monitored by cleavage products of collagen metabolism that pass into the circulation and/or are excreted in the urine and can be used as markers of bone turnover[31]. In the fibril assembly phase, *de novo* synthesis of collagen leads to release of collagen propeptides P1NP and P1CP. On the other hand, osteoclasts resorb the matrix through the action of CTSK leading to the release of cross-linked telopeptides, NTX and CTX[32]. Results have shown that both P1NP and CTX are increased in SKG animals depicting higher bone remodeling rate. Collagen metabolism is relevant for bone biomechanics at two levels. First of all, collagen fiber orientation determines the deposition of hydroxyapatite crystals (stiffness) in the extracellular matrix, directly influencing the elasticity of bone. Secondly, collagen fibers *per se* directly determine the ability to absorb energy through plastic deformation, thus determining ductility and ultimately fracture strength[604]. Therefore, the high remodeling rate of collagen might be associated with decreased bone mineralization that may reduce its stiffness and ductility.

As observed in the SKG mice model, results from the compression of trabecular cylinders extracted from femoral epiphysis of RA patients reflect impairment of biomechanical behavior, particularly strength and stiffness. We have detailed the implications of these observations through an evaluation of gene expression of bone microenvironment. We have found that genes that code for pro-inflammatory cytokines were upregulated in RA patients, particularly IL-17, which plays an important role in stimulating osteoclastogenesis. In accordance, RANKL/OPG expression ratio was increased in RA. Overall osteoclast gene expression was similar between RA and primary OP patients, with the exception of β3 subunit of αvβ3 integrin, which was lower in RA patients, suggesting an intriguing disturbance in osteoclast adherence to bone matrix[138]. RA patients had an upregulation of OSX, which together with increased FGF2 and IGF-I, might represent a compensatory mechanism for osteoblastic activity response that have been previously observed in a mice model of arthritis[605]. Interestingly, OSX is involved in DKK1 induction[222], which is coherent with our observation of an increase in this gene expression in the bone of RA patients. In addition, DKK1 has a high affinity for LRP6 and induces its accumulation both at the cell surface and in endosomes[606] and in fact our observations showed that increased expression of DKK1 in RA was paralleled by an upregulation of LRP6. DKK1 upregulation in RA patients is limiting the effects of the pro-osteoblastic factors, as can be inferred by the low collagen expression in RA bone. Therefore, RA bone microenvironment has a gene expression profile characterized by upregulated pro-osteoclastogenic cytokines and DKK1, increased RANKL/OPG expression ratio, paralleled by raised expression of factors that promote osteoblastic activity. The marked DKK1 expression observed in RA patients might limit this tentative repairing effort through osteoblastic activity, as suggested by the low type I collagen expression. Bone loss in chronic inflammatory diseases thus appears to result from enhanced bone resorption and impaired bone formation, which constitutes a detrimental imbalance of bone remodeling and precipitates the rapid loss of bone mass in the course of inflammatory disease.

Differences were observed in gene expression between RA bone and established primary OP bone in spite of the fact that these two patient groups were matched for BMD and major fracture risk factors and had similar bone microarchitecture and biomechanics properties. These observations might indicate that the differences in gene expression that were observed reflect biologically specific mechanisms responsible for bone fragility in RA. Of interest, RA patients had a relatively short disease duration, low erosive rate and low microstructural damage (as evaluated by microCT) reinforcing the idea that these differences in gene expression occurred in the absence of major clinically meaningful bone damage in RA.

Unlike the unregulated and prolonged inflammation seen in RA, fracture healing is a highly regulated and brief process mainly characterized by altered levels of TNF, IL-1, and IL-6[551]. In accordance with this we observed that cytokine gene expression was more pronounced during the first days after fracture and specifically the decrease in IL-6 expression levels was far more pronounced than what was observed with the other pro-inflammatory cytokines evaluated. In fact, this is in line with a previous observation in which IL-6 ablation during fracture healing significantly reduced osteoclastogenesis and impaired callus formation[607]. Paralleling this cytokine rise, OPG expression diminished gradually after fracture, releasing the inhibitory signal for osteoclast differentiation. Concordantly, RANKL peaked at 4^{th}-7^{th} day after trauma, creating a stimulus for osteoclast differentiation from its precursors. We found that osteoclast-specific genes were significantly increased from day 8 onwards after fracture, pointing to an activation of osteoclast function. Specifically, CTSK values were increased from the 8^{th} day post fracture onwards, indicating that during 4-7 days after fracture, osteoclastogenesis stimulus was ongoing intensively, allowing that by day 8 osteoclasts containing CTSK had already been formed in relatively high numbers. The active role of osteoclasts during the early phase of fracture healing was already described in a sheep model, where it was proposed that these cells not only resorb bone but adjust the system, together with osteoblasts, in order to improve bone strength[596]. Concerning osteoblast differentiation and activity, RUNX2 increased from the initial phase of bone healing, whereas OSX increased after 4 days post-fracture sustaining the evidence that OSX acts later than RUNX2 in osteoblast lineage commitment[222]. SOST expression decreased significantly from the beginning of the healing cascade, in a parallel way to IL-6 decrease, suggesting that there is an initial blockage of osteoblast proliferation and differentiation that is subsequently released over the period of fracture healing, which is in accordance with a study in young mice[581]. In addition, in a closed femoral fracture model in rats and a fibular osteotomy model in cynomolgus monkeys, treatment with anti-SOST antibody significantly enhanced fracture healing by improvement of bone formation, bone mass and bone strength[608]. Taken together, these observations are highly suggestive of the existence of a two step process in bone healing, dependent on an initial inflammatory stimulus and a latter decrease in SOST-related effects. Therefore local promotion of these sequential events constitutes a medical intervention that worth to be tested in fracture healing.

CONCLUSION

Chronic inflammation has a harmful effect upon bone. Inflammatory cells express high levels of RANKL and secrete pro-inflammatory cytokines, which activate osteoclast differentiation and increase bone resorption. On the other hand, there is also an increase in pro-osteoblastogenic factors that try to compensate this destructive effect. However, this feedback mechanism is hampered by the osteoblast inhibition imposed by DKK1. The net effect is an impaired bone matrix organization, which leads to an inadequate mineralization and altered structural properties of collagen. This constitutes the main cause of the deterioration of bone mechanical properties and consequent bone fragility observed in RA.

Although it might seem paradoxical, these same proinflammatory factors orchestrate the sequence of events that promote bone fracture healing, balancing osteoclastic activity, sclerostin expression and osteoblastic activity.

The work herein discussed clearly shows that inflammation has a complex role in bone regulation. The identification of key regulators of this system will be crucial for the future management of both RA and fracture healing.

REFERENCES

1. Wain HM, Bruford EA, Lovering RC, Lush MJ, Wright MW, Povey S. Guidelines for human gene nomenclature. Genomics 2002;79:464-70.

2. Fratzl P, Weinkamer R. Nature's hierarchical materials. Progress in Materials Science 2007;52:1263-334.

3. Seeman E, Delmas PD. Bone quality--the material and structural basis of bone strength and fragility. N Engl J Med 2006;354:2250-61.

4. Lakes R, Saha S. Cement line motion in bone. Science 1979;204:501-3.

5. Khurana JS, ed. Bone Pathology. New York: Humana Press; 2009.

6. Bouxsein ML. Determinants of skeletal fragility. Best Pract Res Clin Rheumatol 2005;19:897-911.

7. Myllyharju J, Kivirikko KI. Collagens, modifying enzymes and their mutations in humans, flies and worms. Trends Genet 2004;20:33-43.

8. van der Rest M, Garrone R. Collagen family of proteins. Faseb J 1991;5:2814-23.

9. Knott L, Bailey AJ. Collagen cross-links in mineralizing tissues: a review of their chemistry, function, and clinical relevance. Bone 1998;22:181-7.

10. Kadler KE, Holmes DF, Trotter JA, Chapman JA. Collagen fibril formation. Biochem J 1996;316 (Pt 1):1-11.

11. Traub W, Yonath A, Segal DM. On the Molecular Structure of Collagen. Nature 1969;221:914-7.

12. Ramshaw JA, Shah NK, Brodsky B. Gly-X-Y tripeptide frequencies in collagen: a context for host-guest triple-helical peptides. J Struct Biol 1998;122:86-91.

13. Bilezikian JP, Raisz LG, Rodan GA. Principles of bone biology. San Diego: Academic Press; 2002.

14. Lazarides E, Lukens LN. Collagen synthesis on polysomes in vivo and in vitro. Nat New Biol 1971;232:37-40.

15. Bornstein P, McKay J, Morishima JK, Devarayalu S, Gelinas RE. Regulatory elements in the first intron contribute to transcriptional control of the human alpha 1(I) collagen gene. Proc Natl Acad Sci U S A 1987;84:8869-73.

16. Kern B, Shen J, Starbuck M, Karsenty G. Cbfa1 contributes to the osteoblast-specific expression of type I collagen genes. J Biol Chem 2001;276:7101-7.

17. Roberts AB, Sporn MB, Assoian RK, et al. Transforming growth factor type beta: rapid induction of fibrosis and angiogenesis in vivo and stimulation of collagen formation in vitro. Proc Natl Acad Sci U S A 1986;83:4167-71.

18. McCarthy TL, Centrella M, Canalis E. Regulatory effects of insulin-like growth factors I and II on bone collagen synthesis in rat calvarial cultures. Endocrinology 1989;124:301-9.

19. Thiebaud D, Guenther HL, Porret A, Burckhardt P, Fleisch H, Hofstetter W. Regulation of collagen type I and biglycan mRNA levels by hormones and growth factors in normal and immortalized osteoblastic cell lines. J Bone Miner Res 1994;9:1347-54.

20. Kawaguchi Y, Hara M, Wright TM. Endogenous IL-1alpha from systemic sclerosis fibroblasts induces IL-6 and PDGF-A. J Clin Invest 1999;103:1253-60.

21. Kouba DJ, Chung KY, Nishiyama T, et al. Nuclear factor-kappa B mediates TNF-alpha inhibitory effect on alpha 2(I) collagen (COL1A2) gene transcription in human dermal fibroblasts. J Immunol 1999;162:4226-34.

22. Kahari VM, Chen YQ, Su MW, Ramirez F, Uitto J. Tumor necrosis factor-alpha and interferon-gamma suppress the activation of human type I collagen gene expression by transforming growth factor-beta 1. Evidence for two distinct mechanisms of inhibition at the transcriptional and posttranscriptional levels. J Clin Invest 1990;86:1489-95.

23. Harrison JR, Vargas SJ, Petersen DN, Lorenzo JA, Kream BE. Interleukin-1 alpha and phorbol ester inhibit collagen synthesis in osteoblastic MC3T3-E1 cells by a transcriptional mechanism. Mol Endocrinol 1990;4:184-90.

24. Kream BE, Rowe D, Smith MD, Maher V, Majeska R. Hormonal regulation of collagen synthesis in a clonal rat osteosarcoma cell line. Endocrinology 1986;119:1922-8.

25. Harrison JR, Petersen DN, Lichtler AC, Mador AT, Rowe DW, Kream BE. 1,25-Dihydroxyvitamin D3 inhibits transcription of type I collagen genes in the rat osteosarcoma cell line ROS 17/2.8. Endocrinology 1989;125:327-33.

26. Bailey AJ, Light ND, Atkins EDT. Chemical cross-linking restrictions on models for the molecular organization of the collagen fibre. Nature 1980;288:408-10.

27. Kadler KE, Hulmes DJ, Hojima Y, Prockop DJ. Assembly of type I collagen fibrils de novo by the specific enzymic cleavage of pC collagen. The fibrils formed at about 37 degrees C are similar in diameter, roundness, and apparent flexibility to the collagen fibrils seen in connective tissue. Ann N Y Acad Sci 1990;580:214-24.

28. Kuc IM, Scott PG. Increased diameters of collagen fibrils precipitated in vitro in the presence of decorin from various connective tissues. Connect Tissue Res 1997;36:287-96.

29. Vogel KG, Trotter JA. The effect of proteoglycans on the morphology of collagen fibrils formed in vitro. Coll Relat Res 1987;7:105-14.

30. Iozzo RV. The biology of the small leucine-rich proteoglycans. Functional network of interactive proteins. J Biol Chem 1999;274:18843-6.

31. Civitelli R, Armamento-Villareal R, Napoli N. Bone turnover markers: understanding their value in clinical trials and clinical practice. Osteoporos Int 2009;20:843-51.

32. Seibel MJ. Molecular markers of bone turnover: biochemical, technical and analytical aspects. Osteoporos Int 2000;11 Suppl 6:S18-29.

33. Leeming DJ, Alexandersen P, Karsdal MA, Qvist P, Schaller S, Tanko LB. An update on biomarkers of bone turnover and their utility in biomedical research and clinical practice. Eur J Clin Pharmacol 2006;62:781-92.

34. Brown JP, Albert C, Nassar BA, et al. Bone turnover markers in the management of postmenopausal osteoporosis. Clin Biochem 2009;42:929-42.

35. Garnero P, Ferreras M, Karsdal MA, et al. The type I collagen fragments ICTP and CTX reveal distinct enzymatic pathways of bone collagen degradation. J Bone Miner Res 2003;18:859-67.

36. Herring GM, Ashton BA. The isolation of soluble proteins, glycoproteins, and proteoglycans from bone. Prep Biochem 1974;4:179-200.

37. Young MF, Kerr JM, Ibaraki K, Heegaard AM, Robey PG. Structure, expression, and regulation of the major noncollagenous matrix proteins of bone. Clin Orthop Relat Res 1992:275-94.

38. Bianco P, Fisher LW, Young MF, Termine JD, Robey PG. Expression and localization of the two small proteoglycans biglycan and decorin in developing human skeletal and non-skeletal tissues. J Histochem Cytochem 1990;38:1549-63.

39. Bonewald LF. Mechanosensation and Transduction in Osteocytes. Bonekey Osteovision 2006;3:7-15.

40. Xu T, Bianco P, Fisher LW, et al. Targeted disruption of the biglycan gene leads to an osteoporosis-like phenotype in mice. Nat Genet 1998;20:78-82.

41. Corsi A, Xu T, Chen XD, et al. Phenotypic effects of biglycan deficiency are linked to collagen fibril abnormalities, are synergized by decorin deficiency, and mimic Ehlers-Danlos-like changes in bone and other connective tissues. J Bone Miner Res 2002;17:1180-9.

42. Termine JD, Belcourt AB, Conn KM, Kleinman HK. Mineral and collagen-binding proteins of fetal calf bone. J Biol Chem 1981;256:10403-8.

43. Gundberg CM. Matrix proteins. Osteoporos Int 2003;14 Suppl 5:S37-40; discussion S-2.

44. Delany AM, Amling M, Priemel M, Howe C, Baron R, Canalis E. Osteopenia and decreased bone formation in osteonectin-deficient mice. J Clin Invest 2000;105:915-23.

45. Mansergh FC, Wells T, Elford C, et al. Osteopenia in Sparc (osteonectin)-deficient mice: characterization of phenotypic determinants of femoral strength and changes in gene expression. Physiol Genomics 2007;32:64-73.

46. Sodek J, Ganss B, McKee MD. Osteopontin. Crit Rev Oral Biol Med 2000;11:279-303.

47. Stein GS, Lian JB, Owen TA. Relationship of cell growth to the regulation of tissue-specific gene expression during osteoblast differentiation. Faseb J 1990;4:3111-23.

48. Yoshitake H, Rittling SR, Denhardt DT, Noda M. Osteopontin-deficient mice are resistant to ovariectomy-induced bone resorption. Proc Natl Acad Sci U S A 1999;96:8156-60.

49. Bianco P, Fisher LW, Young MF, Termine JD, Robey PG. Expression of bone sialoprotein (BSP) in developing human tissues. Calcif Tissue Int 1991;49:421-6.

50. Ganss B, Kim RH, Sodek J. Bone sialoprotein. Crit Rev Oral Biol Med 1999;10:79-98.

51. McKee MD, Nanci A. Osteopontin: an interfacial extracellular matrix protein in mineralized tissues. Connect Tissue Res 1996;35:197-205.

52. Petruska JA, Hodge AJ. A Subunit Model for the Tropocollagen Macromolecule. Proc Natl Acad Sci U S A 1964;51:871-6.

53. Weiner S, Traub W. Bone structure: from angstroms to microns. Faseb J 1992;6:879-85.

54. Robinson RA. An electron-microscopic study of the crystalline inorganic component of bone and its relationship to the organic matrix. J Bone Joint Surg Am 1952;34-A:389-435; passim.

55. Gupta HS, Zioupos P. Fracture of bone tissue: The 'hows' and the 'whys'. Med Eng Phys 2008;30:1209-26.

56. Fratzl P, Fratzl-Zelman N, Klaushofer K, Vogl G, Koller K. Nucleation and growth of mineral crystals in bone studied by small-angle X-ray scattering. Calcif Tissue Int 1991;48:407-13.

57. Rey C, Combes C, Drouet C, Glimcher MJ. Bone mineral: update on chemical composition and structure. Osteoporos Int 2009;20:1013-21.

58. Boskey AL. Biomineralization: conflicts, challenges, and opportunities. J Cell Biochem Suppl 1998;30-31:83-91.

59. Golub EE. Role of matrix vesicles in biomineralization. Biochim Biophys Acta 2009;1790:1592-8.

60. Wuthier RE. Lipids of matrix vesicles. Fed Proc 1976;35:117-21.

61. Ali SY. Constitutive enzymes of matrix vesicles. Bone Miner 1992;17:168-71.

62. Genge BR, Wu LN, Wuthier RE. Identification of phospholipid-dependent calcium-binding proteins as constituents of matrix vesicles. J Biol Chem 1989;264:10917-21.

63. Skrtic D, Eanes ED. Membrane-mediated precipitation of calcium phosphate in model liposomes with matrix vesicle-like lipid composition. Bone Miner 1992;16:109-19.

64. Anderson HC. Molecular biology of matrix vesicles. Clin Orthop Relat Res 1995:266-80.

65. Colfen H. Biomineralization: A crystal-clear view. Nat Mater 2010;9:960-1.

66. Kawasaki K, Buchanan AV, Weiss KM. Biomineralization in humans: making the hard choices in life. Annu Rev Genet 2009;43:119-42.

67. Apostol L, Boudousq V, Basset O, et al. Relevance of 2D radiographic texture analysis for the assessment of 3D bone micro-architecture. Med Phys 2006;33:3546-56.

68. Millard J, Augat P, Link TM, et al. Power spectral analysis of vertebral trabecular bone structure from radiographs: orientation dependence and correlation with bone mineral density and mechanical properties. Calcif Tissue Int 1998;63:482-9.

69. Lespessailles E, Roux JP, Benhamou CL, et al. Fractal analysis of bone texture on os calcis radiographs compared with trabecular microarchitecture analyzed by histomorphometry. Calcif Tissue Int 1998;63:121-5.

70. Parfitt AM, Drezner MK, Glorieux FH, et al. Bone histomorphometry: standardization of nomenclature, symbols, and units. Report of the ASBMR Histomorphometry Nomenclature Committee. J Bone Miner Res 1987;2:595-610.

71. Lespessailles E, Chappard C, Bonnet N, Benhamou CL. Imaging techniques for evaluating bone microarchitecture. Joint Bone Spine 2006;73:254-61.

72. Genant HK, Engelke K, Prevrhal S. Advanced CT bone imaging in osteoporosis. Rheumatology (Oxford) 2008;47 Suppl 4:iv9-16.

73. Genant HK, Engelke K, Fuerst T, et al. Noninvasive assessment of bone mineral and structure: state of the art. J Bone Miner Res 1996;11:707-30.

74. Brandi ML. Microarchitecture, the key to bone quality. Rheumatology (Oxford) 2009;48 Suppl 4:iv3-8.

75. Lang TF, Keyak JH, Heitz MW, et al. Volumetric quantitative computed tomography of the proximal femur: precision and relation to bone strength. Bone 1997;21:101-8.

76. Laib A, Hauselmann HJ, Ruegsegger P. In vivo high resolution 3D-QCT of the human forearm. Technol Health Care 1998;6:329-37.

77. Bouxsein ML, Boyd SK, Christiansen BA, Guldberg RE, Jepsen KJ, Muller R. Guidelines for assessment of bone microstructure in rodents using micro-computed tomography. J Bone Miner Res 2010;25:1468-86.

78. Barbier A, Martel C, de Vernejoul MC, et al. The visualization and evaluation of bone architecture in the rat using three-dimensional X-ray microcomputed tomography. J Bone Miner Metab 1999;17:37-44.

79. Muller R, Van Campenhout H, Van Damme B, et al. Morphometric analysis of human bone biopsies: a quantitative structural comparison of histological sections and micro-computed tomography. Bone 1998;23:59-66.

80. Chappard D, Retailleau-Gaborit N, Legrand E, Basle MF, Audran M. Comparison insight bone measurements by histomorphometry and microCT. J Bone Miner Res 2005;20:1177-84.

81. Griffith JF, Engelke K, Genant HK. Looking beyond bone mineral density : Imaging assessment of bone quality. Ann N Y Acad Sci 2010;1192:45-56.

82. Boyde A, Jones SJ. Scanning electron microscopy of bone: instrument, specimen, and issues. Microsc Res Tech 1996;33:92-120.

83. Chen H, Washimi Y, Kubo KY, Onozuka M. Gender-related changes in three-dimensional microstructure of trabecular bone at the human proximal tibia with aging. Histol Histopathol 2011;26:563-70.

84. Boyde A. The real response of bone to exercise. J Anat 2003;203:173-89.

85. Sahar ND, Hong SI, Kohn DH. Micro- and nano-structural analyses of damage in bone. Micron 2005;36:617-29.

86. Braidotti P, Bemporad E, D'Alessio T, Sciuto SA, Stagni L. Tensile experiments and SEM fractography on bovine subchondral bone. J Biomech 2000;33:1153-7.

87. Cox G, Kable E. Second-harmonic imaging of collagen. Methods Mol Biol 2006;319:15-35.

88. Cox G, Kable E, Jones A, Fraser I, Manconi F, Gorrell MD. 3-dimensional imaging of collagen using second harmonic generation. J Struct Biol 2003;141:53-62.

89. Johnson AW, Ammar DA, Kahook MY. Two-Photon Imaging of the Mouse Eye. Invest Ophthalmol Vis Sci 2011.

90. Chen MH, Chen WL, Sun Y, Fwu PT, Dong CY. Multiphoton autofluorescence and second-harmonic generation imaging of the tooth. J Biomed Opt 2007;12:064018.

91. Theodossiou TA, Thrasivoulou C, Ekwobi C, Becker DL. Second harmonic generation confocal microscopy of collagen type I from rat tendon cryosections. Biophys J 2006;91:4665-77.

92. Rao RA, Mehta MR, Leithem S, Toussaint KC, Jr. Quantitative analysis of forward and backward second-harmonic images of collagen fibers using Fourier transform second-harmonic-generation microscopy. Opt Lett 2009;34:3779-81.

93. Mansfield JC, Winlove CP, Moger J, Matcher SJ. Collagen fiber arrangement in normal and diseased cartilage studied by polarization sensitive nonlinear microscopy. J Biomed Opt 2008;13:044020.

94. Tiwari N, Chabra S, Mehdi S, et al. Imaging of normal and pathologic joint synovium using nonlinear optical microscopy as a potential diagnostic tool. J Biomed Opt 2010;15:056001.

95. Torkian BA, Yeh AT, Engel R, Sun CH, Tromberg BJ, Wong BJ. Modeling aberrant wound healing using tissue-engineered skin constructs and multiphoton microscopy. Arch Facial Plast Surg 2004;6:180-7.

96. Pena AM, Fabre A, Debarre D, et al. Three-dimensional investigation and scoring of extracellular matrix remodeling during lung fibrosis using multiphoton microscopy. Microsc Res Tech 2007;70:162-70.

97. Condeelis J, Segall JE. Intravital imaging of cell movement in tumours. Nat Rev Cancer 2003;3:921-30.

98. Voura EB, Jaiswal JK, Mattoussi H, Simon SM. Tracking metastatic tumor cell extravasation with quantum dot nanocrystals and fluorescence emission-scanning microscopy. Nat Med 2004;10:993-8.

99. Deng X, Williams ED, Thompson EW, Gan X, Gu M. Second-harmonic generation from biological tissues: effect of excitation wavelength. Scanning 2002;24:175-8.

100. Yan J, Chen G, Chen J, et al. A pilot study of using multiphoton microscopy to diagnose gastric cancer. Surg Endosc 2011;25:1425-30.

101. Wang CC, Li FC, Wu RJ, et al. Differentiation of normal and cancerous lung tissues by multiphoton imaging. J Biomed Opt 2009;14:044034.

102. Hompland T, Erikson A, Lindgren M, Lindmo T, de Lange Davies C. Second-harmonic generation in collagen as a potential cancer diagnostic parameter. J Biomed Opt 2008;13:054050.

103. Nadiarnykh O, Plotnikov S, Mohler WA, Kalajzic I, Redford-Badwal D, Campagnola PJ. Second harmonic generation imaging microscopy studies of osteogenesis imperfecta. J Biomed Opt 2007;12:051805.

104. Reshak AH. High second harmonic generation signal from muscles and fascia pig's muscles using the two-photon laser scanning microscope. J Microsc 2009;234:280-6.

105. Helmchen F, Denk W. Deep tissue two-photon microscopy. Nat Methods 2005;2:932-40.

106. Williams RM, Zipfel WR, Webb WW. Interpreting second-harmonic generation images of collagen I fibrils. Biophys J 2005;88:1377-86.

107. Schenke-Layland K. Non-invasive multiphoton imaging of extracellular matrix structures. J Biophotonics 2008;1:451-62.

108. Konig K, Weinigel M, Hoppert D, et al. Multiphoton tissue imaging using high-NA microendoscopes and flexible scan heads for clinical studies and small animal research. J Biophotonics 2008;1:506-13.

109. Konig K, Ehlers A, Riemann I, Schenkl S, Buckle R, Kaatz M. Clinical two-photon microendoscopy. Microsc Res Tech 2007;70:398-402.

110. Dunlop JWC, Fatzl P. Biological Composites. Annual Review of Materials Research 2010;40:1-24.

111. Fung YC. Biomechanics : mechanical properties of living tissues. 2nd ed. New York: Springer-Verlag; 1993.

112. Nordin M, Frankel VH. Basic biomechanics of the musculoskeletal system. 3rd ed. Philadelphia: Lippincott Williams & Wilkins; 2001.

113. Ashby MF, Gibson LJ, Wegst U, Olive R. The Mechanical Properties of Natural Materials. I. Material Property Charts. Proceedings: Mathematical and Physical Sciences 1995;450:123-40.

114. Martin RB, Ishida J. The relative effects of collagen fiber orientation, porosity, density, and mineralization on bone strength. J Biomech 1989;22:419-26.

115. Carter DR, Hayes WC. Bone compressive strength: the influence of density and strain rate. Science 1976;194:1174-6.

116. Riggs BL, Melton Iii LJ, 3rd, Robb RA, et al. Population-based study of age and sex differences in bone volumetric density, size, geometry, and structure at different skeletal sites. J Bone Miner Res 2004;19:1945-54.

117. Schuit SC, van der Klift M, Weel AE, et al. Fracture incidence and association with bone mineral density in elderly men and women: the Rotterdam Study. Bone 2004;34:195-202.

118. Amling M, Herden S, Posl M, Hahn M, Ritzel H, Delling G. Heterogeneity of the skeleton: comparison of the trabecular microarchitecture of the spine, the iliac crest, the femur, and the calcaneus. J Bone Miner Res 1996;11:36-45.

119. Goldstein SA. The mechanical properties of trabecular bone: dependence on anatomic location and function. J Biomech 1987;20:1055-61.

120. Nazarian A, Muller J, Zurakowski D, Muller R, Snyder BD. Densitometric, morphometric and mechanical distributions in the human proximal femur. J Biomech 2007;40:2573-9.

121. Beaupied H, Lespessailles E, Benhamou CL. Evaluation of macrostructural bone biomechanics. Joint Bone Spine 2007;74:233-9.

122. Al Nazer R, Rantalainen T, Heinonen A, Sievanen H, Mikkola A. Flexible multibody simulation approach in the analysis of tibial strain during walking. J Biomech 2008;41:1036-43.

123. Lanyon LE, Hampson WG, Goodship AE, Shah JS. Bone deformation recorded in vivo from strain gauges attached to the human tibial shaft. Acta Orthop Scand 1975;46:256-68.

124. Carter DR. Anisotropic analysis of strain rosette information from cortical bone. J Biomech 1978;11:199-202.

125. Guo XE, Kim CH. Mechanical consequence of trabecular bone loss and its treatment: a three-dimensional model simulation. Bone 2002;30:404-11.

126. Ritchie RO. How does human bone resist fracture? Ann N Y Acad Sci 2010;1192:72-80.

127. Smith BL, Schaffer TE, Viani M, et al. Molecular mechanistic origin of the toughness of natural adhesives, fibres and composites. Nature 1999;399:761-3.

128. Zaidi M. Skeletal remodeling in health and disease. Nat Med 2007;13:791-801.

129. Hattner R, Epker BN, Frost HM. Suggested sequential mode of control of changes in cell behaviour in adult bone remodelling. Nature 1965;206:489-90.

130. Robling AG, Castillo AB, Turner CH. Biomechanical and molecular regulation of bone remodeling. Annu Rev Biomed Eng 2006;8:455-98.

131. Eriksen EF. Cellular mechanisms of bone remodeling. Rev Endocr Metab Disord 2010.

132. Manolagas SC, Parfitt AM. What old means to bone. Trends Endocrinol Metab 2010;21:369-74.

133. Hartmann C. A Wnt canon orchestrating osteoblastogenesis. Trends Cell Biol 2006;16:151-8.

134. Krane SM. Identifying genes that regulate bone remodeling as potential therapeutic targets. J Exp Med 2005;201:841-3.

135. Martin TJ, Sims NA. Osteoclast-derived activity in the coupling of bone formation to resorption. Trends Mol Med 2005;11:76-81.

136. Ishii M, Saeki Y. Osteoclast cell fusion: mechanisms and molecules. Mod Rheumatol 2008;18:220-7.

137. Bar-Shavit Z. The osteoclast: a multinucleated, hematopoietic-origin, bone-resorbing osteoimmune cell. J Cell Biochem 2007;102:1130-9.

138. Zou W, Teitelbaum SL. Integrins, growth factors, and the osteoclast cytoskeleton. Ann N Y Acad Sci 2010;1192:27-31.

139. Yavropoulou MP, Yovos JG. Osteoclastogenesis--current knowledge and future perspectives. J Musculoskelet Neuronal Interact 2008;8:204-16.

140. Menaa C, Kurihara N, Roodman GD. CFU-GM-derived cells form osteoclasts at a very high efficiency. Biochem Biophys Res Commun 2000;267:943-6.

141. Tondravi MM, McKercher SR, Anderson K, et al. Osteopetrosis in mice lacking haematopoietic transcription factor PU.1. Nature 1997;386:81-4.

142. Kawaguchi N, Noda M. Mitf is expressed in osteoclast progenitors in vitro. Exp Cell Res 2000;260:284-91.

143. Hu R, Sharma SM, Bronisz A, Srinivasan R, Sankar U, Ostrowski MC. Eos, MITF, and PU.1 recruit corepressors to osteoclast-specific genes in committed myeloid progenitors. Mol Cell Biol 2007;27:4018-27.

144. Grigoriadis AE, Wang ZQ, Cecchini MG, et al. c-Fos: a key regulator of osteoclast-macrophage lineage determination and bone remodeling. Science 1994;266:443-8.

145. Miyamoto T, Ohneda O, Arai F, et al. Bifurcation of osteoclasts and dendritic cells from common progenitors. Blood 2001;98:2544-54.

146. Fujikawa Y, Quinn JM, Sabokbar A, McGee JO, Athanasou NA. The human osteoclast precursor circulates in the monocyte fraction. Endocrinology 1996;137:4058-60.

147. Komano Y, Nanki T, Hayashida K, Taniguchi K, Miyasaka N. Identification of a human peripheral blood monocyte subset that differentiates into osteoclasts. Arthritis Res Ther 2006;8:R152.

148. Takahashi N, Yamana H, Yoshiki S, et al. Osteoclast-like cell formation and its regulation by osteotropic hormones in mouse bone marrow cultures. Endocrinology 1988;122:1373-82.

149. Lacey DL, Timms E, Tan HL, et al. Osteoprotegerin ligand is a cytokine that regulates osteoclast differentiation and activation. Cell 1998;93:165-76.

150. Yasuda H, Shima N, Nakagawa N, et al. Osteoclast differentiation factor is a ligand for osteoprotegerin/osteoclastogenesis-inhibitory factor and is identical to TRANCE/RANKL. Proc Natl Acad Sci U S A 1998;95:3597-602.

151. Atkins GJ, Kostakis P, Vincent C, et al. RANK Expression as a cell surface marker of human osteoclast precursors in peripheral blood, bone marrow, and giant cell tumors of bone. J Bone Miner Res 2006;21:1339-49.

152. Burgess TL, Qian Y, Kaufman S, et al. The ligand for osteoprotegerin (OPGL) directly activates mature osteoclasts. J Cell Biol 1999;145:527-38.

153. Asagiri M, Takayanagi H. The molecular understanding of osteoclast differentiation. Bone 2007;40:251-64.

154. Darnay BG, Haridas V, Ni J, Moore PA, Aggarwal BB. Characterization of the intracellular domain of receptor activator of NF-kappaB (RANK). Interaction with tumor necrosis factor receptor-associated factors and activation of NF-kappab and c-Jun N-terminal kinase. J Biol Chem 1998;273:20551-5.

155. Galibert L, Tometsko ME, Anderson DM, Cosman D, Dougall WC. The involvement of multiple tumor necrosis factor receptor (TNFR)-associated factors in the signaling mechanisms of receptor activator of NF-kappaB, a member of the TNFR superfamily. J Biol Chem 1998;273:34120-7.

156. Feng X. RANKing intracellular signaling in osteoclasts. IUBMB Life 2005;57:389-95.

157. Liu W, Xu D, Yang H, et al. Functional identification of three receptor activator of NF-kappa B cytoplasmic motifs mediating osteoclast differentiation and function. J Biol Chem 2004;279:54759-69.

158. Lomaga MA, Yeh WC, Sarosi I, et al. TRAF6 deficiency results in osteopetrosis and defective interleukin-1, CD40, and LPS signaling. Genes Dev 1999;13:1015-24.

159. Cappellen D, Luong-Nguyen NH, Bongiovanni S, Grenet O, Wanke C, Susa M. Transcriptional program of mouse osteoclast differentiation governed by the macrophage colony-stimulating factor and the ligand for the receptor activator of NFkappa B. J Biol Chem 2002;277:21971-82.

160. Kadono Y, Okada F, Perchonock C, et al. Strength of TRAF6 signalling determines osteoclastogenesis. EMBO Rep 2005;6:171-6.

161. Vaira S, Alhawagri M, Anwisye I, Kitaura H, Faccio R, Novack DV. RelA/p65 promotes osteoclast differentiation by blocking a RANKL-induced apoptotic JNK pathway in mice. J Clin Invest 2008;118:2088-97.

162. Iotsova V, Caamano J, Loy J, Yang Y, Lewin A, Bravo R. Osteopetrosis in mice lacking NF-kappaB1 and NF-kappaB2. Nat Med 1997;3:1285-9.

163. Novack DV, Teitelbaum SL. The osteoclast: friend or foe? Annu Rev Pathol 2008;3:457-84.

164. Yoshida H, Hayashi S, Kunisada T, et al. The murine mutation osteopetrosis is in the coding region of the macrophage colony stimulating factor gene. Nature 1990;345:442-4.

165. Boyle WJ, Simonet WS, Lacey DL. Osteoclast differentiation and activation. Nature 2003;423:337-42.

166. Nakahama K. Cellular communications in bone homeostasis and repair. Cell Mol Life Sci 2010;67:4001-9.

167. Kim MS, Day CJ, Morrison NA. MCP-1 is induced by receptor activator of nuclear factor-{kappa}B ligand, promotes human osteoclast fusion, and rescues granulocyte macrophage colony-stimulating factor suppression of osteoclast formation. J Biol Chem 2005;280:16163-9.

168. Novack DV, Faccio R. Osteoclast motility: putting the brakes on bone resorption. Ageing Res Rev 2011;10:54-61.

169. Kim K, Lee SH, Ha Kim J, Choi Y, Kim N. NFATc1 induces osteoclast fusion via up-regulation of Atp6v0d2 and the dendritic cell-specific transmembrane protein (DC-STAMP). Mol Endocrinol 2008;22:176-85.

170. Yagi M, Miyamoto T, Sawatani Y, et al. DC-STAMP is essential for cell-cell fusion in osteoclasts and foreign body giant cells. J Exp Med 2005;202:345-51.

171. Zeng Z-Y, Chen J-M. Cell-cell fusion: human multinucleated osteoclasts. Central European Journal of Biology 2009;4:543-8.

172. Kukita T, Wada N, Kukita A, et al. RANKL-induced DC-STAMP is essential for osteoclastogenesis. J Exp Med 2004;200:941-6.

173. Lee SH, Rho J, Jeong D, et al. v-ATPase V0 subunit d2-deficient mice exhibit impaired osteoclast fusion and increased bone formation. Nat Med 2006;12:1403-9.

174. Vignery A. Macrophage fusion: are somatic and cancer cells possible partners? Trends Cell Biol 2005;15:188-93.

175. Helming L, Gordon S. Molecular mediators of macrophage fusion. Trends Cell Biol 2009;19:514-22.

176. Zhao H, Ito Y, Chappel J, Andrews NW, Teitelbaum SL, Ross FP. Synaptotagmin VII regulates bone remodeling by modulating osteoclast and osteoblast secretion. Dev Cell 2008;14:914-25.

177. Destaing O, Saltel F, Geminard JC, Jurdic P, Bard F. Podosomes display actin turnover and dynamic self-organization in osteoclasts expressing actin-green fluorescent protein. Mol Biol Cell 2003;14:407-16.

178. McHugh KP, Hodivala-Dilke K, Zheng MH, et al. Mice lacking beta3 integrins are osteosclerotic because of dysfunctional osteoclasts. J Clin Invest 2000;105:433-40.

179. Faccio R, Grano M, Colucci S, et al. Localization and possible role of two different alpha v beta 3 integrin conformations in resting and resorbing osteoclasts. J Cell Sci 2002;115:2919-29.

180. Faccio R, Novack DV, Zallone A, Ross FP, Teitelbaum SL. Dynamic changes in the osteoclast cytoskeleton in response to growth factors and cell attachment are controlled by beta3 integrin. J Cell Biol 2003;162:499-509.

181. Faccio R, Takeshita S, Colaianni G, et al. M-CSF regulates the cytoskeleton via recruitment of a multimeric signaling complex to c-Fms Tyr-559/697/721. J Biol Chem 2007;282:18991-9.

182. Nakamura I, Duong le T, Rodan SB, Rodan GA. Involvement of alpha(v)beta3 integrins in osteoclast function. J Bone Miner Metab 2007;25:337-44.

183. Baron R, Neff L, Louvard D, Courtoy PJ. Cell-mediated extracellular acidification and bone resorption: evidence for a low pH in resorbing lacunae and localization of a 100-kD lysosomal membrane protein at the osteoclast ruffled border. J Cell Biol 1985;101:2210-22.

184. Riihonen R, Supuran CT, Parkkila S, Pastorekova S, Vaananen HK, Laitala-Leinonen T. Membrane-bound carbonic anhydrases in osteoclasts. Bone 2007;40:1021-31.

185. Blair HC, Teitelbaum SL, Ghiselli R, Gluck S. Osteoclastic bone resorption by a polarized vacuolar proton pump. Science 1989;245:855-7.

186. Teti A, Blair HC, Teitelbaum SL, et al. Cytoplasmic pH regulation and chloride/bicarbonate exchange in avian osteoclasts. J Clin Invest 1989;83:227-33.

187. Kornak U, Kasper D, Bosl MR, et al. Loss of the ClC-7 chloride channel leads to osteopetrosis in mice and man. Cell 2001;104:205-15.

188. Saftig P, Hunziker E, Wehmeyer O, et al. Impaired osteoclastic bone resorption leads to osteopetrosis in cathepsin-K-deficient mice. Proc Natl Acad Sci U S A 1998;95:13453-8.

189. Canhão H, Fonseca JE, Queiroz MV. Epidemiologia da osteoporose. Mecanismos de remodelação óssea e factores protectores do osso. Acta Reumatológica Portuguesa 2005;30:225-40.

190. Gori F, Hofbauer LC, Dunstan CR, Spelsberg TC, Khosla S, Riggs BL. The expression of osteoprotegerin and RANK ligand and the support of osteoclast formation by stromal-osteoblast lineage cells is developmentally regulated. Endocrinology 2000;141:4768-76.

191. Ducy P, Schinke T, Karsenty G. The osteoblast: a sophisticated fibroblast under central surveillance. Science 2000;289:1501-4.

192. Komori T. Regulation of osteoblast differentiation by transcription factors. J Cell Biochem 2006;99:1233-9.

193. Marie PJ. Transcription factors controlling osteoblastogenesis. Arch Biochem Biophys 2008;473:98-105.

194. Neve A, Corrado A, Cantatore FP. Osteoblast physiology in normal and pathological conditions. Cell Tissue Res 2011;343:289-302.

195. Yamaguchi A, Katagiri T, Ikeda T, et al. Recombinant human bone morphogenetic protein-2 stimulates osteoblastic maturation and inhibits myogenic differentiation in vitro. J Cell Biol 1991;113:681-7.

196. Stein G, Lian J, Owen T. Relationship of cell growth to the regulation of tissue-specific gene expression during osteoblast differentiation. The FASEB Journal 1990;4:3111-23.

197. Mackie EJ. Osteoblasts: novel roles in orchestration of skeletal architecture. Int J Biochem Cell Biol 2003;35:1301-5.

198. Whitson SW, Harrison W, Dunlap MK, et al. Fetal bovine bone cells synthesize bone-specific matrix proteins. J Cell Biol 1984;99:607-14.

199. Nagata T, Bellows CG, Kasugai S, Butler WT, Sodek J. Biosynthesis of bone proteins [SPP-1 (secreted phosphoprotein-1, osteopontin), BSP (bone sialoprotein) and SPARC (osteonectin)] in association with mineralized-tissue formation by fetal-rat calvarial cells in culture. Biochem J 1991;274 (Pt 2):513-20.

200. Gerstenfeld LC, Chipman SD, Glowacki J, Lian JB. Expression of differentiated function by mineralizing cultures of chicken osteoblasts. Dev Biol 1987;122:49-60.

201. Lian JB, Stein GS. Development of the osteoblast phenotype: molecular mechanisms mediating osteoblast growth and differentiation. Iowa Orthop J 1995;15:118-40.

202. Owen TA, Aronow M, Shalhoub V, et al. Progressive development of the rat osteoblast phenotype in vitro: reciprocal relationships in expression of genes associated with osteoblast proliferation and differentiation during

formation of the bone extracellular matrix. J Cell Physiol 1990;143:420-30.

203. Komori T, Yagi H, Nomura S, et al. Targeted disruption of Cbfa1 results in a complete lack of bone formation owing to maturational arrest of osteoblasts. Cell 1997;89:755-64.

204. Prince M, Banerjee C, Javed A, et al. Expression and regulation of Runx2/Cbfa1 and osteoblast phenotypic markers during the growth and differentiation of human osteoblasts. J Cell Biochem 2001;80:424-40.

205. Liu W, Toyosawa S, Furuichi T, et al. Overexpression of Cbfa1 in osteoblasts inhibits osteoblast maturation and causes osteopenia with multiple fractures. J Cell Biol 2001;155:157-66.

206. Franceschi RT, Xiao G, Jiang D, Gopalakrishnan R, Yang S, Reith E. Multiple signaling pathways converge on the Cbfa1/Runx2 transcription factor to regulate osteoblast differentiation. Connect Tissue Res 2003;44 Suppl 1:109-16.

207. Tsuji K, Ito Y, Noda M. Expression of the PEBP2alphaA/AML3/CBFA1 gene is regulated by BMP4/7 heterodimer and its overexpression suppresses type I collagen and osteocalcin gene expression in osteoblastic and nonosteoblastic mesenchymal cells. Bone 1998;22:87-92.

208. Inman CK, Shore P. The osteoblast transcription factor Runx2 is expressed in mammary epithelial cells and mediates osteopontin expression. J Biol Chem 2003;278:48684-9.

209. Javed A, Barnes GL, Jasanya BO, et al. runt homology domain transcription factors (Runx, Cbfa, and AML) mediate repression of the bone sialoprotein promoter: evidence for promoter context-dependent activity of Cbfa proteins. Mol Cell Biol 2001;21:2891-905.

210. Nakashima K, Zhou X, Kunkel G, et al. The novel zinc finger-containing transcription factor osterix is required for osteoblast differentiation and bone formation. Cell 2002;108:17-29.

211. Celil AB, Hollinger JO, Campbell PG. Osx transcriptional regulation is mediated by additional pathways to BMP2/Smad signaling. J Cell Biochem 2005;95:518-28.

212. Koga T, Matsui Y, Asagiri M, et al. NFAT and Osterix cooperatively regulate bone formation. Nat Med 2005;11:880-5.

213. Winslow MM, Pan M, Starbuck M, et al. Calcineurin/NFAT signaling in osteoblasts regulates bone mass. Dev Cell 2006;10:771-82.

214. Koay MA, Brown MA. Genetic disorders of the LRP5-Wnt signalling pathway affecting the skeleton. Trends Mol Med 2005;11:129-37.

215. Little RD, Carulli JP, Del Mastro RG, et al. A mutation in the LDL receptor-related protein 5 gene results in the autosomal dominant high-bone-mass trait. Am J Hum Genet 2002;70:11-9.

216. Westendorf JJ, Kahler RA, Schroeder TM. Wnt signaling in osteoblasts and bone diseases. Gene 2004;341:19-39.

217. Krishnan V, Bryant HU, Macdougald OA. Regulation of bone mass by Wnt signaling. J Clin Invest 2006;116:1202-9.

218. Cadigan KM, Liu YI. Wnt signaling: complexity at the surface. J Cell Sci 2006;119:395-402.

219. Day TF, Guo X, Garrett-Beal L, Yang Y. Wnt/beta-catenin signaling in mesenchymal progenitors controls osteoblast and chondrocyte differentiation during vertebrate skeletogenesis. Dev Cell 2005;8:739-50.

220. Johnson ML, Harnish K, Nusse R, Van Hul W. LRP5 and Wnt signaling: a union made for bone. J Bone Miner Res 2004;19:1749-57.

221. Zhang C, Cho K, Huang Y, et al. Inhibition of Wnt signaling by the osteoblast-specific transcription factor Osterix. Proc Natl Acad Sci U S A 2008;105:6936-41.

222. Zhang C. Transcriptional regulation of bone formation by the osteoblast-specific transcription factor Osx. J Orthop Surg Res 2010;5:37.

223. Bennett CN, Longo KA, Wright WS, et al. Regulation of osteoblastogenesis and bone mass by Wnt10b. Proc Natl Acad Sci U S A 2005;102:3324-9.

224. Gaur T, Lengner CJ, Hovhannisyan H, et al. Canonical WNT signaling promotes osteogenesis by directly stimulating Runx2 gene expression. J Biol Chem 2005;280:33132-40.

225. Yang F, Tang W, So S, de Crombrugghe B, Zhang C. Sclerostin is a direct target of osteoblast-specific transcription factor osterix. Biochem Biophys Res Commun 2010;400:684-8.

226. Kato M, Patel MS, Levasseur R, et al. Cbfa1-independent decrease in osteoblast proliferation, osteopenia, and persistent embryonic eye vascularization in mice deficient in Lrp5, a Wnt coreceptor. J Cell Biol 2002;157:303-14.

227. Glass DA, 2nd, Bialek P, Ahn JD, et al. Canonical Wnt signaling in differentiated osteoblasts controls osteoclast differentiation. Dev Cell 2005;8:751-64.

228. Silkstone D, Hong H, Alman BA. Beta-catenin in the race to fracture repair: in it to Wnt. Nat Clin Pract Rheumatol 2008;4:413-9.

229. Kawano Y, Kypta R. Secreted antagonists of the Wnt signalling pathway. J Cell Sci 2003;116:2627-34.

230. Mason JJ, Williams BO. SOST and DKK: Antagonists of LRP Family Signaling as Targets for Treating Bone Disease. J Osteoporos 2010;2010.

231. Bafico A, Liu G, Yaniv A, Gazit A, Aaronson SA. Novel mechanism of Wnt signalling inhibition mediated by Dickkopf-1 interaction with LRP6/Arrow. Nat Cell Biol 2001;3:683-6.

232. Mao B, Wu W, Davidson G, et al. Kremen proteins are Dickkopf receptors that regulate Wnt/beta-catenin signalling. Nature 2002;417:664-7.

233. Li J, Sarosi I, Cattley RC, et al. Dkk1-mediated inhibition of Wnt signaling in bone results in osteopenia. Bone 2006;39:754-66.

234. Morvan F, Boulukos K, Clement-Lacroix P, et al. Deletion of a single allele of the Dkk1 gene leads to an increase in bone formation and bone mass. J Bone Miner Res 2006;21:934-45.

235. Ellwanger K, Saito H, Clement-Lacroix P, et al. Targeted disruption of the Wnt regulator Kremen induces limb defects and high bone density. Mol Cell Biol 2008;28:4875-82.

236. Li X, Liu P, Liu W, et al. Dkk2 has a role in terminal osteoblast differentiation and mineralized matrix formation. Nat Genet 2005;37:945-52.

237. Poole KE, van Bezooijen RL, Loveridge N, et al. Sclerostin is a delayed secreted product of osteocytes that inhibits bone formation. Faseb J 2005;19:1842-4.

238. Robling AG, Niziolek PJ, Baldridge LA, et al. Mechanical stimulation of bone in vivo reduces osteocyte expression of Sost/sclerostin. J Biol Chem 2008;283:5866-75.

239. Krause C, Korchynskyi O, de Rooij K, et al. Distinct modes of inhibition by sclerostin on bone morphogenetic protein and Wnt signaling pathways. J Biol Chem 2010;285:41614-26.

240. Li X, Ominsky MS, Niu QT, et al. Targeted deletion of the sclerostin gene in mice results in increased bone formation and bone strength. J Bone Miner Res 2008;23:860-9.

241. Winkler DG, Sutherland MK, Geoghegan JC, et al. Osteocyte control of bone formation via sclerostin, a novel BMP antagonist. Embo J 2003;22:6267-76.

242. Moester MJ, Papapoulos SE, Lowik CW, van Bezooijen RL. Sclerostin: current knowledge and future perspectives. Calcif Tissue Int 2010;87:99-107.

243. Ahrens M, Ankenbauer T, Schroder D, Hollnagel A, Mayer H, Gross G. Expression of human bone morphogenetic proteins-2 or -4 in murine mesenchymal progenitor C3H10T1/2 cells induces differentiation into distinct mesenchymal cell lineages. DNA Cell Biol 1993;12:871-80.

244. Ducy P, Zhang R, Geoffroy V, Ridall AL, Karsenty G. Osf2/Cbfa1: a transcriptional activator of osteoblast differentiation. Cell 1997;89:747-54.

245. Theoleyre S, Wittrant Y, Tat SK, Fortun Y, Redini F, Heymann D. The molecular triad OPG/RANK/RANKL: involvement in the orchestration of pathophysiological bone remodeling. Cytokine Growth Factor Rev 2004;15:457-75.

246. Anderson DM, Maraskovsky E, Billingsley WL, et al. A homologue of the TNF receptor and its ligand enhance T-cell growth and dendritic-cell function. Nature 1997;390:175-9.

247. Horwood NJ, Kartsogiannis V, Quinn JM, Romas E, Martin TJ, Gillespie MT. Activated T lymphocytes support osteoclast formation in vitro. Biochem Biophys Res Commun 1999;265:144-50.

248. Fata JE, Kong YY, Li J, et al. The osteoclast differentiation factor osteoprotegerin-ligand is essential for mammary gland development. Cell 2000;103:41-50.

249. Han X, Kawai T, Taubman MA. Interference with immune-cell-mediated bone resorption in periodontal disease. Periodontol 2000 2007;45:76-94.

250. Kim HH, Shin HS, Kwak HJ, et al. RANKL regulates endothelial cell survival through the phosphatidylinositol 3'-kinase/Akt signal transduction pathway. Faseb J 2003;17:2163-5.

251. Khosla S. Minireview: the OPG/RANKL/RANK system. Endocrinology 2001;142:5050-5.

252. Lum L, Wong BR, Josien R, et al. Evidence for a role of a tumor necrosis factor-alpha (TNF-alpha)-converting enzyme-like protease in shedding of TRANCE, a TNF family member involved in osteoclastogenesis and dendritic cell survival. J Biol Chem 1999;274:13613-8.

253. Hikita A, Tanaka S. Ectodomain shedding of receptor activator of NF-kappaB ligand. Adv Exp Med Biol 2007;602:15-21.

254. Nagai M, Kyakumoto S, Sato N. Cancer cells responsible for humoral hypercalcemia express mRNA encoding a secreted form of ODF/TRANCE that induces osteoclast formation. Biochem Biophys Res Commun 2000;269:532-6.

255. O'Brien CA. Control of RANKL gene expression. Bone 2010;46:911-9.

256. Nakashima T, Kobayashi Y, Yamasaki S, et al. Protein expression and functional difference of membrane-bound and soluble receptor activator of NF-kappaB ligand: modulation of the expression by osteotropic factors and cytokines. Biochem Biophys Res Commun 2000;275:768-75.

257. Nakamichi Y, Udagawa N, Kobayashi Y, et al. Osteoprotegerin reduces the serum level of receptor activator of NF-kappaB ligand derived from osteoblasts. J Immunol 2007;178:192-200.

258. Mizuno A, Kanno T, Hoshi M, et al. Transgenic mice overexpressing soluble osteoclast differentiation factor (sODF) exhibit severe osteoporosis. J Bone Miner Metab 2002;20:337-44.

259. Lam J, Nelson CA, Ross FP, Teitelbaum SL, Fremont DH. Crystal structure of the TRANCE/RANKL cytokine reveals determinants of receptor-ligand specificity. J Clin Invest 2001;108:971-9.

260. Kodaira K, Kodaira K, Mizuno A, et al. Cloning and characterization of the gene encoding mouse osteoclast differentiation factor. Gene 1999;230:121-7.

261. Simonet WS, Lacey DL, Dunstan CR, et al. Osteoprotegerin: a novel secreted protein involved in the regulation of bone density. Cell 1997;89:309-19.

262. Hofbauer LC, Heufelder AE. Role of receptor activator of nuclear factor-kappaB ligand and osteoprotegerin in bone cell biology. J Mol Med 2001;79:243-53.

263. Yamaguchi K, Kinosaki M, Goto M, et al. Characterization of structural domains of human osteoclastogenesis inhibitory factor. J Biol Chem 1998;273:5117-23.

264. Bucay N, Sarosi I, Dunstan CR, et al. osteoprotegerin-deficient mice develop early onset osteoporosis and arterial calcification. Genes Dev 1998;12:1260-8.

265. Thomas GP, Baker SU, Eisman JA, Gardiner EM. Changing RANKL/OPG mRNA expression in differentiating murine primary osteoblasts. J Endocrinol 2001;170:451-60.

266. Atkins GJ, Kostakis P, Pan B, et al. RANKL expression is related to the differentiation state of human osteoblasts. J Bone Miner Res 2003;18:1088-98.

267. Karsenty G, Kronenberg HM, Settembre C. Genetic control of bone formation. Annu Rev Cell Dev Biol 2009;25:629-48.

268. Manolagas SC. Birth and death of bone cells: basic regulatory mechanisms and implications for the pathogenesis and treatment of osteoporosis. Endocr Rev 2000;21:115-37.

269. Dallas SL, Bonewald LF. Dynamics of the transition from osteoblast to osteocyte. Ann N Y Acad Sci 2010;1192:437-43.

270. Candeliere GA, Liu F, Aubin JE. Individual osteoblasts in the developing calvaria express different gene repertoires. Bone 2001;28:351-61.

271. Liu F, Malaval L, Aubin JE. The mature osteoblast phenotype is characterized by extensive plasticity. Exp Cell Res 1997;232:97-105.

272. Bonewald LF. Osteocytes as dynamic multifunctional cells. Ann N Y Acad Sci 2007;1116:281-90.

273. Rochefort GY, Pallu S, Benhamou CL. Osteocyte: the unrecognized side of bone tissue. Osteoporos Int 2010;21:1457-69.

274. Franz-Odendaal TA, Hall BK, Witten PE. Buried alive: how osteoblasts become osteocytes. Dev Dyn 2006;235:176-90.

275. Teti A, Zallone A. Do osteocytes contribute to bone mineral homeostasis? Osteocytic osteolysis revisited. Bone 2009;44:11-6.

276. Tanaka-Kamioka K, Kamioka H, Ris H, Lim SS. Osteocyte shape is dependent on actin filaments and osteocyte processes are unique actin-rich projections. J Bone Miner Res 1998;13:1555-68.

277. Dudley HR, Spiro D. The Fine Structure of Bone Cells. J Biophys Biochem Cytol 1961;11:627-49.

278. Knothe Tate ML, Adamson JR, Tami AE, Bauer TW. The osteocyte. Int J Biochem Cell Biol 2004;36:1-8.

279. Palumbo C, Palazzini S, Zaffe D, Marotti G. Osteocyte differentiation in the tibia of newborn rabbit: an ultrastructural study of the formation of cytoplasmic processes. Acta Anat (Basel) 1990;137:350-8.

280. Owen M, Macpherson S. Cell Population Kinetics of an Osteogenic Tissue. Ii. J Cell Biol 1963;19:33-44.

281. Barragan-Adjemian C, Nicolella D, Dusevich V, Dallas MR, Eick JD, Bonewald LF. Mechanism by which MLO-A5 late osteoblasts/early osteocytes mineralize in culture: similarities with mineralization of lamellar bone. Calcif Tissue Int 2006;79:340-53.

282. Bonewald LF. The amazing osteocyte. J Bone Miner Res 2011;26:229-38.

283. Paic F, Igwe JC, Nori R, et al. Identification of differentially expressed genes between osteoblasts and osteocytes. Bone 2009;45:682-92.

284. Petersen DN, Tkalcevic GT, Mansolf AL, Rivera-Gonzalez R, Brown TA. Identification of osteoblast/osteocyte factor 45 (OF45), a bone-specific cDNA encoding an RGD-containing protein that is highly expressed in osteoblasts and osteocytes. J Biol Chem 2000;275:36172-80.

285. Noble BS. The osteocyte lineage. Arch Biochem Biophys 2008;473:106-11.

286. Toyosawa S, Shintani S, Fujiwara T, et al. Dentin matrix protein 1 is predominantly expressed in chicken and rat osteocytes but not in osteoblasts. J Bone Miner Res 2001;16:2017-26.

287. Feng JQ, Ward LM, Liu S, et al. Loss of DMP1 causes rickets and osteomalacia and identifies a role for osteocytes in mineral metabolism. Nat Genet 2006;38:1310-5.

288. Zhang K, Barragan-Adjemian C, Ye L, et al. E11/gp38 selective expression in osteocytes: regulation by mechanical strain and role in dendrite elongation. Mol Cell Biol 2006;26:4539-52.

289. Inoue K, Mikuni-Takagaki Y, Oikawa K, et al. A crucial role for matrix metalloproteinase 2 in osteocytic canalicular formation and bone metabolism. J Biol Chem 2006;281:33814-24.

290. Kartsogiannis V, Zhou H, Horwood NJ, et al. Localization of RANKL (receptor activator of NF kappa B ligand) mRNA and protein in skeletal and extraskeletal tissues. Bone 1999;25:525-34.

291. Zhao S, Zhang YK, Harris S, Ahuja SS, Bonewald LF. MLO-Y4 osteocyte-like cells support osteoclast formation and activation. J Bone Miner Res 2002;17:2068-79.

292. Mikuni-Takagaki Y, Suzuki Y, Kawase T, Saito S. Distinct responses of different populations of bone cells to mechanical stress. Endocrinology 1996;137:2028-35.

293. Sun YQ, McLeod KJ, Rubin CT. Mechanically induced periosteal bone formation is paralleled by the upregulation of collagen type one mRNA in osteocytes as measured by in situ reverse transcript-polymerase chain reaction. Calcif Tissue Int 1995;57:456-62.

294. Noble BS, Reeve J. Osteocyte function, osteocyte death and bone fracture resistance. Mol Cell Endocrinol 2000;159:7-13.

295. Noble BS, Stevens H, Loveridge N, Reeve J. Identification of apoptotic changes in osteocytes in normal and pathological human bone. Bone 1997;20:273-82.

296. Sims NA, Gooi JH. Bone remodeling: Multiple cellular interactions required for coupling of bone formation and resorption. Semin Cell Dev Biol 2008;19:444-51.

297. Proff P, Romer P. The molecular mechanism behind bone remodelling: a review. Clin Oral Investig 2009;13:355-62.

298. Hauge EM, Qvesel D, Eriksen EF, Mosekilde L, Melsen F. Cancellous bone remodeling occurs in specialized compartments lined by cells expressing osteoblastic markers. J Bone Miner Res 2001;16:1575-82.

299. Eghbali-Fatourechi GZ, Lamsam J, Fraser D, Nagel D, Riggs BL, Khosla S. Circulating osteoblast-lineage cells in humans. N Engl J Med 2005;352:1959-66.

300. Marotti G, Ferretti M, Muglia MA, Palumbo C, Palazzini S. A quantitative evaluation of osteoblast-osteocyte relationships on growing endosteal surface of rabbit tibiae. Bone 1992;13:363-8.

301. Civitelli R. Cell-cell communication in the osteoblast/osteocyte lineage. Arch Biochem Biophys 2008;473:188-92.

302. Silvestrini G, Ballanti P, Patacchioli F, et al. Detection of osteoprotegerin (OPG) and its ligand (RANKL) mRNA and protein in femur and tibia of the rat. J Mol Histol 2005;36:59-67.

303. Cardoso L, Herman BC, Verborgt O, Laudier D, Majeska RJ, Schaffler MB. Osteocyte apoptosis controls activation of intracortical resorption in response to bone fatigue. J Bone Miner Res 2009;24:597-605.

304. Noble BS, Peet N, Stevens HY, et al. Mechanical loading: biphasic osteocyte survival and targeting of osteoclasts for bone destruction in rat cortical bone. Am J Physiol Cell Physiol 2003;284:C934-43.

305. Mann V, Huber C, Kogianni G, Jones D, Noble B. The influence of mechanical stimulation on osteocyte apoptosis and bone viability in human trabecular bone. J Musculoskelet Neuronal Interact 2006;6:408-17.

306. Heino TJ, Hentunen TA, Vaananen HK. Osteocytes inhibit osteoclastic bone resorption through transforming growth factor-beta: enhancement by estrogen. J Cell Biochem 2002;85:185-97.

307. Heino TJ, Kurata K, Higaki H, Vaananen HK. Evidence for the role of osteocytes in the initiation of targeted remodeling. Technol Health Care 2009;17:49-56.

308. Carman CV, Sage PT, Sciuto TE, et al. Transcellular diapedesis is initiated by invasive podosomes. Immunity 2007;26:784-97.

309. Carman CV, Springer TA. A transmigratory cup in leukocyte diapedesis both through individual vascular endothelial cells and between them. J Cell Biol 2004;167:377-88.

310. Yang CM, Chien CS, Yao CC, Hsiao LD, Huang YC, Wu CB. Mechanical strain induces collagenase-3 (MMP-13) expression in MC3T3-E1 osteoblastic cells. J Biol Chem 2004;279:22158-65.

311. Teitelbaum SL. Bone resorption by osteoclasts. Science 2000;289:1504-8.

312. Everts V, Delaisse JM, Korper W, et al. The bone lining cell: its role in cleaning Howship's lacunae and initiating bone formation. J Bone Miner Res 2002;17:77-90.

313. Tran Van P, Vignery A, Baron R. An electron-microscopic study of the bone-remodeling sequence in the rat. Cell Tissue Res 1982;225:283-92.

314. Chang MK, Raggatt LJ, Alexander KA, et al. Osteal tissue macrophages are intercalated throughout human and mouse bone lining tissues and regulate osteoblast function in vitro and in vivo. J Immunol 2008;181:1232-44.

315. Henriksen K, Neutzsky-Wulff AV, Bonewald LF, Karsdal MA. Local communication on and within bone controls bone remodeling. Bone 2009;44:1026-33.

316. Pederson L, Ruan M, Westendorf JJ, Khosla S, Oursler MJ. Regulation of bone formation by osteoclasts involves Wnt/BMP signaling and the chemokine sphingosine-1-phosphate. Proc Natl Acad Sci U S A 2008;105:20764-9.

317. Zhao C, Irie N, Takada Y, et al. Bidirectional ephrinB2-EphB4 signaling controls bone homeostasis. Cell Metab 2006;4:111-21.

318. van Bezooijen RL, Roelen BA, Visser A, et al. Sclerostin is an osteocyte-expressed negative regulator of bone formation, but not a classical BMP antagonist. J Exp Med 2004;199:805-14.

319. Yuan B, Takaiwa M, Clemens TL, et al. Aberrant Phex function in osteoblasts and osteocytes alone underlies murine X-linked hypophosphatemia. J Clin Invest 2008;118:722-34.

320. Raggatt LJ, Partridge NC. Cellular and molecular mechanisms of bone remodeling. J Biol Chem 2010;285:25103-8.

321. Feng X, McDonald JM. Disorders of bone remodeling. Annu Rev Pathol 2011;6:121-45.

322. Rachner TD, Khosla S, Hofbauer LC. Osteoporosis: now and the future. Lancet 2011.

323. Osteoporosis prevention, diagnosis, and therapy. NIH Consens Statement 2000;17:1-45.

324. Cummings SR, Bates D, Black DM. Clinical use of bone densitometry: scientific review. JAMA 2002;288:1889-97.

325. Eastell R, Ebeling PR. Bone turnover markers: a key tool for understanding osteoporosis. Osteoporos Int 2009;20 Suppl 3:S237-8.

326. Szulc P, Delmas PD. Biochemical markers of bone turnover: potential use in the investigation and management of postmenopausal osteoporosis. Osteoporos Int 2008;19:1683-704.

327. Li WF, Hou SX, Yu B, Li MM, Ferec C, Chen JM. Genetics of osteoporosis: accelerating pace in gene identification and validation. Hum Genet 2010;127:249-85.

328. Rivadeneira F, Styrkarsdottir U, Estrada K, et al. Twenty bone-mineral-density loci identified by large-scale meta-analysis of genome-wide association studies. Nat Genet 2009;41:1199-206.

329. Pietschmann P, Rauner M, Sipos W, Kerschan-Schindl K. Osteoporosis: an age-related and gender-specific disease--a mini-review. Gerontology 2009;55:3-12.

330. Riggs BL, Khosla S, Melton LJ, 3rd. Sex steroids and the construction and conservation of the adult skeleton. Endocr Rev 2002;23:279-302.

331. Khosla S. Update in male osteoporosis. J Clin Endocrinol Metab 2010;95:3-10.

332. Frenkel B, Hong A, Baniwal SK, et al. Regulation of adult bone turnover by sex steroids. J Cell Physiol 2010;224:305-10.

333. Khosla S. Update on estrogens and the skeleton. J Clin Endocrinol Metab 2010;95:3569-77.

334. Garnero P, Sornay-Rendu E, Chapuy MC, Delmas PD. Increased bone turnover in late postmenopausal women is a major determinant of osteoporosis. J Bone Miner Res 1996;11:337-49.

335. Eghbali-Fatourechi G, Khosla S, Sanyal A, Boyle WJ, Lacey DL, Riggs BL. Role of RANK ligand in mediating increased bone resorption in early postmenopausal women. J Clin Invest 2003;111:1221-30.

336. Saika M, Inoue D, Kido S, Matsumoto T. 17beta-estradiol stimulates expression of osteoprotegerin by a mouse stromal cell line, ST-2, via estrogen receptor-alpha. Endocrinology 2001;142:2205-12.

337. Jilka RL. Cytokines, bone remodeling, and estrogen deficiency: a 1998 update. Bone 1998;23:75-81.

338. Everts V, de Vries TJ, Helfrich MH. Osteoclast heterogeneity: lessons from osteopetrosis and inflammatory conditions. Biochim Biophys Acta 2009;1792:757-65.

339. Michou L, Brown JP. Genetics of bone diseases: Paget's disease, fibrous dysplasia, osteopetrosis, and osteogenesis imperfecta. Joint Bone Spine 2010.

340. Van Wesenbeeck L, Odgren PR, MacKay CA, et al. The osteopetrotic mutation toothless (tl) is a loss-of-function frameshift mutation in the rat Csf1 gene: Evidence of a crucial role for CSF-1 in osteoclastogenesis and endochondral ossification. Proc Natl Acad Sci U S A 2002;99:14303-8.

341. Dougall WC, Glaccum M, Charrier K, et al. RANK is essential for osteoclast and lymph node development. Genes Dev 1999;13:2412-24.

342. Sobacchi C, Frattini A, Guerrini MM, et al. Osteoclast-poor human osteopetrosis due to mutations in the gene encoding RANKL. Nat Genet 2007;39:960-2.

343. Guerrini MM, Sobacchi C, Cassani B, et al. Human osteoclast-poor osteopetrosis with hypogammaglobulinemia due to TNFRSF11A (RANK) mutations. Am J Hum Genet 2008;83:64-76.

344. Tolar J, Teitelbaum SL, Orchard PJ. Osteopetrosis. N Engl J Med 2004;351:2839-49.

345. Maricic M. Osteomalacia. Curr Osteoporos Rep 2008;6:130-3.

346. Ros I, Alvarez L, Guanabens N, et al. Hypophosphatemic osteomalacia: a report of five cases and evaluation of bone markers. J Bone Miner Metab 2005;23:266-9.

347. Holick MF. High prevalence of vitamin D inadequacy and implications for health. Mayo Clin Proc 2006;81:353-73.

348. Suda T, Ueno Y, Fujii K, Shinki T. Vitamin D and bone. J Cell Biochem 2003;88:259-66.

349. Saito T, Nishii Y, Yasuda T, et al. Familial hypophosphatemic rickets caused by a large deletion in PHEX gene. Eur J Endocrinol 2009;161:647-51.

350. Morales-Piga AA, Rey-Rey JS, Corres-Gonzalez J, Garcia-Sagredo JM, Lopez-Abente G. Frequency and characteristics of familial aggregation of Paget's disease of bone. J Bone Miner Res 1995;10:663-70.

351. Siris ES, Ottman R, Flaster E, Kelsey JL. Familial aggregation of Paget's disease of bone. J Bone Miner Res 1991;6:495-500.

352. Daroszewska A, Ralston SH. Mechanisms of disease: genetics of Paget's disease of bone and related disorders. Nat Clin Pract Rheumatol 2006;2:270-7.

353. Seitz S, Priemel M, Zustin J, et al. Paget's disease of bone: histologic analysis of 754 patients. J Bone Miner Res 2009;24:62-9.

354. Alvarez L, Guanabens N, Peris P, et al. Discriminative value of biochemical markers of bone turnover in assessing the activity of Paget's disease. J Bone Miner Res 1995;10:458-65.

355. Torres R, de la Piedra C, Rapado A. Clinical usefulness of serum tartrate-resistant acid phosphatase in Paget's disease of bone: correlation with other biochemical markers of bone remodelling. Calcif Tissue Int 1991;49:14-6.

356. Garnero P, Fledelius C, Gineyts E, Serre CM, Vignot E, Delmas PD. Decreased beta-isomerization of the C-terminal telopeptide of type I

collagen alpha 1 chain in Paget's disease of bone. J Bone Miner Res 1997;12:1407-15.

357. Roodman GD. Insights into the pathogenesis of Paget's disease. Ann N Y Acad Sci 2010;1192:176-80.

358. Cody JD, Singer FR, Roodman GD, et al. Genetic linkage of Paget disease of the bone to chromosome 18q. Am J Hum Genet 1997;61:1117-22.

359. Hocking LJ, Herbert CA, Nicholls RK, et al. Genomewide search in familial Paget disease of bone shows evidence of genetic heterogeneity with candidate loci on chromosomes 2q36, 10p13, and 5q35. Am J Hum Genet 2001;69:1055-61.

360. Laurin N, Brown JP, Morissette J, Raymond V. Recurrent mutation of the gene encoding sequestosome 1 (SQSTM1/p62) in Paget disease of bone. Am J Hum Genet 2002;70:1582-8.

361. Sparks AB, Peterson SN, Bell C, et al. Mutation screening of the TNFRSF11A gene encoding receptor activator of NF kappa B (RANK) in familial and sporadic Paget's disease of bone and osteosarcoma. Calcif Tissue Int 2001;68:151-5.

362. Goode A, Layfield R. Recent advances in understanding the molecular basis of Paget disease of bone. J Clin Pathol 2010;63:199-203.

363. Seibenhener ML, Geetha T, Wooten MW. Sequestosome 1/p62--more than just a scaffold. FEBS Lett 2007;581:175-9.

364. Visconti MR, Langston AL, Alonso N, et al. Mutations of SQSTM1 are associated with severity and clinical outcome in paget disease of bone. J Bone Miner Res 2010;25:2368-73.

365. Layfield R, Hocking LJ. SQSTM1 and Paget's disease of bone. Calcif Tissue Int 2004;75:347-57.

366. Duran A, Serrano M, Leitges M, et al. The atypical PKC-interacting protein p62 is an important mediator of RANK-activated osteoclastogenesis. Dev Cell 2004;6:303-9.

367. Chamoux E, Couture J, Bisson M, Morissette J, Brown JP, Roux S. The p62 P392L mutation linked to Paget's disease induces activation of human osteoclasts. Mol Endocrinol 2009;23:1668-80.

368. Arron JR, Choi Y. Bone versus immune system. Nature 2000;408:535-6.

369. Bianco P. Bone and the hematopoietic niche: a tale of two stem cells. Blood 2011.

370. Yin T, Li L. The stem cell niches in bone. J Clin Invest 2006;116:1195-201.

371. Taichman RS, Emerson SG. The role of osteoblasts in the hematopoietic microenvironment. Stem Cells 1998;16:7-15.

372. Otto F, Thornell AP, Crompton T, et al. Cbfa1, a candidate gene for cleidocranial dysplasia syndrome, is essential for osteoblast differentiation and bone development. Cell 1997;89:765-71.

373. Nilsson SK, Johnston HM, Whitty GA, et al. Osteopontin, a key component of the hematopoietic stem cell niche and regulator of primitive hematopoietic progenitor cells. Blood 2005;106:1232-9.

374. Stier S, Ko Y, Forkert R, et al. Osteopontin is a hematopoietic stem cell niche component that negatively regulates stem cell pool size. J Exp Med 2005;201:1781-91.

375. Zhang J, Niu C, Ye L, et al. Identification of the haematopoietic stem cell niche and control of the niche size. Nature 2003;425:836-41.

376. Arai F, Hirao A, Ohmura M, et al. Tie2/angiopoietin-1 signaling regulates hematopoietic stem cell quiescence in the bone marrow niche. Cell 2004;118:149-61.

377. Kollet O, Dar A, Shivtiel S, et al. Osteoclasts degrade endosteal components and promote mobilization of hematopoietic progenitor cells. Nat Med 2006;12:657-64.

378. Lorenzo J, Choi Y. Osteoimmunology. Immunol Rev 2005;208:5-6.

379. Marriott I, Rati DM, McCall SH, Tranguch SL. Induction of Nod1 and Nod2 intracellular pattern recognition receptors in murine osteoblasts following bacterial challenge. Infect Immun 2005;73:2967-73.

380. Grassi F, Manferdini C, Cattini L, et al. T cell suppression by osteoclasts in vitro. J Cell Physiol 2011;226:982-90.

381. Kiesel JR, Buchwald ZS, Aurora R. Cross-presentation by osteoclasts induces FoxP3 in CD8+ T cells. J Immunol 2009;182:5477-87.

382. Klareskog L, Catrina AI, Paget S. Rheumatoid arthritis. Lancet 2009;373:659-72.

383. Alamanos Y, Drosos AA. Epidemiology of adult rheumatoid arthritis. Autoimmun Rev 2005;4:130-6.

384. Rantapaa-Dahlqvist S, de Jong BA, Berglin E, et al. Antibodies against cyclic citrullinated peptide and IgA rheumatoid factor predict the development of rheumatoid arthritis. Arthritis Rheum 2003;48:2741-9.

385. Firestein GS. Evolving concepts of rheumatoid arthritis. Nature 2003;423:356-61.

386. MacGregor AJ, Snieder H, Rigby AS, et al. Characterizing the quantitative genetic contribution to rheumatoid arthritis using data from twins. Arthritis Rheum 2000;43:30-7.

387. Isomaki H, Nissila M, Koota K, Martio J, Tiilikainen A. Letter: HL-A 27 and rheumatoid arthritis. Lancet 1974;2:1212-3.

388. Kueppers F, Brackertz D, Mueller-Eckhardt C. HL-A antigens in sarcoidosis and rheumatoid arthritis. Lancet 1972;2:1425.

389. Panayi GS, Wooley P, Batchelor JR. Genetic basis of rheumatoid disease: HLA antigens, disease manifestations, and toxic reactions to drugs. Br Med J 1978;2:1326-8.

390. Padyukov L, Seielstad M, Ong RT, et al. A genome-wide association study suggests contrasting associations in ACPA-positive versus ACPA-negative rheumatoid arthritis. Ann Rheum Dis 2011;70:259-65.

391. Begovich AB, Carlton VE, Honigberg LA, et al. A missense single-nucleotide polymorphism in a gene encoding a protein tyrosine phosphatase (PTPN22) is associated with rheumatoid arthritis. Am J Hum Genet 2004;75:330-7.

392. James EA, Moustakas AK, Bui J, et al. HLA-DR1001 presents "altered-self" peptides derived from joint-associated proteins by accepting citrulline in three of its binding pockets. Arthritis Rheum 2010;62:2909-18.

393. Raychaudhuri S, Thomson BP, Remmers EF, et al. Genetic variants at CD28, PRDM1 and CD2/CD58 are associated with rheumatoid arthritis risk. Nat Genet 2009;41:1313-8.

394. Orstavik RE, Haugeberg G, Mowinckel P, et al. Vertebral deformities in rheumatoid arthritis: a comparison with population-based controls. Arch Intern Med 2004;164:420-5.

395. van Staa TP, Geusens P, Bijlsma JW, Leufkens HG, Cooper C. Clinical assessment of the long-term risk of fracture in patients with rheumatoid arthritis. Arthritis Rheum 2006;54:3104-12.

396. Bromley M, Woolley DE. Chondroclasts and osteoclasts at subchondral sites of erosion in the rheumatoid joint. Arthritis Rheum 1984;27:968-75.

397. Ritchlin CT, Haas-Smith SA, Li P, Hicks DG, Schwarz EM. Mechanisms of TNF-alpha- and RANKL-mediated osteoclastogenesis and bone resorption in psoriatic arthritis. J Clin Invest 2003;111:821-31.

398. Lubberts E, Oppers-Walgreen B, Pettit AR, et al. Increase in expression of receptor activator of nuclear factor kappaB at sites of bone erosion correlates with progression of inflammation in evolving collagen-induced arthritis. Arthritis Rheum 2002;46:3055-64.

399. Crotti TN, Smith MD, Weedon H, et al. Receptor activator NF-kappaB ligand (RANKL) expression in synovial tissue from patients with

rheumatoid arthritis, spondyloarthropathy, osteoarthritis, and from normal patients: semiquantitative and quantitative analysis. Ann Rheum Dis 2002;61:1047-54.

400. Leibbrandt A, Penninger JM. RANK/RANKL: regulators of immune responses and bone physiology. Ann N Y Acad Sci 2008;1143:123-50.

401. Cohen SB, Dore RK, Lane NE, et al. Denosumab treatment effects on structural damage, bone mineral density, and bone turnover in rheumatoid arthritis: a twelve-month, multicenter, randomized, double-blind, placebo-controlled, phase II clinical trial. Arthritis Rheum 2008;58:1299-309.

402. Dore RK, Cohen SB, Lane NE, et al. Effects of denosumab on bone mineral density and bone turnover in patients with rheumatoid arthritis receiving concurrent glucocorticoids or bisphosphonates. Ann Rheum Dis 2010;69:872-5.

403. Sharp JT, Tsuji W, Ory P, Harper-Barek C, Wang H, Newmark R. Denosumab prevents metacarpal shaft cortical bone loss in patients with erosive rheumatoid arthritis. Arthritis Care Res (Hoboken) 2010;62:537-44.

404. Deodhar A, Dore RK, Mandel D, et al. Denosumab-mediated increase in hand bone mineral density associated with decreased progression of bone erosion in rheumatoid arthritis patients. Arthritis Care Res (Hoboken) 2010;62:569-74.

405. Herman S, Kronke G, Schett G. Molecular mechanisms of inflammatory bone damage: emerging targets for therapy. Trends Mol Med 2008.

406. McInnes IB, Schett G. Cytokines in the pathogenesis of rheumatoid arthritis. Nat Rev Immunol 2007;7:429-42.

407. Husby G, Williams RC, Jr. Synovial localization of tumor necrosis factor in patients with rheumatoid arthritis. J Autoimmun 1988;1:363-71.

408. Feldmann M, Brennan FM, Chantry D, et al. Cytokine production in the rheumatoid joint: implications for treatment. Ann Rheum Dis 1990;49 Suppl 1:480-6.

409. Nouri AM, Panayi GS, Goodman SM. Cytokines and the chronic inflammation of rheumatic disease. I. The presence of interleukin-1 in synovial fluids. Clin Exp Immunol 1984;55:295-302.

410. Symons JA, McDowell TL, di Giovine FS, Wood NC, Capper SJ, Duff GW. Interleukin 1 in rheumatoid arthritis: potentiation of immune responses within the joint. Lymphokine Res 1989;8:365-72.

411. Houssiau FA, Devogelaer JP, Van Damme J, de Deuxchaisnes CN, Van Snick J. Interleukin-6 in synovial fluid and serum of patients with rheumatoid arthritis and other inflammatory arthritides. Arthritis Rheum 1988;31:784-8.

412. Hirano T, Matsuda T, Turner M, et al. Excessive production of interleukin 6/B cell stimulatory factor-2 in rheumatoid arthritis. Eur J Immunol 1988;18:1797-801.

413. Yu DT, Peter JB, Paulus HE, Nies KM. Human lymphocyte subpopulations. Study of T and B cells and their density distribution. Clin Immunol Immunopathol 1974;2:333-42.

414. Vernon-Roberts B, Currey HL, Perrin J. T and B cells in the blood and synovial fluid of rheumatoid patients. Ann Rheum Dis 1974;33:430-4.

415. Choi SI, Brahn E. Rheumatoid arthritis therapy: advances from bench to bedside. Autoimmunity 2010;43:478-92.

416. Kong YY, Feige U, Sarosi I, et al. Activated T cells regulate bone loss and joint destruction in adjuvant arthritis through osteoprotegerin ligand. Nature 1999;402:304-9.

417. Takayanagi H, Ogasawara K, Hida S, et al. T-cell-mediated regulation of osteoclastogenesis by signalling cross-talk between RANKL and IFN-gamma. Nature 2000;408:600-5.

418. Wong BR, Josien R, Lee SY, et al. TRANCE (tumor necrosis factor [TNF]-related activation-induced cytokine), a new TNF family member predominantly expressed in T cells, is a dendritic cell-specific survival factor. J Exp Med 1997;186:2075-80.

419. Rivollier A, Mazzorana M, Tebib J, et al. Immature dendritic cell transdifferentiation into osteoclasts: a novel pathway sustained by the rheumatoid arthritis microenvironment. Blood 2004;104:4029-37.

420. Gruber R. Cell biology of osteoimmunology. Wien Med Wochenschr 2010;160:438-45.

421. Gallois A, Lachuer J, Yvert G, et al. Genome-wide expression analyses establish dendritic cells as a new osteoclast precursor able to generate bone-resorbing cells more efficiently than monocytes. J Bone Miner Res 2010;25:661-72.

422. Miltenburg AM, van Laar JM, de Kuiper R, Daha MR, Breedveld FC. T cells cloned from human rheumatoid synovial membrane functionally represent the Th1 subset. Scand J Immunol 1992;35:603-10.

423. Mauri C, Williams RO, Walmsley M, Feldmann M. Relationship between Th1/Th2 cytokine patterns and the arthritogenic response in collagen-induced arthritis. Eur J Immunol 1996;26:1511-8.

424. Hirota K, Hashimoto M, Yoshitomi H, et al. T cell self-reactivity forms a cytokine milieu for spontaneous development of IL-17+ Th cells that cause autoimmune arthritis. J Exp Med 2007;204:41-7.

425. Hu Y, Shen F, Crellin NK, Ouyang W. The IL-17 pathway as a major therapeutic target in autoimmune diseases. Ann N Y Acad Sci 2011;1217:60-76.

426. Miossec P. Interleukin-17 in rheumatoid arthritis: if T cells were to contribute to inflammation and destruction through synergy. Arthritis Rheum 2003;48:594-601.

427. Chabaud M, Fossiez F, Taupin JL, Miossec P. Enhancing effect of IL-17 on IL-1-induced IL-6 and leukemia inhibitory factor production by rheumatoid arthritis synoviocytes and its regulation by Th2 cytokines. J Immunol 1998;161:409-14.

428. Chen G, Zhang X, Li R, et al. Role of osteopontin in synovial Th17 differentiation in rheumatoid arthritis. Arthritis Rheum 2010;62:2900-8.

429. Sato K, Suematsu A, Okamoto K, et al. Th17 functions as an osteoclastogenic helper T cell subset that links T cell activation and bone destruction. J Exp Med 2006;203:2673-82.

430. Takayanagi H. New immune connections in osteoclast formation. Ann N Y Acad Sci 2010;1192:117-23.

431. David JP. Osteoimmunology: a view from the bone. Adv Immunol 2007;95:149-65.

432. Lubberts E, van den Bersselaar L, Oppers-Walgreen B, et al. IL-17 promotes bone erosion in murine collagen-induced arthritis through loss of the receptor activator of NF-kappa B ligand/osteoprotegerin balance. J Immunol 2003;170:2655-62.

433. Lubberts E, Koenders MI, Oppers-Walgreen B, et al. Treatment with a neutralizing anti-murine interleukin-17 antibody after the onset of collagen-induced arthritis reduces joint inflammation, cartilage destruction, and bone erosion. Arthritis Rheum 2004;50:650-9.

434. Chabaud M, Durand JM, Buchs N, et al. Human interleukin-17: A T cell-derived proinflammatory cytokine produced by the rheumatoid synovium. Arthritis Rheum 1999;42:963-70.

435. Church LD, Filer AD, Hidalgo E, et al. Rheumatoid synovial fluid interleukin-17-producing CD4 T cells have abundant tumor necrosis factor-alpha co-expression, but little interleukin-22 and interleukin-23R expression. Arthritis Res Ther 2010;12:R184.

436. Shen H, Goodall JC, Hill Gaston JS. Frequency and phenotype of peripheral blood Th17 cells in ankylosing spondylitis and rheumatoid arthritis. Arthritis Rheum 2009;60:1647-56.

437. Notley CA, Ehrenstein MR. The yin and yang of regulatory T cells and inflammation in RA. Nat Rev Rheumatol 2010;6:572-7.

438. Mottonen M, Heikkinen J, Mustonen L, Isomaki P, Luukkainen R, Lassila O. CD4+ CD25+ T cells with the phenotypic and functional characteristics of regulatory T cells are enriched in the synovial fluid of patients with rheumatoid arthritis. Clin Exp Immunol 2005;140:360-7.

439. Ruprecht CR, Gattorno M, Ferlito F, et al. Coexpression of CD25 and CD27 identifies FoxP3+ regulatory T cells in inflamed synovia. J Exp Med 2005;201:1793-803.

440. Han GM, O'Neil-Andersen NJ, Zurier RB, Lawrence DA. CD4+CD25high T cell numbers are enriched in the peripheral blood of patients with rheumatoid arthritis. Cell Immunol 2008;253:92-101.

441. Oh S, Rankin AL, Caton AJ. CD4+CD25+ regulatory T cells in autoimmune arthritis. Immunol Rev 2010;233:97-111.

442. de Kleer IM, Wedderburn LR, Taams LS, et al. CD4+CD25bright regulatory T cells actively regulate inflammation in the joints of patients with the remitting form of juvenile idiopathic arthritis. J Immunol 2004;172:6435-43.

443. Ehrenstein MR, Evans JG, Singh A, et al. Compromised function of regulatory T cells in rheumatoid arthritis and reversal by anti-TNFalpha therapy. J Exp Med 2004;200:277-85.

444. Valencia X, Stephens G, Goldbach-Mansky R, Wilson M, Shevach EM, Lipsky PE. TNF downmodulates the function of human CD4+CD25hi T-regulatory cells. Blood 2006;108:253-61.

445. Yuan FL, Li X, Lu WG, et al. Regulatory T cells as a potent target for controlling bone loss. Biochem Biophys Res Commun 2010;402:173-6.

446. Schett G. Osteoimmunology in rheumatic diseases. Arthritis Res Ther 2009;11:210.

447. Kim YG, Lee CK, Nah SS, Mun SH, Yoo B, Moon HB. Human CD4+CD25+ regulatory T cells inhibit the differentiation of osteoclasts from peripheral blood mononuclear cells. Biochem Biophys Res Commun 2007;357:1046-52.

448. Askenasy N, Kaminitz A, Yarkoni S. Mechanisms of T regulatory cell function. Autoimmun Rev 2008;7:370-5.

449. Axmann R, Herman S, Zaiss M, et al. CTLA-4 directly inhibits osteoclast formation. Ann Rheum Dis 2008;67:1603-9.

450. Zaiss MM, Axmann R, Zwerina J, et al. Treg cells suppress osteoclast formation: a new link between the immune system and bone. Arthritis Rheum 2007;56:4104-12.

451. Kelchtermans H, Geboes L, Mitera T, Huskens D, Leclercq G, Matthys P. Activated CD4+CD25+ regulatory T cells inhibit osteoclastogenesis and collagen-induced arthritis. Ann Rheum Dis 2009;68:744-50.

452. Zaiss MM, Frey B, Hess A, et al. Regulatory T cells protect from local and systemic bone destruction in arthritis. J Immunol 2010;184:7238-46.

453. Li X, Yuan FL, Lu WG, et al. The role of interleukin-17 in mediating joint destruction in rheumatoid arthritis. Biochem Biophys Res Commun 2010;397:131-5.

454. Scheel T, Gursche A, Zacher J, Haupl T, Berek C. V-region gene analysis of locally defined synovial B and plasma cells reveals selected B cell expansion and accumulation of plasma cell clones in rheumatoid arthritis. Arthritis Rheum 2011;63:63-72.

455. Takemura S, Klimiuk PA, Braun A, Goronzy JJ, Weyand CM. T cell activation in rheumatoid synovium is B cell dependent. J Immunol 2001;167:4710-8.

456. Walsh MC, Kim N, Kadono Y, et al. Osteoimmunology: interplay between the immune system and bone metabolism. Annu Rev Immunol 2006;24:33-63.

457. Wu JY, Purton LE, Rodda SJ, et al. Osteoblastic regulation of B lymphopoiesis is mediated by Gs{alpha}-dependent signaling pathways. Proc Natl Acad Sci U S A 2008;105:16976-81.

458. Zhu J, Garrett R, Jung Y, et al. Osteoblasts support B-lymphocyte commitment and differentiation from hematopoietic stem cells. Blood 2007;109:3706-12.

459. Calvi LM, Adams GB, Weibrecht KW, et al. Osteoblastic cells regulate the haematopoietic stem cell niche. Nature 2003;425:841-6.

460. von Freeden-Jeffry U, Vieira P, Lucian LA, McNeil T, Burdach SE, Murray R. Lymphopenia in interleukin (IL)-7 gene-deleted mice identifies IL-7 as a nonredundant cytokine. J Exp Med 1995;181:1519-26.

461. Nagasawa T, Hirota S, Tachibana K, et al. Defects of B-cell lymphopoiesis and bone-marrow myelopoiesis in mice lacking the CXC chemokine PBSF/SDF-1. Nature 1996;382:635-8.

462. Datta HK, Ng WF, Walker JA, Tuck SP, Varanasi SS. The cell biology of bone metabolism. J Clin Pathol 2008;61:577-87.

463. Li Y, Toraldo G, Li A, et al. B cells and T cells are critical for the preservation of bone homeostasis and attainment of peak bone mass in vivo. Blood 2007;109:3839-48.

464. Horowitz MC, Fretz JA, Lorenzo JA. How B cells influence bone biology in health and disease. Bone 2010;47:472-9.

465. Mansour A, Anginot A, Mancini SJ, et al. Osteoclast activity modulates B-cell development in the bone marrow. Cell Res 2011.

466. Gierut A, Perlman H, Pope RM. Innate immunity and rheumatoid arthritis. Rheum Dis Clin North Am 2010;36:271-96.

467. Sun JC, Beilke JN, Lanier LL. Adaptive immune features of natural killer cells. Nature 2009;457:557-61.

468. Soderstrom K, Stein E, Colmenero P, et al. Natural killer cells trigger osteoclastogenesis and bone destruction in arthritis. Proc Natl Acad Sci U S A 2010;107:13028-33.

469. Maruotti N, Crivellato E, Cantatore FP, Vacca A, Ribatti D. Mast cells in rheumatoid arthritis. Clin Rheumatol 2007;26:1-4.

470. Hueber AJ, Asquith DL, Miller AM, et al. Mast cells express IL-17A in rheumatoid arthritis synovium. J Immunol 2010;184:3336-40.

471. Edwards SW, Hallett MB. Seeing the wood for the trees: the forgotten role of neutrophils in rheumatoid arthritis. Immunol Today 1997;18:320-4.

472. Nathan C. Neutrophils and immunity: challenges and opportunities. Nat Rev Immunol 2006;6:173-82.

473. Lisignoli G, Toneguzzi S, Pozzi C, et al. Proinflammatory cytokines and chemokine production and expression by human osteoblasts isolated from patients with rheumatoid arthritis and osteoarthritis. J Rheumatol 1999;26:791-9.

474. Chung R, Cool JC, Scherer MA, Foster BK, Xian CJ. Roles of neutrophil-mediated inflammatory response in the bony repair of injured growth plate cartilage in young rats. J Leukoc Biol 2006;80:1272-80.

475. Chakravarti A, Raquil MA, Tessier P, Poubelle PE. Surface RANKL of Toll-like receptor 4-stimulated human neutrophils activates osteoclastic bone resorption. Blood 2009;114:1633-44.

476. Poubelle PE, Chakravarti A, Fernandes MJ, Doiron K, Marceau AA. Differential expression of RANK, RANK-L, and osteoprotegerin by synovial fluid neutrophils from patients with rheumatoid arthritis and by healthy human blood neutrophils. Arthritis Res Ther 2007;9:R25.

477. Keffer J, Probert L, Cazlaris H, et al. Transgenic mice expressing human tumour necrosis factor: a predictive genetic model of arthritis. EMBO J 1991;10:4025-31.

478. Alonzi T, Fattori E, Lazzaro D, et al. Interleukin 6 is required for the development of collagen-induced arthritis. J Exp Med 1998;187:461-8.

479. Brandao FM, Coelho P, Pinto P, Combe B. Tocilizumab - a new step in rheumatoid arthritis treatment. Acta Reumatol Port 2010;35:302-12.

480. Smolen JS, Aletaha D. Interleukin-6 receptor inhibition with tocilizumab and attainment of disease remission in rheumatoid arthritis: the role of acute-phase reactants. Arthritis Rheum 2011;63:43-52.

481. Fonseca JE, Santos MJ, Canhao H, Choy E. Interleukin-6 as a key player in systemic inflammation and joint destruction. Autoimmun Rev 2009;8:538-42.

482. Axmann R, Bohm C, Kronke G, Zwerina J, Smolen J, Schett G. Inhibition of interleukin-6 receptor directly blocks osteoclast formation in vitro and in vivo. Arthritis Rheum 2009;60:2747-56.

483. Nowell MA, Williams AS, Carty SA, et al. Therapeutic targeting of IL-6 trans signaling counteracts STAT3 control of experimental inflammatory arthritis. J Immunol 2009;182:613-22.

484. Kato A, Matsuo S, Takai H, Uchiyama Y, Mihara M, Suzuki M. Early effects of tocilizumab on bone and bone marrow lesions in a collagen-induced arthritis monkey model. Exp Mol Pathol 2008;84:262-70.

485. Garnero P, Thompson E, Woodworth T, Smolen JS. Rapid and sustained improvement in bone and cartilage turnover markers with the anti-interleukin-6 receptor inhibitor tocilizumab plus methotrexate in rheumatoid arthritis patients with an inadequate response to methotrexate: results from a substudy of the multicenter double-blind, placebo-controlled trial of tocilizumab in inadequate responders to methotrexate alone. Arthritis Rheum 2010;62:33-43.

486. Dayer JM, Bresnihan B. Targeting interleukin-1 in the treatment of rheumatoid arthritis. Arthritis Rheum 2002;46:574-8.

487. Bendele A, McAbee T, Sennello G, Frazier J, Chlipala E, McCabe D. Efficacy of sustained blood levels of interleukin-1 receptor antagonist in animal models of arthritis: comparison of efficacy in animal models with human clinical data. Arthritis Rheum 1999;42:498-506.

488. Kobayashi N, Kadono Y, Naito A, et al. Segregation of TRAF6-mediated signaling pathways clarifies its role in osteoclastogenesis. Embo J 2001;20:1271-80.

489. Abramson SB, Amin A. Blocking the effects of IL-1 in rheumatoid arthritis protects bone and cartilage. Rheumatology (Oxford) 2002;41:972-80.

490. Polzer K, Joosten L, Gasser J, et al. Interleukin-1 is essential for systemic inflammatory bone loss. Ann Rheum Dis 2010;69:284-90.

491. Probert L, Plows D, Kontogeorgos G, Kollias G. The type I interleukin-1 receptor acts in series with tumor necrosis factor (TNF) to induce arthritis in TNF-transgenic mice. Eur J Immunol 1995;25:1794-7.

492. Sfikakis PP. The first decade of biologic TNF antagonists in clinical practice: lessons learned, unresolved issues and future directions. Curr Dir Autoimmun 2010;11:180-210.

493. Jin J, Chang Y, Wei W. Clinical application and evaluation of anti-TNF-alpha agents for the treatment of rheumatoid arthritis. Acta Pharmacol Sin 2010;31:1133-40.

494. Lacey DC, Simmons PJ, Graves SE, Hamilton JA. Proinflammatory cytokines inhibit osteogenic differentiation from stem cells: implications for bone repair during inflammation. Osteoarthritis Cartilage 2009;17:735-42.

495. O'Gradaigh D, Ireland D, Bord S, Compston JE. Joint erosion in rheumatoid arthritis: interactions between tumour necrosis factor alpha, interleukin 1, and receptor activator of nuclear factor kappaB ligand (RANKL) regulate osteoclasts. Ann Rheum Dis 2004;63:354-9.

496. Kim N, Kadono Y, Takami M, et al. Osteoclast differentiation independent of the TRANCE-RANK-TRAF6 axis. J Exp Med 2005;202:589-95.

497. Gilbert L, He X, Farmer P, et al. Inhibition of osteoblast differentiation by tumor necrosis factor-alpha. Endocrinology 2000;141:3956-64.

498. Panagakos FS, Fernandez C, Kumar S. Ultrastructural analysis of mineralized matrix from human osteoblastic cells: effect of tumor necrosis factor-alpha. Mol Cell Biochem 1996;158:81-9.

499. Gorny G, Shaw A, Oursler MJ. IL-6, LIF, and TNF-alpha regulation of GM-CSF inhibition of osteoclastogenesis in vitro. Exp Cell Res 2004;294:149-58.

500. Hiasa M, Abe M, Nakano A, et al. GM-CSF and IL-4 induce dendritic cell differentiation and disrupt osteoclastogenesis through M-CSF receptor shedding by up-regulation of TNF-alpha converting enzyme (TACE). Blood 2009;114:4517-26.

501. Houde N, Chamoux E, Bisson M, Roux S. Transforming growth factor-beta1 (TGF-beta1) induces human osteoclast apoptosis by up-regulating Bim. J Biol Chem 2009;284:23397-404.

502. Gingery A, Bradley EW, Pederson L, Ruan M, Horwood NJ, Oursler MJ. TGF-beta coordinately activates TAK1/MEK/AKT/NFkB and SMAD pathways to promote osteoclast survival. Exp Cell Res 2008;314:2725-38.

503. Ehnert S, Baur J, Schmitt A, et al. TGF-beta1 as possible link between loss of bone mineral density and chronic inflammation. PLoS One 2010;5:e14073.

504. Wang R, Zhang L, Zhang X, et al. Regulation of activation-induced receptor activator of NF-kappaB ligand (RANKL) expression in T cells. Eur J Immunol 2002;32:1090-8.

505. Choy EH, Panayi GS. Cytokine pathways and joint inflammation in rheumatoid arthritis. N Engl J Med 2001;344:907-16.

506. Koga T, Inui M, Inoue K, et al. Costimulatory signals mediated by the ITAM motif cooperate with RANKL for bone homeostasis. Nature 2004;428:758-63.

507. Kaifu T, Nakahara J, Inui M, et al. Osteopetrosis and thalamic hypomyelinosis with synaptic degeneration in DAP12-deficient mice. J Clin Invest 2003;111:323-32.

508. Mocsai A, Humphrey MB, Van Ziffle JA, et al. The immunomodulatory adapter proteins DAP12 and Fc receptor gamma-chain (FcRgamma) regulate development of functional osteoclasts through the Syk tyrosine kinase. Proc Natl Acad Sci U S A 2004;101:6158-63.

509. Joyce-Shaikh B, Bigler ME, Chao CC, et al. Myeloid DAP12-associating lectin (MDL)-1 regulates synovial inflammation and bone erosion associated with autoimmune arthritis. J Exp Med 2010;207:579-89.

510. Takayanagi H. Osteoimmunology: shared mechanisms and crosstalk between the immune and bone systems. Nat Rev Immunol 2007;7:292-304.

511. Bar-Shavit Z. Taking a toll on the bones: regulation of bone metabolism by innate immune regulators. Autoimmunity 2008;41:195-203.

512. Hurst J, von Landenberg P. Toll-like receptors and autoimmunity. Autoimmun Rev 2008;7:204-8.

513. Asagiri M, Hirai T, Kunigami T, et al. Cathepsin K-dependent toll-like receptor 9 signaling revealed in experimental arthritis. Science 2008;319:624-7.

514. Kim KW, Cho ML, Oh HJ, et al. TLR-3 enhances osteoclastogenesis through upregulation of RANKL expression from fibroblast-like synoviocytes in patients with rheumatoid arthritis. Immunol Lett 2009;124:9-17.

515. Kim KW, Cho ML, Lee SH, et al. Human rheumatoid synovial fibroblasts promote osteoclastogenic activity by activating RANKL via TLR-2 and TLR-4 activation. Immunol Lett 2007;110:54-64.

516. Okada Y, Naka K, Kawamura K, et al. Localization of matrix metalloproteinase 9 (92-kilodalton gelatinase/type IV collagenase = gelatinase B) in osteoclasts: implications for bone resorption. Lab Invest 1995;72:311-22.

517. Ji JD, Park-Min KH, Shen Z, et al. Inhibition of RANK expression and osteoclastogenesis by TLRs and IFN-gamma in human osteoclast precursors. J Immunol 2009;183:7223-33.

518. Durand M, Boire G, Komarova SV, et al. The increased in vitro osteoclastogenesis in patients with rheumatoid arthritis is due to increased percentage of precursors and decreased apoptosis - The In Vitro Osteoclast Differentiation in Arthritis (IODA) study. Bone 2011;48:588-96.

519. Nose M, Yamazaki H, Hagino H, Morio Y, Hayashi S, Teshima R. Comparison of osteoclast precursors in peripheral blood mononuclear cells

from rheumatoid arthritis and osteoporosis patients. J Bone Miner Metab 2009;27:57-65.

520. Trebec DP, Chandra D, Gramoun A, Li K, Heersche JN, Manolson MF. Increased expression of activating factors in large osteoclasts could explain their excessive activity in osteolytic diseases. J Cell Biochem 2007;101:205-20.

521. Hirayama T, Danks L, Sabokbar A, Athanasou NA. Osteoclast formation and activity in the pathogenesis of osteoporosis in rheumatoid arthritis. Rheumatology (Oxford) 2002;41:1232-9.

522. Takano H, Tomita T, Toyosaki-Maeda T, et al. Comparison of the activities of multinucleated bone-resorbing giant cells derived from CD14-positive cells in the synovial fluids of rheumatoid arthritis and osteoarthritis patients. Rheumatology (Oxford) 2004;43:435-41.

523. Walsh NC, Reinwald S, Manning CA, et al. Osteoblast function is compromised at sites of focal bone erosion in inflammatory arthritis. J Bone Miner Res 2009;24:1572-85.

524. MacDonald BT, Joiner DM, Oyserman SM, et al. Bone mass is inversely proportional to Dkk1 levels in mice. Bone 2007;41:331-9.

525. Diarra D, Stolina M, Polzer K, et al. Dickkopf-1 is a master regulator of joint remodeling. Nat Med 2007;13:156-63.

526. Heiland GR, Zwerina K, Baum W, et al. Neutralisation of Dkk-1 protects from systemic bone loss during inflammation and reduces sclerostin expression. Ann Rheum Dis 2010;69:2152-9.

527. Schett G, Saag KG, Bijlsma JW. From bone biology to clinical outcome: state of the art and future perspectives. Ann Rheum Dis 2010;69:1415-9.

528. Garnero P, Tabassi NC, Voorzanger-Rousselot N. Circulating dickkopf-1 and radiological progression in patients with early rheumatoid arthritis treated with etanercept. J Rheumatol 2008;35:2313-5.

529. Wang SY, Liu YY, Ye H, et al. Circulating Dickkopf-1 Is Correlated with Bone Erosion and Inflammation in Rheumatoid Arthritis. J Rheumatol 2011.

530. Daoussis D, Andonopoulos AP, Liossis SN. Wnt pathway and IL-17: novel regulators of joint remodeling in rheumatic diseases. Looking beyond the RANK-RANKL-OPG axis. Semin Arthritis Rheum 2010;39:369-83.

531. Daoussis D, Liossis SN, Solomou EE, et al. Evidence that Dkk-1 is dysfunctional in ankylosing spondylitis. Arthritis Rheum 2010;62:150-8.

532. Uderhardt S, Diarra D, Katzenbeisser J, et al. Blockade of Dickkopf (DKK)-1 induces fusion of sacroiliac joints. Ann Rheum Dis 2010;69:592-7.

533. Dalbeth N, Pool B, Smith T, et al. Circulating mediators of bone remodeling in psoriatic arthritis: implications for disordered osteoclastogenesis and bone erosion. Arthritis Res Ther 2010;12:R164.

534. Lane NE, Nevitt MC, Lui LY, de Leon P, Corr M. Wnt signaling antagonists are potential prognostic biomarkers for the progression of radiographic hip osteoarthritis in elderly Caucasian women. Arthritis Rheum 2007;56:3319-25.

535. Appel H, Ruiz-Heiland G, Listing J, et al. Altered skeletal expression of sclerostin and its link to radiographic progression in ankylosing spondylitis. Arthritis Rheum 2009;60:3257-62.

536. Kronke G, Uderhardt S, Kim KA, et al. R-spondin 1 protects against inflammatory bone damage during murine arthritis by modulating the Wnt pathway. Arthritis Rheum 2010;62:2303-12.

537. Schindeler A, McDonald MM, Bokko P, Little DG. Bone remodeling during fracture repair: The cellular picture. Semin Cell Dev Biol 2008;19:459-66.

538. Alexander K, Chang M, Maylin E, et al. Osteal macrophages promote in vivo intramembranous bone healing in a mouse tibial injury model. J Bone Miner Res 2011.

539. Bais M, McLean J, Sebastiani P, et al. Transcriptional analysis of fracture healing and the induction of embryonic stem cell-related genes. PLoS One 2009;4:e5393.

540. Bastian O, Pillay J, Alblas J, Leenen L, Koenderman L, Blokhuis T. Systemic inflammation and fracture healing. J Leukoc Biol 2011.

541. Marzona L, Pavolini B. Play and players in bone fracture healing match. Clinical cases in Mineral and Bone Metabolism 2009;6:159-62.

542. Schmidt-Bleek K, Schell H, Kolar P, et al. Cellular composition of the initial fracture hematoma compared to a muscle hematoma: a study in sheep. J Orthop Res 2009;27:1147-51.

543. Andrew JG, Andrew SM, Freemont AJ, Marsh DR. Inflammatory cells in normal human fracture healing. Acta Orthop Scand 1994;65:462-6.

544. Einhorn TA, Majeska RJ, Rush EB, Levine PM, Horowitz MC. The expression of cytokine activity by fracture callus. J Bone Miner Res 1995;10:1272-81.

545. Giannoudis PV, Einhorn TA, Marsh D. Fracture healing: the diamond concept. Injury 2007;38 Suppl 4:S3-6.

546. Grundnes O, Reikeras O. The importance of the hematoma for fracture healing in rats. Acta Orthop Scand 1993;64:340-2.

547. Mizuno K, Mineo K, Tachibana T, Sumi M, Matsubara T, Hirohata K. The osteogenetic potential of fracture haematoma. Subperiosteal and

intramuscular transplantation of the haematoma. J Bone Joint Surg Br 1990;72-B:822-9.

548. Street J, Winter D, Wang JH, Wakai A, McGuinness A, Redmond HP. Is human fracture hematoma inherently angiogenic? Clin Orthop Relat Res 2000:224-37.

549. Glass GE, Chan JK, Freidin A, Feldmann M, Horwood NJ, Nanchahal J. TNF-alpha promotes fracture repair by augmenting the recruitment and differentiation of muscle-derived stromal cells. Proc Natl Acad Sci U S A 2011;108:1585-90.

550. Ai-Aql ZS, Alagl AS, Graves DT, Gerstenfeld LC, Einhorn TA. Molecular mechanisms controlling bone formation during fracture healing and distraction osteogenesis. J Dent Res 2008;87:107-18.

551. Tsiridis E, Upadhyay N, Giannoudis P. Molecular aspects of fracture healing: which are the important molecules? Injury 2007;38 Suppl 1:S11-25.

552. Dimitriou R, Tsiridis E, Giannoudis PV. Current concepts of molecular aspects of bone healing. Injury 2005;36:1392-404.

553. Reikeras O, Shegarfi H, Wang JE, Utvag SE. Lipopolysaccharide impairs fracture healing: an experimental study in rats. Acta Orthop 2005;76:749-53.

554. Gordon S, Martinez FO. Alternative activation of macrophages: mechanism and functions. Immunity 2010;32:593-604.

555. De AK, Laudanski K, Miller-Graziano CL. Failure of monocytes of trauma patients to convert to immature dendritic cells is related to preferential macrophage-colony-stimulating factor-driven macrophage differentiation. J Immunol 2003;170:6355-62.

556. Horgan AF, Mendez MV, O'Riordain DS, Holzheimer RG, Mannick JA, Rodrick ML. Altered gene transcription after burn injury results in depressed T-lymphocyte activation. Ann Surg 1994;220:342-51; discussion 51-2.

557. Colburn NT, Zaal KJ, Wang F, Tuan RS. A role for gamma/delta T cells in a mouse model of fracture healing. Arthritis Rheum 2009;60:1694-703.

558. Hauser CJ, Zhou X, Joshi P, et al. The immune microenvironment of human fracture/soft-tissue hematomas and its relationship to systemic immunity. J Trauma 1997;42:895-903; discussion -4.

559. Tsangari H, Findlay DM, Kuliwaba JS, Atkins GJ, Fazzalari NL. Increased expression of IL-6 and RANK mRNA in human trabecular bone from fragility fracture of the femoral neck. Bone 2004;35:334-42.

560. Yang X, Ricciardi BF, Hernandez-Soria A, Shi Y, Pleshko Camacho N, Bostrom MP. Callus mineralization and maturation are delayed during fracture healing in interleukin-6 knockout mice. Bone 2007;41:928-36.

561. Lange J, Sapozhnikova A, Lu C, et al. Action of IL-1beta during fracture healing. J Orthop Res 2010;28:778-84.

562. Gerstenfeld LC, Cho TJ, Kon T, et al. Impaired fracture healing in the absence of TNF-alpha signaling: the role of TNF-alpha in endochondral cartilage resorption. J Bone Miner Res 2003;18:1584-92.

563. Kon T, Cho TJ, Aizawa T, et al. Expression of osteoprotegerin, receptor activator of NF-kappaB ligand (osteoprotegerin ligand) and related proinflammatory cytokines during fracture healing. J Bone Miner Res 2001;16:1004-14.

564. Shintaku Y, Murakami T, Yanagita T, et al. Sox9 Expression during Fracture Repair. Cells Tissues Organs 2011.

565. Phillips AM. Overview of the fracture healing cascade. Injury 2005;36 Suppl 3:S5-7.

566. Schmid GJ, Kobayashi C, Sandell LJ, Ornitz DM. Fibroblast growth factor expression during skeletal fracture healing in mice. Dev Dyn 2009;238:766-74.

567. Cho TJ, Gerstenfeld LC, Einhorn TA. Differential temporal expression of members of the transforming growth factor beta superfamily during murine fracture healing. J Bone Miner Res 2002;17:513-20.

568. Tsuji K, Bandyopadhyay A, Harfe BD, et al. BMP2 activity, although dispensable for bone formation, is required for the initiation of fracture healing. Nat Genet 2006;38:1424-9.

569. Duvall CL, Taylor WR, Weiss D, Wojtowicz AM, Guldberg RE. Impaired angiogenesis, early callus formation, and late stage remodeling in fracture healing of osteopontin-deficient mice. J Bone Miner Res 2007;22:286-97.

570. Kobayashi T, Onodera S, Kondo E, et al. Impaired fracture healing in macrophage migration inhibitory factor-deficient mice. Osteoporos Int 2010.

571. Rundle CH, Wang H, Yu H, et al. Microarray analysis of gene expression during the inflammation and endochondral bone formation stages of rat femur fracture repair. Bone 2006;38:521-9.

572. Khan SN, Solaris J, Ramsey KE, et al. Identification of novel gene expression in healing fracture callus tissue by DNA microarray. HSS J 2008;4:149-60.

573. Chen Y, Whetstone HC, Lin AC, et al. Beta-catenin signaling plays a disparate role in different phases of fracture repair: implications for therapy to improve bone healing. PLoS Med 2007;4:e249.

574. Zhong N, Gersch RP, Hadjiargyrou M. Wnt signaling activation during bone regeneration and the role of Dishevelled in chondrocyte proliferation and differentiation. Bone 2006;39:5-16.

575. Kahler RA, Westendorf JJ. Lymphoid enhancer factor-1 and beta-catenin inhibit Runx2-dependent transcriptional activation of the osteocalcin promoter. J Biol Chem 2003;278:11937-44.

576. Kakar S, Einhorn TA, Vora S, et al. Enhanced chondrogenesis and Wnt signaling in PTH-treated fractures. J Bone Miner Res 2007;22:1903-12.

577. Secreto FJ, Hoeppner LH, Westendorf JJ. Wnt signaling during fracture repair. Curr Osteoporos Rep 2009;7:64-9.

578. Minear S, Leucht P, Jiang J, et al. Wnt proteins promote bone regeneration. Sci Transl Med 2010;2:29ra30.

579. Einhorn TA. The Wnt signaling pathway as a potential target for therapies to enhance bone repair. Sci Transl Med 2010;2:42ps36.

580. Kim JB, Leucht P, Lam K, et al. Bone regeneration is regulated by wnt signaling. J Bone Miner Res 2007;22:1913-23.

581. Dean DB, Watson JT, Jin W, et al. Distinct functionalities of bone morphogenetic protein antagonists during fracture healing in mice. J Anat 2010:In press.

582. Ominsky MS, Li C, Li X, et al. Inhibition of sclerostin by monoclonal antibody enhances bone healing and improves bone density and strength of non-fractured bones. J Bone Miner Res 2010.

583. Agholme F, Li X, Isaksson H, Ke HZ, Aspenberg P. Sclerostin antibody treatment enhances metaphyseal bone healing in rats. J Bone Miner Res 2010;25:2412-8.

584. Giannoudis P, Tzioupis C, Almalki T, Buckley R. Fracture healing in osteoporotic fractures: is it really different? A basic science perspective. Injury 2007;38 Suppl 1:S90-9.

585. Namkung-Matthai H, Appleyard R, Jansen J, et al. Osteoporosis influences the early period of fracture healing in a rat osteoporotic model. Bone 2001;28:80-6.

586. Walsh WR, Sherman P, Howlett CR, Sonnabend DH, Ehrlich MG. Fracture healing in a rat osteopenia model. Clin Orthop Relat Res 1997:218-27.

587. Nikolaou VS, Efstathopoulos N, Kontakis G, Kanakaris NK, Giannoudis PV. The influence of osteoporosis in femoral fracture healing time. Injury 2009;40:663-8.

588. Desai BJ, Meyer MH, Porter S, Kellam JF, Meyer RA, Jr. The effect of age on gene expression in adult and juvenile rats following femoral fracture. J Orthop Trauma 2003;17:689-98.

589. Meyer RA, Jr., Desai BR, Heiner DE, Fiechtl J, Porter S, Meyer MH. Young, adult, and old rats have similar changes in mRNA expression of many skeletal genes after fracture despite delayed healing with age. J Orthop Res 2006;24:1933-44.

590. Lu C, Miclau T, Hu D, et al. Cellular basis for age-related changes in fracture repair. J Orthop Res 2005;23:1300-7.

591. Roholl PJ, Blauw E, Zurcher C, Dormans JA, Theuns HM. Evidence for a diminished maturation of preosteoblasts into osteoblasts during aging in rats: an ultrastructural analysis. J Bone Miner Res 1994;9:355-66.

592. Beresford JN, Bennett JH, Devlin C, Leboy PS, Owen ME. Evidence for an inverse relationship between the differentiation of adipocytic and osteogenic cells in rat marrow stromal cell cultures. J Cell Sci 1992;102 (Pt 2):341-51.

593. Ivaska KK, Gerdhem P, Akesson K, Garnero P, Obrant KJ. Effect of fracture on bone turnover markers: a longitudinal study comparing marker levels before and after injury in 113 elderly women. J Bone Miner Res 2007;22:1155-64.

594. Ikegami S, Kamimura M, Nakagawa H, et al. Comparison in bone turnover markers during early healing of femoral neck fracture and trochanteric fracture in elderly patients Orthopedic Reviews 2009;1:e21.

595. Cox G, Einhorn TA, Tzioupis C, Giannoudis PV. Bone-turnover markers in fracture healing. J Bone Joint Surg Br 2010;92:329-34.

596. Schell H, Lienau J, Epari DR, et al. Osteoclastic activity begins early and increases over the course of bone healing. Bone 2006;38:547-54.

597. Veitch SW, Findlay SC, Hamer AJ, Blumsohn A, Eastell R, Ingle BM. Changes in bone mass and bone turnover following tibial shaft fracture. Osteoporos Int 2006;17:364-72.

598. Moghaddam A, Muller U, Roth HJ, Wentzensen A, Grutzner PA, Zimmermann G. TRACP 5b and CTX as osteological markers of delayed fracture healing. Injury 2010.

599. Busti AJ, Hooper JS, Amaya CJ, Kazi S. Effects of perioperative antiinflammatory and immunomodulating therapy on surgical wound healing. Pharmacotherapy 2005;25:1566-91.

600. Bogoch ER, Ouellette G, Hastings DE. Intertrochanteric fractures of the femur in rheumatoid arthritis patients. Clin Orthop Relat Res 1993:181-6.

601. Bogoch ER, Moran EL. Bone abnormalities in the surgical treatment of patients with rheumatoid arthritis. Clin Orthop Relat Res 1999:8-21.

602. Sakaguchi N, Takahashi T, Hata H, et al. Altered thymic T-cell selection due to a mutation of the ZAP-70 gene causes autoimmune arthritis in mice. Nature 2003;426:454-60.

603. Matsuura M, Eckstein F, Lochmuller EM, Zysset PK. The role of fabric in the quasi-static compressive mechanical properties of human trabecular bone from various anatomical locations. Biomech Model Mechanobiol 2008;7:27-42.

604. Viguet-Carrin S, Garnero P, Delmas PD. The role of collagen in bone strength. Osteoporos Int 2006;17:319-36.

605. Baek WY, de Crombrugghe B, Kim JE. Postnatally induced inactivation of Osterix in osteoblasts results in the reduction of bone formation and maintenance. Bone 2010;46:920-8.

606. Li Y, Lu W, King TD, Liu CC, Bijur GN, Bu G. Dkk1 stabilizes Wnt co-receptor LRP6: implication for Wnt ligand-induced LRP6 down-regulation. PLoS One 2010;5:e11014.

607. Wallace A, Cooney TE, Englund R, Lubahn JD. Effects of Interleukin-6 Ablation on Fracture Healing in Mice. J Orthop Res 2011.

608. Ominsky MS, Li C, Li X, et al. Inhibition of sclerostin by monoclonal antibody enhances bone healing and improves bone density and strength of nonfractured bones. J Bone Miner Res 2011;26:1012-21.

A presente dissertação foi realizada na Unidade de Investigação em Reumatologia do Instituto de Medicina Molecular, Faculdade de Medicina da Universidade de Lisboa, Lisboa, Portugal.

O trabalho aqui apresentado foi realizado no âmbito do projecto “Repercussão da inflamação sobre a estrutura do osso e cartilagem: padrão de organização do colagénio e propriedades mecânicas” - financiado pela Fundação para a Ciência e Tecnologia (referência PTDC/SAU-BEB/65992/2006).

Bolsa de Doutoramento conferida pela Fundação para a Ciência e Tecnologia (referência SFRH/BD/36825/2007).